uOttawa

L'Université canadienne
Canada's university

FACULTÉ DES ÉTUDES SUPÉRIEURES ET POSTOCTORALES

uOttawa

L'Université canadienne
Canada's university

FACULTY OF GRADUATE AND POSDOCTORAL STUDIES

Annick Danielle St-Amand
AUTEUR DE LA THÈSE / AUTHOR OF THESIS

Ph.D. (Chemistry)
GRADE / DEGREE

Department of Chemistry
FACULTÉ, ÉCOLE, DÉPARTEMENT / FACULTY, SCHOOL, DEPARTMENT

Modeling Atmospheric Vegetation Uptake of PBDE's and PHADs Using Field Measurements

TITRE DE LA THÈSE / TITLE OF THESIS

Paul Mayer
DIRECTEUR (DIRECTRICE) DE LA THÈSE / THESIS SUPERVISOR

Jules Blais
CO-DIRECTEUR (CO-DIRECTRICE) DE LA THÈSE / THESIS CO-SUPERVISOR

EXAMINATEURS (EXAMINATRICES) DE LA THÈSE / THESIS EXAMINERS

Robert Burk (absent)

David Lean

Natalie Goto

Tom Harner

Gary W. Slater
Le Doyen de la Faculté des études supérieures et postdoctorales / Dean of the Faculty of Graduate and Postdoctoral Studies

MODELING ATMOSPHERIC VEGETATION UPTAKE OF PBDES AND PAHS USING FIELD MEASUREMENTS

by

Annick D. St-Amand, M.Sc.

Thesis submitted to the Faculty of Graduate and Postdoctoral Studies

In partial fulfillment of the requirements for the PhD degree in chemistry

Ottawa-Carleton Chemistry Institute

Department of Chemistry, Faculty of Science

University of Ottawa

Candidate	Supervisors
Annick D. St-Amand	Dr Paul M. Mayer & Dr Jules M. Blais

Your file Votre référence
ISBN: 978-0-494-41646-4
Our file Notre référence
ISBN: 978-0-494-41646-4

À mes parents et grand-parents

Sources d'amour et d'inspiration

ACKNOWLEDGEMENTS

I would first like to thank my two supervisors, Dr Paul M. Mayer and Dr Jules M. Blais. Your guidance and direction in the development and realization of this project is much valued. Thanks for your many comments, suggestions, and questions that help shaped papers, presentations, and the course of this study. Your unwavering support in my academic endeavours is appreciated.

I would also like to express my gratitude to Dr John Holmes, Dr A. A. (Sander) Mommers, and Dr Clem Kazakoff from the Mass Spectrometry Centre for "good morning"s and their resourcefulness. Special thanks also to Lynda Kimpe for our fascinating discussions and for sharing with me her invaluable technical knowledge regarding method development and instrumental analysis. I am also grateful to past and present colleagues from both research groups for filling this journey with discussions, laughs, and smiles; from chemistry particularly Emma Rennie, Julie Grabowy, Xian Wang, Clement Poon, Abdul Alhazmi, Mohammad Qadura, Annie Vallières, Laura Vanier, and last, but certainly not least, my office mate Anne-Marie Boulanger; and from biology: Eva Kruemmel, Tania Delongchamp, Susanna Atkinson, Bradley Mills, and Karen Foster. Special thanks also go out to Holly Shaw for help with sample collection and preparation as well as everybody who has lent a hand in sampling.

I would also like to thank the city of Ottawa for their cooperation and access to the sampling site, as well as the following for financial support: the Natural Sciences and Engineering Research Council of Canada, the Ontario Graduate Scholarship in Science and Technology program, the University of Ottawa, and the Leonard and Kathleen O'Brien Humanitarian Trust.

Finally, I would like to thank my partner Gaëtan for his strength and understanding and my family; parents, grandparents and brother for their support, encouragements and many phone calls. You truly are a source of love and inspiration...

ABSTRACT

This thesis examines the accumulation of polybrominated diphenyl ethers (PBDEs) and polycyclic aromatic hydrocarbons (PAHs) in vegetation in order to develop an interpretative scheme to determine deposition velocities of semi-volatile organic compounds (SVOCs) onto vegetation.

PBDEs are flame retardants used in a variety of consumables. Although relatively non-volatile, these compounds have been quantified around the world extending to otherwise pristine ecosystems providing empirical evidence for their long-range transport. However, modeling studies indicate that their long-range atmospheric transport (LRAT) potential is at best moderate. However, recent modeling studies have suggested that vegetation may play an important role in their global distribution. PAHs are also ubiquitous contaminants. These can be released through both natural and anthropogenic sources. Some are considered highly carcinogenic and their potential impact on human health may be due to their association to particulates. Although their environmental fate is perhaps better understood, the processes involved in surface-air exchange, particularly with vegetation, have not been well documented.

Spruce needles and atmospheric (gaseous and particulate-bound) PBDE and PAH concentrations were monitored bi-weekly from February 2004 to June 2005 to examine potential weather-related and seasonal effects. An efficient extraction method for PBDEs from spruce needles was developed. Finally, using measured concentrations, surface-air exchange was considered and a modeling concept was developed to determine deposition velocities to vegetation.

Following their emergence, spruce needle PBDE and PAH concentrations increase gradually over time although decreasing briefly following snowmelt with a minimum coinciding with the following year's bud burst. Atmospheric concentrations of PBDE and PAH, both gaseous and particulate-bound, were linked to daily weather events. PBDE gaseous concentrations increased with temperature, whereas PAH concentrations were generally highest in the winter, likely reflecting increased emission. Analysis of air mass back trajectories and local wind directions revealed that particulate-bound PBDEs, along with both gaseous and particulate-bound PAHs originated from local sources, whereas gaseous PBDEs were likely from distant sources.

Using measured atmospheric PBDE and PAH concentrations, particulate-gas partitioning was examined. Particulate-gas distributions correlated significantly with log K_{OA} values and a significant temperature dependence was observed for most compounds considered, except the higher PBDE congeners. From compounds exclusively associated to particulates, the particulate-bound deposition velocities were calculated at 3.8 and 10.8 m/h for PBDEs and PAHs, respectively. The different v_P values obtained for PBDEs and PAHs may indicate association with different particulates. Net gaseous transfer velocities correlated significantly with log K_{OA} values and ranged from 2.4 to 62.2 m/h for PBDEs and from negligible to 75.6 m/h for PAHs. These derived values were then used to monitor PBDE and PAH accumulation in vegetation through time, and these agreed well with measured values. This study provides the necessary background for modeling PBDE and PAH transport between air and coniferous vegetation globally.

RÉSUMÉ

Les polybromodiphényl éthers (PBDEs) sont des composés ignifuges ajoutés à divers produits destinés à la consommation afin d'augmenter leur résistance au feu. Ces derniers sont maintenant retrouvés un peu partout à travers le monde, jusqu'en Arctique ce qui démontre que ceux-ci peuvent être transportés sur de longues distances. Cependant, des études modélisant leur destin environnemental indique que leur transport atmosphérique sur de longues distances serait limité. Des études récentes utilisant une approche similaire ont cependant démontrées que la végétation pourrait jouer un rôle à cet égard. Les composés d'hydrocarbure aromatique polycycliques (PAHs) sont aussi omniprésents dans l'environnement. Ils peuvent être émis lors de processus naturels et anthropogéniques. Certains PAHs possèdent des propriétés cancérigènes et leur toxicité pourrait être liée à leur association avec les particules suspendues dans l'air. Bien que leur comportement environnemental soit mieux connu, des questions demeurent en ce qui concerne leurs échanges entre les surfaces, telle la végétation, et l'air.

Les concentrations de PBDEs et PAHs dans des aiguilles d'épinettes et l'air (espèces gazeuses et associées aux particules) furent évaluées bi-hebdomadairement près d'un site d'enfouissement sanitaire de février 2004 à juin 2005 afin d'étudier l'impact des saisons et de la météorologie locale. Une méthode efficace pour l'extraction des PBDEs d'aiguilles d'épinettes fut aussi développée. Finalement, les processus impliqués dans l'échange entre la végétation et l'air furent considérés afin de concevoir un concept permettant la détermination des vélocités de déposition.

Dès leur bourgeonnement, les concentrations de PBDEs et PAHs retrouvés dans les aiguilles d'épinettes ont augmenté graduellement et ce jusqu'en hiver. Suite à la fonte

des neiges ces concentrations diminuèrent légèrement. Les concentrations atmosphériques étaient cependant beaucoup plus variables, sujets aux conditions météorologiques quotidiennes. Les concentrations de PBDEs en phase gazeuse, augmentèrent avec la température, alors que celles les concentrations atmosphériques de PAHs étaient plus élevées en hiver probablement à cause d'une augmentation de leur émission. Finalement, en analysant les trajectoires antérieures des masses d'air, il fut possible de déterminer que les PBDEs associés aux particules atmosphériques ainsi que les PAHs en phase gazeuse et associés aux particules provenaient de sources locales alors que les PBDEs en phase gazeuse provenaient de sources plus éloignées.

La distribution des PBDEs et PAHs entre les particules et la phase gazeuse fut aussi examinée. Ces distributions corrèlent significativement avec les valeurs de log K_{OA} de ces composés. De plus, un lien avec la température fut aussi observé. En utilisant les concentrations des composés associés exclusivement aux particules il fut possible de calculer les vélocités de déposition pour les composés associés aux particules pour les PBDEs et les PAHs de 3.8 et 10.8 m/h respectivement. Les vélocités d'échange en phase gazeuse furent aussi déterminées. Ces dernières étaient de 2.4 à 62.2 m/h pour les PBDEs et variaient de nulles à 75.6 m/h pour les PAHs et augmentèrent selon les valeurs de log K_{OA}. Ces valeurs de vélocités furent ensuite utilisées afin d'examiner l'évolution des concentrations en PBDEs et PAHs retrouvées dans les aguilles d'épinettes et les valeurs calculées étaient similaires à celles mesurées. Cette étude procure l'arrière-plan nécessaire à la compréhension du rôle de la végétation dans le transport global de ces composés.

TABLE OF CONTENTS

LIST OF TABLES

LIST OF FIGURES

LIST OF ABBREVIATIONS

ASE	Accelerated Solvent Extraction
BDL	Below Detection Limit
BFRs	Brominated Flame Retardants
DDT	Dichlorodiphenyltrichloroethane
dw	dry weight
GC	Gas Chromatography
GMF	Glass Membrane Filter
HCs	Hydrocarbons
LRAT	Long-Range Atmospheric Transport
MDL	Method Detection Limit
MS	Mass Spectrometry
ND	Not Detected
OCs	Organochlorines
OCN	Octachloronaphthalene
PAHs	Polycyclic Aromatic Hydrocarbons
PBBs	Polybrominated Biphenyls
PBDEs	Polybrominated Diphenyl Ethers

PCBs	Polychlorinated Biphenyls
PCDDs	Dibenzo-p-dioxins
PCNs	Polychlorinated Naphthalenes
PUF	Polyurethane Foam
RDL	Regression Detection Limit
SEM	Standard error of the mean
SIM	Selected Ion Monitoring
SVOCs	Semi-volatile Organic Compounds
TaPL3	Transport and Persistence Level III (Fugacity Model)
TWF	Trail Road Waste Facility
VOCs	Volatile Organic Compounds

Polycyclic Aromatic Hydrocarbons

AceN	Acenaphthylene
Ant	Anthracene
BaA	Benzo(a)anthracene
BbF	Benzo(b)fluoranthene
BkF	Benzo(k)fluoranthene
BghiP	Benzo(ghi)perylene
BaP	Benzo(a)pyrene
Chry	Chrysene
Flu	Fluorene
IndP	Indeno(123-cd)pyrene
Phe	Phenanthrene
Pyr	Pyrene

Chapter 1 - INTRODUCTION

1.1 GENERAL INTRODUCTION

The publication in 1962 of Rachel Carson's Silent Spring [1] brought forth a new generation of environmental consciousness. That book along with local pollution events such as the Love Canal [2] and the Hudson River contamination [3] in the United States, as well as the Great Lakes pollution [4] and the Sydney Tar Ponds in Canada [5], have all promoted a certain modern environmental pollution awareness. Since its publication, many persistent organic pollutants such as the notorious DDT, polychlorinated biphenyls (PCBs), polybrominated biphenyls (PBBs), as well as many pesticides are no longer in use because of their related health and environmental concerns [4, 6]. However, these chemicals still linger in the environment due to their high stability and large quantities used in the past. Some, on the other hand, have been replaced. In that context, it could be said that the problems facing the environment today are not dramatically different; they have evolved.

In the 1970s PBBs were widely used in the flame retardant industry. However their usage was dramatically cut short in 1973 because of cattle feed contamination and they were somewhat quickly replaced with PBDEs [7, 8]. Because of their increased usage over the last decades PBDEs have now reached ubiquitous status. Like most persistent organic pollutants, PBDEs are subject to bioaccumulation and biomagnification and there are several concerns regarding their adverse health effects ranging from

endocrine disruption to neurotoxicity, in addition to their potential risk to the environment [9].

Some persistent organic pollutants can be released from naturally occurring events and thus have always been found in the environment. Such is the case of polycyclic aromatic hydrocarbons (PAHs), which can be released by forest fires. However, environmental concentrations of PAHs started to increase dramatically with the onset of the American Industrial Revolution due to an increase in energy consumption as they are emitted during the incomplete combustion of organic material, such as fossil fuels. PAHs are known carcinogens [7, 10].

Both PBDEs and PAHs have been quantified in various environmental and biological media throughout the world extending to very remote pristine locations, such as the Arctic [11-15]. PAHs are considered sufficiently volatile to be transported via long-range atmospheric transport (LRAT) [16, 17]. On the other hand, PBDEs have very low vapour pressures and their long-range atmospheric transport (LRAT) potential has been questioned [18, 19]; in fact relatively little is known about their overall environmental fate. A recent modeling study has shown that vegetation may play an important role by promoting surface-air exchange of PBDEs [20]. As for PAHs, questions still remain regarding their particulate-gas partitioning and surface-air exchange processes, which may help improve understanding of their toxicity action [21]. This study considers vegetation uptake of both semi-volatile organic compounds (SVOCs) near a point source to study the processes involved in air-vegetation exchange and gain insight into the role of vegetation in the global distribution of these compounds.

1.2 POLYBROMINATED DIPHENYL ETHERS (PBDES)

1.2.1 DESCRIPTION, USAGE AND TECHNICAL FORMULATIONS

As mentioned previously, PBDEs are used as flame retardants. Flame retardants are chemicals used in a variety of consumer's products to increase their fire resistance and thus prevent fires. As such, they are used in plastics, textiles, furniture, and electronic devices; for example, furniture foam can contain between 1-10% by weight of PBDEs [22]. The use of flame retardants has increased over the past few decades to meet stricter fire regulations. Although there are a variety of chemicals used as flame retardants ranging from metal oxides to inorganic salts, brominated flame retardants (BFRs) are generally preferred since they are the cheapest and easiest manufacturing alternative [23]. BFRs include PBDEs, hexabromocyclododecane (HBCD), tetrabromobisphenol A (TBBPA), and PBBs, the last of which are no longer being produced and, as stated above, have been replaced with PBDEs [12, 23-25]. Their structures are presented in figure 1.1. In contrast to their obvious and direct benefits, several concerns have arisen from their widespread usage, namely their persistence and potential toxicity of BFRs [23].

Flame retardants are either additive or reactive. For example, TBBPA is a reactive flame retardant because it is chemically bound to the polymer. However, most BFRs, such as PBDEs, are additive flame retardants, since they are essentially mixed in with the polymers and are not chemically bonded. It is thus foreseeable that these chemicals have the potential to leach from their final products and be released in our homes and in the environment [12, 24-26].

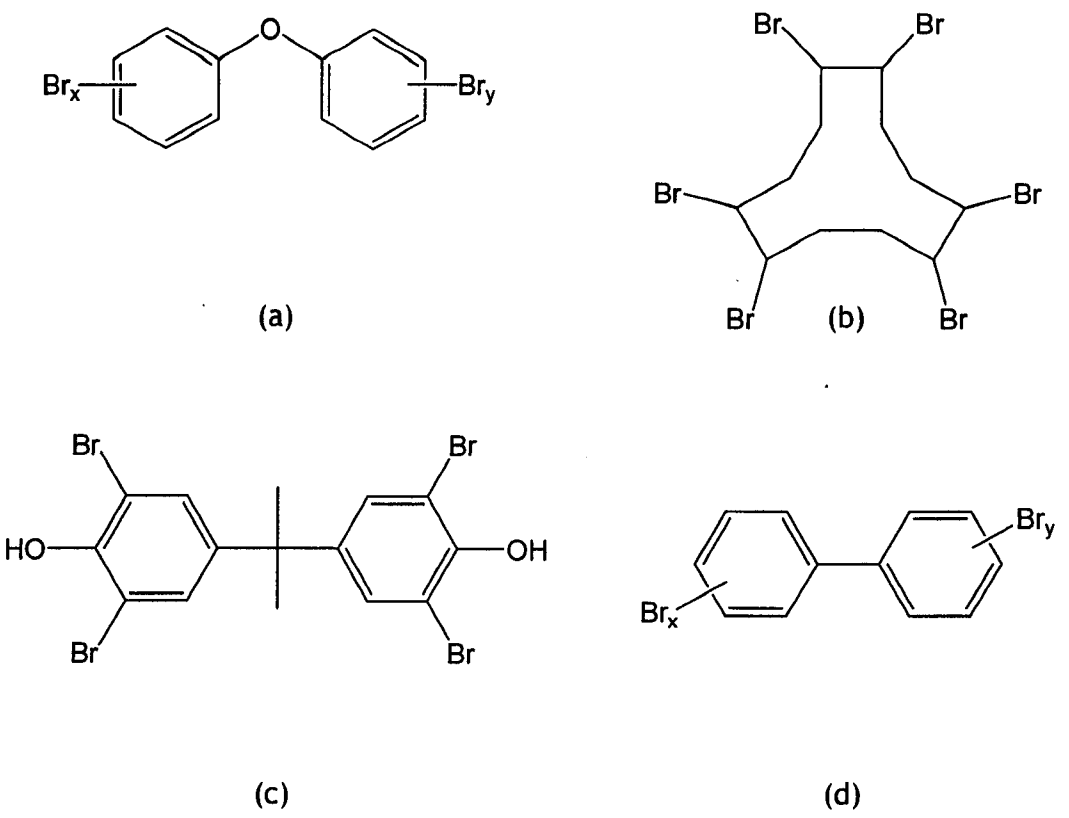

Figure 1.1 - Structures of (a) PBDEs, (b) HBCD, (c) TBBPA, and (d) PBBs.

PBDEs are structurally similar to PBBs and to polychlorinated biphenyls (PCBs) and present similar properties [9]. They also have 209 possible congeners ranging from mono-brominated to deca-brominated diphenyl ethers (see figure 1.1). However, because of steric effects, the bromination process of diphenyl ethers is rather specific and only a few congeners are formed [12, 23]. This has also been observed for PBBs [23]. The individual PBDE congeners are numbered in the same manner as PCBs and PBBs as described by the International Union of Pure and Applied Chemistry (IUPAC) which is based on the number and position of the halogen atoms on the phenyl rings [23, 24].

Three technical PBDE formulations are typically manufactured and named according to their average bromine content: PentaBDE, OctaBDE and DecaBDE. As seen in

table 1.1, PentaBDEs consist primarily of BDE-47 and BDE-99 which usually account for more than 70% of the total weight. Other congeners include triBDEs 17 and 28, tetraBDE 66, pentaBDEs 85 and 100, and hexaBDEs 138, 153, and 154. These last two congeners are also present in the OctaBDE formulation, along with heptaBDE 183 (major congener), some octaBDEs, and nonaBDEs. Finally, the DecaBDE formulation contains almost exclusively BDE-209, the fully brominated congener [9, 12, 24]. Congeners found in these technical formulations will be the focus of this study and are listed in table 1.1.

Table 1.1 - Technical formulations of PBDE-based flame retardants in percentage of BDE congener present [9, 12, 24].

Formulation	PBDE congener (%)
PentaBDE	47 (41-42%), 99 (35%), 100 (7%), 153/154 (6-7%)
	Minor components: 17, 28, 66, 85, 138, and 183
OctaBDE	183 (44%), octaBDEs (31-35%), 153/154 (10-12%), nonaBDEs (10-11%)
DecaBDE	209 (97-98%), nonaBDEs (< 3%)

The main uses of these three PBDE technical formulations are listed in table 1.2. In general, PentaBDE is mainly used in the furniture industry, applied to foams and textiles; OctaBDE is usually produced in lowest quantity with usage almost limited to poly(acrylonitrile butadiene styrene); and DecaBDE is generally considered a general purpose flame retardant and is used in a wide variety of consumables, particularly electronic devices. It should be noted that the PentaBDE formulation is not currently used in Japanese and European markets where restrictions were established in the 1990s, making North America its principal consumer [9, 12].

Table 1.2 - Uses of technical formulations of PBDE-based flame retardants [12, 24].

Formulation	Main uses
PentaBDE	Polyurethane foam and textiles
OctaBDE	Poly(acrylonitrile butadiene styrene) and polycarbonates
DecaBDE	Polycarbonates, polyvinyl chloride, polyesters, textiles and rubber

1.2.2 Current demand and presence in the environment

As mentioned previously, usage of PBDEs was initiated in the mid-1970s. Since then, stricter fire regulations have been implemented causing increased demand and production of PBDEs and other BFRs. Levels of PentaBDE produced throughout the world for 1980-2000 are presented in figure 1.2. Despite their obvious benefits PBDEs have found their way into the environment and have been quantified in various environmental media as well as in biota and in humans. Numerous trends have been published, all of which show rising concentrations [11, 12, 14, 15, 23, 24, 27-32]. Even more interesting, PBDE concentrations in the environment reflect the increase in production and use of PBDEs at the end of the 20th century. For example, BDE-47 concentrations in Canadian Arctic ringed seals have increased exponentially from 1981 to 2000 similarly to that of the worldwide PentaBDE production (seen in figure 1.2). Mother's milk from Sweden also follows a similar trend, from 1972 to 1997-1998 when concentrations started decreasing. Many authors have hypothesised that this reduction may be due to the implementation of stricter regulations regarding the use and production of PentaBDE by the European Union in 1996. The continued use of PentaBDE in North America (until 2004) would explain the continued increase in BDE-47 concentrations in Arctic ringed seals. This phenomenon is

not limited to BDE-47 as all the congeners surveyed in these studies generally show similar trends [11, 14, 15, 23, 28, 29, 31, 32].

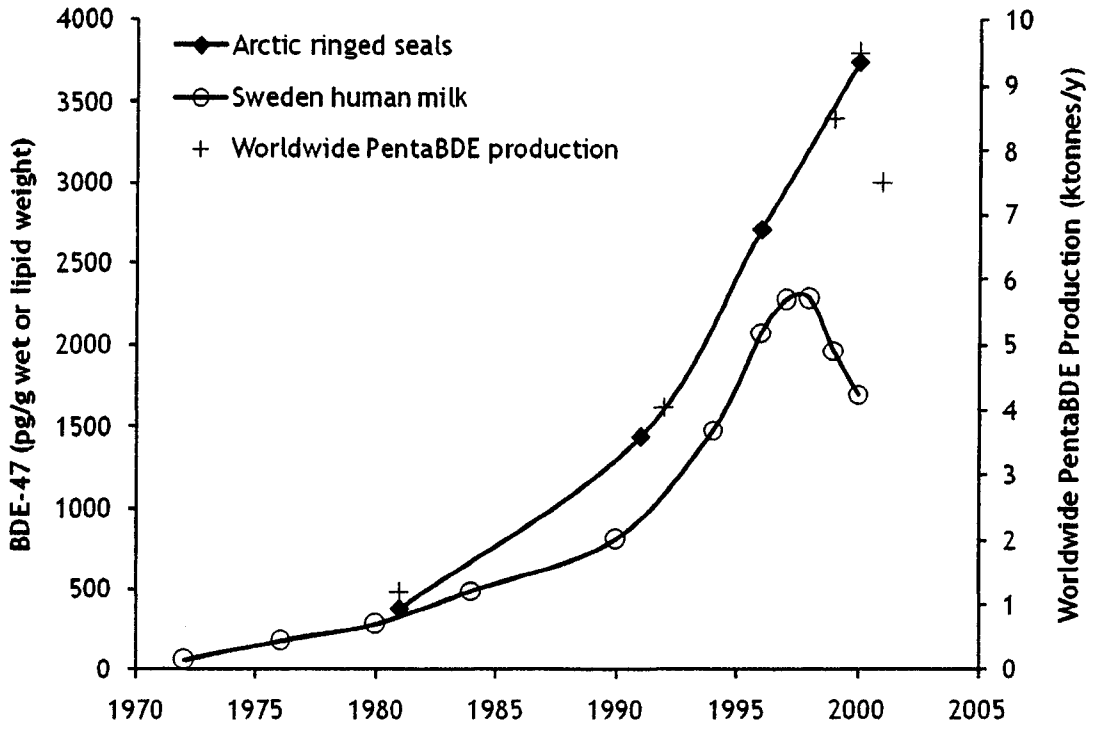

Figure 1.2 - Comparison of BDE-47 concentrations in ringed seals from the Canadian Arctic and mother's milk from Sweden against worldwide PentaBDE production [11, 28, 29, 33].

Concentrations of PBDEs found in Canadian mother's milk have been found to be magnitudes higher than that of Swedish mothers, indicating higher body burden in Canada. Furthermore, concentrations have not yet peaked and are still increasing at an alarming rate (seen in figure 1.3) [23, 28-30]. This is thought to be due to the continued use of PentaBDE in North America; where the only US manufacturer of PentaBDE and OctaBDE voluntarily ceased production in December 2004. The impacts of those actions have yet to be quantified [34].

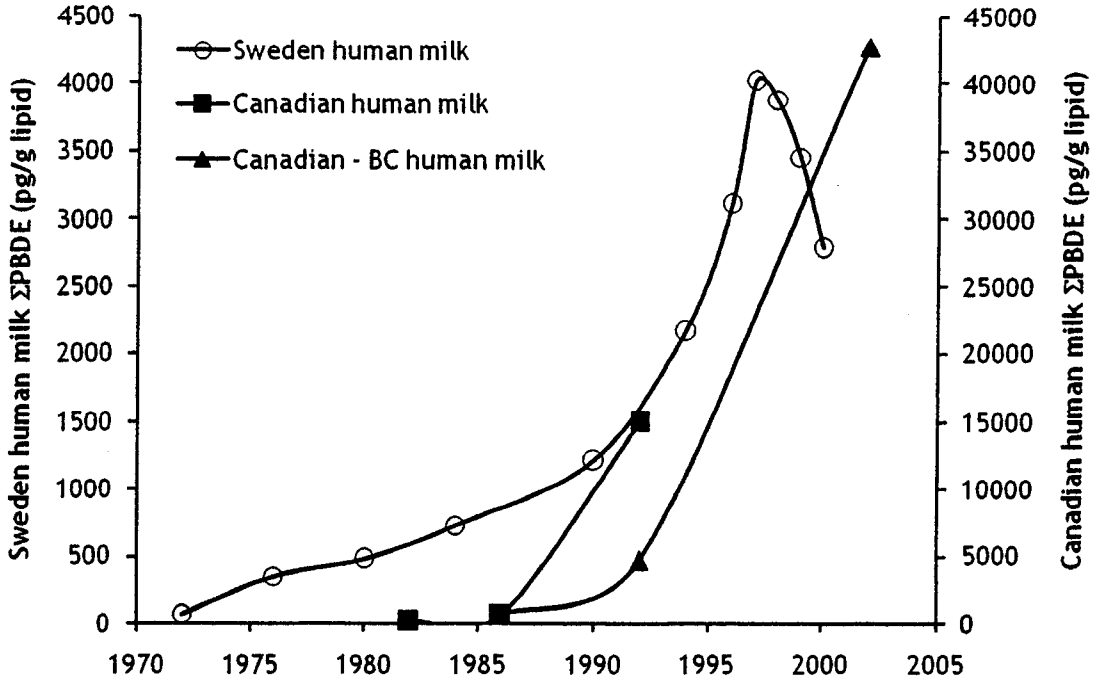

Figure 1.3 - Comparison of total PBDE concentrations of mother's milk from Sweden and Canada [28-30].

Furthermore, studies indicate that, in contrast to PBDEs, the body burden for many persistent organic pollutants is decreasing. A recent study compared concentrations of several classes of pollutants found in blood and blood serum in pooled blood samples from the United States from 1973 and 2003 [27]. Results showed that serum concentrations of highly toxic dioxins, furans and PCBs have decreased whereas those of PBDEs have increased, some of which are the highest reported in the world. Predominant congeners were BDE-47 and BDE-99. Current PBDE concentrations are lower than PCB concentrations encountered in 1973, however this may be changing as PBDEs, namely DecaBDE, are still being produced [27]. Furthermore, PBDE blood concentrations in North America have been estimated to be about 20 times higher than in Europe [22].

Lower molecular weight congeners are generally considered more toxic than higher molecular weight congeners, explaining recent regulations which did not include the DecaBDE formulation. Studies in mice and rats have shown that possible toxicological effects include endocrine disruption, developmental neurotoxicity as well as behavioural and cognitive effects. Studies have also shown that PBDEs alter thyroid hormone homeostasis and may impact brain development [23, 24, 27, 35]. However, there have always been questions about whether animal studies can be applied to human toxicology. Recently, a ground-breaking epidemiological study considering the impact of PBDEs on newborn baby boys was published [36]. It has long been suspected that children were more susceptible to endocrine disruption caused by PBDEs. This study found that PBDE concentrations in mother's breast milk were highest for newborns with cryptorchidism, a condition in which one or both testes fail to descend during fetal development. Cryptorchidism is the most common birth defect of male genitalia and incidence around the world is increasing [36]. This condition has been linked to reduced fertility, increased risk of testicular tumours, inguinal hernias and psychological problems [37].

Exposure routes to PBDEs are still under investigation and possibly include occupational exposure, diet, indoor and outdoor dust, volatilization and leaching from consumer's product, such as textiles and electronic devices [22, 23, 27, 38-45]. PBDEs have also been shown to leach from electronic refuse [26].

Estimated worldwide demands for PBDEs in 2001 are presented in table 1.3. In 2001 the largest consumer of PentaBDE was North America (close to 95%), whereas DecaBDE was used in highest amounts by both North America and Asia.

Table 1.3 - Estimated 2001 worldwide demand for PBDEs (in metric tonnes) [46].

	PentaBDE	OctaBDE	DecaBDE	Total
Americas	7100	1500	24500	33100
Europe	150	610	7600	8360
Asia	150	1500	23000	24650
Other	100	180	1050	1330
Total	7500	3790	56150	67440

It should be noted that PBDEs are not manufactured in Canada; all are imported either as chemical formulations (from the United States), substrates containing PBDEs (resins, polymers), semi-finished components or finished products (some are also exported as finished products). At the beginning of this century, approximately 1300 tonnes/year was used in Canada, most of which was imported from the United States as the following: PentaBDE > DecaBDE >> OctaBDE. However, this does not include amounts entering as finished products which are thought to account for the largest quantities of PBDEs in Canada. However, as PentaBDE and OctaBDE are no longer manufactured in the United States, their usage in Canada has substantially diminished [46].

A number of restrictions and regulations on the use and production of technical PBDE formulations have been implemented recently. In fact, PentaBDE and OctaBDE have been banned in Europe since August 2004 and some regulations were reinforced as early as 1996. In the United States manufacturing of both PentaBDE and OctaBDE voluntarily ceased at the end of 2004. Regulations however do not apply to DecaBDE [23]. In fact, DecaBDE is not currently regulated and continues to be used around the world [9]. Because of these various regulations it is hard to gain insight on the current world market for these flame retardants. However, it is foreseeable that the European and North American markets for PentaBDE and OctaBDE have diminished significantly.

1.2.3 PHYSICOCHEMICAL PROPERTIES

The following congeners were considered for this study: BDE-17, 28, 47, 66, 71, 85, 99, 100, 138, 153, 154, 183, 190, and 209. These congeners make up the three technical formulations discussed above and have been the focus of many studies due to their prevalence in the environment. Their structures are presented in figure 1.4.

PBDEs are persistent highly lipophilic compounds with low volatility and water solubility which is reflected in their relatively high log K_{OA} (octanol-air partition coefficient) and log K_{OW} (octanol-water partition coefficient) values. A comparison of PBDEs' log K_{OA} values with those of environmentally relevant contaminants is presented in figure 1.5. Shown in the figure are volatile organic compounds (VOCs), monoaromatic hydrocarbons (HCs), chlorobenzenes, PAHs, polychlorinated naphthalenes (PCNs), PCBs, dioxins (PCDDs), organochlorine (OC) pesticides, and PBDEs. Log K_{OA} values typically ranged from 9 (triBDEs) to 15 (DecaBDE), increasing with degree of bromination [47].

Tri-BDE

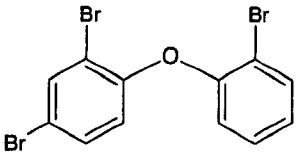

17

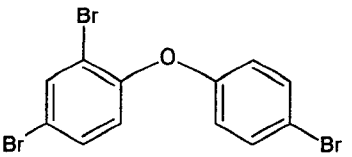

28

Tetra-BDE

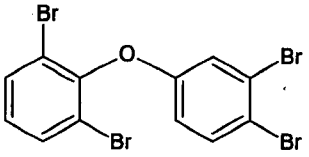

71

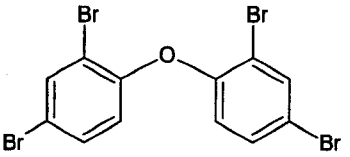

47

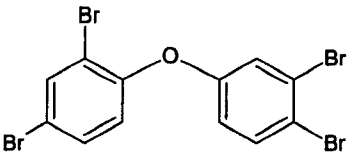

66

Penta-BDE

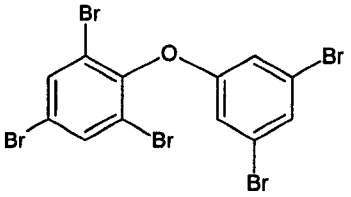

100

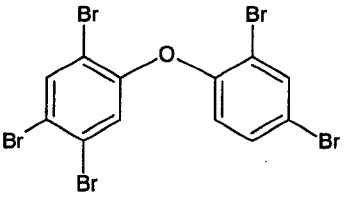

99

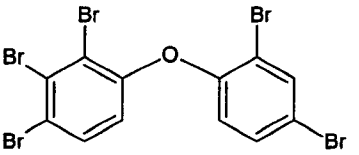

85

Hexa-BDE

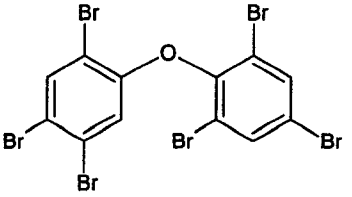

154

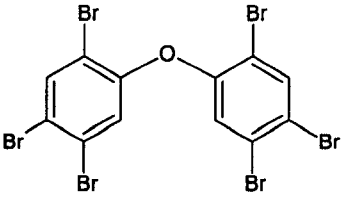

153

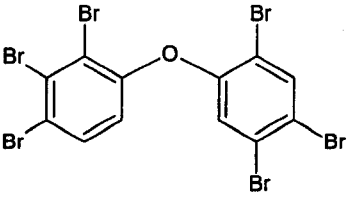

138

Hepta-BDE

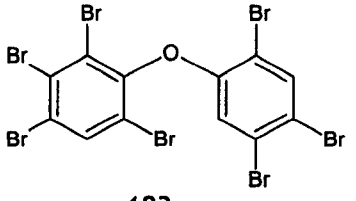

183

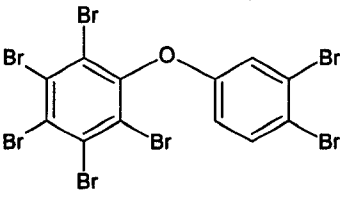

190

Deca-BDE

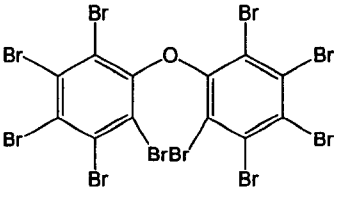

209

Figure 1.4 - PBDEs considered in this study.

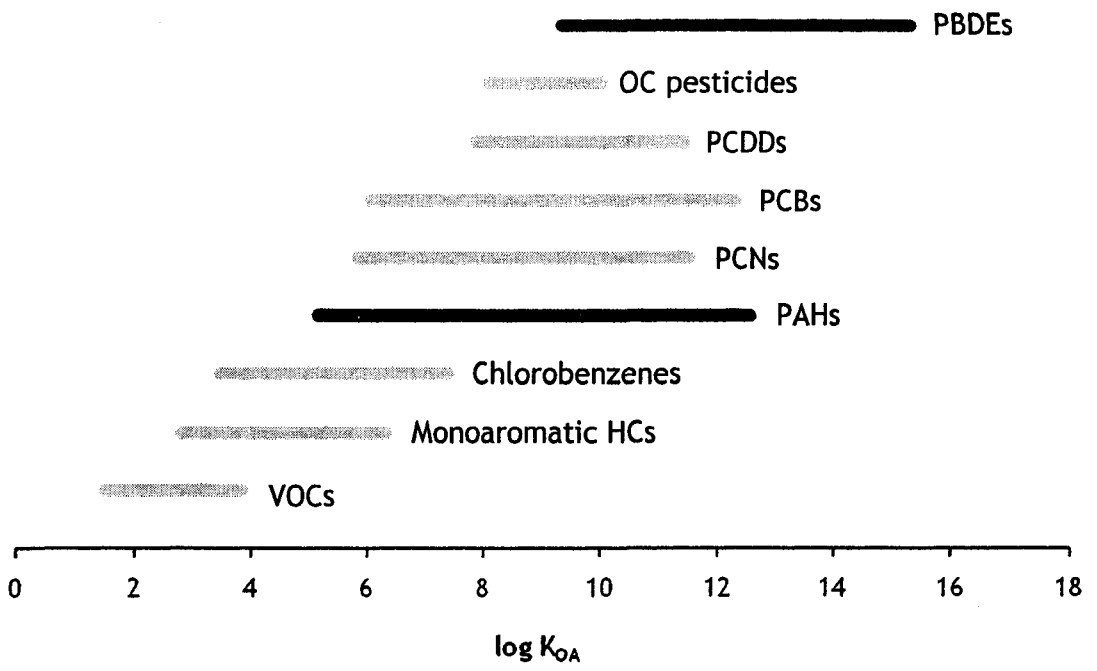

Figure 1.5 - Broad comparison of log K_{OA} for a range of organic pollutants.

Although measurements of log K_{OW} values have not been realized for all congeners, these typically range from 5.5 - 5.6 for triBDEs, 5.9 - 6.2 for tetraBDEs, 6.6 - 7.0 for pentaBDEs, 6.9 -7.9 for hexaBDEs, 8.4 - 8.9 for octaBDEs and 10 for decaBDE [24, 47]. Because of these physicochemical properties, PBDEs tend to accumulate in sediments and bind to particulates [24]. Furthermore, lower PBDE congeners (tetra to hexa congeners) are highly bioaccumulative and highest concentrations are usually present in animals higher in the foodweb [24, 46, 48]. A summary of their physicochemical properties is shown in table 1.4. It should be noted that the PBDE congeners are presented in chronological order of elution to facilitate physicochemical properties comparison and overall discussion. Also listed are BDE-77 and BDE-118 recovery surrogates used in this study.

Table 1.4 - Physicochemical properties of polybrominated diphenyl ethers [47]. Surrogate standards from this study are noted with an asterisk.

BDE	# Br	MM (g/mol)	Vapour pressure (Pa) supercooled liquid P_L	log K_{OA}	log K_{OW}
17	3	406.9	-	9.30	-
28	3	406.9	2.19×10^{-3}	9.41	5.80
71	4	485.8	-	-	-
47	4	485.8	1.86×10^{-4}	10.44	6.39
66	4	485.8	1.22×10^{-4}	10.82	-
77 *	4	485.8	6.79×10^{-4}	10.87	-
100	5	564.7	2.86×10^{-5}	11.13	-
99	5	564.7	1.76×10^{-5}	11.26	6.76
118 *	5	564.7	-	-	-
85	5	564.7	9.86×10^{-6}	11.66	-
154	6	643.6	3.80×10^{-6}	11.92	-
153	6	643.6	2.09×10^{-6}	11.89	7.08
138	6	643.6	1.58×10^{-6}	-	-
183	7	722.5	4.68×10^{-7}	11.96	7.14
190	7	722.5	2.82×10^{-7}	-	8.36
209	10	959.2	2.95×10^{-9}	15.27	9.97

1.3 Polycyclic aromatic hydrocarbons (PAHs)

1.3.1 Description, emissions and presence in the environment

Polycyclic aromatic hydrocarbons (PAHs) are organic compounds constructed of two or more fused aromatic rings. They have been the focus of many studies because of their environmental prevalence, persistence, and toxicity. In fact, the PAH benzo(a)pyrene holds the distinction of being the first identified carcinogen [49, 50].

They are found in petroleum and can be released in the environment due to the incomplete combustion of organic matter. As such they can be divided into petrogenic and pyrogenic origins and can be released from natural, combustion and anthropogenic (industrial) sources. Natural sources include forest fires and volcanoes whereas domestic heating, combustion of fossil fuels, transportation and waste incineration activities make up the list of combustion sources [7, 51, 52]. The formation of PAHs during the combustion of organic biomass has been reviewed recently [10]. Briefly, organic compounds are fragmented into free radicals, which react with each other to form a first aromatic ring, which is then further stabilized by the addition of subsequent rings [10]. Because PAHs can be emitted in the environment from naturally occurring processes they have always been found in the environment. However, the current widespread occurance of both natural and anthropogenic sources has increased concentrations in the environment to ubiquitous levels [7, 53].

PAH concentrations in the environment started increasing during the Industrial Revolution presumably due to an increase in energy consumption [7, 10]. Typically, PAH

concentration profiles in sediment started rising at the end of the 19th century, which corresponds to the beginning of the American Industrial Revolution, peaked in the 1950s and started declining in the 1960s when cleaner fuels such as oil and natural gas began replacing coal. As for the current trend, recent literature seems to disagree; some recent studies have shown that PAH concentrations in sediment have recently started increasing again whilst others report relatively constant PAH concentrations for 1980-2000 [10, 54-56]. Increased vehicle usage and diesel consumption are suspected to contribute increasingly to the overall environmental PAH burden [54, 55].

Canadian atmospheric emissions of PAHs have been estimated for 1990 at a little over 4300 tonnes and relative contributions are summarized in table 1.5. Forest fires were identified as the largest contributors, followed by industrial activities, particularly aluminium smelters [51].

However, most studies do not consider forest fires as a significant source to the overall PAH environmental burden, although numbers are seldom provided [53, 57]. This is shown in table 1.5, for American emissions where the contribution of forest fires is estimated at 7% compared to 47% for Canada. By considering only the industrial and combustion processes, emission sources in Canada are relatively similar to those in the United States, except for a few differences. For examples, domestic heating in Canada is estimated to contribute more to the overall PAH emissions than in the United States, the consequence of a colder climate. Also, transportation is potentially a bigger contributor in the United States than in Canada. It should be noted however, that it is generally difficult to compare these values directly as emission sources are often divided quite differently and can vary greatly from one location to another (i.e. urban versus rural locations). However domestic heating, transportation, and industrial activities are commonly listed as major PAH sources. Other miscellaneous sources reported include

accidental fuel spills and leakages, industrial wastewater, and the wood preservative creosote [51, 53, 57, 58].

Table 1.5 - Relative contributions of natural, combustion and anthropogenic sources to the overall atmospheric PAH burden [51, 58].

Sources	Contribution (without forest fires) (%)	
	1990 Canada	United States
Anthropogenic sources		
Aluminium smelters	21.0 (39.6)	40.6 (43.7)
Other	0.8 (1.5)	0.1 (0.1)
Combustion sources		
Domestic heating	11.7 (22.1)	16.1 (17.3)
Open air fires	8.3 (15.7)	5.8 (6.3)
Incineration	5.9 (11.1)	0.6 (0.6)
Transportation	4.7 (8.9)	25.2 (27.1)
Tobacco smoke	< 0.1 (< 0.1)	-
Other	0.6 (1.1)	4.6 (4.9)
Natural sources		
Forest fires	47.0	7.0

As mentioned previously, PAHs constitute of two or more aromatic rings. Although the structure possibilities are almost endless, PAH composition can vary considerably for different emission sources [7]. Petrogenic PAHs (generated from geochemical alterations of organic matter) usually include lower molecular weights PAHs such as acenaphthylene, whereas pyrogenic PAHs (formed from the incomplete combustion of organic matter) are generally composed of at least 4 aromatic rings [7].

PAHs are considered toxic and carcinogenic. The most potent carcinogens included the benzofluoranthenes, benzo(a)pyrene, benzo(a)anthracene, and indeno(123-cd)pyrene. They are metabolized by enzymes of cytochrome P-450 to form a wide variety of carcinogenic metabolites which can bind to and disrupt RNA and DNA [51, 59]. The toxicity of PAHs may be linked to their association with airborne particulate matter, especially particulates that are less than 5 μm in diameter as these can penetrate deeper into the respiratory system [21, 60].

Exposure to PAHs can occur through various routes including occupational exposure, diet, air, water, and tobacco smoke which is an important direct exposure route [51, 52, 60, 61]. PAHs typically found in tobacco smoke include benzofluoranthenes, benzo(a)pyrene, and indeno(123-cd)pyrene [51].

1.3.2 Physicochemical properties

The United States Environmental Protection Agency has regrouped 16 high priority PAHs according to their carcinogenicity potential [7]. Of this list, 12 were chosen to pursue this study: acenaphthylene, fluorene, phenanthrene, anthracene, pyrene, benzo(a)anthracene, chrysene, benzo(b)fluoranthene, benzo(k)fluoranthene, benzo(a)pyrene, indeno(123-cd)pyrene, and benzo(ghi)perylene, covering a wide range of physicochemical properties, emissions sources and prevalence in the environment. Their structures are presented in figure 1.6.

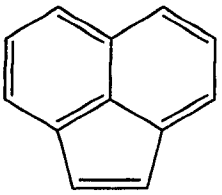

Acenaphthylene

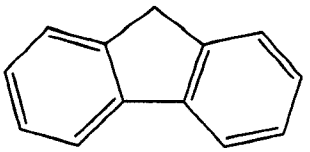

Fluorene

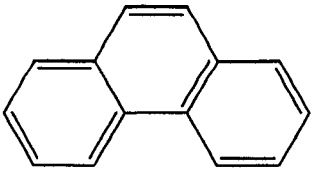

Phenanthrene

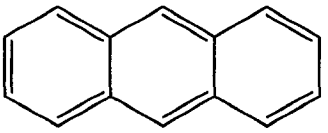

Anthracene

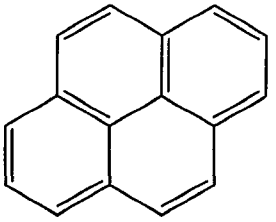

Pyrene

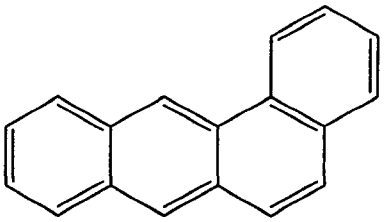

Benzo(a)anthracene

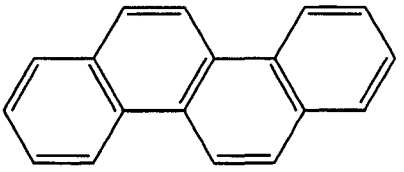

Chrysene

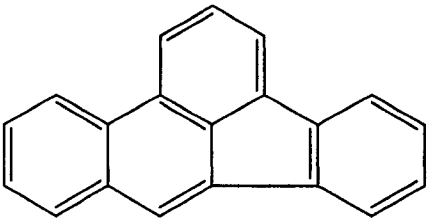

Benzo(b)fluoranthene

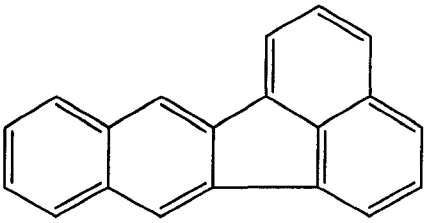

Benzo(k)fluoranthene

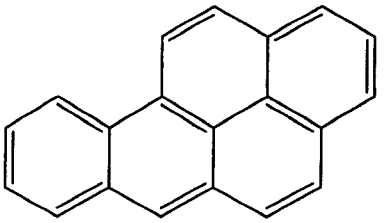

Benzo(a)pyrene

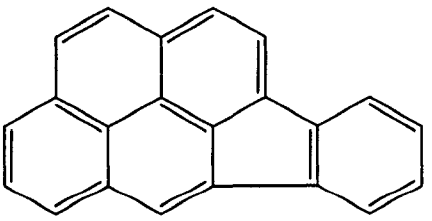

Indeno(123-cd)pyrene

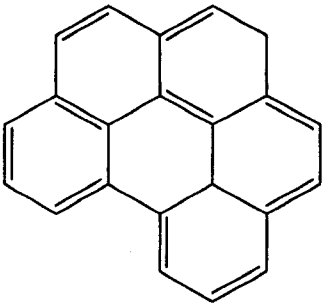

Benzo(ghi)perylene

Figure 1.6 - PAHs considered in this study.

Similarly to PBDEs, PAHs present a wide range of physicochemical properties. For example, naphthalene is considered slightly soluble in water, whereas the bigger PAHs, such as benzo(ghi)perylene, are extremely insoluble. Although vapour pressures are an order of magnitude higher than PBDEs these decrease dramatically with the number of aromatic rings. As demonstrated previously in figure 1.5, most PAHs have moderate log K_{OA} values typically ranging from 5 to 12.5 increasing with the number of aromatic rings [47]. The most volatile PAH considered in this study, acenaphthylene, has a log K_{OA} of 6.34. Like PBDEs, their log K_{OW} values indicate a high affinity for atmospheric or water borne suspended particulates, as well as possible accumulation in organisms [51]. A summary of the physicochemical properties of PAHs considered in this study is shown in table 1.6. As in the case of PBDEs, PAH congeners are presented in order of elution.

Table 1.6 - Physicochemical properties of polycyclic aromatic hydrocarbons [47].

PAH	# rings	MM (g/mol)	Vapour pressure (Pa) supercooled liquid P_L	log K_{OA}	log K_{OW}
AceN	3	152.2	2.01	6.34	-
Flu	3	166.2	7.29×10^{-1}	6.90	4.18
Phe	3	178.2	1.16×10^{-1}	7.68	4.46
Ant	3	178.2	5.65×10^{-2}	7.71	4.45
Pyr	4	202.3	1.52×10^{-2}	8.75	4.88
BaA	4	228.3	5.28×10^{-4}	10.29	5.91
Chr	4	228.3	5.90×10^{-5}		5.86
BbF	5	252.3	1.31×10^{-6}	11.36	5.78
BkF	5	252.3	4.21×10^{-6}		-
BaP	5	252.3	5.33×10^{-5}	11.56	6.35
IndP	6	276.3	2.30×10^{-7}	12.43	-
BghiP	6	276.3	1.85×10^{-6}	12.55	6.90

Chapter 2 - Environmental Fate of SVOCs

2.1 Environmental Fate Modeling

Although several approaches can be used to model the environmental fate of pollutants, fugacity-based models are widely used to understand both fate and distribution amongst environmental media [62, 63]. The following description is intended as a brief overview of the various concepts used in environmental modeling which are pertinent to this study. Additional details can be found elsewhere [62, 63].

The underlying frame of these models is fugacity; the tendency of a chemical to escape from its original phase or medium, which can be used to describe partitioning between phases or compartments [62]. Typically, a simple environment is generated and divided into four primary compartments: air, soil, water and sediment as shown in figure 2.1.

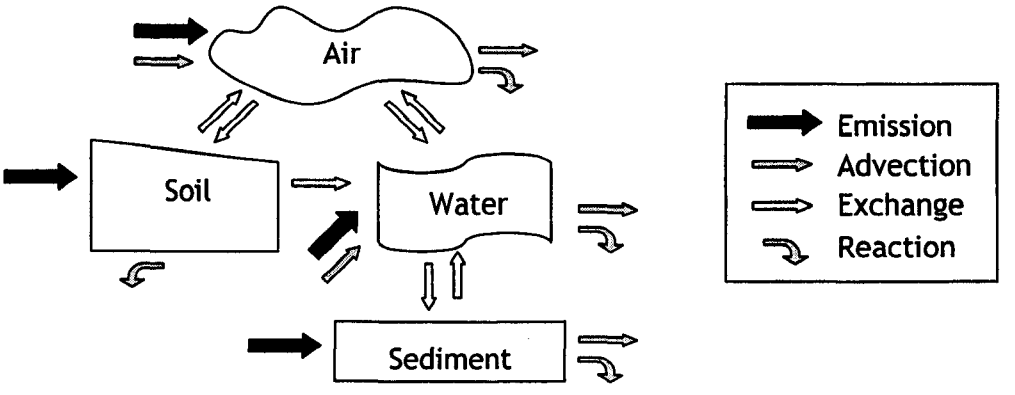

Figure 2.1 - Generic level III fugacity-based model.

When a chemical is released into the environment it is distributed among these four compartments. This distribution can be calculated and the exchange processes involved can be described according to various levels of complexity, ranging from level I to level III calculations. Both level I and II calculations assume that equilibrium is achieved between the four compartments named previously, which is unrealistically simplistic and may even be misleading [62]. Level III calculations on the other hand consider non-equilibrium partitioning between compartments, as well as advection and reaction losses, thus progressing towards a more environmentally realistic model. Also, compartments can be further sub-categorized into sub-compartments where the equilibrium condition is maintained; for example, the air compartment can be further divided into the gaseous phase and suspended particulates [62]. By considering non-equilibrium partitioning between compartments, each compartment is at a different fugacity and exchange between two compartments can be described as

$$N = D_{12}(f_1 - f_2) \tag{2.1}$$

where N is the transfer rate between compartments (mol/h), D is the transfer coefficient (mol/h Pa), and f is the fugacity of each compartment. Transfer coefficients are process specific and are related to mass transfer coefficients, transport velocities, and precipitation or deposition rates, just to name a few. At low concentrations, the fugacity of a chemical is directly proportional to its concentration as

$$C = f \times Z \tag{2.2}$$

where Z, the fugacity capacity (mol/m^3 Pa) depends on the temperature, the physicochemical properties of the chemical and the compartment [62].

2.2 POLYBROMINATED DIPHENYL ETHERS

As noted previously, PBDEs are ubiquitous contaminants found throughout the world in various matrices. They have been quantified in air [9, 13, 45, 64, 65], soil [9, 65], sediment [9, 14], vegetation [66, 67], biota [9, 11, 15], and human [22, 27, 29, 43, 68] and in locations as far away as the Arctic [11-15].

Atmospheric PBDEs have been quantified both in the gaseous phase and associated with particulates [13, 65, 69-71]. Because of their apparent affinity with organic matter which increases with log K_{OA} values, their association to particulates is relatively higher than most SVOCs; BDE-47 has been found predominantly in the gaseous phase, whereas the opposite has been observed for higher congeners, such as BDE-153 [71, 72]. This however depends on a number of environmental and meteorological factors. For example, PBDEs' log K_{OA} values decrease with temperature; consequently as temperature decreases, association to particulates increases [73]. Association with particulates can reduce overall mobility as particulates deposit onto available surfaces [74]. Lower congeners found mainly in the gaseous phase may be more available in the environment and may thus present a greater environmental risk [19]. Particulate-gas partitioning concepts are described in more detail in chapter 3.

Environmental congener profiles often reflect those of technical formulations [23, 34, 75, 76]. However, vapour pressures decrease according to the degree of bromination, and this can have consequences on the environmental fate and composition of PBDE congeners. For example, because of their prevalence in the PentaBDE technical formulation, and relatively high vapour pressures, BDE-47 and BDE-99 are often major congeners found in atmospheric samples. BDE-100 and BDE-153/154 are also both

constituents of the PentaBDE technical formulation, but because of its relatively higher vapour pressure, only BDE-100 is usually found in appreciable amounts in the gaseous phase [23, 24].

Environmental fate modeling is an invaluable tool when studying the environmental fate of contaminants, especially when field measurements are limited. PBDEs have been studied using level III fugacity-based modeling. These studies indicate that at steady-state, PBDEs should be found predominantly in soil and sediments with little partitioning to water and air, which is a direct consequence of their low water solubility and vapour pressures [19, 20, 34]. A typical environmental partitioning of BDE-47 is shown in figure 2.2.

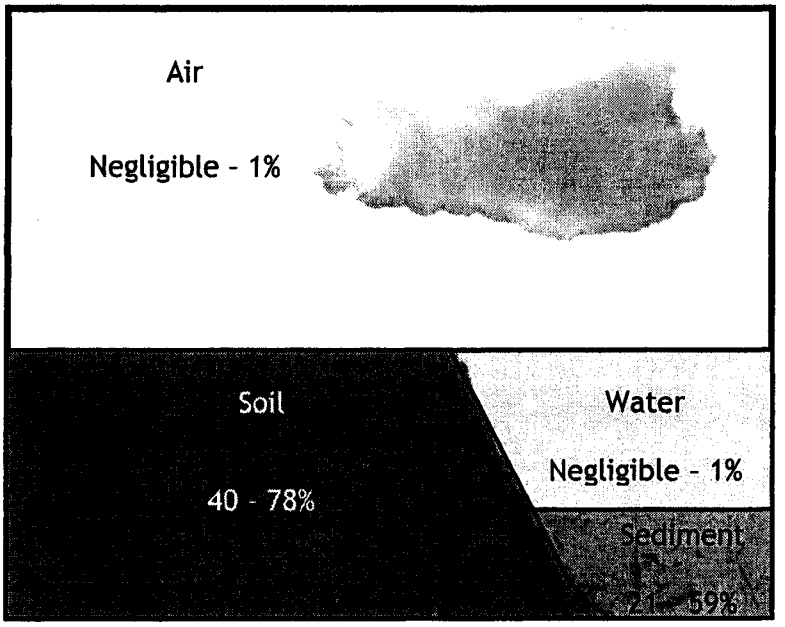

Figure 2.2 - Range of predicted partitioning of BDE-47 using a level III fugacity-based model.

PBDEs are generally considered extremely stable. However, relatively little is known about their degradation pathways and corresponding rates are only available for a selected few PBDE congeners. PBDEs are expected to be more reactive than PCBs due to their relatively weaker carbon-bromine bond and thus should be less persistent [23, 77]. Half-lives in air, water, and soil/sediments have been reported as more than 2 days, 2 months and 6 months respectively [23]. However these vary largely. For example, in the modeling study discussed above, the following half-lives were used for BDE-47: in air 100-300 hours (4 to 12 days), in water and in soil 10000-30000 hours (14 to 42 months), and in sediments more than 30000 hours (more than 42 months) [20]. Nevertheless, persistence is expected to increase with the degree of bromination [20, 77].

PBDEs may react very similarly in the environment as other halogenated SVOCs, undergoing oxidation by hydroxyl radicals in the atmosphere and aerobic degradation in other media such as soil, water, and sediments [77]. Several laboratory studies have considered the debromination of BDE-209 which has been shown to degrade to lower brominated congeners ranging from hexa to nonaBDEs in organic solvents under ultraviolet radiation [78]. Other studies have shown that lower congeners are more stable to photodecomposition than higher congeners. Other degradation products identified include polybrominated dibenzofurans. Although there is a clear indication that PBDEs undergo debromination and photodecomposition in laboratory settings, this has not yet been established in the environment [23, 24].

2.3 POLYCYCLIC AROMATIC HYDROCARBONS

PAHs are also considered ubiquitous contaminants. In contrast to PBDEs however, their environmental behaviour has been studied extensively for more than 30 years. They have been quantified in the atmosphere [7, 16, 79, 80], vegetation [81-83], soil [84], and sediment [7, 85]. Soil and sediment are considered their biggest sinks [51]. PAHs can be transported over long distances through the atmosphere and have been quantified in remote pristine ecosystems [7, 17, 79, 86].

PAHs are mostly released in the atmosphere where they are found both in the gaseous phase and associated to particulates. Some very volatile congeners, such as naphthalene, have been found exclusively in the gaseous phase; however most partition between both compartments. They can react with hydroxyl and peroxyl radicals as well as ozone, NO_X, and SO_X [10, 53, 57]. Reactions with NO_X are particularly important as these can be emitted simultaneously with PAHs and may lead to the formation of mutagenic nitro-PAHs [53, 57]. Photodecomposition is thought to be very important as many of these reactions are enhanced by sunlight [10]. Conversely, association with particulates seems to increase their stability [10, 53].

Also, PAHs bind to organic matter in soil and suspended particulates in water [51, 53, 57]. Soil PAH concentrations have been found higher near emission sources, such as highway roadsides and urban centers [80, 84, 87]. Microbial activity is responsible for their degradation in soil and in water where they are also subject to photolysis, hydrolysis, and sedimentation [10, 51]. PAHs have also been shown to accumulate in vegetation [51, 81, 82, 88].

The overall environmental fate and global distribution of PAHs is perhaps better understood than PBDEs as they have been studied extensively over several decades using extensive field measurements. However, just as in the previous case, the processes involved in surface-air exchange, particularly with vegetation, have not been well documented. Further research is thus needed to understand the role of vegetation in the overall environmental fate and global distribution of SVOCs.

2.4 The role of vegetation in the overall environmental fate of SVOCs

As mentioned previously, PBDEs and PAHs are ubiquitous pollutants found throughout the world including very remote pristine ecosystems, where industry and population are both scarce. Numerous studies have quantified both SVOCs in the Arctic wildlife, soil, sediment and atmospheric samples [11, 13-15, 89], providing empirical evidence for their long-range atmospheric transport [14]. Models however, have demonstrated that only the more volatile PBDEs (up to PentaBDEs) have a moderate LRAT potential, lower than that of PCBs, and almost negligible for higher congeners [18, 19]. It has been suggested that current modeling schemes do not effectively represent the overall environmental fate of these compounds and that other processes may be involved [20].

As noted previously, fugacity-based models typically consider four environmental media: air, soil, water and sediment. However, it is widely recognized that vegetation plays an important role in the overall environmental fate of PAHs and many SVOCs. In

fact, vegetation is commonly used as a passive air sampler for many SVOCs [82, 90-98]. Field measurements of atmospheric PBDEs have shown that concentrations decrease with the emergence of new foliage in the spring [99].

Following these observations, the role of vegetation in the environmental fate of BDE-47 was investigated by incorporating a vegetation compartment in an otherwise typical transport and persistence level III fugacity-based model [20]. Figure 2.3 presents the results for BDE-47 without and with vegetation as well as the various surface-air exchange processes. Firstly, in the absence of vegetation BDE-47 was found almost entirely distributed between the soil and sediment with 69 and 31% respectively; however this was greatly reduced to 41 and 19% upon the inclusion of vegetation which became an important compartment with nearly 40%. In both cases, the presence of BDE-47 in the atmospheric and water compartments was negligible. Also of interest are the surface-air exchange processes which are compared in the same figure. Without vegetation atmospheric BDE-47 partitions largely to soil and water with negligible revolatilization. Whereas this is also true for these compartments even in the presence of vegetation, the vegetation-air interface however shows an unprecedented exchange with the possibility of revolatilization. In fact, at the vegetation-air interface, the model predicted that as much as 50% of BDE-47 deposited could be subsequently revolatilized. These modeling results suggest that vegetation likely plays an important role in the overall environmental fate and global distribution of PBDEs by promoting surface-air exchange. BDE-47, and compounds with similar properties, could then migrate to remote locations through a series of hops; a phenomenon called the grasshopper effect [20, 100].

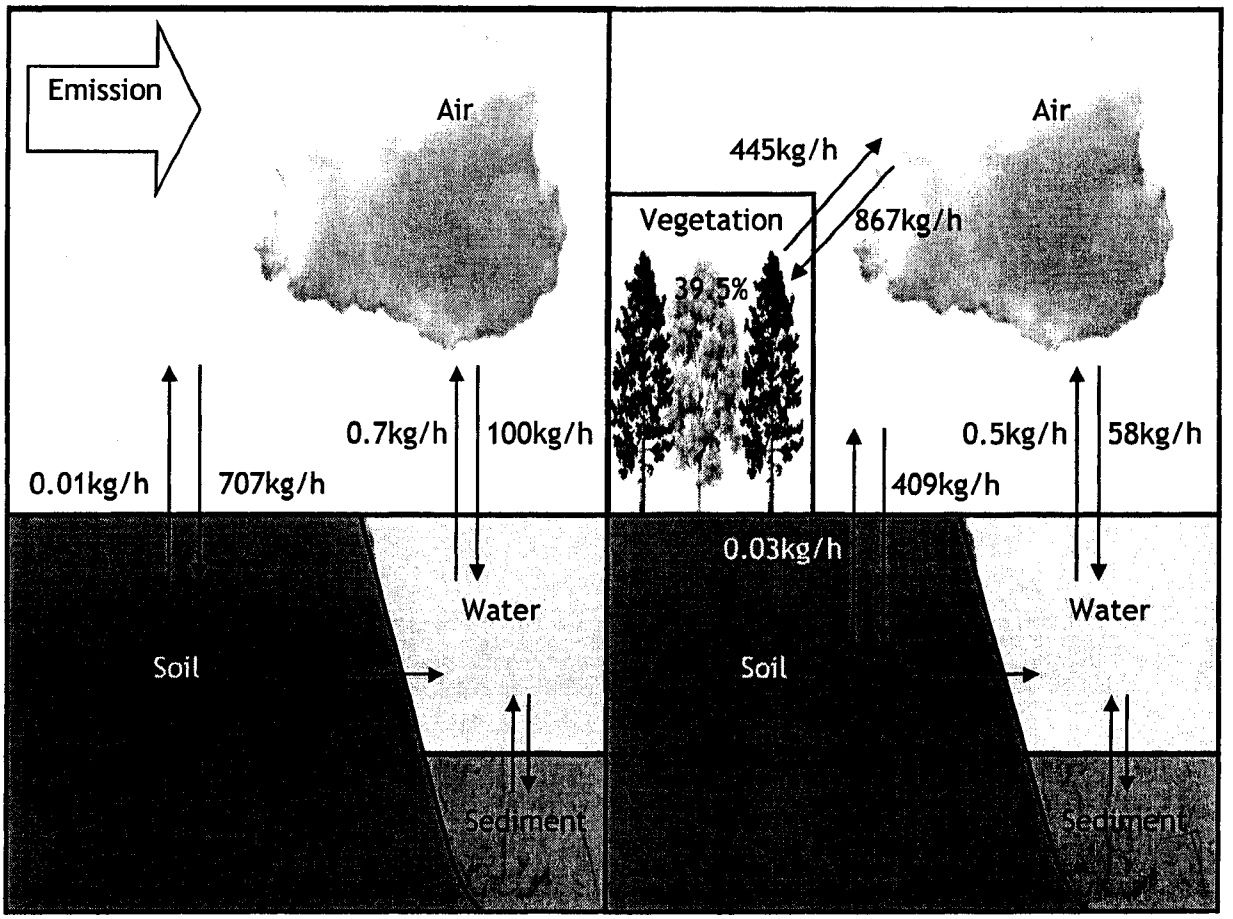

a) without vegetation b) with vegetation

Figure 2.3 - Distribution of BDE-47 in a steady-state environment a) without and b) with a vegetation compartment and comparison of surface-air exchange processes [20].

It should be noted however that the mass fraction of BDE-47 found in the vegetation compartment is highly dependent on its degradation half-lives in vegetation. Thus the mass fraction of BDE-47 in the vegetation compartment was found to vary from 2%, if the half-life in vegetation is equal to that in air, to 55%, if degradation is negligible [20].

Using another modeling approach described previously [98], the authors also showed that BDE-47 would be susceptible to the spring pulse effect, with atmospheric concentrations increasing in early spring as the result of snowmelt releasing accumulated PBDEs and thereafter decreasing following bud burst [20]. Field measurements realized previously, confirm the decrease in atmospheric PBDE concentrations with the emergence of new foliage [99].

Chapter 3 - SURFACE-AIR EXCHANGE OF SVOCS: CONCEPTS

3.1 VEGETATION-AIR EXCHANGE

3.1.1 MCLACHLAN INTERPRETATIVE FRAMEWORK

Although it is widely accepted that vegetation plays a role in the overall environmental fate of many SVOCs, the air-vegetation exchange processes are not fully understood. Vegetation can not only play an important role in the overall environmental fate of SVOCs, but can also act as an important vector in terrestrial food webs. Vegetation can clean the air by removing many SVOCs from the air [101]. In fact many coniferous species have been used as passive air samplers to monitor atmospheric pollution [82, 90-98]. It has been shown that accumulation of SVOCs in vegetation occurs primarily through the atmosphere [101]. The cuticular waxes found at the surface of conifer needles offer the first obstacle to atmospheric vegetation uptake of SVOCs. These soluble waxes are divided into the epi-cuticular wax, found at the surface of the needle, and the intra-cuticular wax, and consist of long chain alcohols, diols, free fatty acids, n-alkanes, n-alkenes, carboxylic esters, ketones, and other aliphatic and terpenoid elements. The composition of these waxes may change during the leaf development, due to ageing processes as well as light, temperature, and pollution [102, 103]. Beneath the wax, insoluble polymeric cutins form a backbone for the cuticle [103].

McLachlan and Horstmann described three mechanisms responsible for the accumulation of SVOCs by vegetation from the atmosphere: gaseous deposition, particulate-bound deposition and wet deposition [91, 104]. For highly hydrophobic SVOCs, such as PBDEs, wet deposition is assumed to be negligible [91]. The relative magnitude of the other two processes relates to gas-particulate partitioning, which in turn depends on the volatility of the compound studied. Relatively volatile compounds tend to partition from particulates to air, therefore preferably undergoing gaseous deposition to vegetation, whereas less volatile compounds have a tendency to deposit onto vegetation via particulates. An equilibrium can be reached between the air and the vegetation compartments; however, if the capacity of the plant for the SVOCs is large, the uptake will be kinetically limited and equilibrium will not be reached. Finally, particulate-bound deposition can be a dry or wet process, the latter likely being negligible for highly lipophilic SVOCs. To improve understanding of SVOC partitioning between air and vegetation, it is useful to determine which processes are active [101].

These processes will depend not only on the physico-chemical properties of the chemical studied, but also on the characteristics of the vegetation and particulates. Equilibrium partitioning will depend on temperature, gaseous concentration and the plant's storage capacity. Kinetically limited gaseous deposition is also a function of gaseous concentration, in addition to the age of the plant, wind speed, atmospheric stability, structure of the canopy, and roughness of the vegetation surface. Finally, particulate-bound deposition depends mainly on particulate-bound concentration and characteristics of particulates such as their size distribution and quantity [101].

It should also be noted that the McLachlan framework considers the plant as a single homogeneous compartment undergoing exchanges with the air. Assuming that the initial concentration of SVOCs in the plant is negligible and that uptake occurs at a

constant rate, with a constant gaseous concentration then gaseous uptake of SVOCs is described as

$$C_{VG} = K_{VG} C_G \left(1 - e^{\left[-\frac{A v_G t}{V K_{VG}} \right]} \right) \tag{3.1}$$

and

$$K_{VG} = m K_{oA}^{n} \tag{3.2}$$

where C_{VG} is the vegetation concentration due to gaseous deposition (mol/m^3), K_{VG} is the equilibrium constant between vegetation and gaseous phase, C_G is the gaseous concentration (mol/m^3), A is the surface area of the vegetation (m^2), v_G is the deposition velocity describing transport from the atmosphere to the plant surface (m/h), t is time (h), and V is the volume of vegetation (m^3). It should be noted that K_{VG}, the volume and surface area of the vegetation are also assumed to be constant [101].

Using similar assumptions as described above, particulate-bound uptake can be described as

$$C_{VP} = \left[\frac{v_P A C_P}{V k_E} \right] \left[1 - e^{(-k_E t)} \right] \tag{3.3}$$

and

$$C_P = B \times TSP \times K_{OA} C_G \tag{3.4}$$

where C_{VP} is the vegetation concentration due to particulate-bound uptake (mol/m^3), v_P is the particulate-bound deposition velocity (m/h), C_P is the particulate-bound concentration (mol/m^3), k_E is the first-order rate for erosion of particulates from the vegetation surface, B is a constant (m^3/μg), and TSP is the total atmospheric suspended particulates (μg/m^3) [101].

Using these equations, plots can be drawn to identify the dominant process involved in the atmospheric uptake of SVOCs: equilibrium partitioning, kinetically limited gaseous deposition and particulate-bound deposition. The first plot relates the vegetation and gaseous concentrations to the log K_{OA} values of the contaminants considered. As seen in figure 3.1, three distinct regions are obtained corresponding to each of the processes described above. SVOCs with log K_{OA} values up to 11 should undergo gaseous deposition possibly reaching an equilibrium (if their log K_{OA} is lower than 8.5), whereas if it is higher than 11, particulate-bound deposition dominates [101].

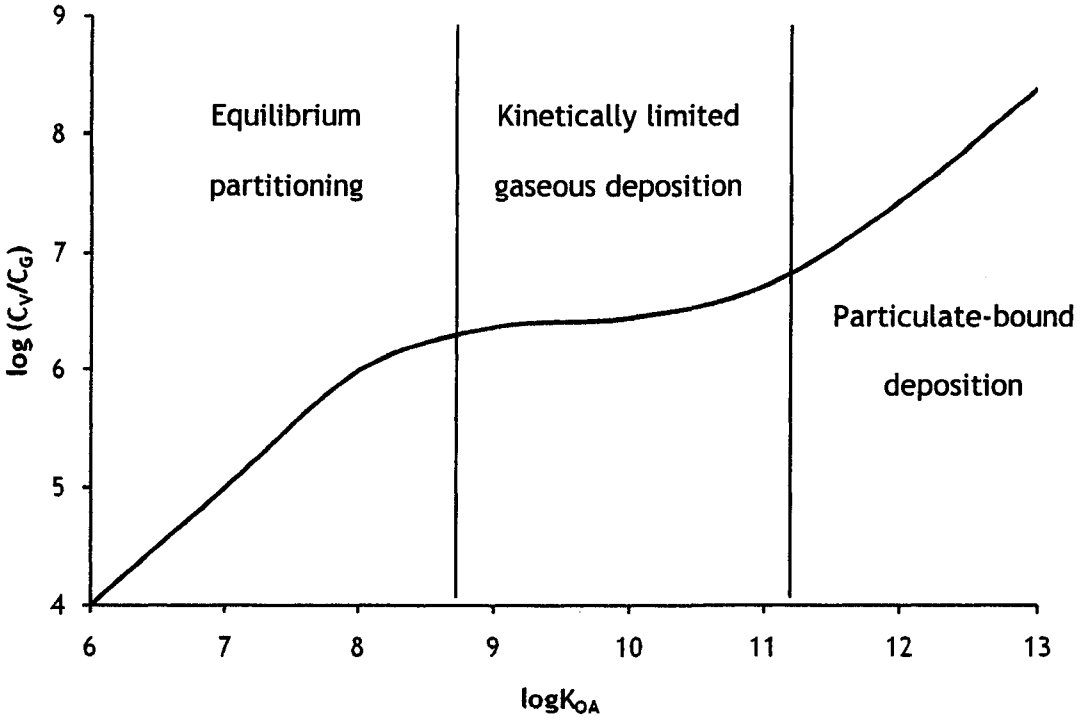

Figure 3.1 - Illustrative McLachlan plots describing processes involved in plant uptake of SVOCs.

Alternatively, a second plot can be used for higher log K_{OA} SVOCs if their quantification in gaseous phase is problematic. In this case, the logarithm of vegetation

concentration to particulate-bound concentration ($\log(C_V/C_P)$) is plotted against the logarithm of particulate-bound concentration to gaseous concentration ($\log(C_P/C_G)$) [101].

Although quite useful, this approach does have limitations. Particulate-bound, gaseous and vegetation concentrations are required. Also, several SVOCs covering a large range of log K_{OA} may need to be analyzed to observe the overall shape of the plot and identify active processes as defined by the theoretical plot. Furthermore, many assumptions are made during the development of this framework. For example, the particulate-bound and gaseous concentrations were assumed constant over time [101]. This may be an issue, especially in the case of SVOCs, such as the PAHs, that present a very noticeable seasonal emission pattern [53, 57].

3.1.2 Traditional methods for the determination of deposition velocity values

Deposition velocities are useful parameters that can be used in various modeling schemes and provide an indication of the potential flux of contaminants to a surface [97, 101].

Traditionally, deposition velocities are determined using deposition fluxes. Deposition fluxes are typically measured using surrogate surfaces such as greased Mylar [105-107], glass jars or filters [108], wet/dry deposition collectors [109, 110], and steel plates [111, 112]. Deposition velocities (v_D) are then calculated according to

$$v_D = Flux / C_{air} \tag{3.5}$$

where the flux ($ng/m^2 \cdot d$) is divided by the atmospheric concentration (ng/m^3) [105, 106, 110]. A summary of reported deposition velocities values for PBDEs and PAHs is presented in tables 3.1 and 3.2. Also added for comparison are results for PCBs.

As it can be seen, reported deposition velocities vary over several orders of magnitude; discrepancies have been attributed to differences in sampling techniques, periods and locations [105, 112]. The deposition process is also a function of the physical and chemical properties of particulates, meteorological conditions, and nature of the deposition surface [113]. Thus the utility of this approach to reflect a natural phenomenon may be limited by the ability of surrogate surfaces to represent the true characteristics of the environmental media [105, 106].

Table 3.1 - Particulate-bound deposition velocities reported in the literature for PBDEs and PAHs.

	v_D (m/h) particulate-bound	Deposition surface	Comments	References
PBDEs	28.8 (optimized)	Glass jars	Deciduous forest	[108]
PBDEs	14.4 - 400	Steel funnels	Incineration plant	[110]
PBDEs	43.2 - 1760	Steel funnels	Urban site	[110]
PAHs	1.4 - 2.2	Glass jars	Coniferous canopy	[104]
PAHs	21.6 - 31.7	Glass jars	Deciduous forest	[104]
PAHs	39.6 - 281	Greased Mylar	Urban site	[105]
PAHs	3.6 - 5.0	Glass jars	Deciduous forest	[108]
PAHs	3.6 - 43.2	Steel	Urban site	[112]

Table 3.2 - Gaseous deposition velocities reported in the literature for PBDEs, PAHs, and PCBs.

	v_D (m/h) gaseous	Deposition surface	Comments	References
PBDEs	61.2 - 108	Glass jars	Deciduous forest	[108]
PAHs	1.3 - 9.0	Glass jars	Coniferous canopy	[104]
PAHs	13.3 - 126	Glass jars	Deciduous forest	[104]
PCBs	0.9 - 50.4	Glass jars	Coniferous canopy	[104]
PCBs	7.6 - 191	Glass jars	Deciduous forest	[104]
PCBs	97.2 ± 18.7	Glass jars	Deciduous forest	[108]

3.2 PARTICULATE-GAS PARTITIONING

As mentioned previously, atmospheric transport is an important pathway in the global distribution of many SVOCs from local point sources, such as cities and industries to remote pristine ecosystems. Many SVOCs, such as PAHs and PBDEs, bind appreciably onto atmospheric particulates which may limit their overall mobility as particulates tend to deposit readily onto available surfaces. In that context, the octanol-air distribution coefficient can also be used to describe particulate-gas partitioning [114].

The particulate-gas partitioning coefficient K_P and the fraction of SVOC associated to particulates ϕ are defined as

$$K_P = {C_P}/{TSP \times C_G} \tag{3.6}$$

$$\phi = {C_P}/{(C_P + C_G)} = {K_P \times TSP}/{(K_P \times TSP + 1)} \tag{3.7}$$

where C_P and C_G are defined as above as the particulate-bound and gaseous concentrations respectively (pg/m^3) and TSP is the total suspended particulate concentration ($\mu g/m^3$).

Conventionally the Junge-Pankow model [115, 116] is used to estimate the fraction of particulate-bound SVOCs

$$\phi = c\theta / \left(p_L^o + c\theta\right) \tag{3.8}$$

where c is a parameter based on the enthalpy of desorption from the particulate surface, the enthalpy of vaporization as well as the number of adsorption sites on the particulate (Pa cm), θ is the particulate surface area per volume of air (cm^2/cm^3), and p_L° is the subcooled liquid vapour pressure of the pure compound (Pa). Typical values are available for c and θ [116, 117].

The Pankow absorption model relating association of SVOCs to particulates to the surface organic matter was subsequently developed [118] and K_P evolved to

$$K_P = 10^{-6} RTf_{om} / M_{om}\gamma_{om}p_L^o \tag{3.9}$$

where R is the gas constant (8.314 m^3 Pa/K mol), T is the temperature (K), f_{om} is the organic matter fraction of the particulate, M_{om} its molecular weight (g/mol), and γ_{om} the activity coefficient of the chemical in the organic layer.

Furthermore, K_P can be linked to K_{OA} [119].

$$K_P = 10^{-9} K_{OA} f_{om} \left(\gamma_{oct}/\gamma_{om}\right)\left(M_{oct}/M_{om}\right)/\rho_{oct} \tag{3.10}$$

Assuming that the ratios of activity coefficients of the chemical in octanol and organic matter is 1 (γ_{oct}/γ_{om} = 1), that the same is true for the ratio of their molecular

weights (M_{oct}/M_{om} = 1), and that the density of octanol is 820 kg/m^3 (at 20°C), then this equation rearranges to

$$\log K_P = \log K_{OA} + \log f_{om} - 11.91 \qquad (3.11)$$

which is defined as the K_{OA} absorption model. This equation along with those described previously can be used to predict association to particulates as a function of the log K_{OA} [114, 119].

Both absorption models can thus be used to predict and compare theoretical association to particulates to experimental values. Studies seem to indicate however, that the Pankow absorption model can sometimes overpredict sorption of SVOCs onto particulates [114, 120]. Furthermore, in order to use the K_{OA} absorption model only the f_{om} and log K_{OA} values are needed [74, 114].

The following figure compares predictions of the two absorption models presented above. These curves were calculated using typical values for c of 17.2 Pa cm and θ of 1.1 × 10^{-5} cm^2/cm^3 for the Junge-Pankow absorption model and typical values of f_{om} and TSP of 0.2 and 25 µg/m^3 respectively for the K_{OA} absorption model. The Junge-Pankow and K_{OA} absorption models predict increased association with particulates with decreasing vapour pressure and increasing log K_{OA} respectively [114, 118, 119].

Both models can thus bring forth insight as to the particulate-gas partitioning of SVOCs. Combining the log K_{OA} absorption model observations with figure 1.5 illustrates that very volatile organic pollutants such as the chlorobenzenes and hydrocarbons are expected to be found predominantly in the gaseous phase (less than 5% associated to particulates), whereas PCBs and PAHs will also be subject to partitioning. PBDEs, having

higher log K_{OA} values, should either be found in both compartments or exclusively associated to particulates (more than 95% associated to particulates).

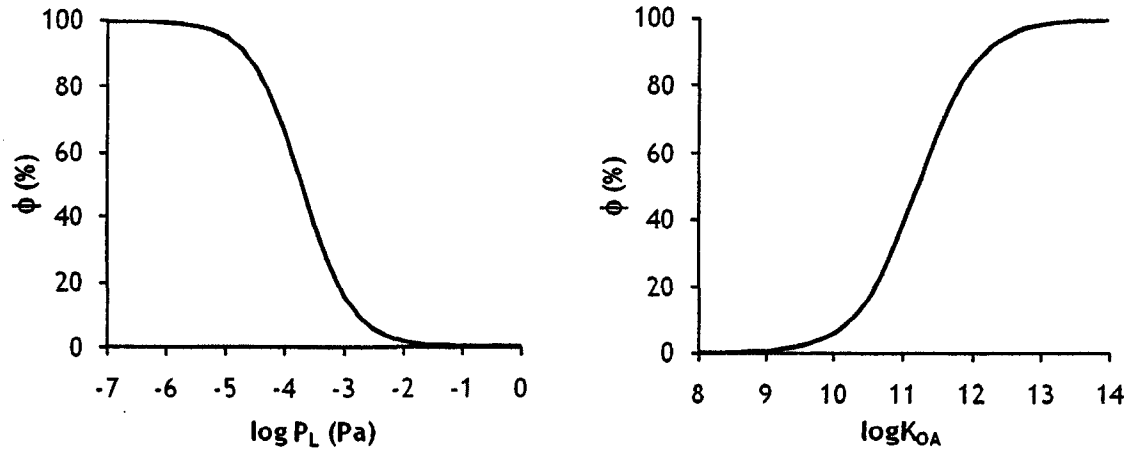

Figure 3.2 - Comparison of Junge-Pankow and K_{OA} absorption models predictions.

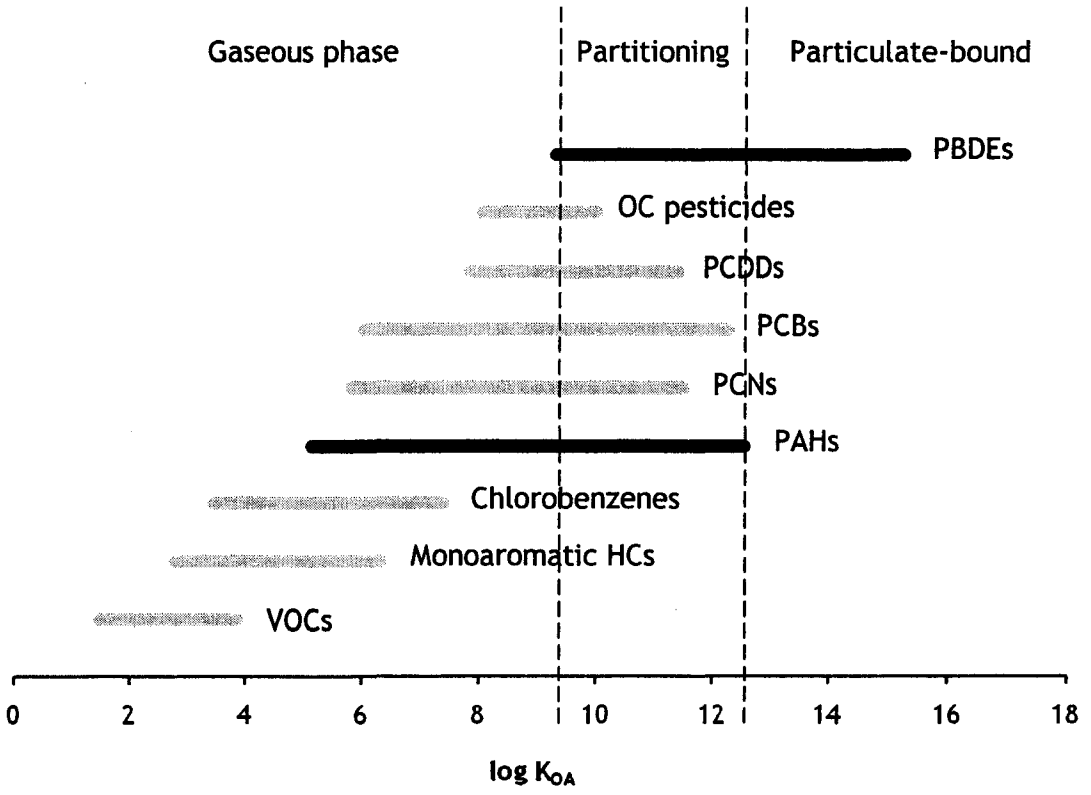

Figure 3.3 - Identification of predicted prevalent particulate-gas partitioning processes for a range of organic pollutants.

Knowledge of the particulate-gas partitioning process is valuable when considering the overall environmental fate and global distribution of a pollutant. Compounds found in the gaseous phase should be able to transport over longer distances than those associated to particulates which are more prone to deposit onto available surfaces, thus reducing overall mobility and transport potential [74].

3.3 Objectives

The overall purpose of this study was to model the transfer of SVOCs from air to vegetation and consider active air-vegetation exchange processes. It is widely acknowledged that vegetation plays a role in the overall environmental fate of SVOCs; this has been shown for a number of SVOCs and more recently for PBDEs, in this case using a modeling approach [20]. However, the processes involved are not completely understood. Furthermore, in the case of PBDEs the scarcity of field measurements in vegetation (tree bark and archived herbage) [66, 67] renders the verification of these models challenging. Thus the following objectives have been identified:

- Evaluate PBDE and PAH concentrations in vegetation and air close to a point source.

  Atmospheric and vegetation concentrations were monitored over an annual cycle (February 2004 to June 2005) on a bi-weekly basis to study possible seasonal and meteorological effects. The atmospheric concentrations were evaluated both as the gaseous phase and particulate-bound. Norway spruce (*Picea abies*) needles

were chosen for the vegetation compartments because of their year-round availability and of their proven efficiency as passive air samplers for a wide variety of SVOCs [81, 82, 90-98].

- Develop an efficient method for the extraction of PBDEs from spruce needles.

  Although methods were available in the literature for the extraction of PBDEs from atmospheric samples and other environmental matrices [121-124], none were found for their extraction from vegetation. A method using accelerated solvent extraction (ASE) offering good recoveries was developed.

- Construct a modeling scheme for the accumulation of PBDEs and PAHs by vegetation.

  The frameworks designed by McLachlan [101] and Horstmann and McLachlan [104], were considered to study air-vegetation exchange. An interpretative scheme was developed to determine particulate-bound and gaseous deposition velocities using field measurements and both processes were examined.

Chapter 4 - EXPERIMENTAL PROCEDURE

4.1 SAMPLING

4.1.1 SAMPLING SITE DESCRIPTION

Samples were collected at the Trail Waste Facility (situated at 45°13'N, 75°46'W), a municipal sanitary landfill for the city of Ottawa, ON, Canada. This landfill is divided into two major areas: general waste and compost. Hazardous waste, tires and appliances are also collected and eventually sent elsewhere. It is located approximately 30 km southwest from the city centre close to a major highway in a mostly residential agricultural area with little industrial activity. During the study period, wind direction was predominantly from the west with an average wind speed of 3.62 m/s. Temperatures ranged from -30.7°C (January 15, 2004) to 32.4°C (July 11, 2005) with lowest temperatures generally encountered in January and highest temperatures in July. Maximum precipitation for a 24h-period was 135.4 mm on September 9, 2004 which was due to a tropical storm remnant. Maximum snow fall for a 24h-period was recorded on March 7, 2005 (15.4 cm) which contributed to a 40 cm maximum snow cover observed between March 8 and 10, 2005. Average wind directions as well as daily average temperatures and precipitation accumulation for the duration of the study (February 2004 to June 2005) are presented in figures 4.1 and 4.2 respectively. Weather data was collected at the Ottawa International Airport (World Meteorological Organization ID # 71628) situated approximately 15 km from the sampling site.

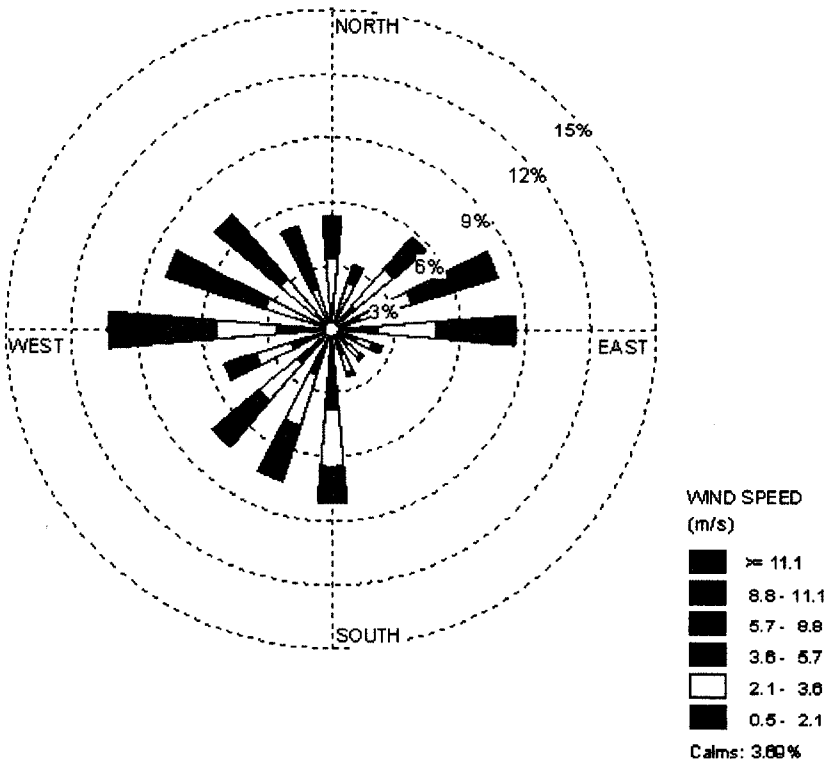

Figure 4.1 - Average wind rose plot for Ottawa during the sampling period.

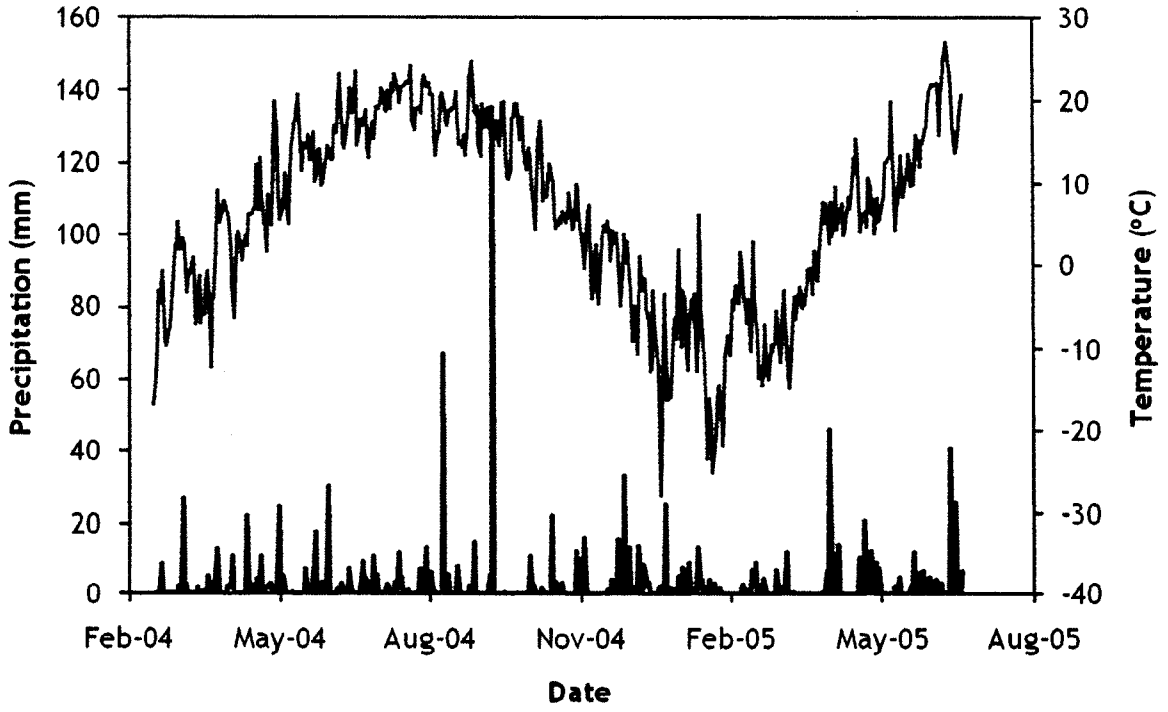

Figure 4.2 - Temperature and precipitation recorded in Ottawa during sampling period.

4.1.2 SAMPLING TECHNIQUES

Atmospheric (particulate-bound and gaseous) and spruce needle samples were collected from February 2004 to June 2005 every two weeks. The 2003 and 2004 growth years of Norway Spruce (*Picea abies*) (between 4 and 6 feet height) were collected from February 2004 to June 2004 and June 2004 to June 2005 respectively. Solvent cleaned pliers which were stored in solvent cleaned aluminium foil were used.

Air samples were collected using a modified high-volume air sampler which was calibrated prior to use by a standard calibration procedure. The flow (m^3/min) through the apparatus was calibrated against magnehilic readings (inches of H_2O) (Dwyer Model 2100). These were measured at the beginning and at the end of each sampling session, averaged and translated to m^3/min to obtain sample volume.

The air sampler was run for approximately 20 hours for an average sample volume size of 750 m^3. Particulates were retained on a glass membrane filter (GMF) of 0.7 μm pore diameter and gaseous species were collected with polyurethane foam (PUF; diameter 6 cm × 7.6 cm length) which was cut in half to assess possible breakthrough. GMFs were kept in solvent cleaned aluminium foil. PUFs were put back in their original solvent cleaned glass jar covered with aluminium foil to limit light exposure as higher PBDE congeners, particularly BDE-209, are suspected to be light sensitive [122]. All samples were kept at -80 °C and thawed at room temperature prior to extraction.

Air sampling observations and weather conditions during each sampling session (including local wind rose plots) along with details of the air sampler calibration procedure can be found in the appendices.

4.2 AIR SAMPLES PREPARATION AND EXTRACTION

4.2.1 SOLID-LIQUID EXTRACTION (SOXHLET)

Air samples were extracted separately following a similar soxhlet procedure as those found in literature [95, 125]. Prior to extraction all samples were spiked with BDE-77 and BDE-118 surrogates for recovery assessment [70, 122]. The structures of these PBDE congeners are presented in figure 4.3.

The GMFs and the two PUF halves were extracted separately with a soxhlet apparatus for 18 hours with 250 mL of hexane. As mentioned previously, PUF were cut in half to assess possible breakthrough. Extracts collected were then concentrated to a few mL using a rotary evaporator, transferred and further concentrated to approximately 200 µL under a nitrogen stream. Finally, these were transferred to GC vials for a final extract volume of 500 µL and octachloronaphthalene (OCN) for PBDE analysis and chrysene-d12 for PAH analysis internal standards were added at 2.5 pg/µL and 1 ng/µL respectively. It should be noted that during the extraction procedures the samples were protected from light to ensure minimal photodegradation.

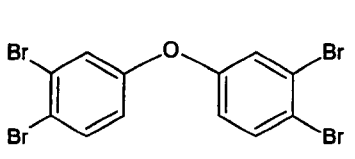

77

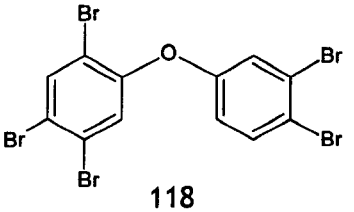

118

Figure 4.3 - Surrogate standards used in this study.

4.3 SPRUCE NEEDLES PREPARATION AND EXTRACTION

4.3.1 SOLID-LIQUID EXTRACTION (ASE) METHOD DEVELOPMENT

In order to meet the overall objectives of this study, method development for the extraction of PBDEs from spruce needles was required. Accelerated solvent extraction was considered as this technique is not only time efficient, it often gives similar or better recoveries than traditional methods and uses less solvent [121-123, 126-128]. Furthermore, this technique has been shown to be efficient in the extraction of many SVOCs from pine needles [127, 128]. A schematic of the instrument is presented in figure 4.4. The sample is put in stainless steel extraction cells generally along with Hydromatrix. The cell is brought in the module where it is filled with solvent, pressurized, and heated when it undergoes a static extraction cycle. The extract is then collected and the extraction cell is rinsed and purged with nitrogen. A few steps can thus be optimized in this procedure: solvent, pressure, temperature, static extraction length, and purge step [121-123, 126-128].

A Dionex ASE-200 accelerated solvent extraction module was used for this study. Method development was inspired by methods previously reported in the literature for the extraction of PCBs from vegetation and PBDEs from solid matrices [121-123, 126-128]. A mixture of 1:1 dichloromethane:hexane was chosen as this solvent mixture has been used previously for PCBs in vegetation and PBDEs from sediment [123, 128]. Pressure was set at 1500 psi and extraction cells were completely purged for 120 s both having been used in PBDE accelerated extraction methods [123]. Attention thus focused on temperature and duration and number of static cycles. Temperatures of 100 - 140°C

were considered. A temperature of 100°C is commonly used in published methods [121, 123]. However, more complex matrices such as waxy needles may need a higher temperature. In fact, temperature not only increases the solubility of the analytes in the extraction solvent, it also disrupts the matrix-analyte interactions [121, 126, 127]. For example, recoveries of PAHs, hexachlorohexane isomers, chlorobenzenes, and DDT/DDE/DDD from mosses were shown to increase significantly from 100 to 120°C [127]. Static cycles ranging from a single 5 minutes to three 10 minutes have been reported [121, 123, 127].

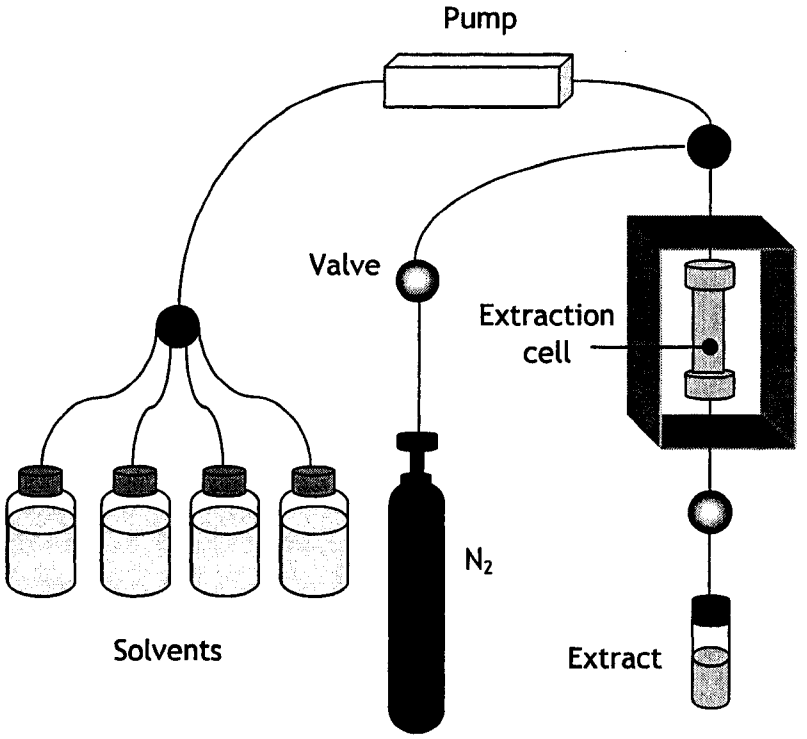

Figure 4.4 - Schematic of an accelerated solvent extraction module.

As a first approach, a low concentration PBDE standard (3.125 pg/µL) was used to assess recoveries. Recovery results for three ASE methods are presented in figure 4.5. Method A consisted of a single static cycle of 5 minutes at 100°C, whereas methods B and

C consisted of two static cycles of 10 minutes at 100°C and 140°C respectively. Recoveries were generally good for all congeners, increasing for methods B and C, but were more precise for the last method. The standard error of the mean was used to draw error bars (n = 3).

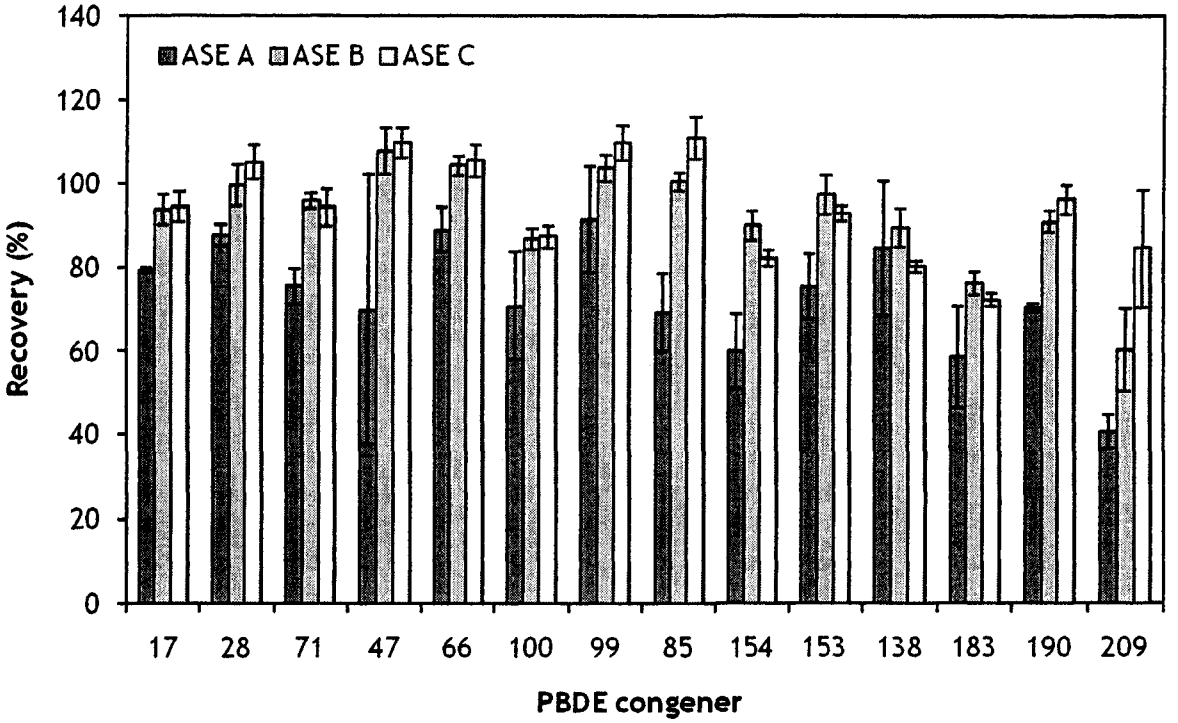

Figure 4.5 - Average recoveries for three ASE test methods.

Efficiency of methods A and C was also assessed using replicate spruce needle samples and results are presented in table 4.1. Although both methods offered good recoveries for spiked blanks, method C extracted a higher quantity of PBDEs from spruce needles both on a fresh weight basis and lipid corrected. This method also completely stripped the wax off the spruce needles surfaces. Method C was thus deemed more efficient and was chosen for the remainder of the study.

Table 4.1 - Efficiency of ASE methods (spruce needle replicates).

ΣPBDE	Method A	Method C
Fresh weight (pg/g)	266	660
Lipid (ng/g)	40.9	59.9

It should be noted that although the ASE conditions were primarily optimized for the extraction of PBDEs from spruce needles, similar ASE conditions for the extraction of PAHs from solid matrices, have been reported [121, 127].

4.3.2 Clean-up method development

In order to remove the wax matrix and green pigments, several adsorbents previously used in clean-up methods for the analysis of PBDE from solid matrices were considered: activated and deactivated florisil, activated and deactivated silica, alumina, and aminopropyl SPE cartridges [122, 123, 129]. Adsorbents were activated by heating at 450°C prior to use for at least 12 hours. Recoveries were calculated using a low concentration PBDE standard (1 pg/μL). Alumina was quickly discarded as this adsorbent presented negligible recoveries for most PBDE congeners and aminopropyl cartridges failed to remove green pigments. Although both combinations of the activated and deactivated silica with florisil columns showed good recoveries for the tri and tetraBDE congeners, poor recoveries were obtained for higher brominated congeners (figure 4.6). Furthermore, it has been demonstrated that the use of florisil can result in the complete loss of BDE-209 [123]. Thus the use of florisil was discontinued.

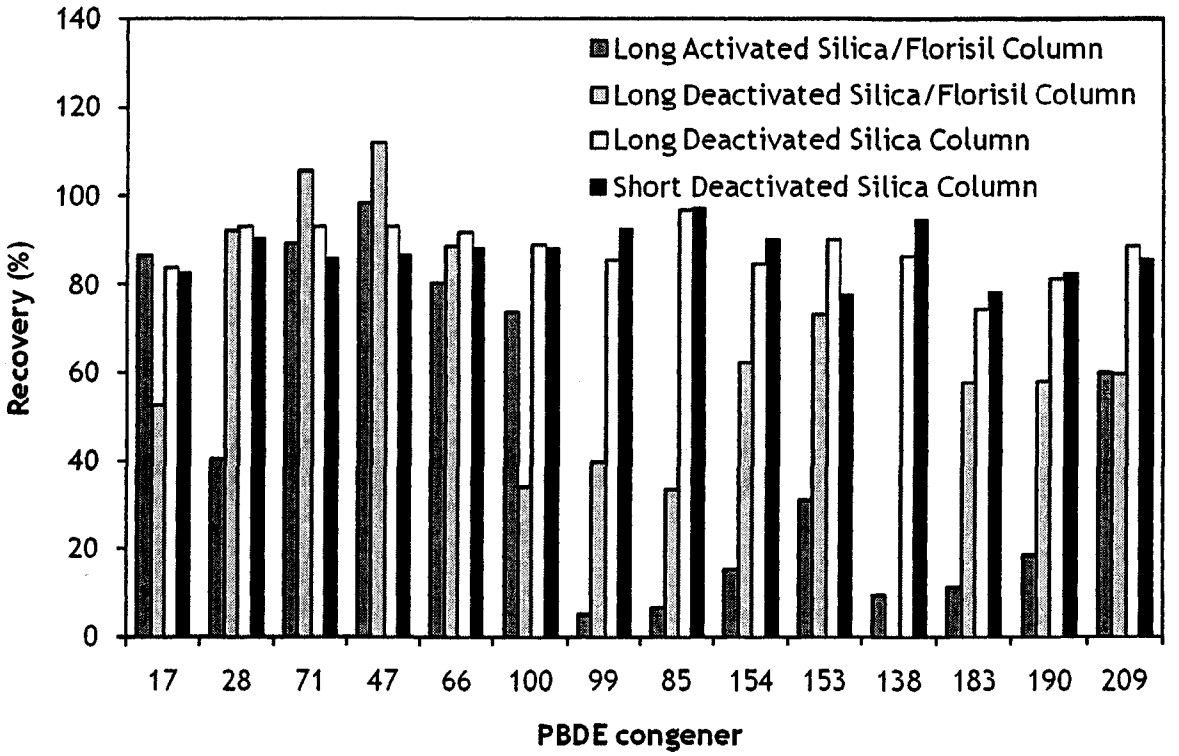

Figure 4.6 - Efficiency of clean-up methods.

Long and short deactivated silica columns showed comparable recoveries with adequate removal of pigments and lipid residue. Since the shorter column using less adsorbent and solvent (25 mL of hexane compared to 100 mL for elution of longer columns) gave similar recoveries it was chosen for the remainder of the study.

4.3.3 Optimized extraction and clean-up method

Spruce needles were thawed at room temperature and needles were cut using solvent cleaned scissors holding the stem. Approximately 8 g of needles were weighed

(defined as the fresh weight), dried in a covered dessicator at room temperature for approximately 36 hours and re-weighed (defined as the dry weight) and moisture content was determined. Initially, several drying periods were considered where samples were put in the dessicator and weighed every 12 hours. After 36 hours, relatively constant weight measurements were achieved.

As mentioned previously, spruce needle samples were also spiked with surrogate standards BDE-77 and BDE-118 prior to extraction. An accelerated solvent extractor (Dionex ASE-200) was used to extract PBDEs from spruce needles at the following working parameters: 33 mL extraction cells filled with Hydromatrix, heated at 140°C, pressurized at 1000 psi with 2 static cycles of 10 minutes and cells were completely purged (120 seconds). The solvent used was a 1:1 mixture of OmniSolv grade hexane and dichloromethane. Collected extracts were concentrated to 10 mL under a gentle stream of nitrogen (UHP) with a TurboVap (Zymark) heated at 35°C and a 10% aliquot was taken for lipid determination. Extracts were then further concentrated to a few mL with a Reacti-Therm heating module (Pierce). Clean-up columns (internal diameter 1 cm) were prepared with pre-cleaned glass wool, deactivated silica (1.7 g) and sodium sulfate and rinsed with hexane prior to use. Extract was eluted with 20 mL of hexane, retained and concentrated to approximately 200 µL under a gentle stream of nitrogen with a TurboVap heated at 35°C. As mentioned previously for atmospheric samples, all final extracts were transferred to GC vials to 500 µL and internal standards OCN and chrysene-d12 were added for PBDE and PAH analysis respectively. Similarly to the atmospheric samples, the spruce needle samples and extracts were protected from light exposure either with amber vials or covering them with aluminium foil.

Lipid determination was done using a 1 mL aliquot of the ASE collected spruce needle extracts which was placed in a pre-weighed aluminium dish. After drying in a

dessicator for several days, the dish was re-weighed and the lipid content was determined. As mentioned previously, moisture content was also determined, so that it was possible to normalize concentrations according to fresh weight, dry weight or lipid content.

4.4 GC-MS Analysis

4.4.1 PBDEs analysis

An Agilent HP 6890 gas chromatograph coupled with a quadrupole mass selective detector HP 5973N was used for all analyses. PBDEs were analyzed using chemical ionization mass spectrometry (GC-CIMS). GC-MS methods were pulled from the literature and optimized for faster acquisition time and higher sensitivity while maintaining good resolution. Several parameters were considered: injection temperature, injection mode, oven program, and source temperature.

Injection temperatures commonly used in PBDE analysis ranging from 250°C to 300°C were considered for this study. As this parameter had limited impact on sensitivity, a temperature of 280°C was chosen. Injections in splitless and pulsed splitless modes were compared with the latter offering a narrower peak shape and overall better sensitivity particularly for the later eluting compounds.

Thirdly, the oven program was optimized for faster analysis. GC-MS methods reported in the literature have long running times (from 30 to 120 minutes) [13, 65, 66, 70, 71, 76, 123, 124, 130], even though many have suggested that longer running times may be detrimental to the analysis of higher congeners particularly BDE-209 as they can undergo thermal degradation [122]. Various oven programs were considered starting from a 90 minute running time, to a brief 12 minutes with good resolution.

Finally, the ion source temperature was considered. As reported in the literature, ion source temperature is an important parameter in increasing sensitivity of the analysis [131]. Ion source temperatures ranging from 150 to 250°C are commonly used [76], although a temperature of 250°C has been reported to demonstrate a higher sensitivity [131]. In this study, increasing the source temperature from 150°C to 250°C resulted in an almost 75% increase in peak height.

4.4.1.2 Optimized GC-MS method for PBDE analysis

Injections of 2 µL were made in pulsed splitless mode at 280°C. In order to achieve optimal resolution, repeatability, and sensitivity, a different GC method was used for lower PBDE congeners (tri to hepta) and for BDE-209.

For lower PBDE congeners, a fused-silica capillary column (15 m × 0.25 mm) coated with 0.25 µm chemically bonded HP-5MS phase (5% phenyl methyl siloxane) with an additional 10 m column guard was used. Initial oven temperature was set at 120°C, followed by an initial ramp of 60°C/min to 180°C and a second ramp of 25°C/min to

300°C which was maintained for 5.20 minutes for a total run time of 11 minutes. Column carrier gas helium was set at a constant flow of 1.1 mL/min.

For BDE-209, an identical column (minus the column guard) was used for GC separation. The oven program was also similar, except that the final temperature of 300°C was kept for 10.20 minutes for a total run of 16 minutes. Helium was again used as the carrier gas, but at an increased constant flow of 3 mL/min.

The mass spectrometry parameters were the same for all PBDE congeners. The GC-MS interface and source were kept at 300°C and 250°C respectively to ensure maximum sensitivity and methane was used as reagent gas. The following mass fragments were monitored in SIM mode: m/z 79 and 81, for quantification and qualification of PBDEs respectively and m/z 404 for internal standard (OCN) monitoring. The following PBDEs were separated and quantified: tri-BDE 17 and 28, tetra-BDE 47, 66, 71 and 77 (surrogate), penta-BDE 85, 99, 100 and 118 (surrogate), hexa-BDE 138, 153, and 154, hepta-BDE 183 and 190 and deca-BDE 209.

A typical standard chromatogram for the GC-MS analysis of lower PBDE congeners is presented below (figure 4.7). This optimized GC-MS method offers good resolution between adjacent peaks as well as a shorter analysis time. Chromatographic characteristics (retention time, peak width, and resolution) for each PBDE congener are presented in the appendices.

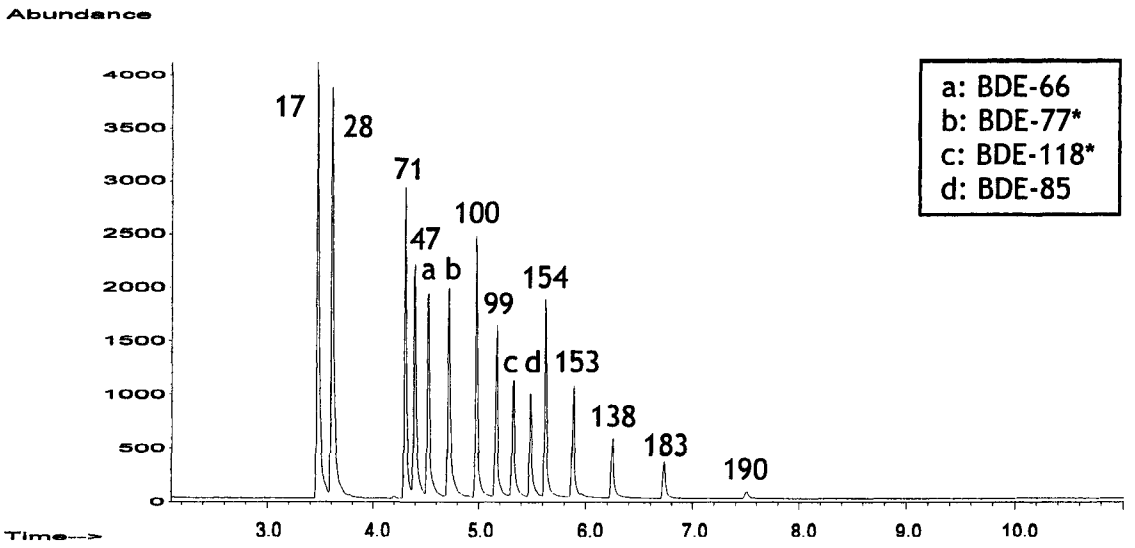

Figure 4.7 - Extracted ion chromatogram (m/z 79) of a 4 pg/µL PBDE standard acquired with the lower PBDE congeners GC-MS method. PBDE congeners are identified with their respective identification number. Surrogate standards are indicated with an asterisk.

4.4.2 PAHs ANALYSIS

PAHs were analyzed using electron ionization mass spectrometry (GC-EIMS). Injections of 1 µL were made in pulsed splitless mode at 280°C. GC separation was realized using the same column as described above (with column guard). Initial oven temperature was set at 150°C and held for 2 minutes, followed by a first ramp of 10°C/min to 240°C and second ramp of 5°C/min to 300°C which was held for 5 minutes. The GC-MS interface was kept at 300°C and the source at 150°C. The following fragments were monitored in SIM mode: m/z 152 for acenaphthylene (AceN), m/z 166 for fluorene (Flu), m/z 178 for phenanthrene (Phe) and anthracene (Ant), m/z 202 for pyrene (Pyr), m/z 228 for benz(a)anthracene and chrysene (BaA + Chr), m/z 240 for chrysene-d12

(internal standard), m/z 252 for benzo(b)fluoranthene and benzo(k)fluoranthene (BbF + BkF), and m/z 276 for indeno(123-cd)pyrene (IndP) and benzo(ghi)perylene (BghiP). Benz(a)anthracene and chrysene as well as benzo(b)fluoranthene and benzo(k)fluoranthene were combined because of poor peak resolution. Additionally, dibenzo(ah)anthracene was also monitored (m/z 278) although not quantified because of poor extraction recoveries. The monitoring fragments were chosen not only for their specificity, but also their intensity in their respective mass spectrum. A typical standard chromatogram is presented in figure 4.8. All peaks were adequately resolved, even phenanthrene and anthracene. Calculated resolutions between adjacent peaks as well as retention time and peak width for each PAH can be found in the appendices.

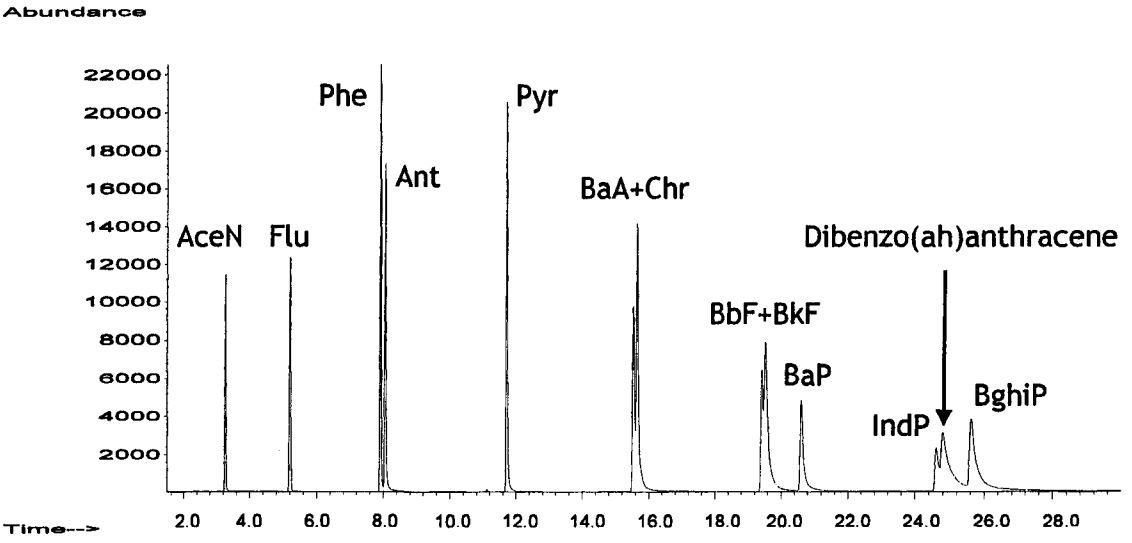

Figure 4.8 - Total ion chromatogram of a 1 ng/µL PAH standard. Compounds are identified using their abbreviations.

4.4.3 Quantification

Parameters used for data acquisition were previously optimized to offer maximum sensitivity and reliable repeat values. Ratios of the peak areas of the analytes and the internal standard were used for quantification. For PBDEs, a 10-point calibration curve forced through the origin was prepared with reference standards ranging from 0 to 5 pg/μL and gave 0.99 or higher coefficients of determination, except for BDE-209 (R^2 > 0.98). For PAHs, 5 calibration standards ranging from 0 to 0.1 ng/μL also gave 0.99 or higher coefficients of determination.

PBDE congeners and PAHs were identified according to their retention time. PBDEs were further confirmed using ratios of m/z 79 and 81 within 15% of the theoretical values. All reported values for PBDEs and PAHs are above detection limit. Typical chromatograms are presented in the appendices.

4.5 Quality Control

4.5.1 Description

Prior to use, all glassware was washed with industrial grade detergent, rinsed with warm tap water and triple-rinsed with distilled water. After air-drying, non-graduated glassware was rinsed with ACS grade acetone and hexane and heated at 200°C for several

hours. Glass Pasteur pipettes were also heated at 200°C for several hours. Graduated glassware was rinsed with OmniSolv acetone and hexane. Aluminium foil used for storage of spruce needle and filter samples was previously rinsed with ACS grade acetone and hexane and heated at 200°C for several hours. Prior to use, GMFs were dried and weighed. PUFs were previously soxhlet washed using hexane (250 mL for approx. 18 hours) which were collected, concentrated and analyzed for PBDEs to ensure they were below detection limit (BDL).

4.5.2 Blanks, detection limits and variability

Blanks

Blanks were also processed every 10 vegetation samples and every 6 air samples (PUF halves and filters) to check for laboratory background contamination. The number of method blanks processed is as follows: 16 for spruce needles samples, 14 for PUF samples and 7 for filter samples. Most PBDE concentrations in blanks were BDL except for BDE-47 and BDE-99, which were found at very low concentrations, and thus the samples were not blank corrected. For BDE-47, average concentrations in blanks were as follows: 0.08 pg/μL (0.02 - 0.13 pg/μL) for spruce needle blanks, 0.17 pg/μL (0.03 - 0.32 pg/μL) for PUF samples blanks and 0.13 pg/μL (0.09 - 0.18 pg/μL) for filter samples blanks. Average concentrations of BDE-99 were: 0.06 pg/μL (0.02 - 0.10 pg/μL) for ASE - spruce needle blanks, 0.11 (BDL - 0.31 pg/μL) for PUF samples blanks and 0.09 pg/μL (0.03 - 0.13 pg/μL) for filter samples blanks. PAH blank levels were below detection limits.

Recovery

Two surrogate standards were used to assess sample recovery: BDE-77 and BDE-118. Recovery of both was averaged. Average recovery for spruce needle, filter, and PUF samples were 70.9 ± 5 %, 86.3 ± 7 %, and 89.0 ± 8 % respectively. Samples were mean recovery corrected if recovery fell outside those ranges.

Recovery was also evaluated on a compound basis by spiking blanks with a low concentration standard. For PBDEs these were found to be 93.8 ± 4% for spruce needle samples, 87.2 ± 5% for filter samples and 83.5 ± 4% for PUF samples. For PAHs these ranged from 7 to 80% for spruce needle samples (the lowest value was for indeno(123,cd)pyrene), from 60 to 110% for filter samples (lowest value for acenaphthylene) and above 90% for PUF samples. PAH sample concentrations were adjusted accordingly.

A correction was also made for the 10% aliquot removed for lipid determination.

Instrumental repeatability

The instrument's repeatability was assessed by injecting a low concentration quality control standard several times ($n \geq 5$) throughout the sequences and by calculating the corresponding relative standard deviation. For PBDEs, these were below 15% (generally 4 to 8%) and the highest variability (~15%) was observed for BDE-209. For PAHs, variability was also below 10% (generally 1 to 4%) and was highest for later eluting compounds such as indeno(123-cd)pyrene.

Detection limits

Using approaches described previously, both the regression and the method detection limits were assessed [132, 133]. The regression detection limits (RDL) were calculated using the standard deviation of the regression (s_r) of calibration curves constructed previously and defined as

$$RDL = 3 \times \frac{s_r}{m} \tag{5.1}$$

where m is the slope [132].

Conversely, method detection limits (MDL) were evaluated for each sample matrix by using a low concentration sample injected at least 7 times and defined as

$$MDL = t \times s_D \tag{5.2}$$

where t is the t-value at the 95% confidence level and s_D is the standard deviation of the replicate analysis [133]. These were then calculated according to an 8 g spruce needle sample size and an atmospheric sample volume of 800 m^3. However, method detection limits could only be assessed for compounds present in the samples. Results for both detection limits for PBDEs and PAHs are presented in tables 4.2 and 4.3 respectively.

For PBDEs, both methods were generally in good agreement. Regression detection limits were generally below 0.1 pg/μL except for BDE-209 (3.0 pg/μL) and method detection limits ranged from 0.002 pg/m^3 to 0.025 pg/m^3 for PUF samples, 0.002 pg/m^3 to 0.29 pg/m^3 for filters and 0.25 to 46.9 pg/g for spruce needles.

For PAHs, the method detection limits were generally better than that of the regression which seemed slightly elevated (although below 0.02 ng/μL). Spruce needles method detection limits ranged from 0.01 to 0.30 ng/g for indeno(123-cd)pyrene. Filters

method detection limits were also very low (< 0.008 ng/m^3). PUFs method detection limits could not be calculated for higher PAHs congeners as these were absent from the samples; these ranged from 0.004 ng/m^3 for acenaphthylene to 0.038 ng/m^3 for phenanthrene.

Table 4.2 - Detection limits for PBDEs. Surrogate standards are denoted with an asterisk.

BDE	Regression detection limit (pg/μL)	Method detection limit (pg/g or pg/m^3)		
		Spruce Needles	GMFs	PUFs
17	0.016	0.50	0.004	0.006
28	0.012	0.69	0.002	0.006
71	0.012	ND	ND	ND
47	0.040	8.13	0.013	0.004
66	0.018	1.56	0.004	ND
77*	0.012	0.40	0.042	0.004
100	0.020	1.00	0.003	0.003
99	0.020	5.31	0.023	0.024
118*	0.009	0.52	0.022	0.005
85	0.018	0.63	0.004	0.002
154	0.016	0.94	0.003	0.009
153	0.016	2.69	0.009	0.008
138	0.027	0.25	ND	ND
183	0.089	0.75	0.003	0.002
190	0.042	ND	ND	ND
209	3.0	46.9	0.288	ND

Table 4.3 - Detection limits for PAHs.

PAH	Regression detection limit (ng/μL)	Method detection limit (ng/g or ng/m^3)		
		Spruce Needles	GMFs	PUFs
AceN	0.004	0.03	< 0.001	0.004
Flu	0.002	0.04	< 0.001	0.015
Phe	0.017	0.02	0.002	0.038
Ant	0.013	0.05	0.001	0.007
Pyr	0.005	0.02	0.003	0.006
BaA + Chr	0.008	0.01	0.003	ND
BbF + BkF	0.009	0.09	0.006	ND
BaP	0.005	0.09	0.005	ND
IndP	0.011	0.30	0.008	ND
BghiP	0.011	0.07	0.005	ND

4.6 BACK TRAJECTORIES ANALYSES AND WIND ROSE PLOTS

Air mass origins were determined using the HYSPLIT transport and dispersion model from the National Oceanic and Atmospheric Administration [134]. Backward trajectories were performed at the end of each sampling period for 96 hours starting at the end of each sampling sessions at 10, 100, and 500 m above sea levels. Backward trajectories for each sampling session can be found in the appendices. Their overall trajectories were then categorized according to 16 cardinal points: N, NNE, NE, ENE, E, ESE, SE, SSE, S, SSW, SW, WSW, W, WNW, NW, and NNW. Wind roses were compiled using hourly weather data collected at the Ottawa International Airport for the duration of the

sampling period. Predominant wind directions were also categorized according to 16 cardinal points. Both were defined categorically and numerically (degrees).

Chapter 5 - Seasonal trends in vegetation and atmospheric PAH and PBDE concentrations near a sanitary landfill

5.1 Summary

In this chapter, the influence of temperature, relative humidity, wind speed and direction on spruce needle and atmospheric (gaseous and particulate-bound) concentrations of PBDEs and PAHs was examined. In general, PBDE and PAH concentrations in spruce needles increased over time and decreased following snowmelt with a minimum coinciding with bud burst of deciduous trees. Atmospheric concentrations of PBDE and PAH, both particulate-bound and gaseous phase, were affected by daily weather parameters (such as temperature and wind direction) and thus showed more variability than those in spruce needles. Highest PAH concentrations were encountered during the winter, likely reflecting increased emission from heating homes. Pseudo Clausius-Clapeyron plots revealed higher PBDE gaseous concentrations with increasing temperature, but showed no correlation between PAH gaseous concentrations and temperature, presumably because of variations in seasonal PAH emission patterns. Finally, air mass back trajectories and local wind directions revealed that particulate-bound PBDEs, along with both gaseous and particulate-bound PAHs were from local sources, whereas gaseous PBDEs were likely from distant sources.

5.2 Spruce needle PBDEs and PAHs

The total PBDE concentration is defined as Σ [PBDE] and includes all PBDEs listed previously unless otherwise noted. It should be noted however that BDE-71 and 190 were BDL in most samples. Similarly, the total PAH concentration is defined as Σ [PAH] and includes all the PAHs named previously unless otherwise mentioned.

Total PBDE spruce needle concentrations generally ranged from 210 to 9940 pg/g dry weight with an average of 2370 pg/g. Table 5.1 presents a summary of spruce needle concentrations for selected PBDEs. Without BDE-209 total PBDE concentrations were much lower ranging from 20 to 3750 pg/g with an average 920 pg/g dry weight. A correlation analysis between individual congeners and total PBDE concentrations revealed that individual congener concentrations increased with the total PBDE concentrations. Correlation coefficients were generally higher than 0.65 except for BDE-17 (0.47), BDE-138 (0.56) and BDE-190 (0.38) which were not major contributors to the total PBDE burden in spruce needles (table 5.2). It should also be noted that BDE-71 was not quantified in spruce needle samples. Predominant PBDE congeners quantified in spruce needles are BDE-209, 99 and 47 which account for more that 85% of the total PBDE burden in spruce needles (figure 5.1) and reflect current usage of Penta and DecaBDE technical formulations [135].

Table 5.1 - Mean and range of selected PBDE and PAH spruce needle concentrations during the sampling period.

Compound	Spruce needles (pg/g)		
	Mean ± SEM	Min	Max
PBDEs			
BDE-28	18 ± 2	0.5	48.5
BDE-47	300 ± 30	1.7	907
BDE-99	350 ± 50	5.2	1680
BDE-153	48 ± 7	2.3	280
BDE-209	1500 ± 200	BDL	6220
TOTAL	2400 ± 300	210	9940
PAHs			
Acenaphthylene	270 ± 40	BDL	1202
Phenanthrene	3600 ± 800	241	26 700
Pyrene	3000 ± 700	97	22 900
Benzo(a)Pyrene	8000 ± 1000	BDL	37 100
Indeno(123-cd)Pyrene	25 000 ± 8000	BDL	246 000
TOTAL	83 000 ± 20 000	10 700	608 000

Table 5.2 - Pearson product moment correlation coefficients for PBDEs in spruce needles.

	17	28	47	66	100	99	85	154	153	138	183	190	209
ΣPBDE	0.47	0.65	0.78	0.75	0.85	0.92	0.87	0.92	0.87	0.56	0.87	0.38	0.97

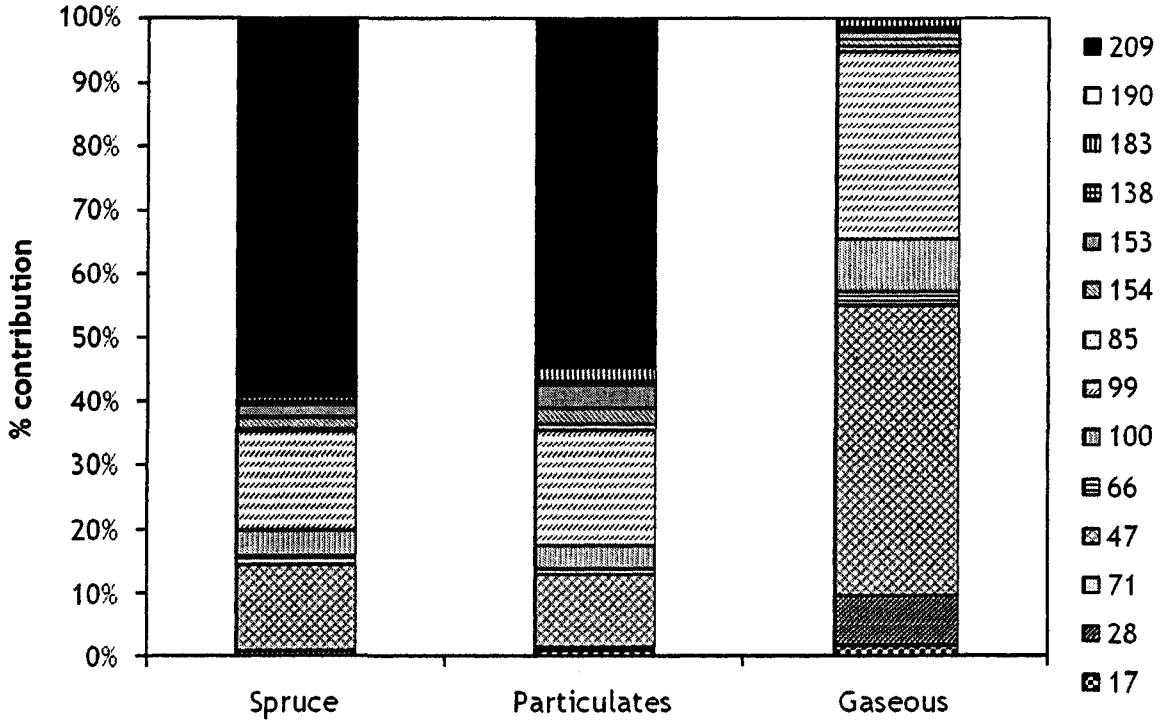

Figure 5.1 - Average congener profiles for PBDEs according to sample type.

Total PAH spruce needle concentrations were significantly higher than PBDEs ranging from 10.7 to 608 ng/g dry weight with an average 82.8 ng/g and were within values reported in the literature [83]. Table 5.1 also presents a summary of spruce needle concentrations for selected PAHs. Individual PAHs were correlated with total PAH concentrations, with coefficients higher than 0.89 (table 5.3). Contributing over 80% of the total PAH spruce needles burden were benzo(b)fluoranthene + benzo(k) fluoranthene, benzo(a)pyrene and indeno(123-cd)pyrene (figure 5.2).

Table 5.3 - Pearson product moment correlation coefficients for PAHs in spruce needles.

	AceN	Flu	Phe	Ant	Pyr	BaA+Chr	BbF+BkF	BaP	IndP	BghiP
ΣPAH	0.87	0.87	0.82	0.90	0.86	0.85	0.98	0.93	0.90	0.91

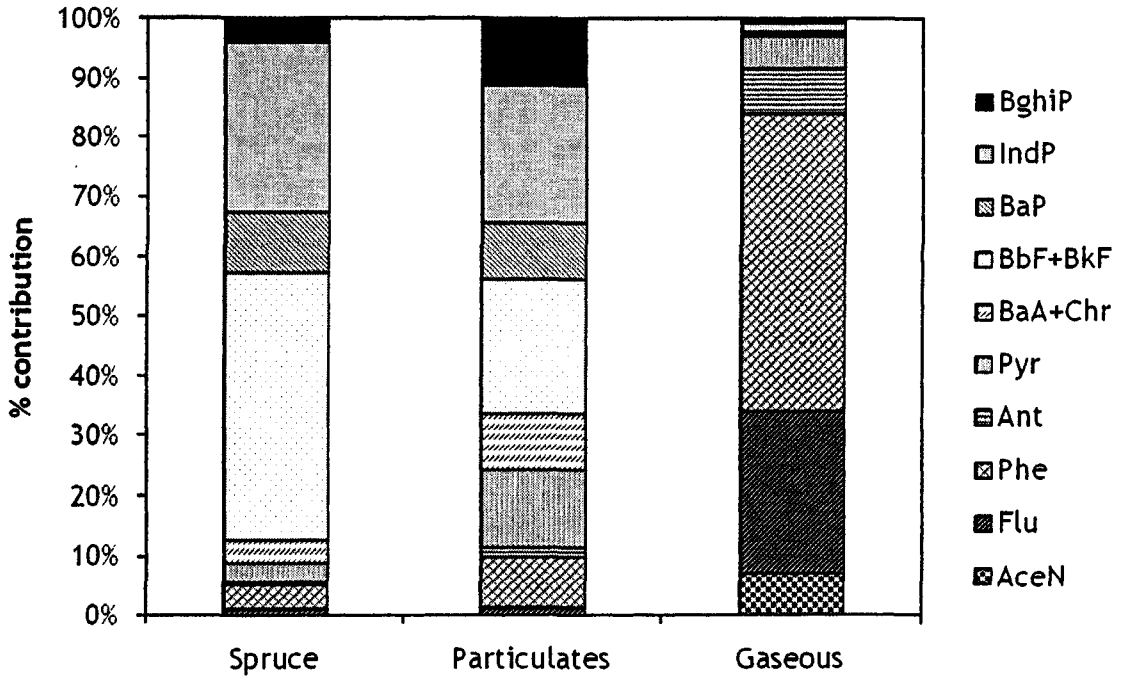

Figure 5.2 - Average congener profiles for PAHs according to sample type.

Spruce needles showed gradual accumulation of both PBDEs and PAHs starting at bud burst (as shown in figure 5.3). PBDE spruce needle concentrations generally increased during the warmer summer months stabilizing in November. This trend is however largely influenced by BDE-209 one of the predominant congeners present in spruce needles, and lighter PBDEs show a more gradual increase (figure 5.4). PAH spruce needle concentrations increased slowly starting at bud burst until November when there

is a sudden increase in concentration. This is most probably due to the arrival of colder temperatures, prompting increased fuel consumption for domestic heating causing higher PAH atmospheric concentrations (see below). With the arrival of spring, a decrease in total PBDE and PAH concentrations is seen following snowmelt (February and March) with a minimum at spring bud burst. Similar trends have also been observed for DDT (and to some extent hexachlorocyclohexanes) in pine needles [136]. This was suggested to be due to the degradation and abrasion of the wax matrix during the winter-to-spring transition. In fact, the winter season brings forth stressful conditions for conifers, such as low water apportionment, windy conditions and sun radiation. As the winter and cold temperatures progress, the protective layer thins out. This protection can decline quite rapidly with the arrival of spring, especially if this transition is dramatic, such as a few days of elevated temperatures [137, 138]. Furthermore, it also has been suggested that during a snowmelt episode, PBDEs, could be re-released in the air and thus possibly re-deposited onto available surfaces [20]. The new leaves of the deciduous trees could offer new deposition surfaces resulting in competitive uptake.

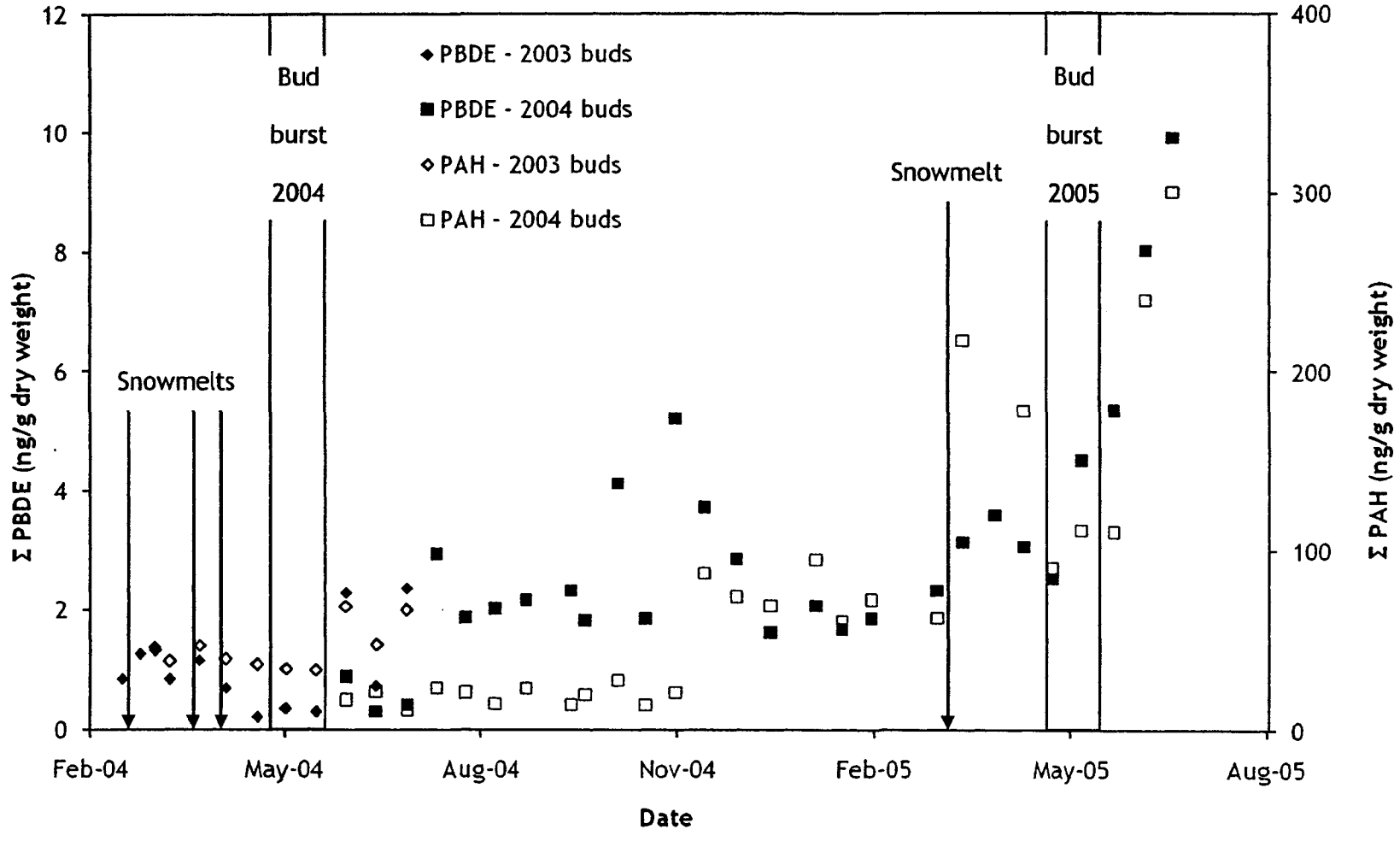

Figure 5.3 - Spruce needle total PAH and PBDE concentrations from February 2004 to June 2005 (2003 and 2004 buds). Bud burst periods and snowmelt episodes are indicated.

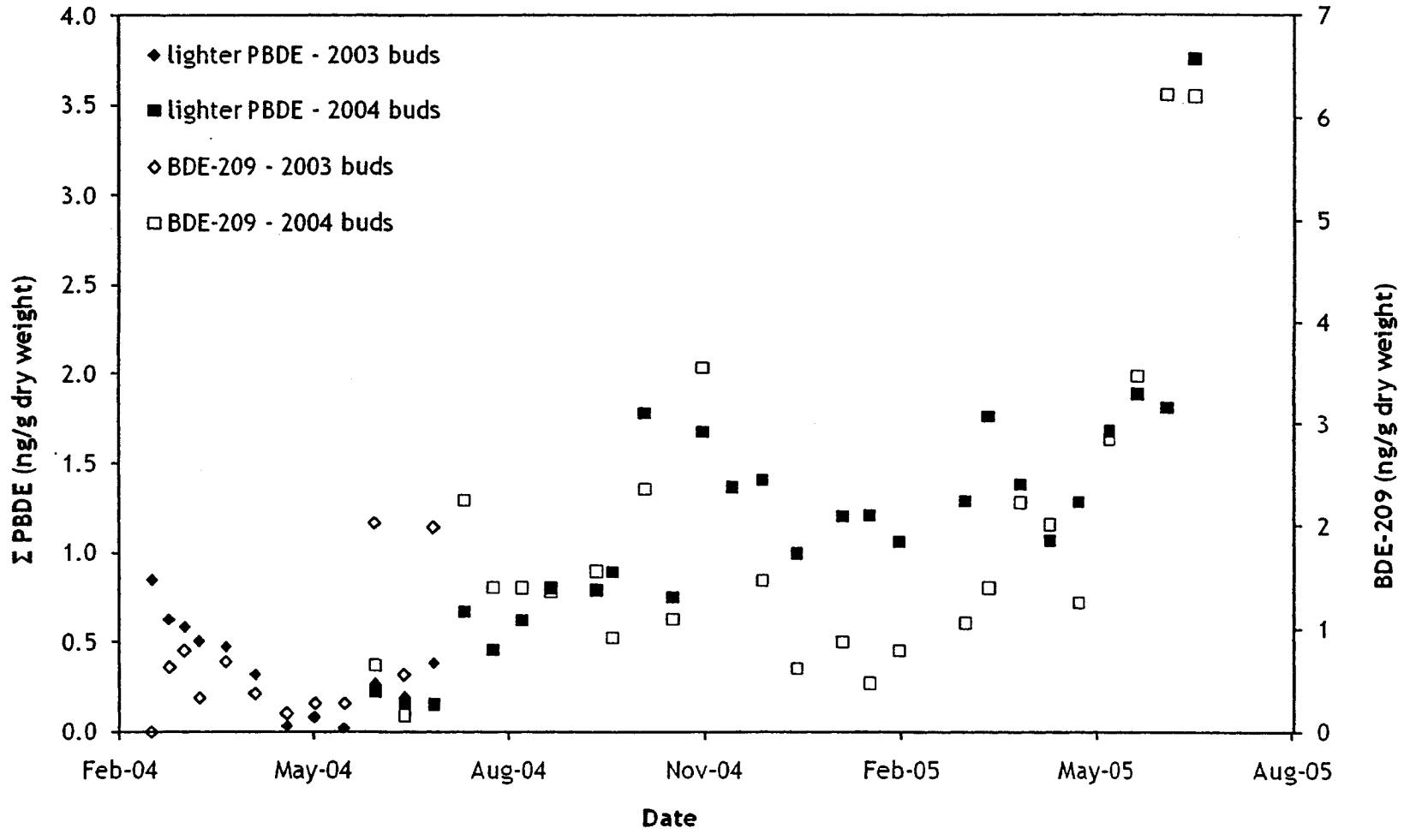

Figure 5.4 - Comparison of spruce needle BDE-209 and lighter (tri to hepta) congeners concentrations from February 2004 to June 2005 (2003 and 2004 buds).

5.3 Atmospheric PBDEs and PAHs

As seen in table 5.4 and figure 5.5, gaseous and particulate-bound total PBDE concentrations were generally below 2 pg/m^3 and 20 pg/m^3, and ranged from 0.36 to 6.9 pg/m^3 and 0.72 to 145 pg/m^3 respectively and are comparable to PBDE atmospheric concentrations reported in the region [45, 139]. Table 5.4 presents a summary of the atmospheric concentrations for selected compounds.

Individual congeners' gaseous concentrations were shown to be highly correlated to total PBDE gaseous concentrations with most correlation coefficients higher than 0.80, except for BDE-17 (0.59), BDE-85 (0.73) and BDE-138 (0.51) (table 5.5). Volatile congeners were predominantly found in the gaseous fraction, with BDE-28, 47 and 99 accounting, on average, for more than 80% of the total concentration (figure 5.1). Correlations for particulate-bound concentrations were lower, but above 0.28, the 99% confidence level critical value for Pearson's product-moment correlation coefficient, except for BDE-17, which was not significantly associated to particulates. PBDEs associated to particulates generally had a higher log K_{OA}; BDE-183 and 209 were found exclusively associated to particulates. BDE-209 contributed on average 55% to the total PBDE particulate burden, with BDE-47 and 99 also present in significant amounts (figure 5.1). The omnipresence of BDE-47, 99 and 209 in all media studied (spruce needles, gaseous and particulate-bound) reflects the current usage pattern of PentaBDE and DecaBDE technical PBDE formulations in North America [135].

Table 5.4 - Mean and range of selected PBDEs and PAHs atmospheric concentrations (gaseous and particulates) during the sampling period.

Compound	Gaseous (pg/m^3)			Particulate-bound (pg/m^3)		
	Mean ± SEM	Min	Max	Mean ± SEM	Min	Max
PBDEs						
BDE-28	0.16 ± 0.03	BDL	0.65	0.06 ± 0.01	BDL	0.37
BDE-47	0.78 ± 0.14	0.14	3.53	1.24 ± 0.33	0.10	11.56
BDE-99	0.42 ± 0.06	0.11	1.84	2.34 ± 0.52	0.11	13.59
BDE-153	0.03 ± 0.01	BDL	0.28	0.48 ± 0.10	BDL	2.53
BDE-209	BDL	BDL	BDL	12.74 ± 4.43	BDL	130
TOTAL	1.68 ± 0.29	0.36	6.93	18.32 ± 4.98	0.72	145
PAHs						
Acenaphthylene	92 ± 17	4.8	406	2.2 ± 0.6	BDL	16
Phenanthrene	563 ± 64	141	1954	32 ± 9	0.34	15
Pyrene	61 ± 6	11	194	50 ± 10	3.8	395
Benzo(a)Pyrene	BDL	BDL	BDL	31 ± 7	2.0	190
Indeno(123-cd)Pyrene	11.4 ± 1.4	BDL	30.6	60 ± 10	6.8	285
TOTAL	1140 ± 120	244	3678	315 ± 67	28	1870

Table 5.5 - Pearson product moment correlation coefficients for PBDEs in atmospheric samples (C_G is defined as gaseous concentrations, whereas C_P is defined as particulate-bound concentrations).

ΣPBDE	17	28	47	66	100	99	85	154	153	138	183	190	209
C_G	0.59	0.94	0.97	0.93	0.97	0.95	0.73	0.85	0.80	0.51	0.54	-	-
C_P	-	0.31	0.36	0.34	0.60	0.63	0.46	0.57	0.56	0.33	0.45	-	0.98

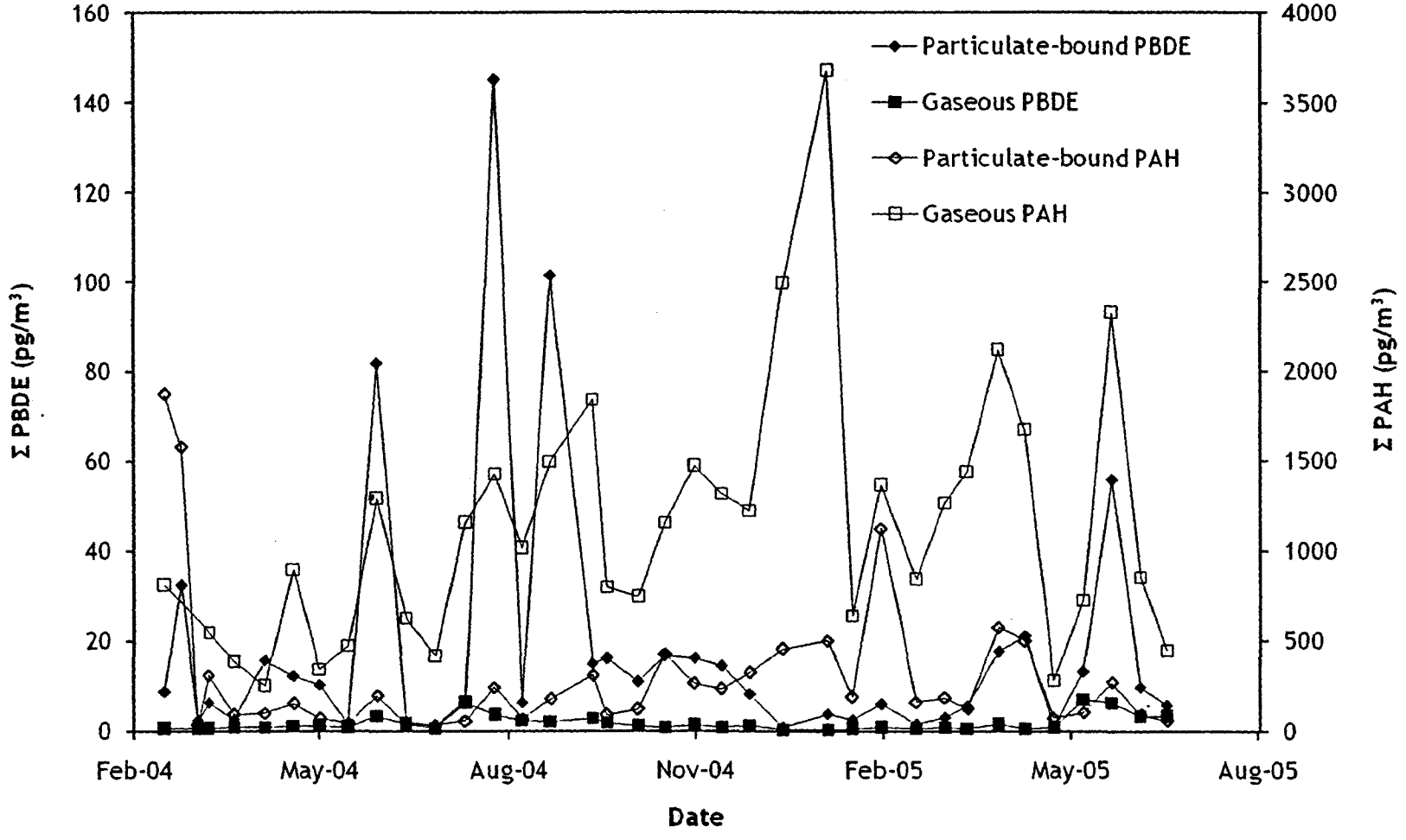

Figure 5.5 - Atmospheric total PBDE and PAH concentrations (pg/m^3) associated to particulates and present in the gas phase.

Atmospheric PAH concentrations were two orders of magnitude higher than those of PBDEs. As shown in figure 5.5, total gaseous PAHs ranged from 244 - 3680 pg/m^3 (generally below 2000 pg/m^3) while particulate-bound concentrations ranged from 28 - 1870 pg/m^3 (generally below 500 pg/m^3) and fell within values reported in the literature for Canada [140].

Individual PAHs were correlated with total PAH concentrations. Correlation coefficients were generally higher than 0.74 for gaseous PAHs, with the exceptions of benzo(a)anthracene + chrysene, benzo(b)fluoranthene + benzo(k)fluoranthene, indeno(123,cd)pyrene and benzo(ghi)perylene which were small contributors to the total PAHs gaseous concentrations (table 5.6). In fact, the three-ring PAHs (acenaphthylene, fluorene, phenanthrene, and anthracene) constituted more than 90% of the total gaseous concentrations (figure 5.2). Correlation coefficients between individual and total particulate-bound PAHs were generally higher than 0.87 (table 5.6). Almost all PAHs were found in appreciable amounts in particulates, except for acenaphthylene, fluorene and anthracene (figure 5.2).

Table 5.6 - Pearson product moment correlation coefficients for PAHs in atmospheric samples (C_G is defined as gaseous concentrations, whereas C_P is defined as particulate-bound concentrations).

ΣPAH	AceN	Flu	Phe	Ant	Pyr	BaA+Chr	BbF+BkF	BaP	IndP	BghiP
C_G	0.74	0.98	0.97	0.27	0.93	0.23	-	-	0.04	0.08
C_P	0.96	0.95	0.98	0.87	0.97	0.99	0.98	0.98	0.97	0.96

5.4 PARTICULATE-GAS PARTITIONING OF PBDES AND PAHS

Particulate-gas partitioning is to be considered in the overall assessment of the environmental fate of SVOCs as more volatile compounds found mainly in the gas phase should travel farther and possibly undergo long-range atmospheric transport to a larger extent than compounds associated to particulates which are more prone to deposit onto available surfaces [74]. Particulate-gas partitioning was assessed by calculating K_P (see chapter 3 - equation 3.6) for each sampling sessions using measured C_P, C_G and TSP values.

$$K_P = {C_P}/{TSP \times C_G}$$

As shown in figure 5.6, particulate-gas partitioning of both PBDEs and PAHs were strongly correlated to log K_{OA} ($p < 0.001$), as the proportion of SVOCs associated to particulates increased with decreasing volatility. On average, penta-BDE and higher congeners (log K_{OA} above 11) were mostly associated to particulates (above 70%) which corroborates previous results [72]. PAHs containing at least 4 rings with a log K_{OA} above 10 (benzo(a)anthracene + chrysene, benzo(b)fluoranthene + benzo(k)fluoranthene, benzo(a)pyrene, indeno(123-cd)pyrene, and benzo(ghi)perylene) were also found predominantly associated to particulates (average also above 70%). This corroborates other studies, except for benzo(a)anthracene + chrysene, which has been found to split more evenly between the gas phase and particulates [141].

The temperature dependence of particulate-gas partitioning was studied by using the van't Hoff equation and plotting log K_P as a function of 1000/T (figure 5.7). Gas-particulate partitioning of both PBDEs and PAHs were found to correlate significantly with

temperature ($p > 0.001$ for most compounds), except for BDE-17, which was found in low concentrations in both gaseous and particulate fractions. As temperature decreases, exchange is thus shifted towards particulates reducing overall mobility and long-range atmospheric transport potential.

It should also be noted that K_P could not be calculated for BDE-183 and benzo(a)pyrene as these two compounds have been found predominantly associated with particulates with C_G below detection limit. Furthermore, their particulate-gas partitioning was not found to be temperature dependent as this was observed in most samples regardless of temperature or season.

Particulate-gas partitioning is intrinsically linked to TSP, which is typically assumed to be 25 $\mu g/m^3$ in most transport models [119]. However, in the present study the average measured TSP was 12 $\mu g/m^3$ (average TSP of 11.77 ± 1.47 $\mu g/m^3$ (3.08 to 41.70 $\mu g/m^3$)) demonstrating that this value is not uniform among regions, (i.e. urban versus rural, agricultural versus open water) and will affect particulate-air partitioning, which influences deposition, degradation, persistence, and uptake by vegetation [101]. In addition, the amount of TSP will influence the amount of PBDEs associated to particulates and their particulate-bound deposition process onto vegetation. It has been suggested that a lower TSP value causes less SVOCs to be associated to particulates and more would be found in the gas phase, even for less volatile species, and thus would result in a higher mobility of these compounds [142]. Therefore, an overestimation of TSP could lead to an underestimation of PBDE mobility and transport potential.

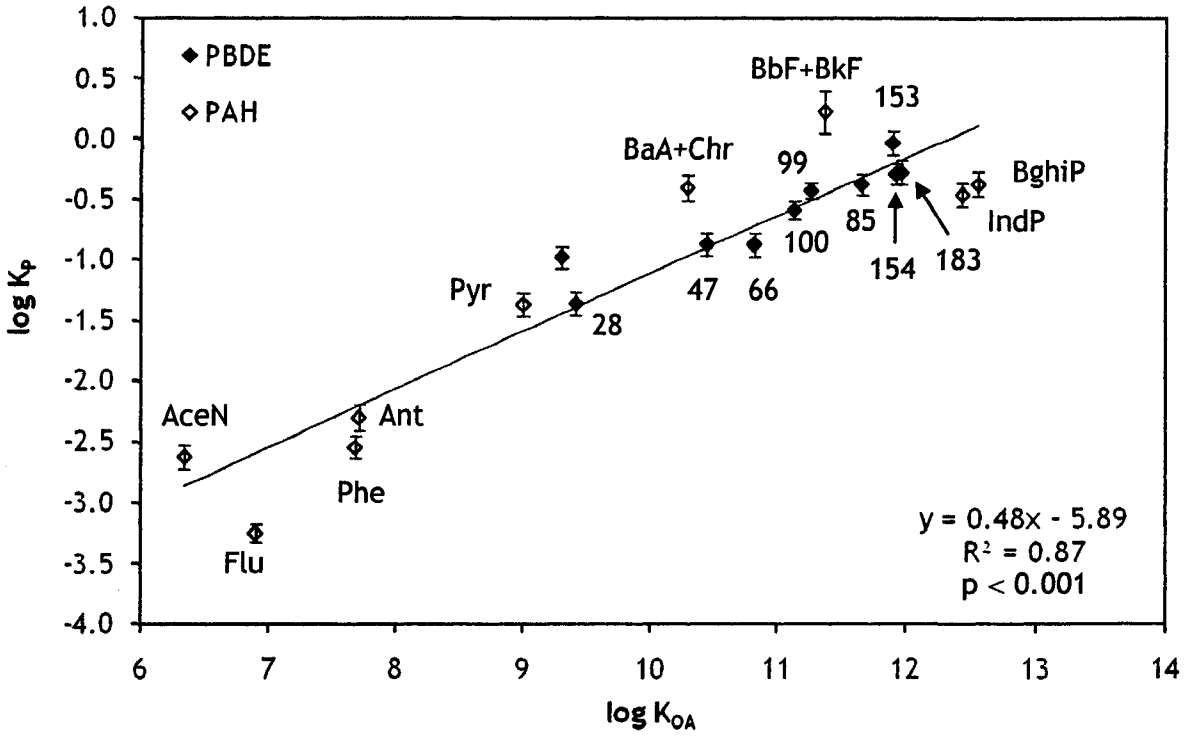

Figure 5.6 - Particulate-gas partitioning of PBDEs and PAHs studied. Individual compounds are indicated. Error bars: standard error of the mean (n=36 PBDEs and n=35 PAHs). PBDEs are identified using their identification number whereas PAHs are indicated using their abbreviation.

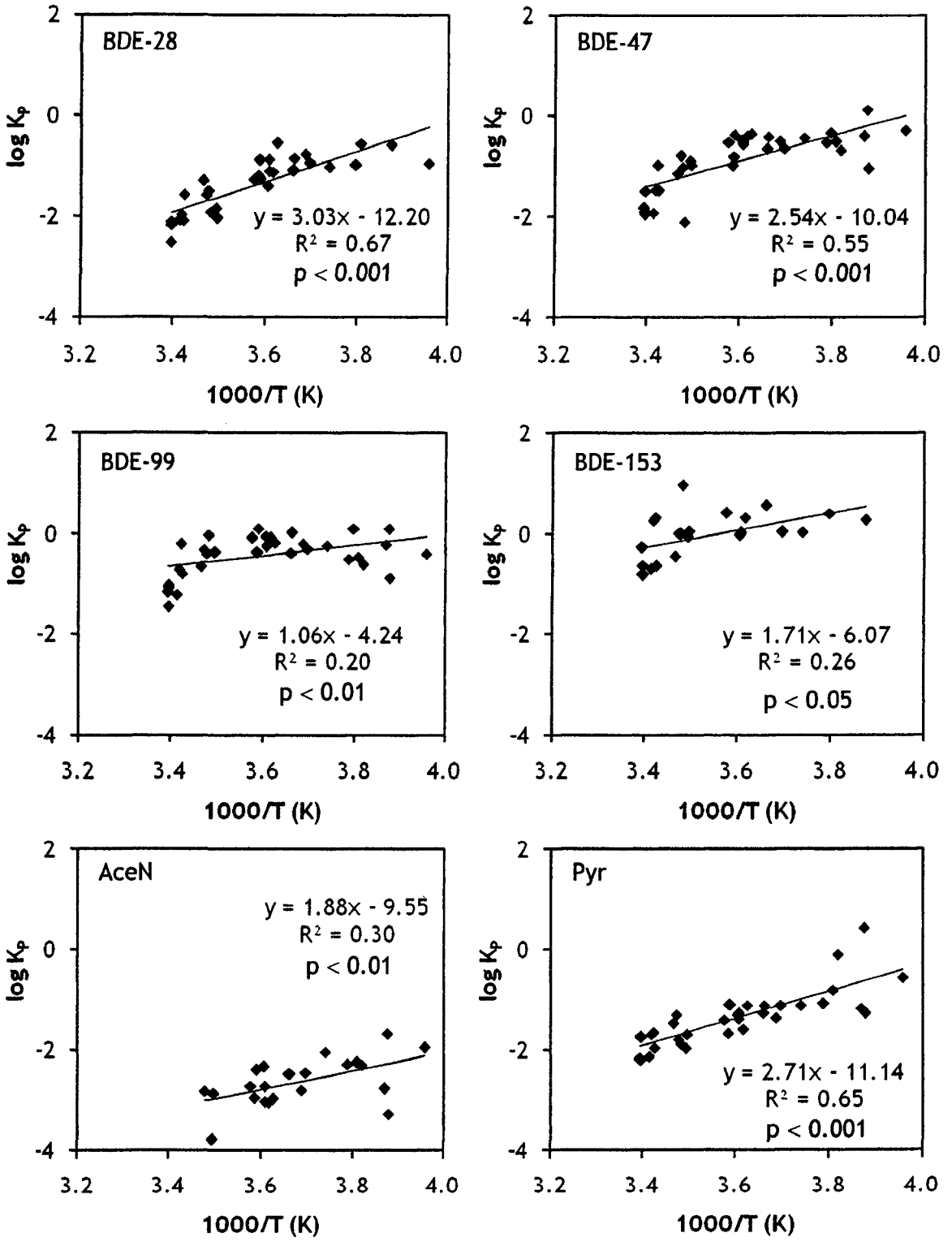

Figure 5.7 - Temperature dependence of particulate-gas partitioning for BDE-28, 47, 99, 153, acenaphthylene, and pyrene.

5.5 Seasonal effects in atmospheric PBDE and PAH concentrations

Statistical analysis revealed that gaseous concentrations of PBDEs, although relatively low, were generally higher in the summer and were significantly correlated with temperature ($p < 0.001$) (table 5.6). Pseudo Clausius-Clapeyron plots were also constructed and results are presented in table 5.7, as well as figure 5.8, which illustrates the results for BDE-28, 47, 99 and 153. For most PBDEs, the natural logarithm of partial pressure correlated significantly ($p < 0.05$) with the reciprocal temperature. Exceptions are BDE-17, 85 and 183 and this may be due to their very low concentrations in the gas phase, which very often were below detection limit. Clausius-Clapeyron plots can also be used to calculate air-surface exchange enthalpies, if the system considered is at equilibrium. These were calculated using their respective pseudo Clausius-Clapeyron plots regression slopes and were smaller than ΔH_{OA} and ΔH_{VAP} reported in the literature [73, 143]. However, it has been suggested by Hoff et al. [144] that Clausius-Clapeyron plots and corresponding slopes can also be used to assess the input of SVOCs from long-range transport and local volatilization. A steeper slope would represent greater contributions from local sources, whereas smaller slopes would be an indication of long-range transport [144]. The smaller slopes and corresponding pseudo enthalpies calculated for PBDEs in this study seem to indicate that gaseous PBDEs originated from distant sources.

Table 5.7 - Calculated p-values for the correlation of total PBDE and PAH gaseous and particulate-bound concentrations with meteorological parameters. Presence of an asterisk indicates significant correlation ($p < 0.05$). Sign of correlation is also indicated.

	PBDE		PAH	
Meteorological parameters	Gaseous	Particulate-bound	Gaseous	Particulate-bound
Temperature (K)	0.000* (+)	0.064	0.184	0.001* (-)
Relative humidity (%)	0.953	0.905	0.110	0.048* (-)
Air masses backward trajectories (categorical)	0.001*	0.045*	0.771	0.956
Air masses backward trajectories (numerical)	0.048*	0.010*	0.471	0.587
Wind direction (categorical)	0.353	0.222	0.005*	0.311
Wind direction (numerical)	0.283	0.004*	0.002*	0.113
Wind speed (km/h)	0.423	0.652	0.189	0.457

Table 5.8 - Summary of regression slopes, correlation coefficients and p-values from pseudo Clausius-Clapeyron plots used to calculate enthalpies for selected PBDEs.

PBDE	Slope	R^2	p-values	ΔH_{calc} (kJ/mol)	ΔH_{VAP} [143] (kJ/mol)	ΔH_{OA} [73] (kJ/mol)
BDE-17	-6.44	0.52	$p < 0.5$	53.5 ± 12.4	-	72.8
BDE-28	-5.50	0.59	$p < 0.001$	45.8 ± 6.6	79.7	74.5
BDE-47	-4.83	0.72	$p < 0.001$	40.1 ± 4.2	94.6	97.0
BDE-66	-4.76	0.43	$p < 0.001$	39.5 ± 9.6	97.8	107.0
BDE-85	-2.97	0.19	$p < 0.1$	24.7 ± 11.8	-	102.0
BDE-99	-2.83	0.42	$p < 0.001$	23.5 ± 4.8	108.0	91.1
BDE-100	-3.33	0.45	$p < 0.001$	27.7 ± 5.3	102.0	105.0
BDE-138	-5.27	0.28	-	43.8 ± 25.0	118.5	-
BDE-153	-2.92	0.18	$p < 0.01$	24.3 ± 11.4	110.0	98.2
BDE-154	-2.24	0.12	$p < 0.05$	18.6 ± 11.2	113.0	94.4
BDE-183	-2.86	0.18	$p < 0.1$	23.8 ± 13.0	118.0	89.5

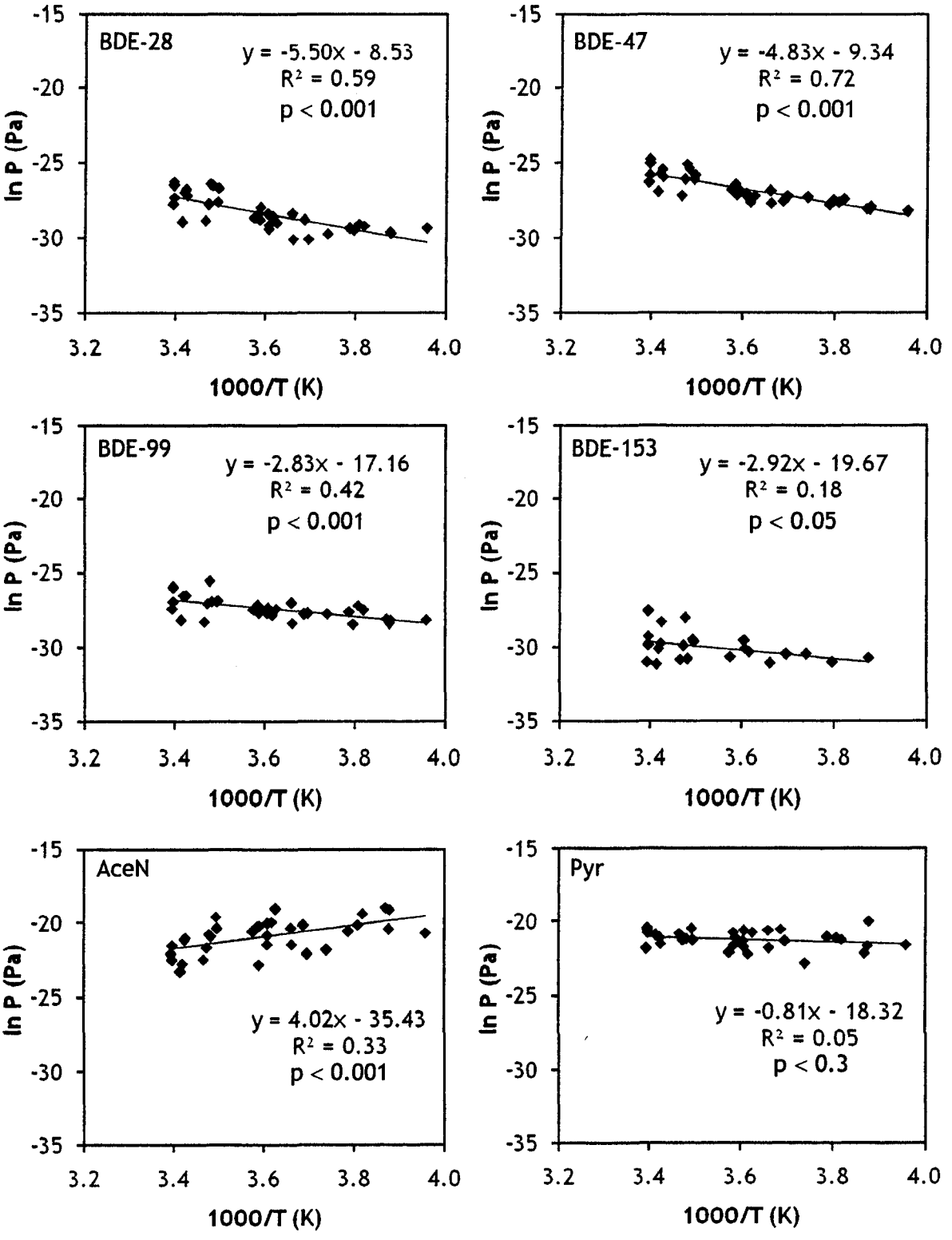

Figure 5.8 - Pseudo Clausius-Clapeyron plots for BDE-28, 47, 99, 153 and PAHs acenaphthylene and pyrene.

Particulate-bound PBDE concentrations were generally highest in the fall and spring seasons and were not significantly correlated to temperature (table 5.6). The lower concentrations encountered in winter could be due to atmospheric scavenging by snowfall, and could be re-released during snowmelt, thus causing an increased concentration in air during spring snowmelt [20].

Seasonal trends for gaseous and particulate-bound PAH concentrations are not as straightforward since meteorological effects are tied to usage patterns. Total PAH gaseous concentrations were not significantly correlated with temperature (table 5.6). Pseudo Clausius-Clapeyron plots were constructed, even though gaseous acenaphthylene was the only PAH to correlate significantly with temperature, though positively (R^2 = 0.31, $p < 0.001$). Other gaseous PAHs did not correlate significantly with temperature. Pyrene is used in figure 5.8 to represent a typical PAH.

Prior investigations have used mass concentration ratios (diagnostic ratios) to identify possible atmospheric PAH sources [90, 145]. For example, the ratio of concentrations of anthracene / (anthracene + phenanthrene) can be used to assess possible combustion versus petroleum sources. If this ratio is higher than 0.1 then combustion sources dominate, whereas a ratio lower than 0.1 indicates prevalence of petroleum sources [90]. For gaseous PAH concentrations, this ratio was lower than 0.1 from February to mid-July 2004, then higher than 0.1 until December, when it decreased below 0.1 till the end of April 2005, indicating both pyrogenic and petroleum origins.

Particulate-bound PAH concentrations were generally higher in the colder winter months as domestic heating increases (figure 5.3) and correlated significantly and negatively with temperature ($p < 0.001$) (table 5.6). For particulate-bound PAH concentrations the diagnostic ratio was always higher than 0.1 suggesting combustion

sources. Furthermore, five and six-ring PAHs have been linked to heating emissions [145] which constituted, on average, 2/3 of particulate-bound PAH burden.

5.6 Other meteorological effects and emission sources

To distinguish between long-range and local emissions as well as meteorologically related effects, and explain some of the variability encountered in atmospheric concentrations for both PBDEs and PAHs, back trajectories using HYSPLIT [134] and wind roses were constructed as described above for each sampling sessions. A thorough statistical analysis using SYSTAT was performed to study the impact of air masses and wind direction which were considered along with other meteorological parameters such as temperature, relative humidity and wind speed to assess their impact. Results are presented in table 5.6.

Gaseous PBDE concentrations were found to be linked to long-range air mass trajectories. In general, air masses deriving from northerly directions resulted in lower PBDE gaseous concentrations, whereas those deriving from the west and south had higher PBDE gaseous concentration. These were found to correlate significantly with air mass directions both categorically ($p < 0.001$) and numerically ($p < 0.05$). These observations demonstrate that gaseous PBDEs found at the sanitary landfill could be from long-range transport, thus corroborating the observations made using pseudo Clausius-Clapeyron plots. PBDE gaseous concentrations did not correlate significantly with local wind direction, relative humidity, or wind speed.

Particulate-bound PBDE concentrations correlated significantly with local wind direction (numerical $p < 0.005$) and to a lesser extent with air mass back trajectories. Previous studies indicate that SVOCs in the gas phase should travel farther and possibly undergo long-range atmospheric transport to a larger extent than compounds associated to particulates which are more prone to deposit onto available surfaces [19, 74]. Wind from the north, west and east were linked to highest particulate-bound PBDEs concentrations demonstrating the possible impact of local sources such as the city centre and the composting, electronic refuse and general waste areas at the sanitary landfill which are respectively situated north, west and east from the sampling station. Temperature, relative humidity or wind speed did not correlate significantly with the particulate-bound PBDE concentrations.

Gaseous PAH concentrations were found to correlate significantly with local wind direction ($p < 0.005$), possibly indicating a local source. In general, winds blowing from the north and east showed highest gaseous PAH concentrations corresponding with the general location of the highway and suburbs of the city. No significant correlations were found with temperature, relative humidity, air mass back trajectories or wind speed. Particulate-bound PAH concentrations did not correlate significantly with local wind direction, air mass back trajectories or wind speed ($p > 0.05$). As mentioned previously, particulate-bound PAH concentrations correlated negatively with temperature ($p < 0.001$) suggesting increased emission during colder months. A significant correlation was also observed with relative humidity ($p < 0.05$).

It is difficult to study the possible trends in concentrations in environmental media for PAHs by only looking at meteorological effects, without considering usage patterns and potential emission sources. Several parameters may have a greater impact on the

particulate-bound and gaseous concentrations comparatively to spruce needle concentrations; vegetation uptake of SVOCs is an accumulative process and thus a sudden short-lived rise in atmospheric concentrations may not be reflected in spruce needle concentrations.

Chapter 6 - DEVELOPMENT OF A MODELING SCHEME FOR ATMOSPHERIC VEGETATION UPTAKE OF PBDES

6.1 SUMMARY

As mentioned previously, processes involved in vegetation uptake of SVOCs can be studied using atmospheric and vegetation concentrations. Using frameworks discussed previously (in chapter 3), an interpretative scheme was developed to study vegetation-air exchange of SVOCs and calculate deposition and transfer velocities using field measurements. Initial SVOC concentrations in new buds were assumed to be negligible and vegetation uptake through time was evaluated as an accumulative process. The 2004 growth year of Norway spruce needles was considered during the development of this modeling concept as field measurements were available for an annual cycle starting from bud burst (end of May 2004) to June 2005. Particulate-gas partitioning was assessed for that time period and revealed that most PBDEs partition between these two compartments. However, BDE-183 and BDE-209 were found exclusively associated to particulates and thus should undergo particulate-bound deposition predominantly; the particulate-bound deposition velocity of PBDEs was calculated to be 3.8 m/h. Net gaseous transfer velocities were calculated for PBDEs found in both compartments and these ranged from 2.4 to 62.2 m/h correlating significantly with log K_{OA} values. These derived values were then used to model PBDE accumulation in vegetation through time, and these agreed well with measured concentrations. This approach provides the

necessary background for modeling PBDE transport between air and coniferous vegetation globally.

6.2 Conception of the modeling approach

It was assumed that vegetation uptake of PBDEs could be due to both particulate-bound and gaseous deposition, as most PBDE congeners are found in both compartments. However, for BDE-183 and 209, which are almost exclusively associated to particulates, gaseous deposition should be negligible and plant uptake should occur primarily through particulate-bound deposition.

Both processes were studied by considering their respective deposition velocities. Usually, surrogate surfaces are used to determine deposition fluxes and these are used to calculate deposition velocities. However, these surrogate surfaces are limited by their ability to represent the true characteristics of the environmental media and to simulate deposition to a natural surface which may be affected by revolatilization and degradation of SVOCs [106]. Instead of measuring deposition fluxes, the accumulation of PBDEs in spruce needles starting at bud burst was studied. Adapting expressions from McLachlan [101] and those developed by Horstmann and McLachlan [104], a diagram was constructed (figure 6.1) and the following equations were applied

$$C_V = C_{VP} + C_{VG} \tag{6.1}$$

$$C_{VP} = \frac{A \times v_P \times t \times C_P}{mass} \tag{6.2}$$

$$C_{VG} = \frac{A \times v_{GT} \times t \times C_G}{mass} \tag{6.3}$$

where C_{VP} and C_{VG} are the concentrations in vegetation due to particulate-bound deposition and gaseous deposition, respectively (pg/g), A is the surface area of the vegetation (m^2), v_P and v_{GT} are the velocities for particulate-bound deposition and net gaseous transfer, respectively (m/h), and t is the time (h) with t_0 at bud burst. For Norway spruce needles, the surface area was calculated using the mass of the sample, mean surface area of a needle (52 ± 1.8 mm^2) and mean weight per needle (9.3 ± 1.8 mg) [146, 147].

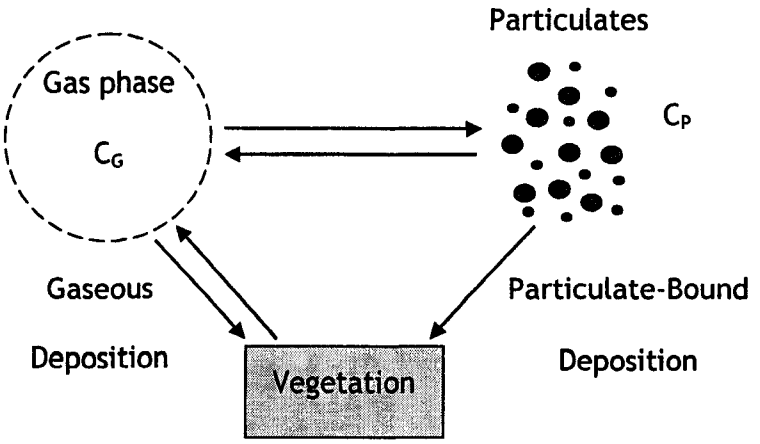

Figure 6.1 - Schematic of vegetation uptake through gaseous and particulate-bound deposition.

Using this approach and field measurements of C_V, C_P and C_G, the deposition and transfer velocities can be calculated for all sampling sessions and seasonal variability can

be assessed. Since C_V is accumulated and averaged through time, C_P and C_G should also be averaged.

6.3 PARTICULATE-GAS PARTITIONING

As a first step, particulate-gas partitioning was assessed for each sampling session over the study period (in this case June 2004 to June 2005) using ϕ instead of K_P (which can not be calculated when $C_G = 0$).

$$\phi = C_P / (C_P + C_G)$$

These were thereafter averaged and compared to summer and winter months (figure 6.2). Association with particulates was strongly correlated to log K_{OA} as the proportion of PBDEs on particulates increased with decreasing volatility. On average, penta-BDE and higher congeners were mostly associated to particulates (above 60 %) rather than being in the gas phase, which is similar to previous results [72].

A temperature effect can be seen for these congeners as the particulate-bound fraction changes quite drastically from summer to winter months. The effect of temperature on the particulate-gas partitioning of PBDEs has been discussed in greater details in the previous chapter and revealed that association with particulates increased with decreasing temperatures. Thus, a decrease in temperature promotes air to particulate exchange reducing the mobility and the long-range atmospheric transport

potential of these compounds. However, as previously discussed, BDE-183 and 209 were found mainly bound to particulates, regardless of ambient temperature.

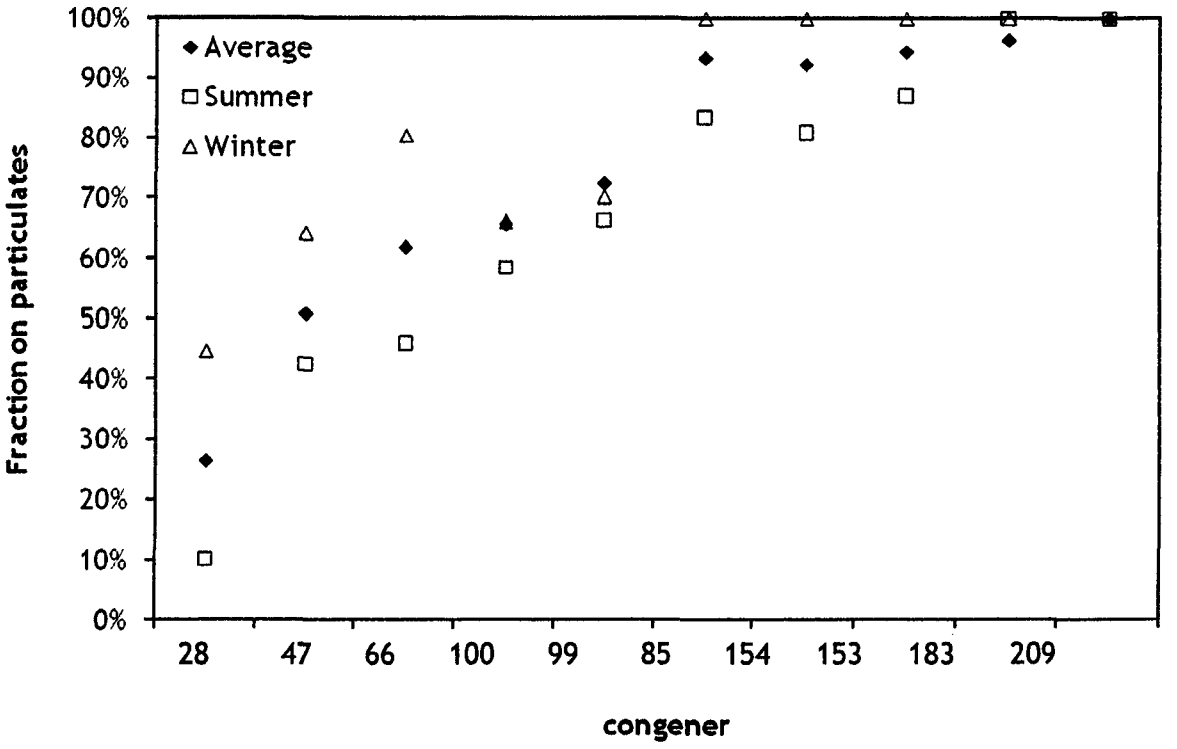

Figure 6.2 - Measured ϕ of selected PBDE congeners: average (June 2004 to June 2005), summer (July 2004 to September 2004), and winter (December 2004 to February 2005). Congeners are identified using their respective identification number.

6.4 PARTICULATE-BOUND DEPOSITION OF PBDES

Particulate-bound deposition of PBDEs could potentially be studied directly with either BDE-183 or BDE-209, since both congeners should only undergo particulate-bound deposition. However, BDE-183 was chosen because of inherent analytical challenges encountered during the quantification of BDE-209, the least of which is a higher detection limit (see chapter 4) [78, 148].

When gaseous deposition and potential wash-off from the surface are negligible $C_V = C_{VP}$ and the particulate-bound deposition velocity can be calculated directly with equation 6.2. As shown in figure 6.3, the v_P for BDE-183 was calculated for each sampling date and was found to be 3.78 ± 0.55 m/h (generally ranging from 1.75 to 8.61 m/h).

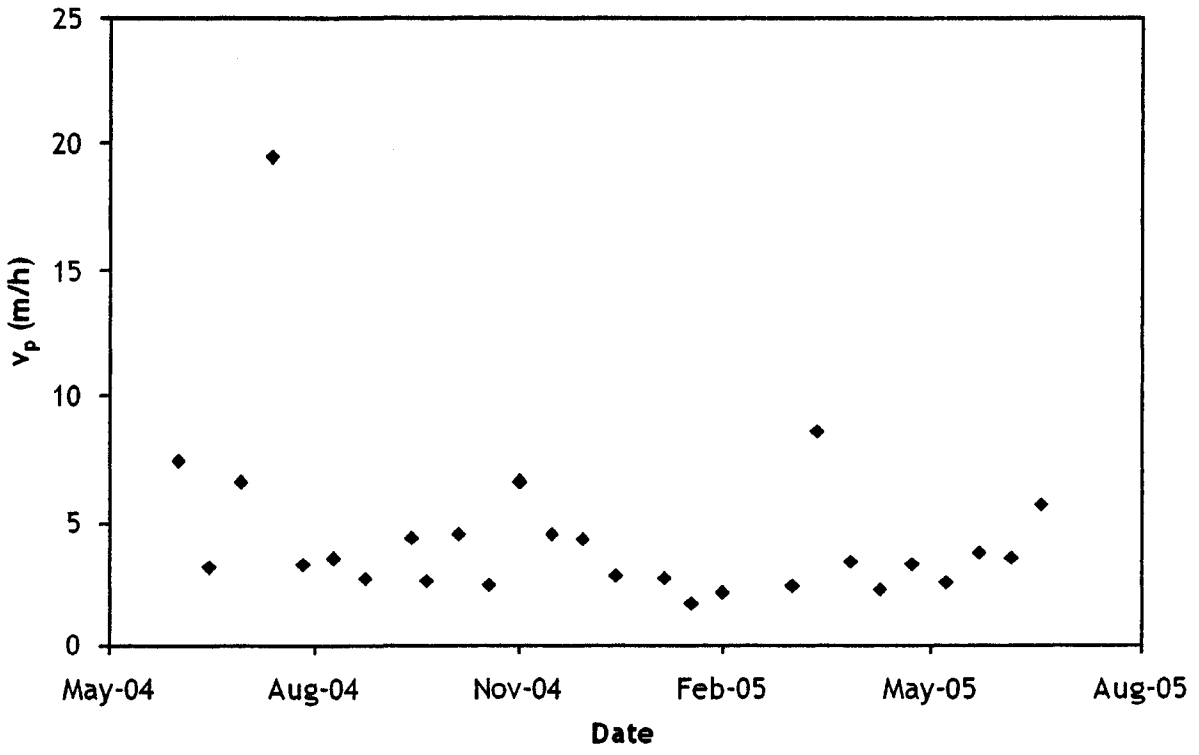

Figure 6.3 - Measured v_P values for BDE-183 according to sampling dates.

The uniformity in the calculated v_P values is probably due to the fact that they were calculated from averaged field measurements. For example, a brief increase in PBDE atmospheric concentration (C_P and C_G), will not necessarily be reflected in C_V. It should be noted that this v_P value should be the same for all PBDEs as the particulate-bound deposition velocity is related to the properties of particulates and compounds within a chemical family should be associated to the same particulates [104]. This v_P value of 3.78 m/h for PBDEs is comparable to values of 1.4 - 2.2 m/h (also for a coniferous canopy) determined for PAHs [104], but lower than reported values for PBDEs [108, 110] although none were available for a coniferous canopy. Reported particulate-bound deposition velocities for PAHs have been shown to be lower for a coniferous canopy [104]. There were no significant relationships ($p > 0.05$) between the particulate-bound deposition velocity and either temperature or wind speed.

6.5 VEGETATION-GASEOUS EXCHANGE OF PBDES

For congeners present in both gas phase and particulates, both deposition processes are possible (seen in figure 6.1) and the net gaseous transfer velocity (v_{GT}) can be calculated by combining equations 6.1, 6.2 and 6.3 and using a v_P of 3.78 m/h (as determined above).

$$v_{GT} = \frac{(C_V - C_{VP}) \times mass}{A \times t \times C_G} \qquad (6.4)$$

The net gaseous transfer velocity (v_{GT}) calculated for all congeners (except for BDE-183) for each sampling session are presented in figure 6.4 and table 6.1. The averaged v_{GT} (ranging from 2.4 - 62.2 m/h) decreased significantly with increasing volatility, indicating not only gaseous deposition. Correlations between v_{GT} and log K_{OA} values have also been observed for PCBs and PAHs with values ranging from 0.3 to 51 m/h and 1.3 to 9 m/h respectively [104].

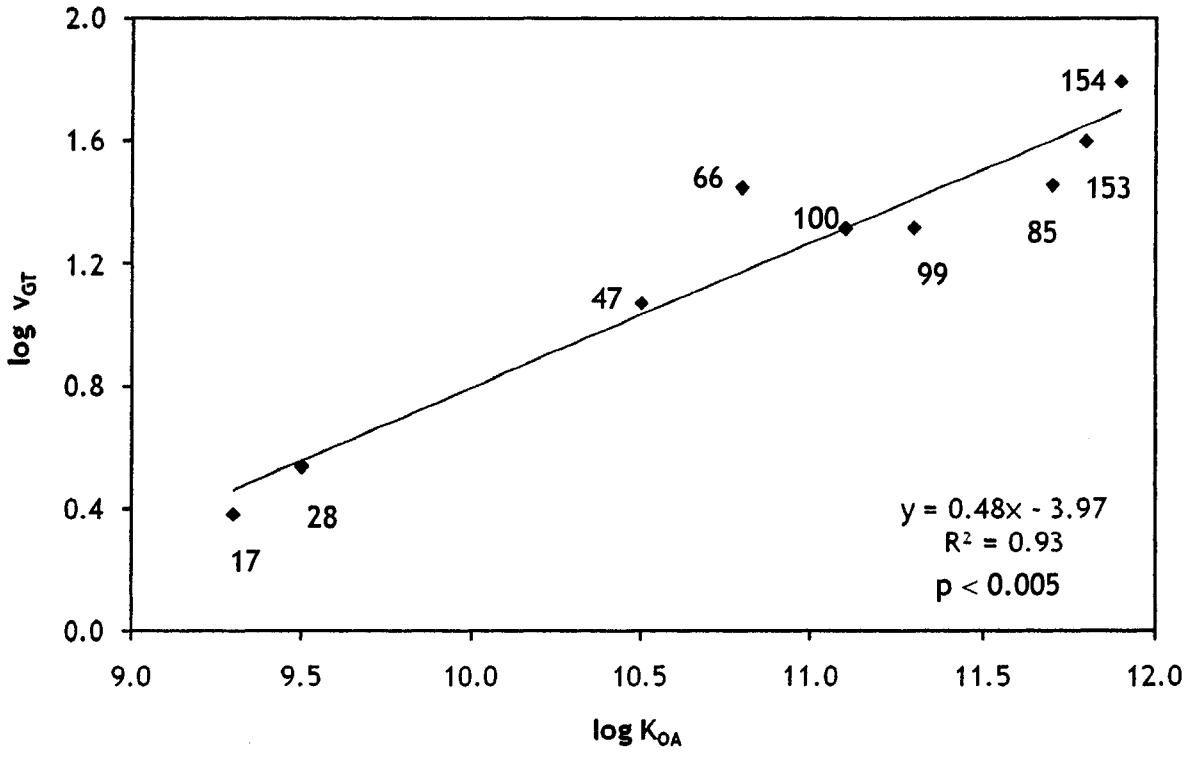

Figure 6.4 - Average log v_{GT} for selected PBDEs. Congeners are identified with their respective identification number.

Table 6.1 - Average measured v_{GT} and calculated v_{VOL} for PBDEs. v_{DEP} is indicated with an asterisk.

BDE	Average measured v_{GT} (m/h)	Average calculated v_{VOL} (m/h)
17	2.41	59.82
28	3.43	58.80
47	11.79	50.44
66	28.06	34.17
100	20.80	41.42
99	20.90	41.32
85	28.56	33.67
153	39.70	22.53
154	62.23*	-

Therefore, the measured v_{GT} describes the net transfer, which incorporates both gaseous deposition and competing processes, which include, but are not limited to volatilization, degradation and debromination. No studies reporting the reactivity of PBDEs in vegetation were found, but if the half-life of PBDEs in vegetation is assumed to be equal or greater to that in water (10000 - 30000 h) [20] then volatilization should be the dominant process and

$$v_{GT} = v_{DEP} - v_{VOL} \tag{6.5}$$

where v_{GT} is the measured net gaseous transfer velocity (m/h), v_{DEP} is the gaseous deposition velocity (m/h) and v_{VOL} represents volatilization (m/h). The gaseous deposition velocity (v_{DEP}) should be the same for compounds having similar diffusivities in air [104]. It was assumed that BDE-154, the least volatile (highest log K_{OA}) congener considered, was unlikely to undergo volatilization from vegetation in appreciable

amounts, and an average v_{DEP} was calculated as 62.23 m/h (v_{VOL} being negligible, v_{GT} = v_{DEP}).

By using equation 6.5, v_{VOL} was calculated for all congeners on a sampling session basis (except BDE-154 and BDE-183) and the volatilization process becomes more important with increasing volatility (Figure 6.5). Additionally, a comparison of v_{GT} and v_{VOL} values is presented in table 6.1.

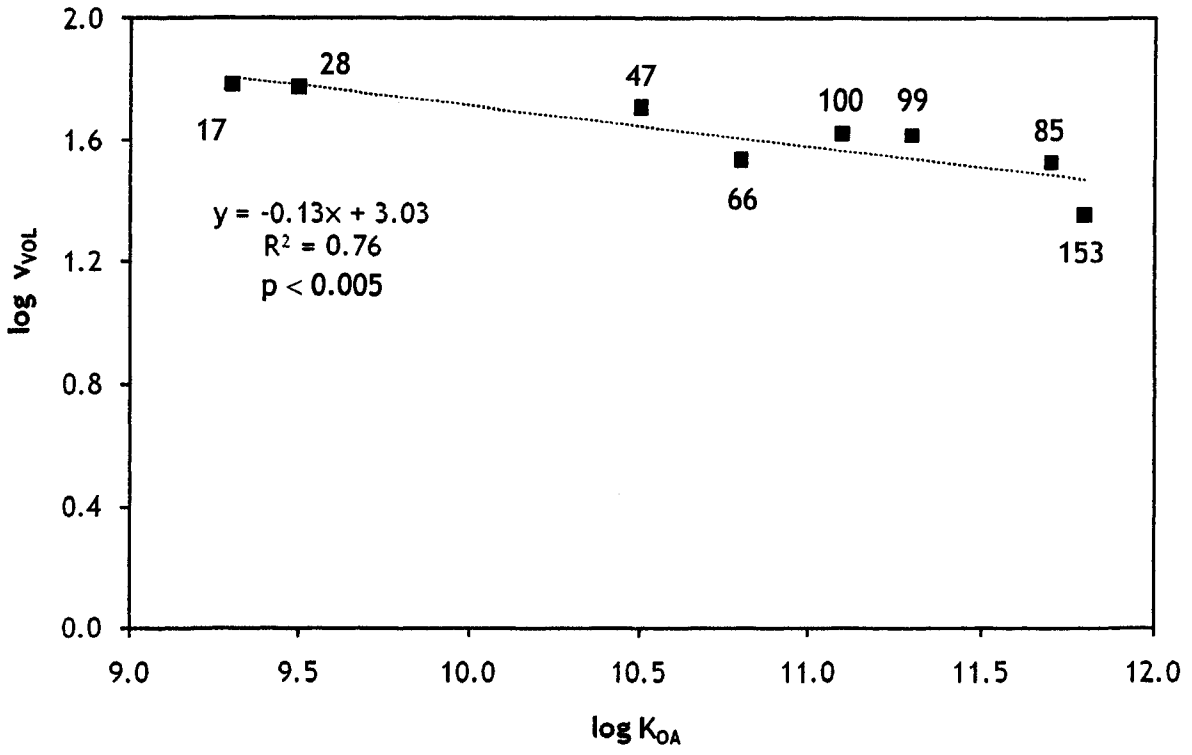

Figure 6.5 - Average log v_{VOL} for selected PBDEs.

Unlike other compartments like soil and sediments that act as true sinks, the vegetation compartment could act as an intermediate between air and soil. Hence air-

surface exchange for relatively volatile PBDEs could be increased by the presence of vegetation [20].

Furthermore, plotting v_{VOL} as a function of temperature revealed a significant positive correlation ($p < 0.01$) for the lighter more volatile tri, tetra and some penta-BDE congeners (figure 6.6). Relatively volatile PBDEs could thus be re-volatilized, especially with increasing temperature possibly promoting surface-air exchange and LRAT potential during the summer. However, volatilization of hexa and higher BDE congeners was not influenced by temperature.

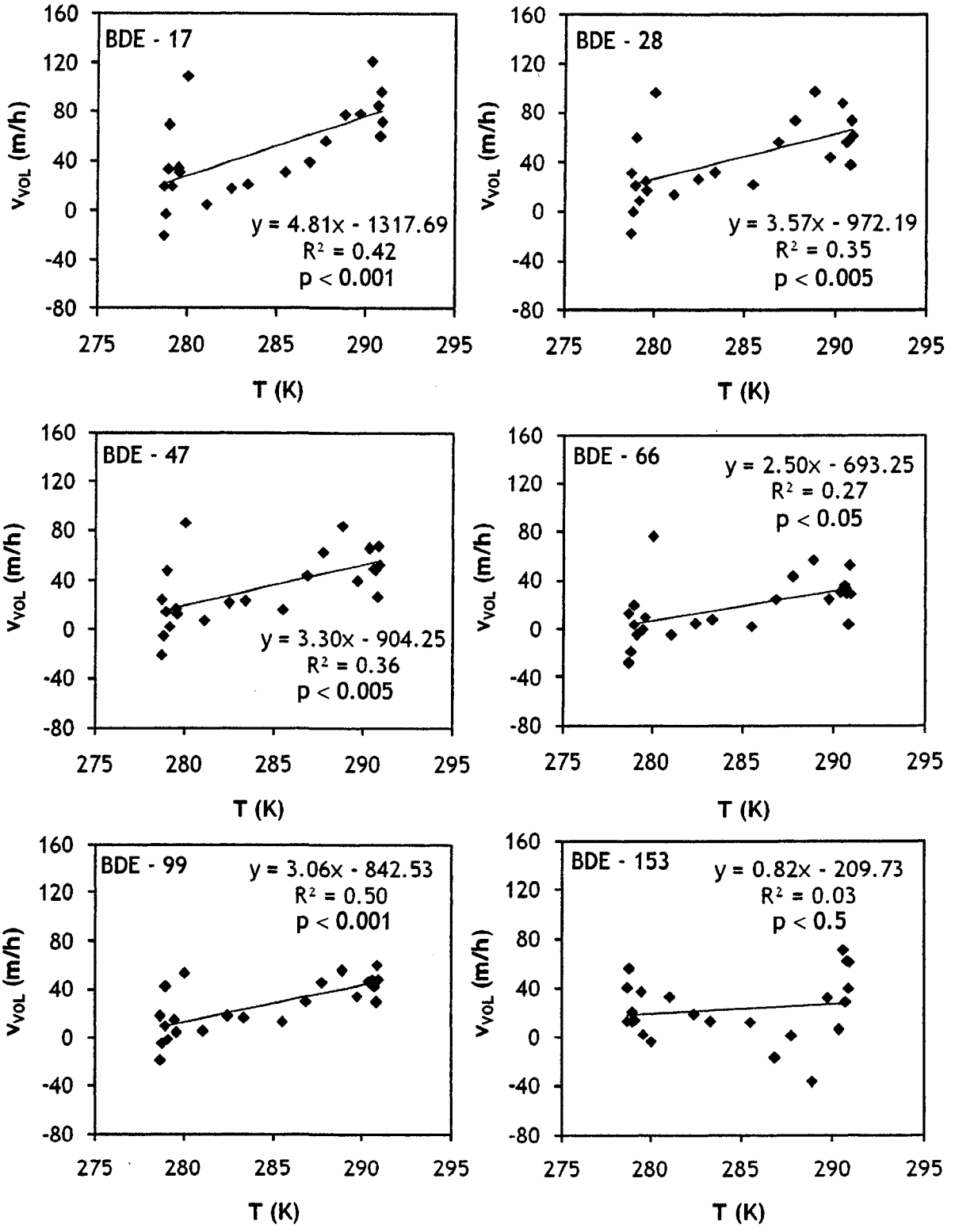

Figure 6.6 - Influence of temperature on the volatilization velocity for selected PBDE congeners.

6.6 CALCULATION OF PBDE VEGETATION CONCENTRATIONS

As stated previously, total PBDE vegetation concentration (C_V) is a contribution of particulate-bound and gaseous deposition processes (equations 6.1 to 6.3).

$$C_V = \frac{A \times v_P \times t \times C_P}{mass} + \frac{A \times v_{GT} \times t \times C_G}{mass} \qquad (6.6)$$

Using this equation, it is possible to calculate C_V and determine the relative contribution of each process (C_{VP} and C_{VG}). The calculations were done using averaged measured atmospheric concentrations as well as v_P and v_{GT} values established previously. Average C_P and C_G values are required because vegetation uptake was considered to be an accumulative process. Results are presented in figure 6.7. The relative contribution of C_{VG} to the total PBDE vegetation concentration is relatively similar for tri and tetra-BDE congeners (around 85%), decreases for penta and hexa-BDE congeners and seems to stabilize for hepta (BDE-183) and higher BDE congeners reflecting higher association to particulates.

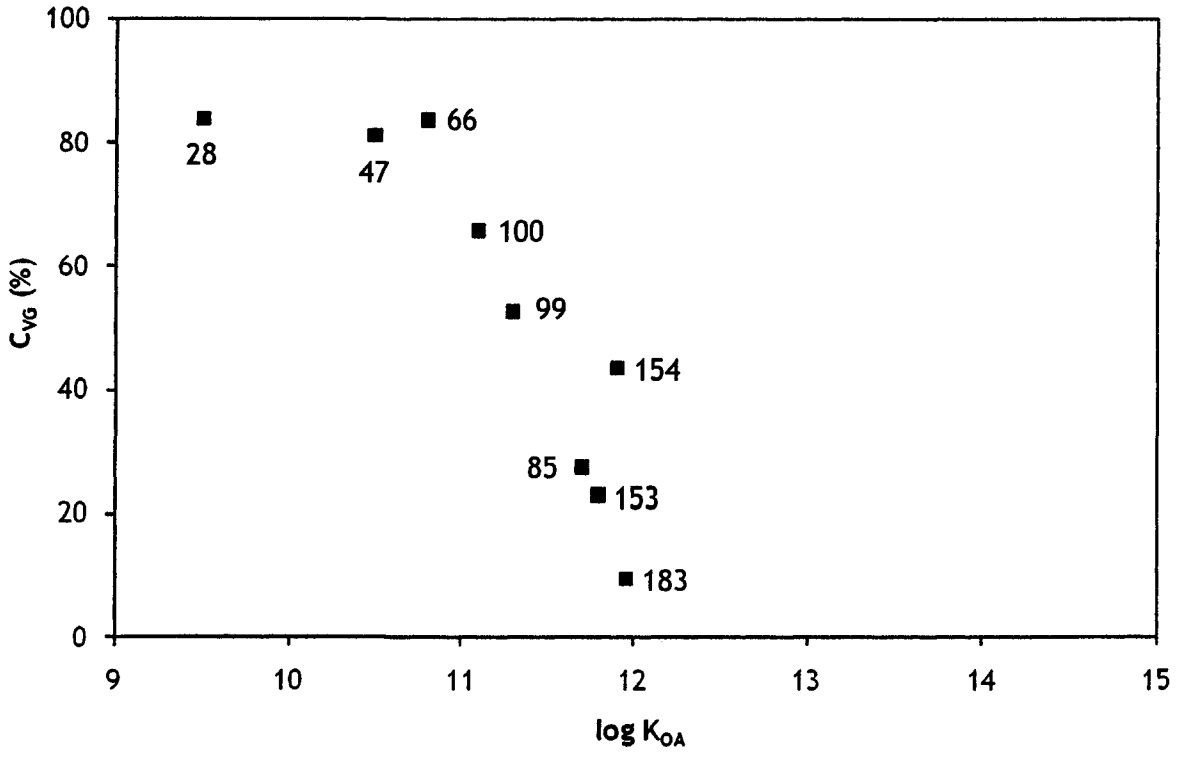

Figure 6.7 - Contribution of gaseous transfer to the total PBDE vegetation concentrations. Congeners are identified with their respective identification number.

Furthermore, it is possible to compare the calculated C_V to measured concentrations. As seen in figures 6.8 and 6.9, calculated C_V values follow the general trend in measured C_V, indicating that the model is self-consistent and robust. The model works well with lighter BDE (in this case BDE-28), as well as heavier congeners (as shown with BDE-99, 153, and 209). It also accommodates low concentrations (as shown with BDE-28), as well as more predominant PBDEs in the environment (like BDE-99 and 209). There is more variability for BDE-28, which may be a consequence of its higher volatility rendering this congener more subject to environmental and meteorological factors.

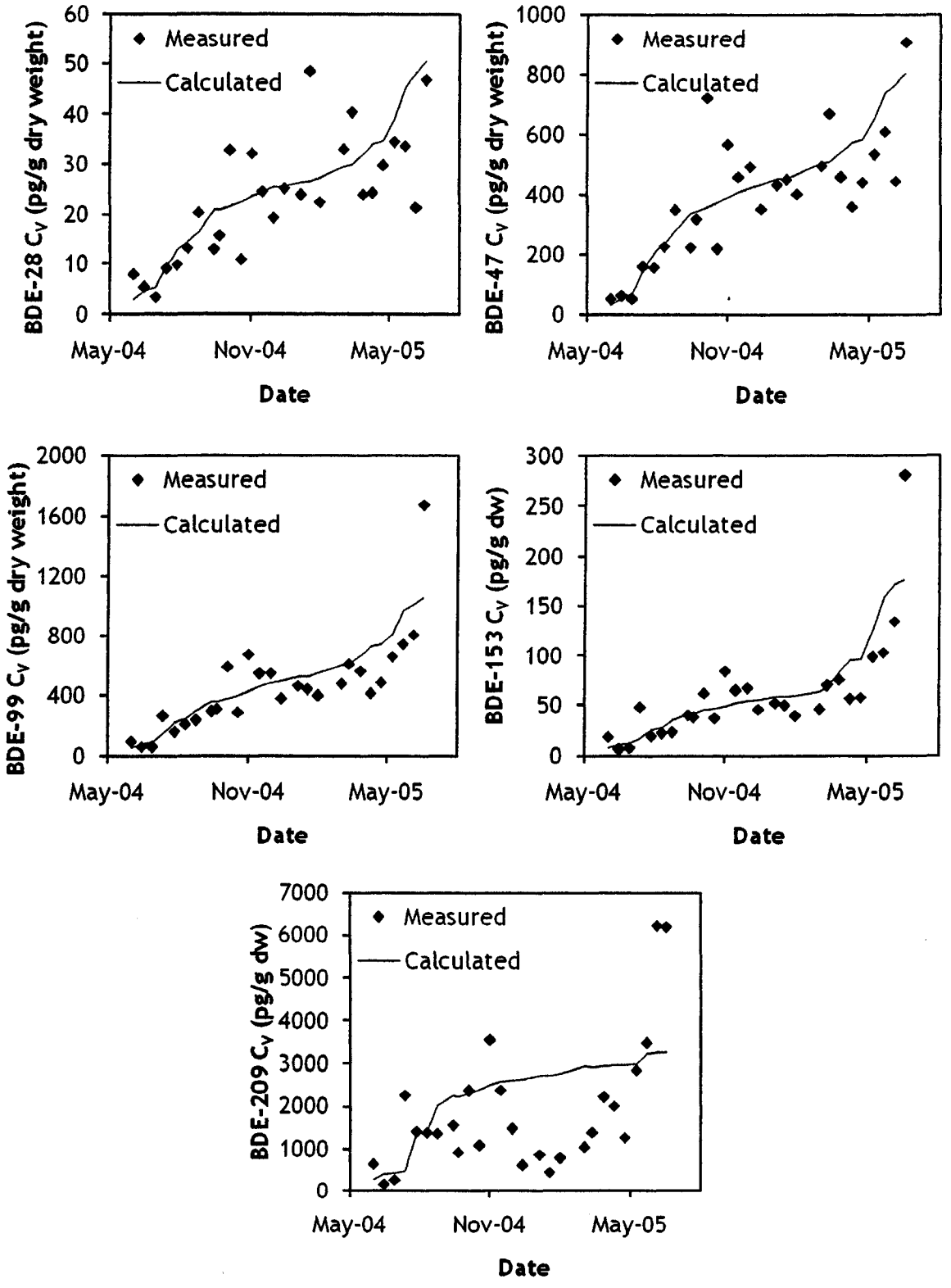

Figure 6.8 - Comparison of measured and calculated vegetation concentrations for selected PBDE congeners.

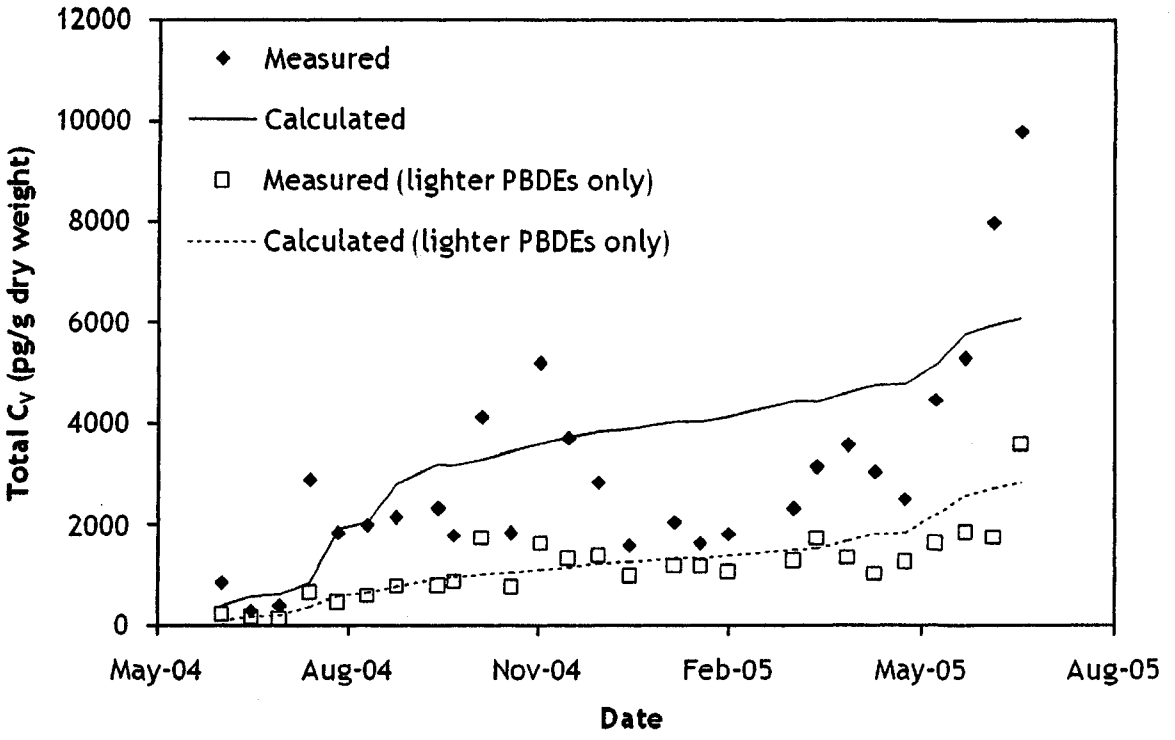

Figure 6.9 - Comparison of measured and calculated total PBDE vegetation concentrations (with and without BDE-209).

By measuring and averaging C_P and C_G through time (starting at bud burst) and by calculating the appropriate deposition and transfer velocities, it is possible to monitor the accumulation of PBDEs in vegetation. Furthermore, since C_P and C_G inherently reflect some environmental and meteorological factors like temperature, bud burst and snow cover, this approach may consider seasonal effects in the accumulative uptake of PBDEs in vegetation leading to a better understanding of the role of vegetation in the environmental fate and transport of PBDEs. Finally, the calculated deposition velocities can be used to improve on-going environmental fate modeling of PBDEs.

Chapter 7 - MODELING VEGETATION UPTAKE OF PAHS

7.1 SUMMARY

Using the interpretative framework developed, the vegetation uptake of PAHs was examined and corresponding deposition and transfer velocities were calculated. As in the previous chapter, samples considered consisted of 2004 Norway spruce buds as well as atmospheric samples collected over an annual cycle (June 2004 to June 2005). Particulate-gas partitioning for this study period revealed that PAHs generally partition between both compartments although one was usually favoured. For example, high log K_{OA} PAHs such as benzo(b)fluoranthene + benzo(k)fluoranthene, benzo(a)pyrene, indeno(123-cd)pyrene, and benzo(ghi)perylene were mostly associated to particulates with little partitioning to the gaseous phase. The particulate-bound deposition velocity of PAHs was calculated at 10.8 m/h using benzo(a)pyrene field measurements. PAHs present in both compartments had net gaseous transfer velocities ranging from negligible values to 75.6 m/h correlating significantly with log K_{OA} values. These derived values were then used to model PAH accumulation in vegetation through time and good agreement was observed between calculated concentrations and field measurements. These results and observations demonstrate that this conceptual model, initially developed with PBDEs, can be applied successfully to other classes of SVOCs to study vegetation-air exchange.

7.2 PARTICULATE-GAS PARTITIONING

PAH association with particulates (ϕ) was calculated for each sampling session over the study period (averages can be found in figure 7.1). Association with particulates was found to correlate significantly with log K_{OA} values and increased with decreasing volatility. The three-ring PAHs were found predominantly in the gaseous phase (below 10% association to particulates), whereas the five and six-ring PAHs were mainly bound to particulates (above 80%).

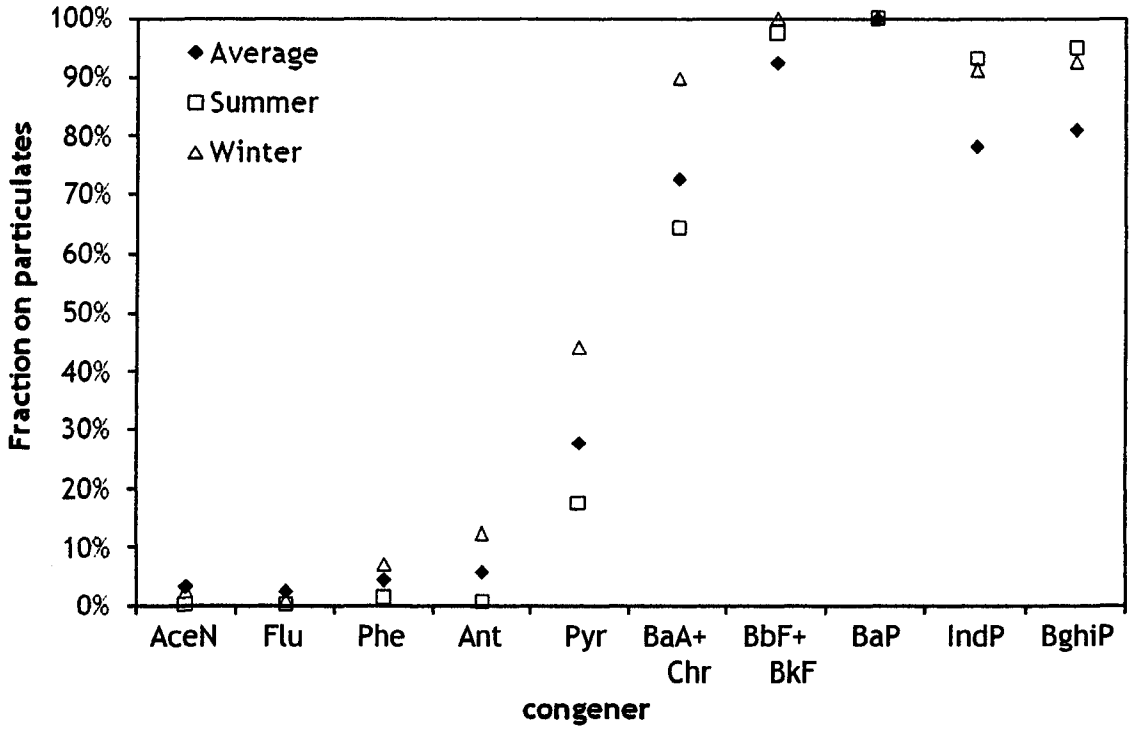

Figure 7.1 - Average measured percentage of selected PAHs on particulates: annual average (June 2004 to June 2005), summer average (July 2004 to September 2004), and winter (December 2004 to February 2005). PAHs are identified using their respective abbreviations.

The annual average was thereafter compared to winter and summer months' averages. As discussed previously (in chapter 5), particulate-gas partitioning of PAHs is temperature dependent; association with particulates decreases with increasing temperature. This can also be seen in figure 7.1 as association with particulates was generally higher during the winter months. An increase in temperature promotes exchange towards the gaseous phase, thus potentially enhancing a compound's mobility and transport potential in the environment. It should also be noted that benzo(a)pyrene was exclusively associated to particulates (BDL in gaseous samples), and did not demonstrate a temperature dependence.

7.3 Particulate-bound deposition of PAHs

As benzo(a)pyrene was found exclusively associated to particulates it was selected to study the particulate-bound deposition of PAHs. The v_P of benzo(a)pyrene was calculated for each sampling session using equation 6.2 and results are presented in figure 7.2. The average v_P was 10.83 ± 1.29 m/h (generally ranging from 4.55 to 23.5 m/h) which seems to be an intermediate value to those reported in the literature [104, 108, 112]. It should be noted that although this v_P may seem more variable than that of BDE-183, its relative error is slightly smaller (12% comparatively to 15%).

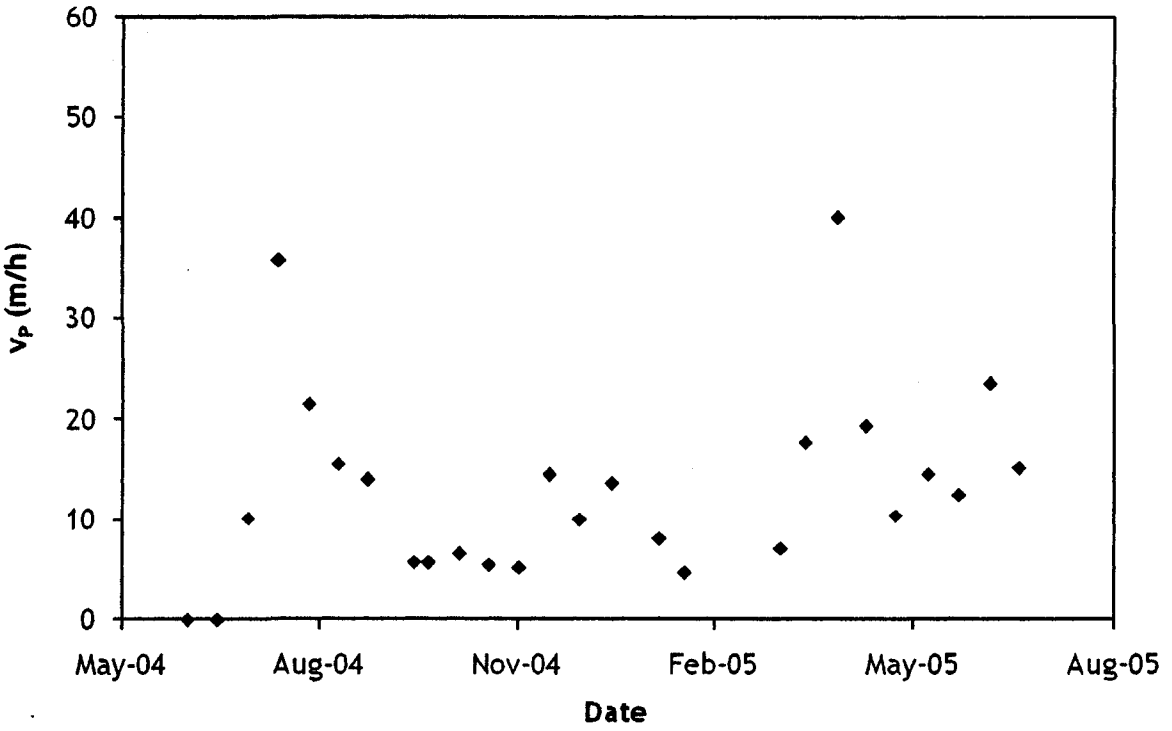

Figure 7.2 - Measured v_P values for benzo(a)pyrene according to sampling date.

7.4 VEGETATION-GASEOUS EXCHANGE OF PAHS

Next, the net gaseous transfer velocities of PAHs were also calculated. Equation 6.4 and a v_P value of 10.83 m/h were employed and v_{GT} values were calculated for each sampling session. Results are presented in figure 7.3 and table 7.1.

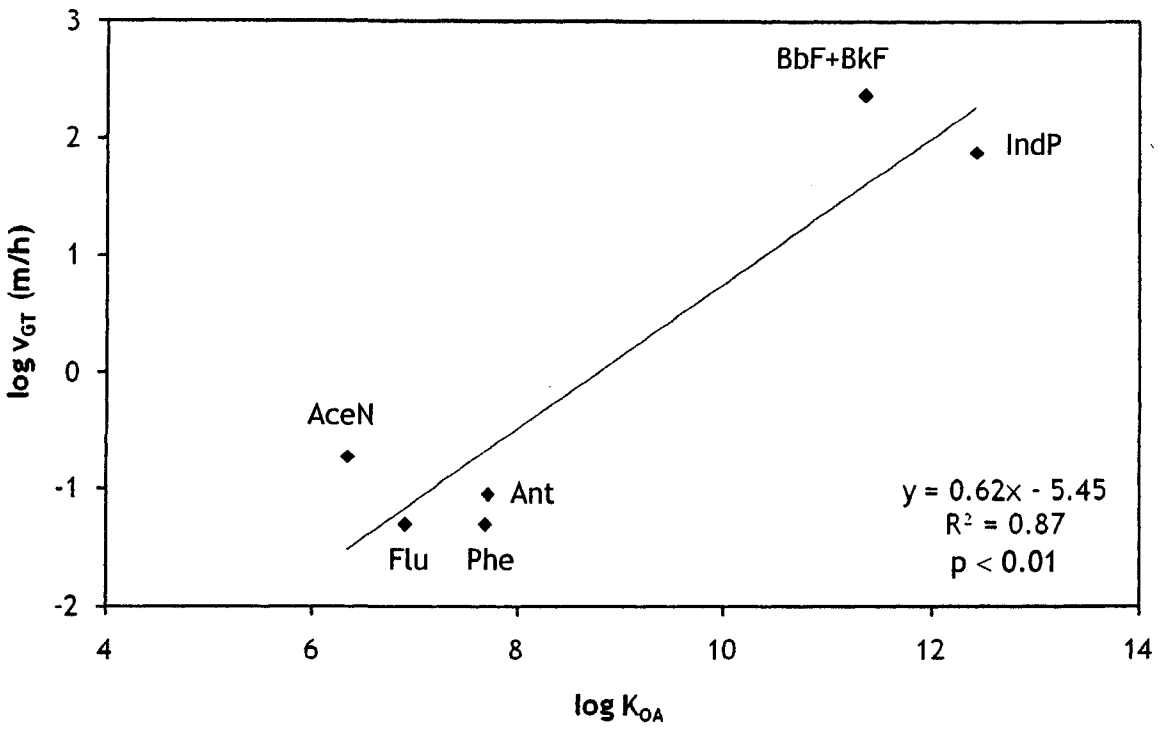

Figure 7.3 - Average log v_{GT} for selected PAHs. Congeners are identified with their respective abbreviation.

Although the relationship between log v_{GT} and log K_{OA} values proved statistically significant, two distinct regions can be identified; low log K_{OA} PAHs have very small v_{GT} values, whereas high log K_{OA} PAHs have remarkably higher v_{GT} values. In the first case, very small v_{GT} values suggest that highly volatile PAHs are approaching equilibrium; the three-ring PAHs have slightly positive v_{GT} values, whereas the four-ring PAHs have slightly negative v_{GT} values (and thus can not be plotted in figure 7.3). Less volatile PAHs may not significantly re-volatilize from the vegetation surface causing higher v_{GT} values. Benzo(b)fluoranthene + benzo(k)fluoranthene exhibits an unusually high v_{GT} value, while indeno(123-cd)pyrene is more reasonable at 75.6 m/h. The v_{GT} value for

benzo(ghi)perylene was slightly negative, hence it probably does not undergo gaseous deposition in appreciable amounts and vegetation uptake should be due to particulate-bound deposition only. For the most part, calculated v_{GT} values fell within values reported in the literature for phenanthrene and pyrene [104]. Finally, a v_{DEP} of 75.6 m/h was selected as indeno(123-cd)pyrene had the highest log K_{OA}.

Table 7.1 - Average measured v_{GT} and calculated v_{VOL} for PAHs. v_{DEP} is identified using an asterisk.

PAH	Average measured v_{GT} (m/h)	Average calculated v_{VOL} (m/h)
Acenaphthylene	0.19	75.42
Fluorene	0.05	75.56
Phenanthrene	0.05	75.56
Anthracene	0.09	75.52
Pyrene	~ 0	75.61
Benz(a)anthracene + Chrysene	~ 0	75.61
Benzo(b)fluoranthene + Benzo(k)fluoranthene	233.07	-
Indeno(123-cd)pyrene	75.61*	-
Benzo(ghi)perylene	~ 0	-

Moreover, volatilization velocities were calculated using equation 6.5 and a v_{DEP} of 75.6 m/h. Results are presented in table 7.1. All were very similar which is a consequence of their very similar v_{GT} values. The v_{VOL} could not be calculated for benzo(b)fluoranthene + benzo(k)fluoranthene and benzo(ghi)perylene for the reasons discussed previously. Finally, temperature dependence for v_{VOL} could not be demonstrated.

7.5 CALCULATION OF PAH VEGETATION CONCENTRATIONS

The relative contribution of the gaseous deposition process (C_{VG}) to the total vegetation uptake was also calculated (as described in section 6.6) for all PAHs considered in this study which revealed a very different trend than that observed for PBDEs. Plotting C_{VG} against log K_{OA} (figure 7.4) reveals that C_{VG} (%) first decreases for the three-ring PAHs reaching negligible values for the four-ring PAHs, after which it increases for bigger PAHs. The following explanation is proposed. Although the three-ring PAHs have very similar v_{GT} values, their gaseous concentrations decrease with increasing log K_{OA}, thus decreasing C_{VG}. Four-ring PAHs (pyrene and benzo(a)anthracene + chrysene), had negligible v_{GT} values so even with quantifiable gaseous phase concentrations the calculated C_{VG} will be negligible. Finally, although the gaseous phase concentrations of benzo(b)fluoranthene + benzo(k)fluoranthene and indeno(123-cd)pyrene were significantly lower than their particulate-bound counterparts, v_{GT} was much larger than v_P translating into a significant gaseous transfer contribution to the total vegetation concentration. Therefore, both v_{GT} and C_G values are important in the assessment of C_{VG}.

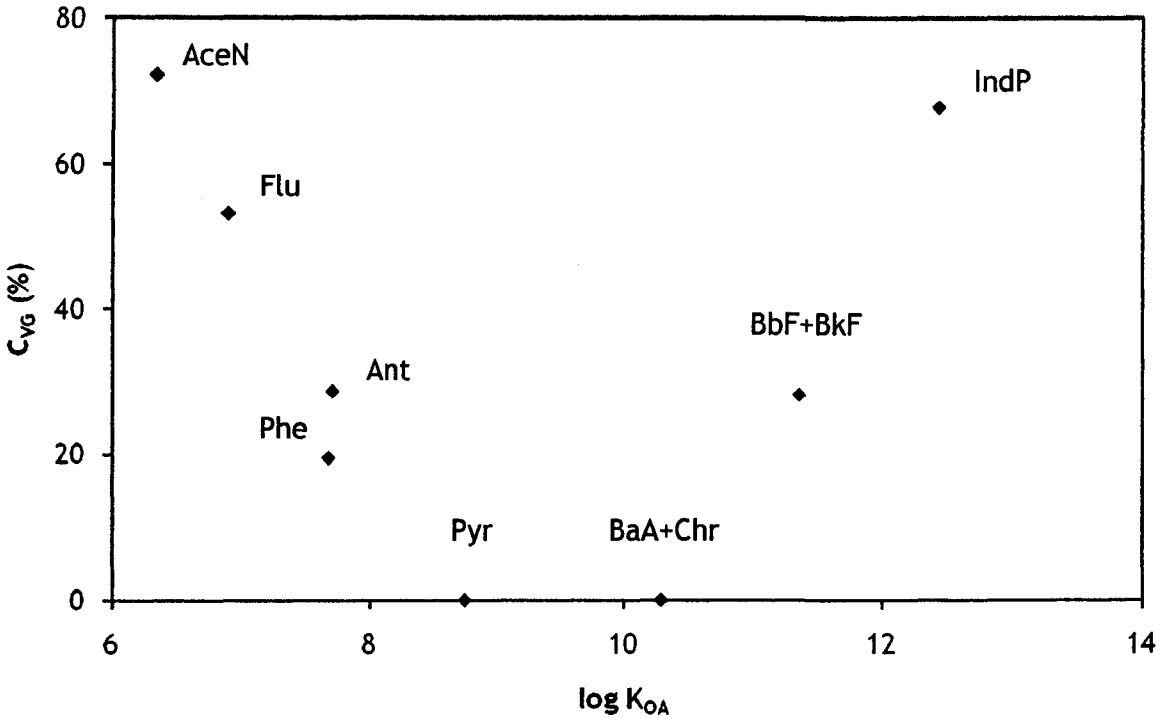

Figure 7.4 - Contribution of gaseous transfer to the total PAH vegetation concentrations. Compounds are identified with their respective abbreviation.

Finally, PAH concentrations in vegetation were calculated with equation 6.6 using averaged atmospheric concentrations and these were compared to field measurements in figures 7.5 and 7.6. In most cases, calculated PAH concentrations in vegetation corroborated measured values. However, in some instances, predicted concentrations were higher than field measurements, which may in part be due to their degradation on vegetation surfaces [149-151]. Similarly to PBDEs, this approach successfully modelled vegetation uptake for a range of physicochemical properties, from low (in the case of fluorene and phenanthrene) to high (benzo(a)pyrene and indeno(123-cd)pyrene) log K_{OA} values. Furthermore, it accommodated low (fluorene, pyrene and benzo(a)pyrene) and

high (phenanthrene and indeno(123-cd)pyrene) concentrations alike. These results demonstrate that this framework can be used successfully for different classes of SVOCs presenting different physicochemical properties and environmental concentrations, as well as different origins and seasonality.

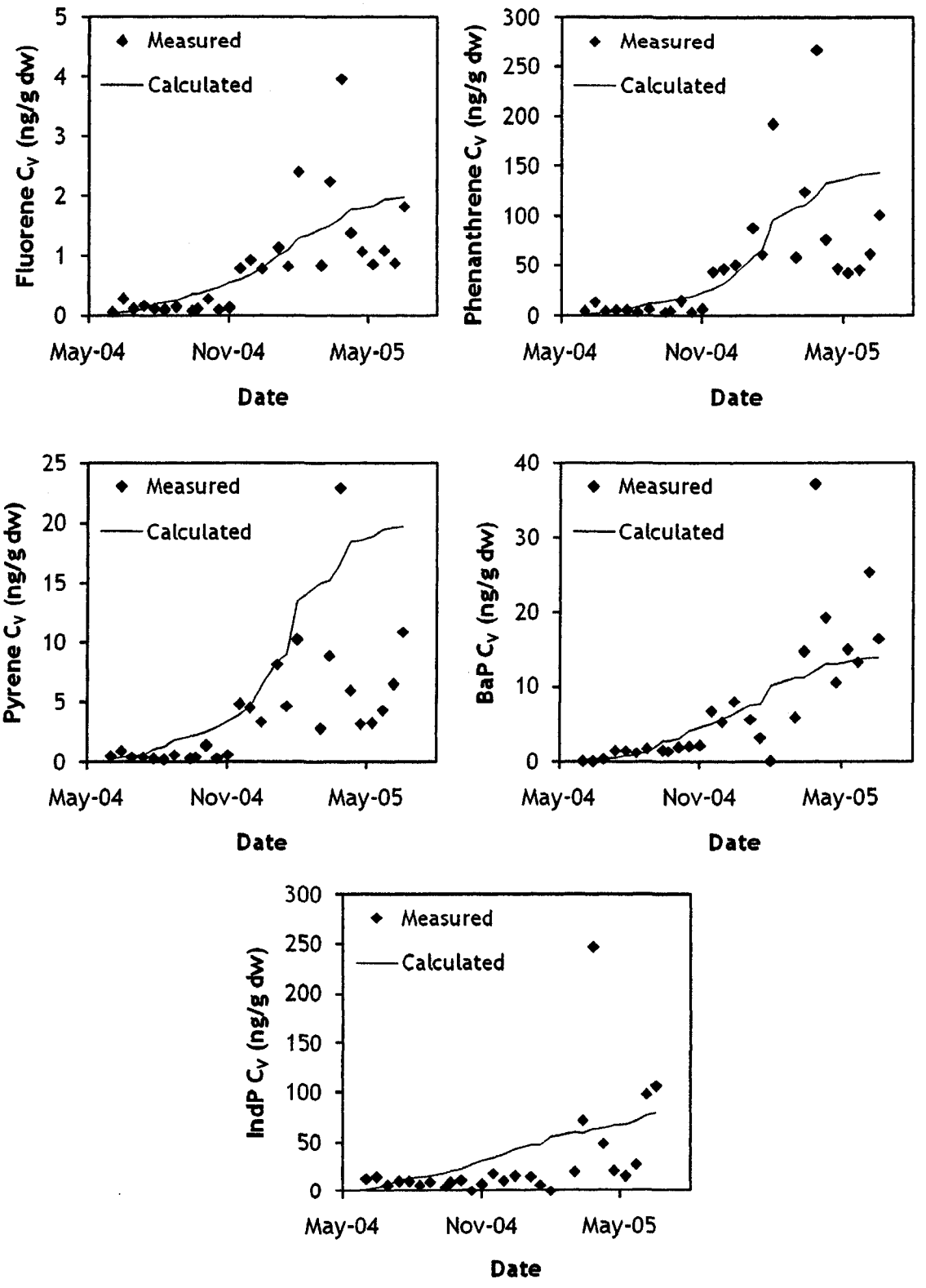

Figure 7.5 - Comparison of measured and calculated PAH vegetation concentrations.

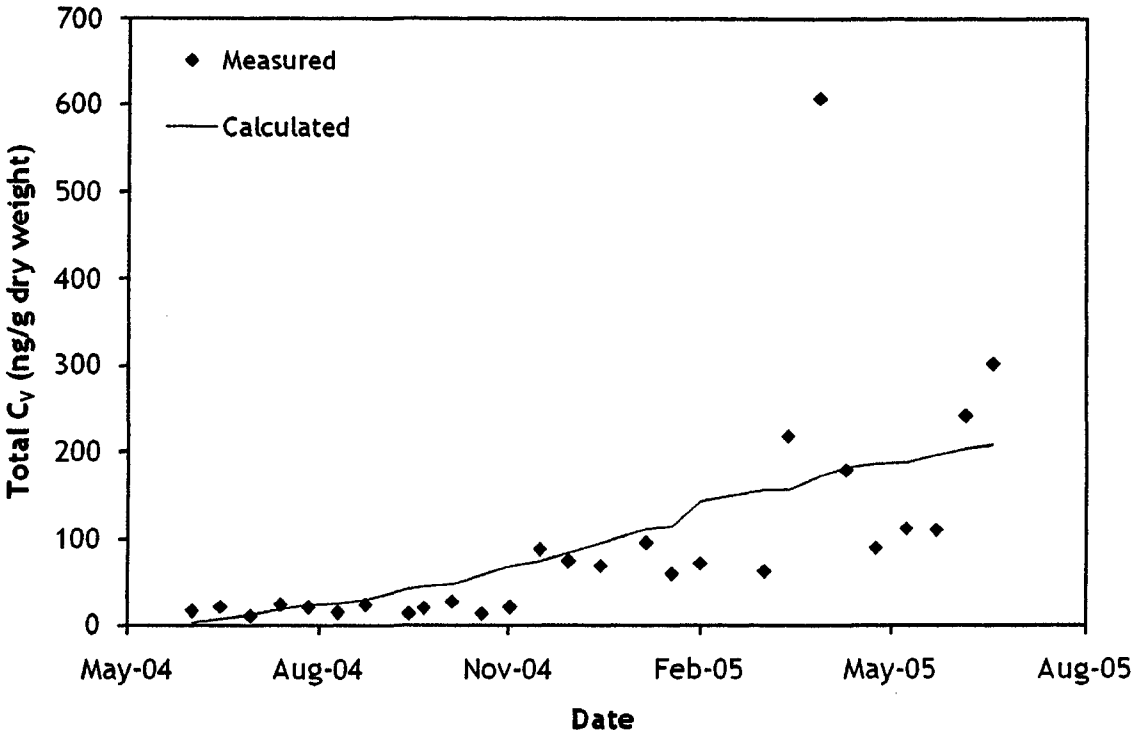

Figure 7.6 - Comparison of measured and calculated total PAH vegetation concentrations.

Chapter 8 - PREDICTIVE ASPECTS OF THE MODELING CONCEPT

8.1 VEGETATION CONCENTRATIONS PREDICTION

The predictive capabilities of this framework were tested using an independent set of data collected at the same location from February to June 2004. Following the 2004 winter-to-spring transition, vegetation concentrations for most compounds were negligible. As mentioned previously, the winter season brings forth stressful conditions for conifers. Although a protective layer is formed at the onset of colder temperatures in the fall, to shield against impairments such as drought (due to freezing temperatures), winds, and solar radiation, this layer usually thins as the winter progresses. Additionally, this protection can degrade quite rapidly with the arrival of spring, particularly if the winter-to-spring transition is characterized by unstable conditions, such as a few days of elevated temperatures [136-138]. Both 2004 and 2005 winter-to-spring transitions are indicated in figures 8.1 and 8.2. In March and April 2004, daily temperatures were highly unstable especially when compared to 2005 where a steady increase of temperature is observed. The snow cover (seen in figure 4.2) for the same time period also follows a similar trend of unsteadiness, corroborating the fact that the 2004 winter-to-spring transition was more erratic than in 2005. This is also reflected in vegetation concentrations. PBDE and PAH concentrations of 2003 buds were found to decrease to negligible values during the spring of 2004. In contrast, 2004 buds were subject to a 30-50% loss in SVOC concentrations during the 2005 winter-to-spring transition.

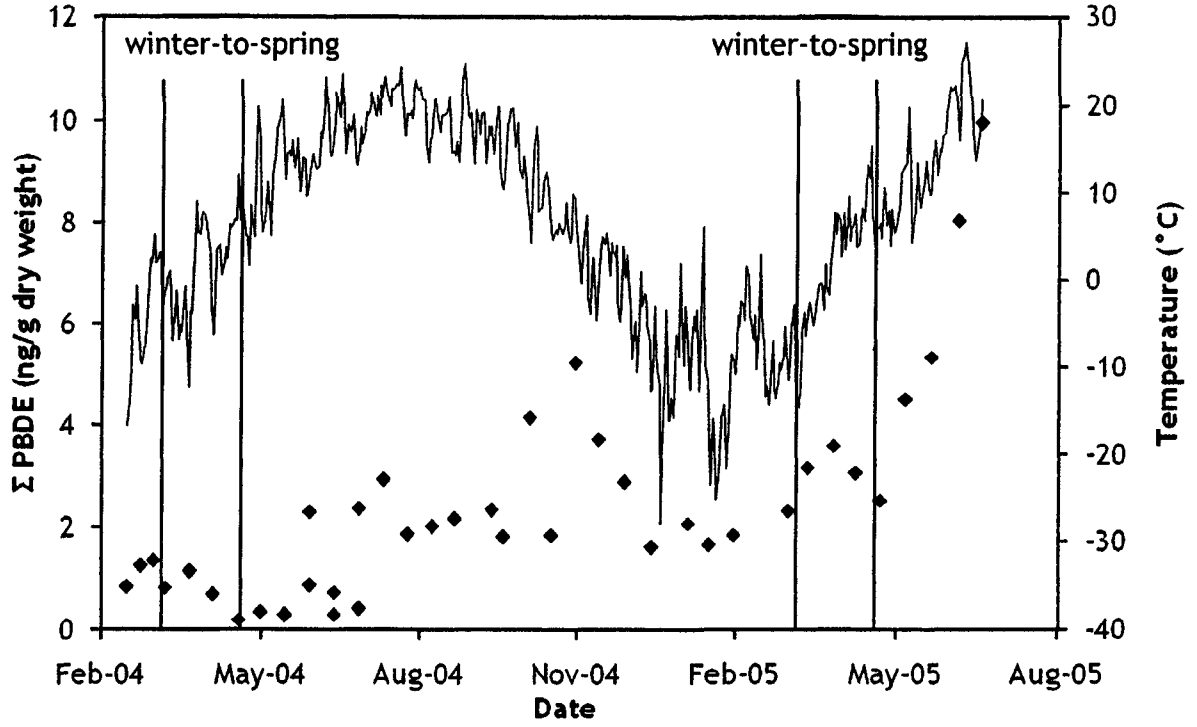

Figure 8.1 - Total PBDE vegetation concentrations and daily temperature values.

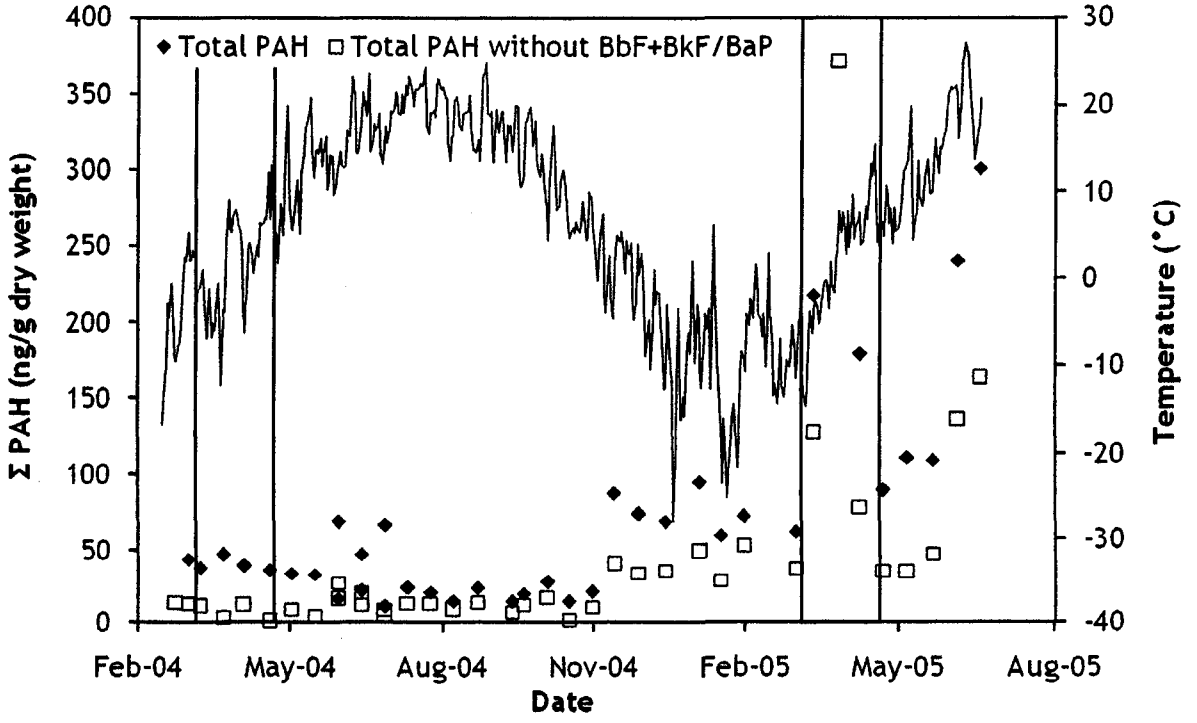

Figure 8.2 - Total PAH vegetation concentrations (with and without BbF + BkF and BaP) and daily temperature values.

Since the model described in this thesis assumes cumulative uptake of SVOCs in vegetation, with initially negligible SVOC concentrations, vegetation uptake following the 2004 winter-to-spring transition (t_0 = April 15, 2004) was modelled for the 2003 buds to test the predictive capabilities of the model. PBDE and PAH vegetation concentrations were calculated using equation 6.6; respective particulate-bound and net gaseous transfer velocities as well as average particulate-bound and gaseous concentrations were applied. Results are presented in figures 8.3 to 8.6 (individual congeners and total concentration).

Generally, the predicted concentrations, agree relatively well with field measurements, even though the number of data points is limited. As with previous comparisons, low to high concentrations are accommodated, as well as a range of physicochemical properties. Exceptions to consider are BDE-209, benzo(b)fluoranthene + benzo(k)fluoranthene, and benzo(a)pyrene, all of which do not reach negligible concentrations following the 2004 winter-to-spring transition. All the same, this test provides evidence that the framework developed in this thesis can efficiently predict vegetation concentrations using measured atmospheric concentrations.

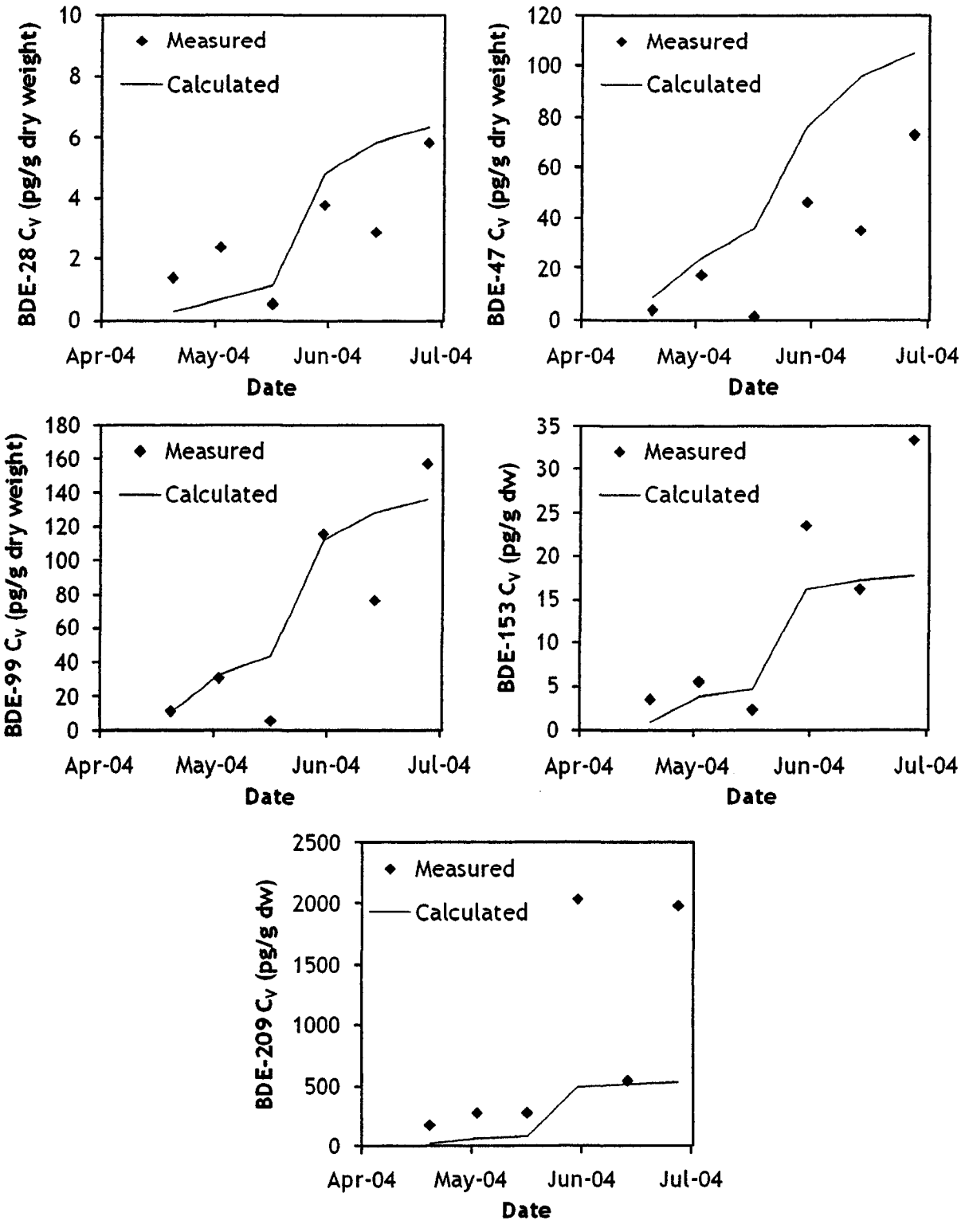

Figure 8.3 - Comparison of measured and predicted vegetation concentrations for selected PBDE congeners following the 2004 winter-to-spring transition.

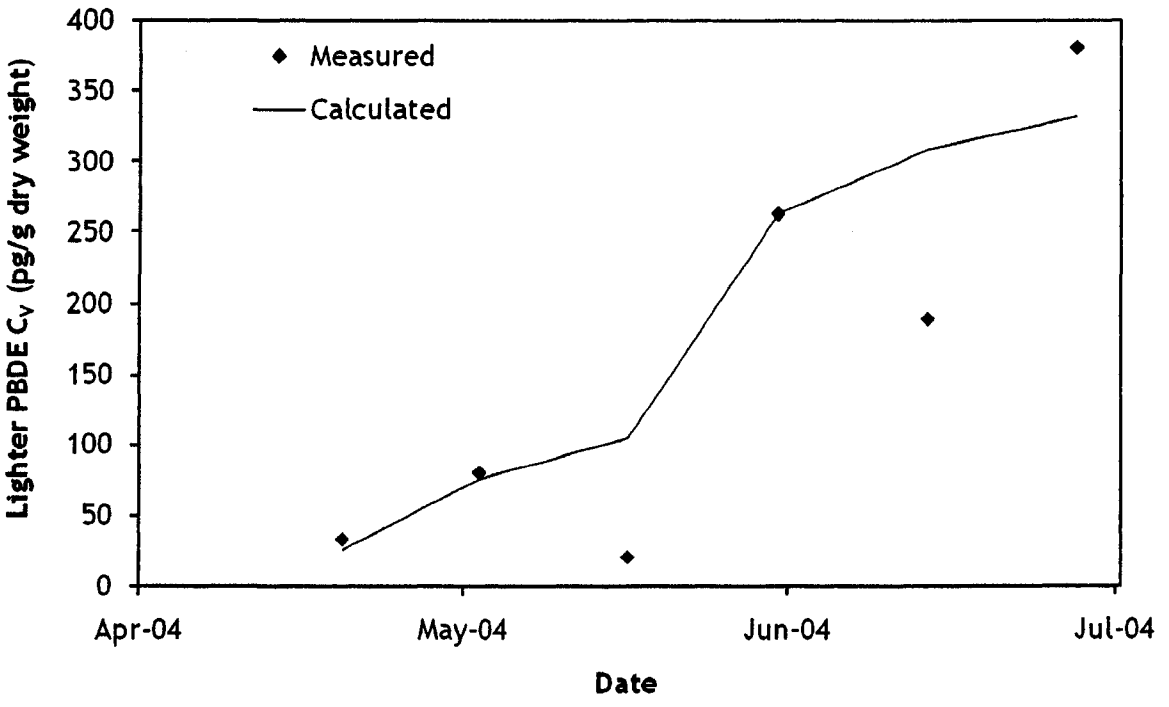

Figure 8.4 - Comparison of measured and predicted lighter PBDE congeners (tri to hepta) vegetation concentrations following the 2004 winter-to-spring transition.

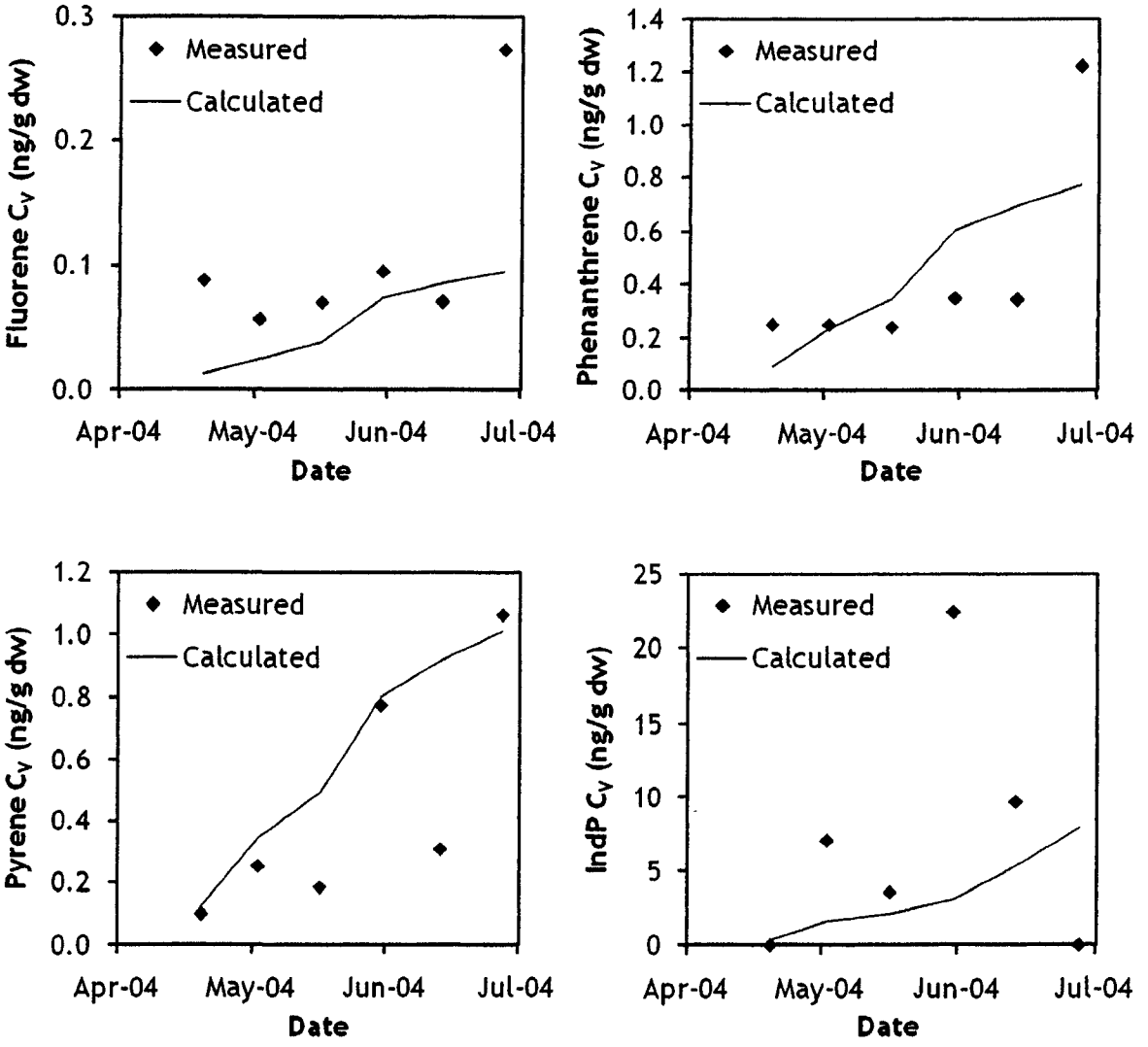

Figure 8.5 - Comparison of measured and predicted vegetation concentrations for selected PAHs following the 2004 winter-to-spring transition.

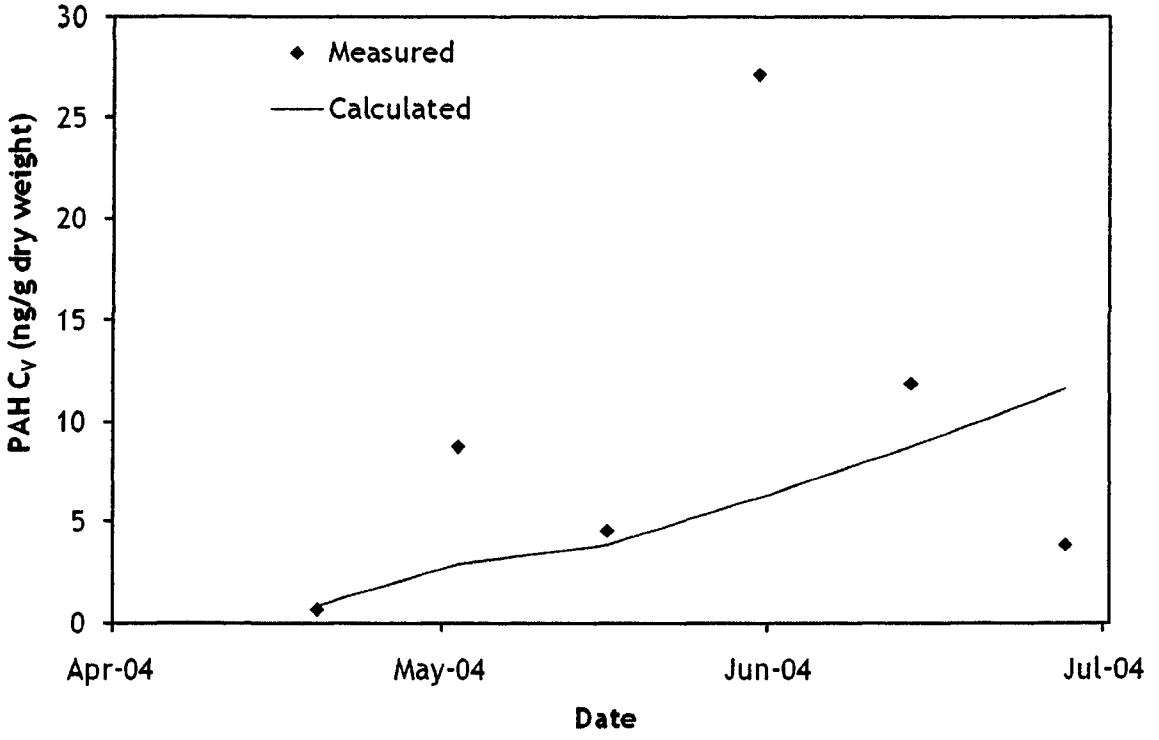

Figure 8.6 - Comparison of measured and predicted total PAH vegetation concentrations (without benzo(b)fluoranthene + benzo(k)fluoranthene and benzo(a)pyrene) following the 2004 winter-to-spring transition.

8.2 ATMOSPHERIC CONCENTRATIONS PREDICTION

As stated previously, conifers can provide an indication of atmospheric pollution levels and, as such, are often used as passive air samplers [82, 90-98]. The possibility of using the present framework to calculate atmospheric concentrations of PBDEs and PAHs using vegetation concentrations was also investigated. Field measurements from February to June 2004 were employed.

C_{VP} and C_{VG} were first determined from measured vegetation concentrations and the average and single-point atmospheric concentrations were calculated using equations 6.2 and 6.3.

$$C_P = \frac{C_{VP} \times mass}{A \times v_P \times t} \qquad C_G = \frac{C_{VG} \times mass}{A \times v_{GT} \times t}$$

As atmospheric concentrations are not due to accumulative processes, only averages are compared below. Measured atmospheric concentrations for February 16 and 24, 2004 are unusually high, which as discussed previously, may be related to snowmelt. The average measured atmospheric concentrations are consequently presented with and without these values. It should also be noted that there is a sharp increase in vegetation concentrations of BDE-209 in June 2004 which contributes largely to exceptionally high predicted particulate-bound concentrations; for this reason results are presented with and without these values.

Table 8.1 - Comparison of average calculated and measured particulate-bound PBDE concentrations from February to June 2004.

BDE	Average calculated C_P (pg/m^3)	Average measured C_P (pg/m^3)	Average measured C_P without February 2004 (pg/m^3)
28	0.011	0.058	0.021
47	0.16	1.63	0.77
66	0.017	0.10	0.043
100	0.16	0.54	0.22
99	0.68	2.67	1.00
85	0.021	0.11	0.041
154	0.15	0.24	0.10
153	0.20	0.38	0.17
183	0.11	0.17	0.14
209	17.94 (3.58)*	8.62	3.64
TOTAL	19.4 (5.1)	14.5	6.1

* Average particulate-bound concentrations without June 2004 values.

Table 8.2 - Comparison of average calculated and measured gaseous PBDE concentrations from February to June 2004.

BDE	Average calculated C_G (pg/m^3)	Average measured C_G (pg/m^3)	Average measured C_G without February 2004 (pg/m^3)
28	0.065	0.091	0.046
47	0.22	0.51	0.37
66	0.012	0.020	0.014
100	0.057	0.068	0.057
99	0.14	0.22	0.19
154	0.007	0.007	0.007
153	0.006	0.007	0.008
TOTAL	0.51	0.92	0.69

Table 8.3 - Comparison of average calculated and measured particulate-bound PAH concentrations from February to June 2004.

BDE	Average calculated C_P (pg/m^3)	Average measured C_P (pg/m^3)	Average measured C_P without February 2004 (pg/m^3)
AceN	0.17	2.22	BDL
Flu	0.32	2.29	0.28
Phe	2.54	44.27	7.03
Ant	0.73	4.01	BDL
Pyr	3.39	69.78	11.04
BaA+Chr	2.30	41.13	9.49
BbF+BkF	79.22	77.37	27.10
BaP	18.90	37.53	8.73
IndP	12.85	63.06	25.56
BghiP	3.91	28.84	10.59
TOTAL	124.3	370.5	99.82

Table 8.4 - Comparison of average calculated and measured gaseous PAH concentrations from February to June 2004.

BDE	Average calculated C_G (pg/m^3)	Average measured C_G (pg/m^3)	Average measured C_G without February 2004 (pg/m^3)
AceN	26.40	34.96	28.60
Flu	77.60	173.1	162.7
Phe	136.2	320.6	309.2
Ant	36.25	17.99	18.99
BbF+BkF	4.46	1.39	1.54
IndP	3.86	5.71	6.34
TOTAL	284.8	553.8	527.4

Agreement between predicted and measured PBDE atmospheric concentrations is good (tables 8.1 and 8.2). Similar observations can also be made for the particulate-bound PAH concentrations (table 8.3). However, the predicted gaseous phase concentrations are lower than field measurements. This may be due to the degradation of PAHs on the vegetation surface which lowers vegetation concentrations [149-151]. Unfortunately, the gaseous concentration could not be predicted for pyrene, benzo(a)anthracene + chrysene, benzo(a)pyrene, and benzo(ghi)perylene since $v_{GT} \approx 0$ for these compounds.

Chapter 9 - CONCLUSIONS

This thesis was designed to survey PBDE and PAH concentrations in spruce needles and air at a sanitary landfill over an annual cycle to study possible seasonal and meteorological effects as well as to develop a framework to model accumulation of SVOCs in vegetation and study their vegetation-air exchange.

Seasonal effects were noted in all media, which were due to weather related phenomena and/or, in the case of PAHs, usage patterns (for example, higher atmospheric PAH concentrations were encountered during the colder months, due to increased domestic heating and fuel consumption). Several meteorological parameters were considered: temperature, wind speed and direction, long-range air mass trajectories, and humidity. Pseudo Clausius-Clapeyron plots showed a high correlation between gaseous concentrations and temperature for PBDEs and calculated pseudo enthalpies suggest that gaseous PBDEs were transported from farther away. However these failed to show a temperature effect for PAHs as this was overshadowed by increased emission during the colder months. Finally, by performing a thorough statistical analysis with air mass back trajectories, wind roses, and meteorological parameters, it was possible to demonstrate that particulate-bound PBDEs, as well as particulate-bound and gaseous PAHs were from local sources (sanitary landfill, highway, and suburbs), whereas gaseous PBDEs underwent transport from more distant sources.

These field measurements were then used to model vegetation uptake of PBDEs and PAHs in vegetation through time. The present study revealed that vegetation uptake of PBDEs and PAHs is related to their particulate-gas partitioning and is a contribution of

both gaseous deposition and particulate-bound deposition. Vegetation uptake was studied by considering gradual accumulation of SVOCs in spruce needles starting at bud burst and assuming an initial SVOC concentration of zero. For PBDEs, BDE-183 was almost exclusively associated to particulates and thus should not undergo gaseous deposition appreciably. Using BDE-183 field measurements a particulate-bound deposition velocity of 3.8 m/h was calculated. By considering both particulate-bound and gaseous depositions, the net gaseous transfer velocities of PBDEs were also calculated. These ranged from 2.4 to 62.2 m/h for BDE-154. Assuming that BDE-154 does not volatilize appreciably then its net gaseous transfer velocity is equal to its deposition velocity. A volatilization velocity could then be calculated for other PBDEs and was found to increase with increasing volatility providing empirical evidence that vegetation does promote surface-air exchange. Penta and hexa-BDE congeners were significantly present as both gaseous and particulate-bound species, and both deposition processes proved important in vegetation uptake for these congeners. As for the tri and tetra-BDE congeners, gaseous deposition was predominant.

As for PAHs, benzo(a)pyrene was used to calculate a particulate-bound deposition velocity of 10.8 m/h. The different v_P values obtained for PBDEs and PAHs may indicate association with different particulates. The net gaseous transfer velocities subsequently determined ranged from negligible values to 75.6 m/h for indeno(123-cd)pyrene. Like PBDEs, the v_{GT} values were significantly correlated to log K_{OA} values and, interestingly, both trends were found to overlap (figure 9.1). Volatilization velocities of most PAHs were very similar to their deposition velocity value (75.6 m/h established with indeno(123-cd)pyrene) as a vegetation-air equilibrium is achieved for highly volatile PAHs. Vegetation uptake of most PAHs occurred through gaseous deposition (equilibrium and non-equilibrium conditions) as well as particulate-bound deposition.

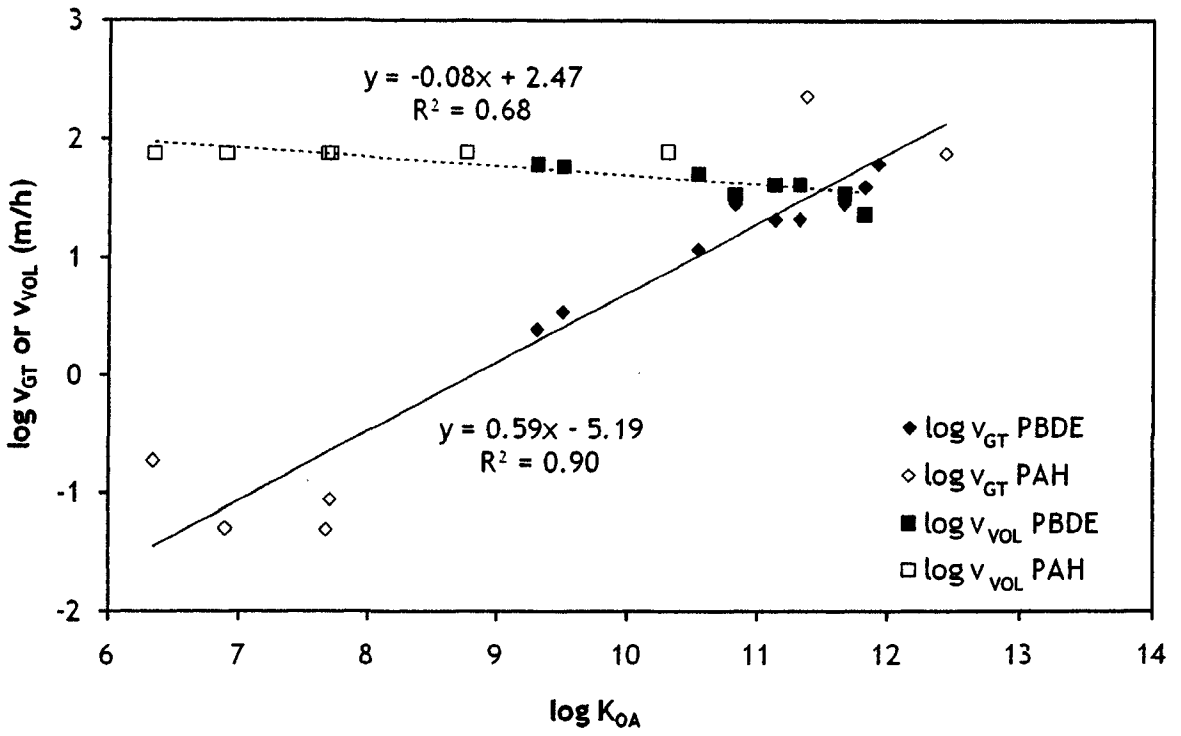

Figure 9.1 - Comparison of log v_{GT} and v_{VOL} values for PBDEs and PAHs.

Finally, the predictive capabilities of this framework were evaluated by applying the v_P and v_{GT} values calculated from one growth year to a second set of independent data collected previously at the same location. In this case, PBDE and PAH vegetation concentrations were calculated following the winter-to-spring transition using measured particulate-bound and gaseous concentrations. Generally, calculated PBDE and PAH vegetation concentrations agreed well with field measurements demonstrating the robustness of this framework. The usefulness of this framework to calculate atmospheric concentrations from measured vegetation concentrations was also assessed. Although this approach worked effectively for PBDEs and particulate-bound PAHs, predicted PAH gaseous phase concentrations were generally well below field measurements.

This developed framework is not without its limitations. The first of which is the need for an exclusively particulate-bound compound to calculate v_P. Secondly, as seen with pyrene and benzo(a)anthracene, if close to perfect equilibrium is achieved then $v_{GT} \approx 0$ and gaseous uptake is considered negligible. Also, losses due to wash-off, vegetation surface deterioration or a compound's degradation are not taken into account, the last of which may not be an issue for presumably highly stable compounds such as PBDEs, but may be important for more reactive SVOCs.

Nevertheless, the usefulness and robustness of this framework have been demonstrated. It considers particulate-gas partitioning dynamics and its role in the overall environmental fate and vegetation uptake of SVOCs and as such, measured TSP values are used, instead of using a single typical value. It can be used to calculate v_P, v_{GT}, v_{DEP}, and v_{VOL} values for each sampling session which can thereafter be averaged to model vegetation uptake and identify the active processes involved and their relative contribution. Moreover, the interpretative framework did well for both PBDEs and PAHs, demonstrating its potential for application to other classes of SVOCs with different physicochemical properties, concentrations, and origins. In conclusion, this interpretative framework can be applied in conjunction with field measurements to study vegetation uptake and vegetation-air exchange through time bringing forth increased understanding in the role of vegetation in the global distribution of SVOCs.

REFERENCES

1. Carson, R., *Silent Spring*. **1962**, New York, NY, USA: Houghton Mifflin Company. 368 pages.
2. Gibbs, L.M., *Love Canal - The story continues...* Revised ed. **1998**, Stoney Creek, CT, USA: New Society Publishers. 223 pages.
3. Limburg, K.E., *PCBs in the Hudson*, in *The Hudson River Ecosystem*, K.E. Limburg, M.A. Moran, and W.H. McDowell, Editors. **1985**, Springer-Verlag: New York, NY, USA. p. 83-130.
4. Hites, R.A., *Persistent Organic Pollutants in the Great Lakes*. The Handbook of Environmental Chemistry. Vol. 5N. **2006**, Berlin, Germany: Springer-Verlag. 441 pages.
5. Barlow, M.; May, E., *Frederick Street - Life and Death on Canada's Love Canal*. **2000**, Toronto, ON, Canada: HarperCollins Canada. 227 pages.
6. Interim Secretariat for the Stockholm Convention, *Stockholm Convention on Persistent Organic Pollutants (POPs)*. **2001**, United Nations Environment Programme (UNEP): Geneva, Switzerland. 34 pages.
7. Simcik, M.F.; Offenberg, J.H., *Polycyclic Aromatic Hydrocarbons in the Great Lakes*, in *Persistent Organic Pollutants in the Great Lakes*, R.A. Hites, Editor. **2006**, Springer-Verlag: Berlin, Germany. p. 307-353.
8. Fries, G.F., The PBB episode in Michigan: an overall appraisal. *Critical Reviews in Toxicology* **1985**, *16*, 105-156.

9. Hites, R.A., *Brominated Flame Retardants in the Great Lakes*, in *Persistent Organic Pollutants in the Great Lakes*, R.A. Hites, Editor. **2006**, Springer-Verlag: Berlin, Germany. p. 355-390.

10. Lima, A.L.C.; Farrington, J.W.; Reddy, C.M., Combustion-Derived Polycyclic Aromatic Hydrocarbons in the Environment - A Review. *Environmental Forensics* **2005**, *6*, 109-131.

11. Ikonomou, M.G.; Rayne, S.; Addison, R.F., Exponential increases of the brominated flame retardants, polybrominated diphenyl ethers, in the Canadian arctic from 1981 to 2000. *Environmental Science & Technology* **2002**, *36*, 1886-1892.

12. Alaee, M.; Arias, P.; Sjodin, A.; Bergman, A., An overview of commercially used brominated flame retardants, their applications, their use patterns in different countries/regions and possible modes of release. *Environment International* **2003**, *29*, 683-689.

13. Wang, X.M.; Ding, X.; Mai, B.X.; Xie, Z.Q.; Xiang, C.H.; Sun, L.G.; Sheng, G.Y.; Fu, J.M.; Zeng, E.Y., Polyhrominated diphenyl ethers in airborne particulates collected during a research expedition from the Bohai Sea to the Arctic. *Environmental Science & Technology* **2005**, *39*, 7803-7809.

14. de Wit, C.A.; Alaee, M.; Muir, D.C.G., Levels and trends of brominated flame retardants in the Arctic. *Chemosphere* **2006**, *64*, 209-233.

15. Braune, B.M.; Mallory, M.L.; Gilchrist, H.G.; Letcher, R.J.; Drouillard, K.G., Levels and trends of organochlorines and brominated flame retardants in Ivory Gull eggs from the Canadian Arctic, 1976 to 2004. *Science of the Total Environment* **2007**, *378*, 403-417.

16. Hung, H.; Blanchard, P.; Halsall, C.J.; Bidleman, T.F.; Stern, G.A.; Fellin, P.; Muir, D.C.G.; Barrie, L.A.; Jantunen, L.M.; Helm, P.A.; Ma, J.; Konoplev, A., Temporal and spatial variabilities of atmospheric polychlorinated biphenyls (PCBs), organichlorine (OC) pesticides and polycyclic aromatic hydrocarbons (PAHs) in the Canadian Arctic: results from a decade of monitoring. *The Science of the Total Environment* **2005**, *342*, 119-144.

17. Halsall, C.J.; Sweetman, A.J.; Barrie, L.A.; Jones, K.C., Modelling the behaviour of PAHs during atmospheric transport from the UK to the Arctic. *Atmospheric Environment* **2001**, *35*, 255-267.

18. Wania, F.; Dugani, C.B., Assessing the long-range transport potential of polybrominated diphenyl ethers: A comparison of four multimedia models. *Environmental Toxicology and Chemistry* **2003**, 22, 1252-1261.

19. Palm, A.; Cousins, I.T.; Mackay, D.; Tysklind, M.; Metcalfe, C.; Alaee, M., Assessing the environmental fate of chemicals of emerging concern: a case study of the polybrominated diphenyl ethers. *Environmental Pollution* **2002**, *117*, 195-213.

20. Gouin, T.; Harner, T., Modelling the environmental fate of the polybrominated diphenyl ethers. *Environment International* **2003**, *29*, 717-724.

21. de Kok, T.M.; Hogervorst, J.G.; Briedé, J.J.; van Herwijnen, M.H.; Maas, L.M.; Moonen, E.J.; Driece, H.A.; Kleinjans, J.C., Genotoxicity and physicochemical characteristics of traffic-related ambient particulate matter. *Environmental and Molecular Mutagenesis* **2005**, *46*, 71-81.

22. Hites, R.A., Polyhrominated diphenyl ethers in the environment and in people: A meta-analysis of concentrations. *Environmental Science & Technology* **2004**, *38*, 945-956.

23. Birnbaum, L.S.; Staskal, D.F., Brominated Flame Retardants: Cause for Concern? *Environmental Health Perspectives* **2004**, *112*, 9-17.

24. de Wit, C.A., An overview of brominated flame retardants in the environment. *Chemosphere* **2002**, *46*, 583-624.

25. Rahman, F.; Langford, K.H.; Scrimshaw, M.D.; Lester, J.N., Polybrominated diphenyl ether (PBDE) flame retardants. *Science of the Total Environment* **2001**, *275*, 1-17.

26. Osako, M.; Kim, Y.-J.; Sakai, S.-i., Leaching of brominated flame retardants in leachate from landfills in Japan. *Chemosphere* **2004**, *57*, 1571-1579.

27. Schecter, A.; Papke, O.; Tung, K.C.; Joseph, J.; Harris, T.R.; Dahlgren, J., Polybrominated diphenyl ether flame retardants in the US population: Current levels, temporal trends, and comparison with dioxins, dibenzofurans, and polychlorinated biphenyls. *Journal of Occupational and Environmental Medicine* **2005**, *47*, 199-211.

28. Meironyté Guvenius, D.; Norén, K. *Polybrominated diphenyl ethers in Swedish human milk. The follow-up study.* in *The Second International Workshop on Brominated Flame Retardants*. 2001. Stockholm, Sweden.

29. Meironyté Guvenius, D.; Norén, K.; Bergman, A., Analysis of polybrominated diphenyl ethers in swedish human milk. A time-related trend study, 1972-1997. *Journal of Toxicology and Environmental Health, Part A* **1999**, *58*, 329-341.

30. Ryan, J.J.; Patry, B.; Mills, P.; Beaudoin, N.G., Recent Trends in Levels of Brominated Diphenyl Ethers (BDEs) in Human Milk from Canada. *Organohalogen Compounds* **2002**, *58*, 173-176.

31. Law, R.J.; Alaee, M.; Allchin, C.R.; Boon, J.P.; Lebeuf, M.; Lepom, P.; Stern, G.A., Levels and trends of polybrominated diphenylethers and other brominated flame retardants in wildlife. *Environment International* **2003**, *29*, 757-770.

32. Lebeuf, M.; Gouteux, B.; Measures, L.; Trottier, S., Levels and Temporal Trends (1988-1999) of Polybrominated Diphenyl Ethers in Beluga Whales (Delphinapterus leucas) from the St. Lawrence Estuary, Canada. *Environmental Science & Technology* **2004**, *38*, 2971-2977.

33. United Nations Environment Programme, *Risk profile on commercial pentabromodiphenyl ether*. **2006**: Geneva. 46 pages.

34. Environment Canada, *Canadian Environmental Protection Act, 1999 - Ecological Screening Assessment Report on Polybrominated Diphenyl Ethers (PBDEs)*. **2006**. 34 pages.

35. U.S. Department of Health and Human Services, *Toxicological Profile for Polybrominated Biphenyls and Polybrominatd Diphenyl Ethers*. **2004**, Agency for Toxic Substances and Disease Registry. 619 pages.

36. Main, K.M.; Kiviranta, H.; Virtanen, H.E.; Sundqvist, E.; Tuomisto, J.T.; Tuomisto, J.; Vartiainen, T.; Skakkebaek, N.E.; Toppari, J., Flame Retardants in Placenta and Breast Milk and Cryptorchisdism in Newborn Boys. *Environmental Health Perspectives* **2007**, *In press*.

37. Olendorf, D.; Jeryan, C.; Boyden, K., *Undescended testes*, in *The Gale Encyclopedia of Medecine*. **1999**, Gale Research: Farmington, MI. 2963-2964 pages.

38. Wenning, R.J., Uncertainties and data needs in risk assessment of three commercial polybrominated diphenyl ethers:probabilistic exposure analysis and comparison with European Commission results. *Chemosphere* **2002**, *46*, 779-796.

39. Rudel, R.A.; Camann, D.E.; Spengler, J.D.; Korn, L.R.; Brody, J.G., Phthalates, alkylphenols, pesticides, polybrominated diphenyl ethers, and other endocrine-disrupting compounds in indoor air and dust. *Environmental Science & Technology* **2003**, *37*, 4543-4553.

40. Jones-Otazo, H.A.; Clarke, J.P.; Diamond, M.L.; Archbold, J.A.; Ferguson, G.; Harner, T.; Richardson, G.M.; Ryan, J.J.; Wilford, B., Is house dust the missing exposure pathway for PBDEs? An analysis of the urban fate and human exposure to PBDEs. *Environmental Science & Technology* **2005**, *39*, 5121-5130.

41. Jakobsson, K.; Thuresson, K.; Rylander, L.; Sjodin, A.; Hagmar, L.; Bergman, A.; B.Sergeant, D., Exposure to polybrominated diphenyl ethers and tetrabromobisphenol A among computer technicians. *Chemosphere* **2002**, *46*, 709-716.

42. Bocio, A.; Llobet, J.M.; Domingo, J.L.; Corbella, J.; Teixido, A.; Casas, C., Polybrominated Diphenyl Ethers (PBDEs) in Foodstuffs: Human Exposure through the Diet. *Journal of Agricultural and Food Chemistry* **2003**, *51*, 3191-3195.

43. Ryan, J.J.; Patry, B., Body Burdens and Food Exposure in Canada for Polybrominated Diphenyl Ethers (BDEs). *Organohalogen Compounds* **2001**, *51*, 226-229.

44. Schecter, A.; Papke, O.; Tung, K.C.; Staskal, D.; Birnbaum, L., Polybrominated diphenyl ethers contamination of United States food. *Environmental Science & Technology* **2004**, *38*, 5306-5311.

45. Wilford, B.H.; Harner, T.; Zhu, J.P.; Shoeib, M.; Jones, K.C., Passive sampling survey of polybrominated diphenyl ether flame retardants in indoor and outdoor air in Ottawa, Canada: Implications for sources and exposure. *Environmental Science & Technology* **2004**, *38*, 5312-5318.

46. Environment Canada, *Proposed Risk Management Strategy for Polybrominated Diphenyl Ethers (PBDEs)*. **2006**. 15 pages.

47. Mackay, D.; Shiu, W.Y.; Ma, K.-C.; Lee, S.C., *Handbook of Physical-Chemical Properties and Environmental Fate of Organic Chemicals*. 2nd ed. **2006**, Boca Raton, FL: CRC Press / Taylor & Francis. 4216 pages.

48. Boon, J.P.; Lewis, W.E.; Tjoen-a-choy, M.R.; Allchin, C.R.; Law, R.J.; Boer, J.D.; Tenhallers-Tjabbes, C.C.; Zegers, B.N., Levels of Polybrominated Diphenyl Ether (PBDE) Flame Retardants in Animals Representing Different Trophic Levels of the North Sea Food Web. *Environmental Science and Technology* **2002**, *36*, 4025-4032.

49. Phillips, D.H., Fifty years of benzo(a)pyrene. *Nature* **1983**, *303*, 468-472.

50. Cook, J.W.; Hewett, C.L.; Hieger, I., The Isolation of a Cancer-producing Hydrocarbon from Coal Tar. Parts I, II, and III. *Journal of the Chemical Society* **1933**, *1933*, 395-405.

51. Environment Canada, *Canadian Environmental Protection Act - Priority Substances List Assessment Report - Polycyclic Aromatic Hydrocarbons*. **1999**. 68 pages.

52. Ayres, D.C.; Hellier, D.G., *Dictionary of Environmentally Important Chemicals*. **1998**, Chicago, Illinois: Fitzroy Dearborn Publishers. 332 pages.

53. Wild, S.R.; Jones, K.C., Polynuclear Aromatic Hydrocarbons in the United Kingdom Environment: A Preliminary Source Inventory and Budget. *Environmental Pollution* **1995**, *88*, 91-108.

54. Van Metre, P.; Mahler, B.; Furlong, E., Urban sprawl leaves its PAH signature. *Environmental Science & Technology* **2000**, *34*, 4064-4070.

55. Lima, A.L.C.; Eglinton, T.I.; Reddy, C.M., High-resolution record of pyrogenic polycyclic aromatic hydrocarbon deposition during the 20th century. *Environmental Science & Technology* **2003**, *37*, 53-61.

56. Schneider, A.; Stapleton, H.M.; Cornwell, J.; Baker, J., Recent development in PAH, PCB, and toxaphene levels in the northern Great Lakes as determined by high resolution sediment cores. *Environmental Science & Technology* **2001**, *35*, 3809-3815.

57. Baek, S.O.; Field, R.A.; Goldstone, M.E.; Kirk, P.W.; Lester, J.N.; Perry, R., A review of atmospheric polycyclic aromatic hydrocarbons: sources, fate and behavior. *Water, Air, and Soil Pollution* **1991**, *60*, 279-300.

58. Ramdhal, T.; Alfheim, I.; Bjorseth, A., *PAH emission from various sources and their evolution over the last decades*, in *Moblie Source Emissions including Polycyclic Aromatic Species*, D. Rondia, M. Cooke, and R.K. Haroz, Editors. **1983**, D. Reidel Publication Company: Dordrecht, Netherlands. p. 277-298.

59. International Agency for Research on Cancer (IARC), *Monographs on the Evaluation of the Carcinogenic Risk of Chemicals to Human: Polynuclear Aromatic Hydrocarbons*. **1983**, World Health Organization (WHO): Lyon, France. Volume 32 pages.

60. Harvey, R.G., *Polycyclic Aromatic Hydrocarbons*. **1997**, New York: Wiley-VCH. 667 pages.

61. Menzie, C.A.; Potocki, B.B.; Santodonato, J., Exposure to Carcinogenic PAHs in the environment. *Environmental Science & Technology* **1992**, *26*, 1278-1284.

62. Mackay, D., *Multimedia Environmental Models: A Fugacity Approach*. 2nd ed. **2001**, Boca Raton, FL, USA: Lewis Publishers. 272 pages.

63. Mackay, D.; Webster, E., Environmental persistence of chemicals. *Environmental Science & Pollution Research* **2006**, *13*, 43-49.

64. Harner, T.; Shoeib, M.; Diamond, M.; Ikonomou, M.; Stern, G., Passive sampler derived air concentrations of PBDEs along an urban-rural transect: Spatial and temporal trends. *Chemosphere* **2006**, *64*, 262-267.

65. Harrad, S.; Hunter, S., Concentrations of Polybrominated Diphenyl Ethers in Air and Soil on a Rural-Urban Transect Across a Major UK Conurbation. *Environmental Science & Technology* **2006**, *40*, 4548-4553.

66. Zhu, L.; Hites, R.A., Brominated Flame Retardants in Tree Bark from North America. *Environmental Science & Technology* **2006**, *40*, 3711-3716.

67. Hassanin, A.; Johnston, A.E.; Thomas, G.O.; Jones, K.C., Time Trends of Atmospheric PBDEs Inferred from Archieved U.K. Herbage. *Environmental Science & Technology* **2005**, *39*, 2436-2441.

68. Meironyté Guvenius, D.; Bergman, A.; Noren, K., Polybrominated diphenyl ethers in Swedish human liver and adipose tissue. *Archives of Environmental Contamination and Toxicology* **2001**, *40*, 564-570.

69. Lee, R.G.M.; Thomas, G.O.; Jones, K.C., PBDEs in the atmosphere of three locations in western Europe. *Environmental Science & Technology* **2004**, *38*, 699-706.

70. Hoh, E.; Hites, R.A., Brominated flame retardants in the atmosphere of the east-central United States. *Environmental Science & Technology* **2005**, *39*, 7794-7802.

71. Strandberg, B.; Dodder, N.G.; Basu, I.; Hites, R.A., Concentrations and Spatial Variations of Polybrominated Diphenyl Ethers and Other Organohalogen Compounds in Great Lakes Air. *Environmental Science and Technology* **2001**, *35*, 1078-1083.

72. Shoeib, M.; Harner, T.; Ikonomou, M.; Kannan, K., Indoor and outdoor air concentrations and phase partitioning of perfluoroalkyl sulfonamides and

polybrominated diphenyl ethers. *Environmental Science & Technology* **2004**, *38*, 1313-1320.

73. Harner, T.; Shoeib, M., Measurements of octanol-air partition coefficients (K-OA) for polybrominated diphenyl ethers (PBDEs): Predicting partitioning in the environment. *Journal of Chemical and Engineering Data* **2002**, *47*, 228-232.

74. Shoeib, M.; Harner, T., Using measured octanol-air partition coefficients to explain environmental partitioning of organochlorine pesticides. *Environmental Toxicology and Chemistry* **2002**, *21*, 984-990.

75. Ikonomou, M.G.; Rayne, S.; Fischer, M.; Fernandez, M.P.; Cretney, W., Occurrence and congener profiles of polybrominated diphenyl ethers (PBDEs) in environmental samples from coastal British Columbia, Canada. *Chemosphere* **2002**, *46*, 649-663.

76. Lacorte, S.; Guillamon, M.; Martinez, E.; Viana, P.; Barcelo, D., Occurrence and specific congener profile of 40 polyhrominated diphenyl ethers in river and coastal sediments from Portugal. *Environmental Science & Technology* **2003**, *37*, 892-898.

77. Cousins, I.T.; Palm, A., *Physical-Chemical Properties and Estimated Environmental Fate of Brominated and Iodinated Organic Compounds*, in *Organic Bromine and Iodine Compounds*, A.H. Neilson, Editor. **2003**, Springer-Verlag: Berlin, Germany.

78. Soderstrom, G.; Sellstrom, U.; De Wit, C.A.; Tysklind, M., Photolytic debromination of decabromodiphenyl ether (BDE 209). *Environmental Science & Technology* **2004**, *38*, 127-132.

79. Ding, X.; Wang, X.-M.; Xie, Z.-Q.; Xiang, C.-H.; Mai, B.-X.; Sun, L.-G.; Zheng, M.; Sheng, G.-Y.; Fu, J.-M.; Pöschl, U., Atmospheric polycyclic aromatic hydrocarbons observed over the North Pacific Ocean and the Arctic area: Spatial distribution and source identification. *Atmospheric Environment* **2007**, *41*, 2061-2072.

80. Vardar, N.; Tasdemir, Y.; Odabasi, M.; Noll, K.E., Characterization of atmospheric concentrations and partitioning of PAHs in the Chicago atmosphere. *Science of the Total Environment* **2004**, *327*, 163-174.

81. Viskari, E.-L., Epicuticular wax of Norway Spruce needles as indicator of traffic pollutant deposition. *Water Air and Soil Pollution* **2000**, *121*, 327-337.

82. Simonich, S.L.; Hites, R.A., Importance of vegetation in removing polycyclic aromatic hydrocarbons from the atmosphere. *Nature* **1994**, *370*, 49-51.

83. Schröter-Kermani, C.; Kreft, D.; Schilling, B.; Herrchen, M.; Wagner, G., Polycyclic aromatic hydrocarbons in pine and spruce shoots - temporal trends and spatial distribution. *Journal of Environmental Monitoring* **2006**, *8*, 806-811.

84. Wong, F.; Harner, T.; Liu, Q.-T.; Diamond, M.L., Using experimental and forest soils to investigate the uptake of polycyclic aromatic hydrocarbons (PAHs) along an urban-rural gradient. *Environmental Pollution* **2004**, *129*, 387-398.

85. El Nemr, A.; Said, T.O.; Khaled, A.; El-Sikaily, A.; Abd-Allah, A.M.A., The distribution and sources of polycyclic aromatic hydrocarbons in surface sediments along the Egyptian Mediterranean coast. *Environmental Monitoring and Assessment* **2007**, *124*, 343-359.

86. Becker, S.; Halsall, C.J.; Tych, W.; Hung, H.; Blanchard, P.; Li, H.; Fellin, P.; Stern, G.; Billeck, B.; Friesen, S., Resolving the Long-Term Trends of Polycyclic Aromatic Hydrocarbons in the Canadian Arctic Atmosphere. *Environmental Science & Technology* **2006**, *40*, 3217-3222.

87. Sitaras, I.E.; Bakeas, E.B.; Siskos, P.A., Gas/particle partitioning of seven volatile polycyclic aromatic hydrocarbons in a heavy traffic urban area. *Science of the Total Environment* **2004**, *327*, 249-264.

88. Alfani, A.; De Nicola, F.; Maisto, G.; Prati, M.V., Long-term PAH accumulation after bud break in Quercus ilex L. leaves in a polluted environment. *Atmospheric Environment* **2005**, *39*, 307-314.

89. Alaee, M.; Muir, D.C.G.; Cannon, C.M.; Helm, P.; Harner, T.; Bidleman, T.F., *New persistent chemicals in air*, in *Sources, Occurences, Trends and Pathways in the Physical Environment, Canadian Arctic Contaminants Assessment Report II*, T.F. Bidleman, R. Macdonald, and J. Stow, Editors. **2003**, Indian and Northern Affairs Canada: Ottawa, ON, Canada. p. 116-124.

90. Blasco, M.; Domeno, C.; Nerin, C., Use of lichens as pollution biomonitors in remote areas: Comparison of PAHs extracted from lichens and atmospheric particles sampled in and around the Somport Tunnel (Pyrenees). *Environmental Science & Technology* **2006**, *40*, 6384-6391.

91. McLachlan, M.S.; Horstmann, M., Forests as Filters of Airborne Organic Pollutants: A Model. *Environmental Science & Technology* **1998**, *32*, 413-420.

92. Barber, J.L.; Thomas, G.O.; Kerstiens, G.; Jones, K.C., Current issues and uncertainties in the measurement and modelling of air-vegetation exchange and within-plant processing of POPs. *Environmental Pollution* **2004**, *128*, 99-138.

93. Buckley, E.H., Accumulation of Airborne Polychlorinated-Biphenyls in Foliage. *Science* **1982**, *216*, 520-522.

94. Collins, C.; Fryer, M.; Grosso, A., Plant Uptake of Non-Ionic Organic Chemicals. *Environmental Science & Technology* **2006**, *40*, 45-52.

95. Davidson, D.A.; Wilkinson, A.C.; Kimpe, L.E.; Blais, J.M., Persistent organic pollutants in air and vegetation from the Canadian Rocky Mountains. *Environmental Toxicology and Chemistry* **2004**, *23*, 540-549.

96. Kylin, H.; Grimvall, E.; Ostman, C., Environmental Monitoring of Polychlorinated-Biphenyls Using Pine Needles as Passive Samplers. *Environmental Science & Technology* **1994**, *28*, 1320-1324.

97. Smith, K.E.C.; Jones, K.C., Particles and vegetation: implications for the transfer of particle-bound organic contaminants to vegetation. *The Science of the Total Environment* **2000**, *246*, 207-236.

98. Wania, F.; McLachlan, M.S., Estimating the Influence of Forests on the Overall Fate of Semivolatile Organic Compounds Using a Multimedia Fate Model. *Environmental Science & Technology* **2001**, *35*, 582-590.

99. Gouin, T.; Thomas, G.O.; Cousins, I.; Barber, J.; Mackay, D.; Jones, K.C., Air-surface exchange of polybrominated biphenyl ethers and polychlorinated biphenyls. *Environmental Science & Technology* **2002**, *36*, 1426-1434.

100. Wania, F.; Mackay, D., Tracking the distribution of persistent organic pollutants. *Environmental Science & Technology* **1996**, *30*, 390A-396A.

101. McLachlan, M.S., Framework for the interpretation of measurements of SOCs in plants. *Environmental Science & Technology* **1999**, *33*, 1799-1804.

102. Prugel, B.; Lognay, G., Composition of the cuticular waxes of Picea abies and P. sitchensis. *Phytochemical Analysis* **1996**, *7*, 29-36.

103. Holloway, P.J., *Structure and histochemistry of plant cuticular membranes: an overview*, in *The Plant Cuticle*, D.F. Cutler, K.L. Alvin, and C.E. Price, Editors. **1982**, Academic Press: New York, USA. p. 1-32.

104. Horstmann, M.; McLachlan, M.S., Atmospheric deposition of semivolatile organic compounds to two forest canopies. *Atmospheric Environment* **1998**, *32*, 1799-1809.

105. Vardar, N.; Odabasi, M.; Holsen, T.M., Particulate Dry Deposition and Overall Deposition Velocities of Polycyclic Aromatic Hydrocarbons. *Journal of Environmental Engineering* **2002**, *128*, 269-274.

106. Franz, T.P.; Eisenreich, S.J.; Holsen, T.M., Dry Deposition of Particulate Polychlorinated Biphenyls and Polycyclic Aromatic Hydrocarbons to Lake Michigan. *Environmental Science & Technology* **1998**, *32*, 3681-3688.

107. Shahin, U.M.; Li, Y.-H.; Holsen, T.M., Dry Deposition of Gas-Phase Polycyclic Aromatic Hydrocarbons to Greased Surrogate Surfaces. *Aerosol Science and Technology* **1999**, *31*, 446-455.

108. Su, Y.; Wania, F.; Harner, T.; Lei, Y.D., Deposition of Polybrominated Diphenyl Ethers, Polychlorinated Biphenyls, and Polycyclic Aromatic Hydrocarbons to a Boreal Deciduous Forest. *Environmental Science & Technology* **2007**, *2007*, 534-540.

109. Terzi, E.; Samara, C., Dry deposition of polycyclic aromatic hydrocarbons in urban and rural sites of Western Greece. *Atmospheric Environment* **2005**, *39*, 6261-6270.

110. ter Schure, A.F.H.; Agrell, C.; Bokenstrand, A.; Sveder, J.; Larsson, P.; Zegers, B.N., Polybrominated diphenyl ethers at a solid wast incineration plant II: atmospheric deposition. *Atmospheric Environment* **2004**, *38*, 5149-5155.

111. Farmer, C.T.; Wade, T.L., Relationship of ambient atmospheric hydrocarbon (C12 - C32) concentrations to deposition. *Water Air and Soil Pollution* **1986**, *29*, 439-452.

112. Tasdemir, Y.; Esen, F., Dry deposition fluxes and deposition velocities of PAHs at an urban site in Turkey. *Atmospheric Environment* **2007**, *41*, 1288-1301.

113. Seinfeld, J.H.; Pandis, S.N., *Atmospheric Chemistry and Physics: From Air Pollution to Climate Change*. 2nd ed. **2006**, New York, NY, USA: Wiley-Interscience. 1203 pages.

114. Harner, T.; Bidleman, T.F., Octanol-air partition coefficient for describing particle/gas partitioning of aromatic compounds in urban air. *Environmental Science & Technology* **1998**, *32*, 1494-1502.

115. Junge, C.E., *Basic considerations about trace constituents in the atmosphere as related to the fate of global pollutants*, in *Fate of Pollutants in the Air and Water Environments*, I.H. Suffet, Editor. **1977**, Wiley-Interscience: New York. p. 7-26.

116. Pankow, J.F., Review and Comparative-Analysis of the Theories on Partitioning between the Gas and Aerosol Particulate Phases in the Atmosphere. *Atmospheric Environment* **1987**, *21*, 2275-2283.

117. Bidleman, T.F., Atmospheric processes - Wet and dry deposition of organic compounds are controlled by their vapor-particle partitioning. *Environmental Science & Technology* **1988**, *22*, 361-367.

118. Pankow, J.F., An absorption model of gas/particle partitioning of organic compounds in the atmosphere. *Atmospheric Environment* **1994**, *28*, 185-188.

119. Finizio, A.; Mackay, D.; Bidleman, T.; Harner, T., Octanol-air partition coefficient as a predictor of partitioning of semi-volatile organic chemicals to aerosols. *Atmospheric Environment* **1997**, *31*, 2289-2296.

120. Cotham, W.E.; Bidleman, T.F., Polycyclic Aromatic Hydrocarbons and Polychlorinated Biphenyls in Air at an Urban and a Rural Site near Lake Michigan. *Environmental Science & Technology* **1995**, *29*, 2782-2789.

121. Bjorklund, E.; Nilsson, T.; Bowadt, S., Pressurised liquid extraction of persistent organic pollutants in environmental analysis. *Trac-Trends in Analytical Chemistry* **2000**, *19*, 434-445.

122. Covaci, A.; Voorspoels, S.; de Boer, J., Determination of brominated flame retardants, with emphasis on polybrominated diphenyl ethers (PBDEs) in environmental and human samples - a review. *Environment International* **2003**, *29*, 735-756.

123. de la Cal, A.; Eljarrat, E.; Barcelo, D., Determination of 39 polybrominated diphenyl ether congeners in sediment samples using fast selective pressurized liquid extraction and purification. *Journal of Chromatography A* **2003**, *1021*, 165-173.

124. Zhu, L.Y.; Hites, R.A., Determination of polybrominated diphenyl ethers in environmental standard reference materials. *Analytical Chemistry* **2003**, *75*, 6696-6700.

125. Vasilakos, C.; Levi, N.; Maggos, T.; Hatzianestis, J.; Michopoulos, J.; Helmis, C., Gas-particle concentration and characterization of sources of PAHs in the atmosphere of a suburban area in Athens, Greece. *Journal of Hazardous Materials* **2007**, *140*, 45-54.

126. Dean, J.R., *Methods for Environmental Trace Analysis*. Analytical Techniques in the Sciences, ed. D.J. Ando. **2003**, West Sussex, England: John Wiley & Sons Ltd. 259 pages.

127. Wenzel, K.D.; Hubert, A.; Manz, M.; Weissflog, L.; Engewald, W.; Schuurmann, G., Accelerated solvent extraction of semivolatile organic compounds from biomonitoring samples of pine needles and mosses. *Analytical Chemistry* **1998**, *70*, 4827-4835.

128. Abrha, Y.; Raghavan, D., Polychlorinated biphenyl (PCB) recovery from spiked organic matrix using accelerated solvent extraction (ASE) and Soxhlet extraction. *Journal of Hazardous Materials* **2000**, *80*, 147-157.

129. Vetter, W., A GC/ECNI-MS method for the identification of lipophilic anthropogenic and natural brominated compounds in marine samples. *Analytical Chemistry* **2001**, *73*, 4951-4957.

130. Agrell, C.; ter Shure, A.F.H.; Sveder, J.; Bokenstrand, A.; Larsson, P.; Zegers, B.N., Polybrominated diphenyl ethers (PBDEs) at a solid waste incineration plant I: Atmospheric concentrations. *Atmospheric Environment* **2004**, *38*, 5139-5148.

131. Eljarrat, E.; Lacorte, S.; Barcelo, D., Optimization of congener-specific analysis of 40 polybrominated diphenyl ethers by gas chromatography/mass spectrometry. *Journal of Mass Spectrometry* **2002**, *37*, 76-84.

132. Funk, W.; Dammann, V.; Donnevert, G., *Quality Assurance in Analytical Chemistry*. 2nd ed. **2007**, Weinheim, Germany: Wiley-VCH Verlag. 277 pages.

133. Eaton, A.D.; Clesceri, L.S.; Rice, E.W.; Greenberg, A.E., *Standard Methods for the Examination of Water and Wastewater*. 21st ed. **2005**, Washington, DC, USA: American Public Health Association.

134. Draxler, R.R.; Rolph, G.D. *HYSPLIT (HYbrid Single-Particle Lagrangian Integrated Trajectory)*. 2003 [cited; Model access via NOAA READY website]. Available from: http://www.arl.noaa.gov/ready/hysplit4.html.

135. Hale, R.C.; Alaee, M.; Manchester-Neesvig, J.B.; Stapleton, H.M.; Ikonomou, M.G., Polybrominated diphenyl ether flame retardants in the North American environment. *Environment International* **2003**, *29*, 771-779.

136. Kylin, H.; Sjodin, A., Accumulation of Airborne Hexachlorocyclohexanes and DDT in Pine Needles. *Environmental Science & Technology* **2003**, *37*, 2350-2355.

137. Fitter, A.H.; Hay, R.K.M., *Environmental Physiology of Plants.* 3rd ed. **2003**, San Diego, CA, USA: Academic Press. 367 pages.

138. Larcher, W., *Physiological Plant Ecology.* 3rd ed. **1996**, New York, NY, USA: Springer-Verlag. 506 pages.

139. Butt, C.M.; Diamond, M.L.; Truong, J.; Ikonomou, M.G.; Ter Schure, A.F.H., Spatial distribution of polybrominated diphenyl ethers in southern Ontario as measured in indoor and outdoor window organic films. *Environmental Science & Technology* **2004**, *38*, 724-731.

140. Sanderson, E.G.; Raqbi, A.; Vyskocil, A.; Farant, J.-P., Comparison of particulate polycyclic aromatic hydrocarbon profiles in different regions of Canada. *Atmospheric Environment* **2004**, *38*, 3417-3429.

141. Su, Y.; Lei, Y.D.; Wania, F.; Shoeib, M.; Harner, T., Regressing gas/particle partitioning data for polycyclic aromatic hydrocarbons. *Environmental Science & Technology* **2006**, *40*, 3558-3564.

142. Chrostowski, P.C.; Foster, S.A., A methodology for assessing congener-specific partitioning and plant uptake of dioxins and dioxin-like compounds. *Chemosphere* **1996**, *32*, 2285-2304.

143. Tittlemier, S.A.; Halldorson, T.; Stern, G.A.; Tomy, G.T., Vapor pressures, aqueous solubilities, and Henry's law constants of some brominated flame retardants. *Environmental Toxicology and Chemistry* **2002**, *21*, 1804-1810.

144. Hoff, R.M.; Brice, K.A.; Halsall, C.J., Nonlinearity in the slopes of Clausius-Clapeyron plots for SVOCs. *Environmental Science & Technology* **1998**, *32*, 1793-1798.

145. Schauer, C.; Niessner, R.; Pöschl, U., Polycyclic Aromatic Hydrocarbons in Urban Air Particulate Air Matter: Decadal and Seasonal Trends, Chemical Degradation, and Sampling Artifacts. *Environmental Science & Technology* **2003**, *37*, 2861-2868.

146. Johansson, T., Biomass Production of Norway Spruce (*Picea abies* (L.) Karst.) Growing on Abondoned Farmland. *Silva Fennica* **2000**, *33*, 261-280.

147. Riederer, M.; Kurbasik, K.; Steinbrecher, R.; Voss, A., Surface areas, lengths and volumes of Picea abies (L.) Karst. needles: determination, biological variability and effect of environmental factors. *Trees* **1988**, *2*, 165-172.

148. de Boer, J.; Wells, D.E., Pitfalls in the analysis of brominated flame retardants in environmental, humand and food samples - including results of three international interlaboratory studies. *Trac-Trends in Analytical Chemistry* **2006**, *25*, 364-372.

149. Niu, J.; Chen, J.; Martens, D.; Henkelmann, B.; Quan, X.; Yang, F.; Seidlitz, H.K.; Schramm, K.W., The role of UV-B on the degradation of PCDD/Fs and PAHs sorbed on surfaces of spruce (Picea Abies (L.) Karst) needles. *Science of the Total Environment* **2004**, *322*, 231-241.

150. Niu, J.; Chen, J.; Martens, D.; Quan, X.; Yang, F.; Kettrup, A.; Schramm, K.-W., Photolysis of polycyclic aromatic hydrocarbons adsorbed on spruce (Picea abies (L.) Karst.) needles under sunlight irradiation. *Environmental Pollution* **2003**, *123*, 39-45.

151. Wild, E.; Dent, J.; Thomas, G.O.; Jones, K.C., Real-Time Visualization and Quantification of PAH Photodegradation on and within Plant Leaves. *Environmental Science & Technology* **2005**, *39*, 268-273.

CLAIMS TO ORIGINAL RESEARCH

1. Although an identified route of exposure to PBDEs is through consumer products, their leaching from refuse is not well characterized and most of the work has focused on leachate concentrations. This is the first study which has surveyed atmospheric and vegetation concentrations of PBDEs at a sanitary landfill which was considered a point-source for PBDEs. Gaseous phase PBDEs, on the other hand, were found to undergo long-range transport. Moreover, the influence of seasonal and meteorological parameters such as temperature, relative humidity, wind speed and direction on PBDE and PAH concentrations were investigated over an annual cycle [1].

2. In order to quantify PBDEs in vegetation an efficient extraction method was required. Although several methods have been reported in the literature for the extraction of PBDEs from solid matrices, none were found for the extraction from vegetation. Furthermore, the extraction of SVOCs from spruce needles can be challenging, comparatively to other surfaces, because of their waxy surfaces. An efficient extraction method using accelerated solvent extraction was developed and optimized to offer recoveries above 80% for most congeners.

3. An interpretative framework was developed to model vegetation uptake of SVOCs using field measurements. This approach considers vegetation uptake as an accumulative process which starts at bud burst when the initial SVOC concentrations are assumed to be negligible. Thus using this modeling scheme it is

possible to study vegetation-air exchange processes through time and determine their corresponding deposition velocities without using surrogate surfaces [2].

a. Particulate-bound deposition and net gaseous transfer velocities for PBDEs and PAHs onto a coniferous canopy were calculated using this approach. These are the first reported deposition velocities established using vegetation concentrations instead of surrogate surfaces [2, 3].
b. Considering that the net gaseous transfer velocity onto vegetation is composed of a both a deposition and a volatilization velocity, these were calculated and reported for the first time in this thesis [2, 3]. Furthermore, these provided empirical evidence of the potential of vegetation to enhance surface-air exchange of PBDEs [2].

4. Finally, evidence was provided to demonstrate the predictive capabilities of this framework using a second independent set of data collected at the same location for a different time period. Although this was tested using a different time frame, PBDE and PAH vegetation concentrations were assumed to be negligible at t_0. As previously, the vegetation concentrations were calculated using averaged measured atmospheric concentrations and were consistent with field measurements [4].

[1] St-Amand, A.D.; Mayer, P.M.; Blais, J.M., Seasonal trends in vegetation and atmospheric concentrations of PAHs and PBDEs near a sanitary landfill. *Atmospheric Environment* **2008**, in press (reference AEA-8046).

[2] St-Amand, A.D.; Mayer, P.M.; Blais, J.M., Modeling Atmospheric Vegetation Uptake of PBDEs using field measurements. *Environmental Science & Technology* **2007**, *41*, 4234-4239.

[3] St-Amand, A.D.; Mayer, P.M.; Blais, J.M., Modeling Atmospheric Vegetation Uptake of PAHs using field measurements, submitted to *Environmental Science & Technology* on December 21st 2007 (manuscript ES-2007-03220X).

[4] St-Amand, A.D.; Mayer, P.M.; Blais, J.M., Predicting PBDE and PAH concentrations in vegetation using atmospheric field measurements, in preparation to be submitted to *Environmental Science & Technology*.

APPENDICES

APPENDIX 1 - SAMPLING AND METEOROLOGICAL DATA

Air sampling observations

Start		End		Duration	Pressure (inches H_2O)		Average flow	Volume (m^3)
Date	Time	Date	Time	(min)	Start	End	(m^3/min)	
16-Feb-04	12:50 PM	17-Feb-04	8:20 AM	1170	42.5	40.0	0.664	777
24-Feb-04	3:10 PM	25-Feb-04	8:25 AM	1035	42.5	40.0	0.648	671
2-Mar-04	2:50 PM	4-Mar-04	8:20 AM	2450	41.5	39.0	0.613	1500
9-Mar-04	11:40 AM	10-Mar-04	3:45 PM	1685	42.0	39.0	0.621	1050
22-Mar-04	2:40 PM	23-Mar-04	3:55 PM	1515	44.0	40.0	0.642	973
5-Apr-04	3:15 PM	6-Apr-04	3:45 PM	1470	44.0	40.0	0.631	927
20-Apr-04	2:15 PM	21-Apr-04	7:30 AM	1035	43.5	40.0	0.624	645
3-May-04	2:35 PM	4-May-04	9:30 AM	1135	45.0	40.0	0.631	716
17-May-04	2:18 PM	18-May-04	10:18 AM	1200	45.0	38.0	0.604	724
31-May-04	2:45 PM	1-Jun-04	9:45 AM	1140	41.0	38.0	0.588	670
14-Jun-04	2:35 PM	15-Jun-04	10:55 AM	1220	41.0	37.0	0.575	701
28-Jun-04	4:32 PM	29-Jun-04	10:06 AM	1054	43.0	37.0	0.592	624
12-Jul-04	2:40 PM	13-Jul-04	8:25 AM	1085	42.0	38.0	0.585	635

26-Jul-04	3:12 PM	27-Jul-04	9:54 AM	1122	42.0	39.0	0.587	658
9-Aug-04	1:53 PM	10-Aug-04	9:40 AM	1187	44.0	39.0	0.591	702
23-Aug-04	2:25 PM	24-Aug-04	10:00 AM	1055	44.0	40.0	0.606	639
13-Sep-04	3:30 PM	14-Sep-04	9:18 AM	1068	44.0	39.0	0.604	645
20-Sep-04	1:45 PM	21-Sep-04	10:05 AM	1220	45.0	39.0	0.607	740
4-Oct-04	1:55 PM	5-Oct-04	8:53 AM	1138	45.0	40.0	0.622	708
18-Oct-04	2:10 PM	19-Oct-04	9:07 AM	1137	45.0	41.0	0.630	717
1-Nov-04	1:25 PM	2-Nov-04	9:13 AM	1188	44.0	40.0	0.620	737
15-Nov-04	1:34 PM	16-Nov-04	9:05 AM	1171	45.0	38.0	0.620	726
29-Nov-04	1:52 PM	30-Nov-04	9:47 AM	1195	47.0	40.0	0.638	763
14-Dec-04	2:49 PM	15-Dec-04	9:51 AM	1142	45.0	40.0	0.653	746
5-Jan-05	2:37 PM	6-Jan-05	8:54 AM	1097	44.0	40.0	0.648	711
17-Jan-05	2:51 PM	18-Jan-05	8:25 AM	1054	45.0	42.0	0.675	712
31-Jan-05	1:17 PM	1-Feb-05	8:41 AM	1164	45.0	41.0	0.656	763
17-Feb-05	12:43 PM	18-Feb-05	10:03 AM	1280	45.0	40.0	0.643	823
3-Mar-05	2:57 PM	4-Mar-05	9:50 AM	1133	45.0	40.0	0.640	725
14-Mar-05	2:11 PM	15-Mar-05	9:12 AM	1141	45.0	40.0	0.631	720

29-Mar-05	10:42 AM	30-Mar-05	8:54 AM	1332	45.0	40.0	0.622	828
11-Apr-05	2:17 PM	12-Apr-05	9:38 AM	1161	45.0	40.0	0.624	724
25-Apr-05	2:05 PM	26-Apr-05	8:40 AM	1118	44.0	39.0	0.606	677
10-May-05	12:39 PM	11-May-05	8:48 AM	1209	42.0	39.0	0.582	704
24-May-05	2:22 PM	25-May-05	9:35 AM	1153	44.0	39.0	0.600	691
7-Jun-05	2:25 PM	8-Jun-05	9:48 AM	1163	44.0	38.0	0.589	685
20-Jun-05	2:43 PM	21-Jun-05	9:42 AM	1139	44.0	38.0	0.589	670

Weather conditions during sampling sessions

Date	Conditions	Average T (°C)	Average RH (%)	Average P (kPa)	Predominant WD		Average WS (km/h)	Precipitation			SC (cm)
					Degree (°)	Cardinal points		Rain (mm)	Snow (cm)	Total (mm)	
16-Feb-04	Clear	-15.2	48.4	102.3	22/7	SW/NEE	11.2	0	0	0	14
24-Feb-04	Clear	-9.9	52.8	100.8	30	NWW	13.7	0	0	0	27
2-Mar-04	Cloudy	2.5	79.5	100.5	24	SWW	14.2	0	0	0	4
9-Mar-04	Clear	-0.1	64.1	101.1	16	SSE	7.5	0	0	0	3
22-Mar-04	Cloudy/Snow	-5.8	63.2	100.6	22	SW	15.4	0	3.6	2.4	5
5-Apr-04	Mainly Clear	-2.7	46.8	99.7	29	NWW	28.3	0	0	0	6
20-Apr-04	Cloudy	6.4	59.3	100.4	11	SEE	12.5	0	0	0	0
3-May-04	Mostly Cloudy	4.0	65.9	100.1	32	NW	18.9	0	0	0	0
17-May-04	Mostly Cloudy	19.7	63.4	100.3	20	SSW	16.1	*	0	*	0
31-May-04	Cloudy/Rain	14.0	70.6	98.8	9	E	13.4	*	0	*	0
14-Jun-04	Cloudy/Rain	21.4	73.6	99.7	23	SW	12.9	1.0	0	1.0	0
28-Jun-04	Mostly Cloudy	15.3	78.3	100.1	21	SSW	10.1	0	0	0	0

12-Jul-04	Cloudy/Fog	21.3	84.9	100.0	15	SSE	8.7	0	0	0	0
26-Jul-04	Cloudy	19.0	71.9	100.6	18/7	S/NEE	6.3	0	0	0	0
9-Aug-04	Mostly Cloudy	21.2	66.0	100.0	20	SSW	8.3	0	0	0	0
23-Aug-04	Mainly Clear	13.1	70.8	100.8	23	SW	14.8	0	0	0	0
13-Sep-04	Clear	12.8	79.0	101.2	9	E	8.1	0	0	0	0
20-Sep-04	Mostly Cloudy	14.7	77.6	101.0	21	SSW	9.1	0	0	0	0
4-Oct-04	Mainly Clear	4.1	81.4	100.9	31	NW	10.7	0	0	0	0
18-Oct-04	Mainly Clear	2.6	75.0	100.9	36	N	9.8	0	0	0	0
1-Nov-04	Cloudy	5.4	74.2	100.8	33/8	NNW/E	7.2	*	0	*	0
15-Nov-04	Mostly Cloudy	4.0	70.1	101.5	24	SWW	7.8	0	0	0	0
29-Nov-04	Cloudy	0.0	69.2	101.1	18	S	6.6	0	0	0	0
14-Dec-04	Mainly Clear	-15.3	85.9	101.3	27	W	11.6	0	0	0	30
5-Jan-05	Cloudy	-14.7	94.0	101.0	32/6	NW/NEE	12.0	0	0	0	13
17-Jan-05	Mainly Clear	-20.5	49.1	101.8	32	NW	25.6	0	0	0	11
31-Jan-05	Clear	-11.3	56.8	101.6	11/29	SEE/NWW	3.6	0	0	0	22
17-Feb-05	Cloudy/Snow	-9.2	73.8	99.6	9/29	E/NWW	13.6	0	2.0	1.2	10
3-Mar-05	Mostly Cloudy	-10.6	49.8	99.6	26	W	13.8	0	0	0	27

14-Mar-05	Mostly Cloudy	-2.0	56.9	100.1	29	NWW	16.8	0	0	0	27
29-Mar-05	Mainly Clear	5.8	68.2	100.3	30/6	NWW/NEE	10.8	0	0	0	0
11-Apr-05	Mainly Clear	3.3	37.3	101.2	1	N	14.7	0	0	0	0
25-Apr-05	Cloudy/Rain	5.5	80.7	98.9	18	S	11.6	1.0	0	1.0	0
10-May-05	Mostly Cloudy	21.2	51.2	99.6	21	SSW	10.3	0	0	0	0
24-May-05	Mainly Clear	14.4	56.8	100.2	5	NE	17.5	0	0	0	0
7-Jun-05	Mostly Cloudy	18.8	71.4	99.8	33	NNW	13.8	0	0	0	0
20-Jun-05	Mainly Clear	19.4	71.9	100.3	22	SW	13.2	0	0	0	0

T = temperature, RH = relative humidity, P = atmospheric pressure, WD = wind direction, WS = wind speed, SC = snow cover, and

* = negligible precipitation

Wind rose plots (winds blowing from)

February 16-17, 2004 (12PM to 9AM)

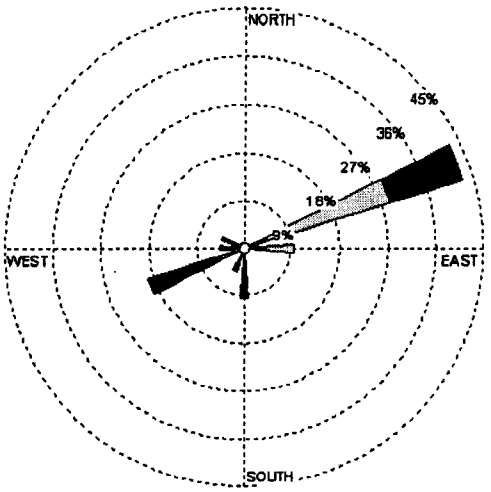

February 24-25, 2004 (3PM to 9AM)

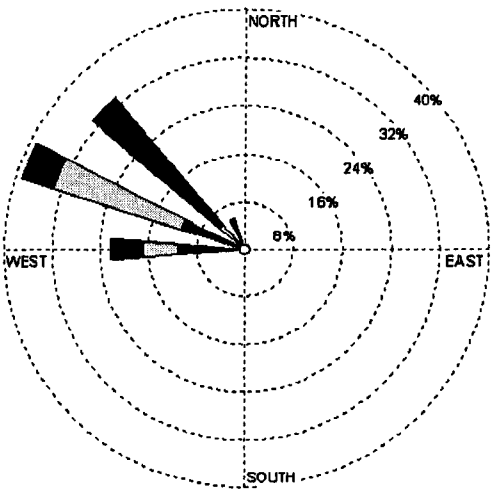

March 2-4, 2004 (2PM to 9AM)

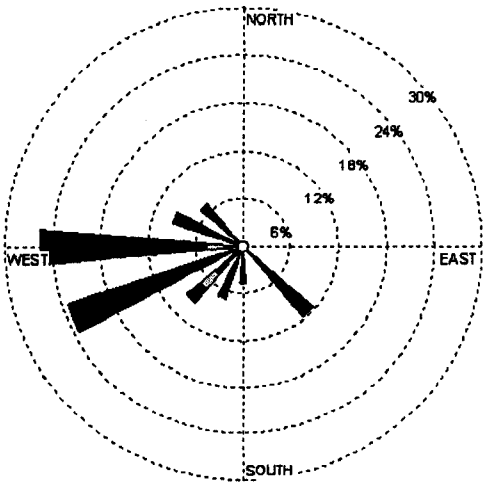

March 9-10, 2004 (11AM to 4PM)

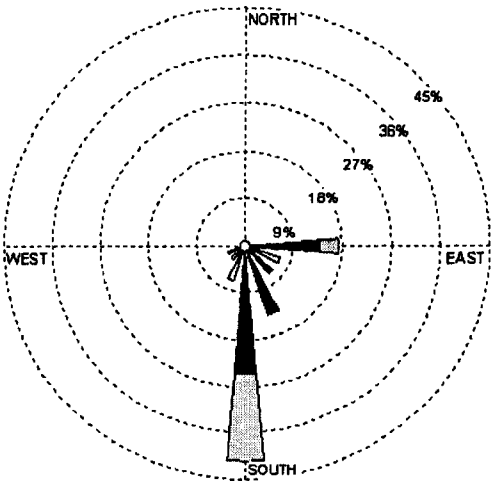

March 22-23, 2004 (2PM to 4PM)

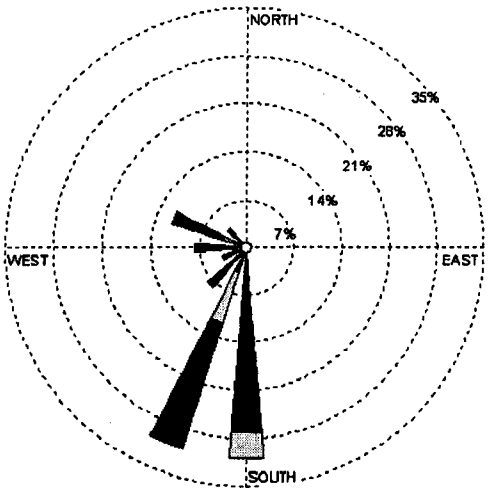

April 5-6, 2004 (3PM to 4PM)

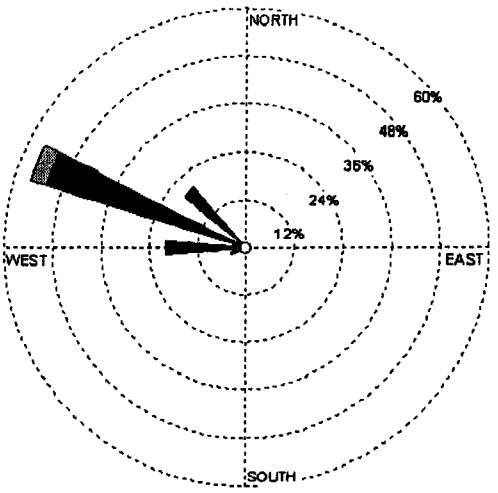

April 20-21, 2004 (2PM to 8AM)

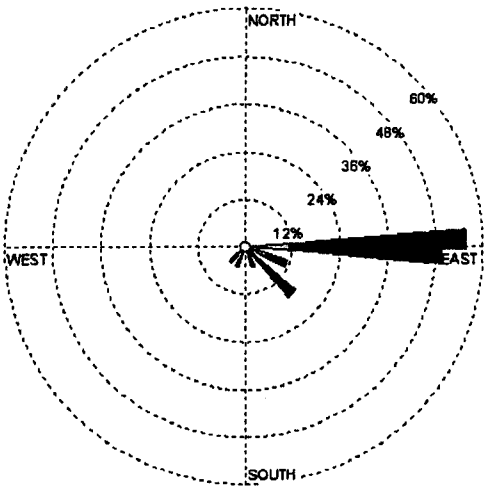

May 3-4, 2004 (2PM to 10AM)

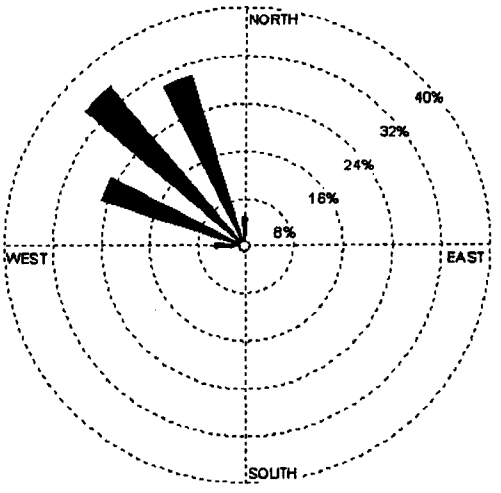

May 17-18, 2004 (2PM to 11AM)

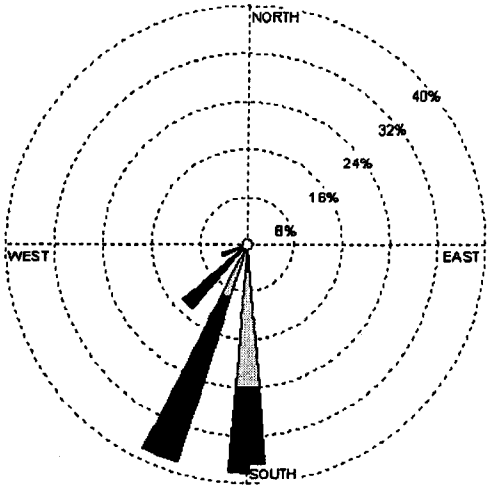

May 31 - June 1, 2004 (2PM to 11AM)

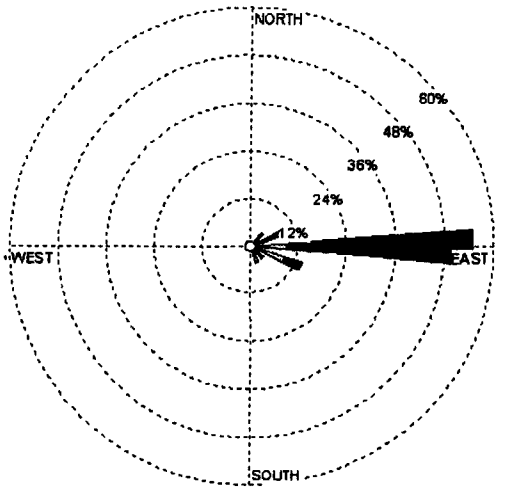

June 14-15, 2004 (2PM to 11AM)

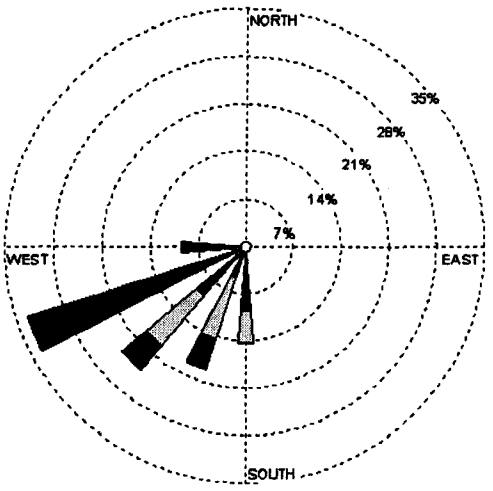

June 28-29, 2004 (4PM to 11AM)

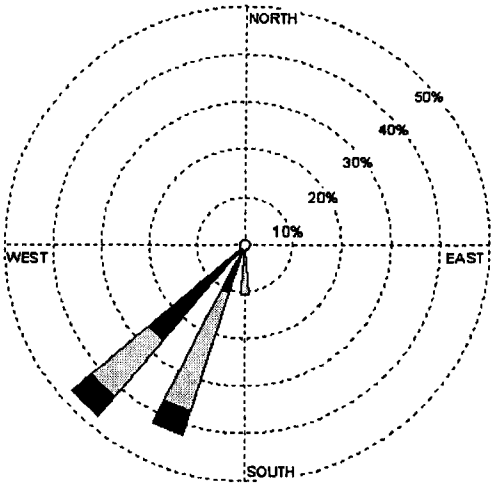

July 12-13, 2004 (2PM to 9AM)

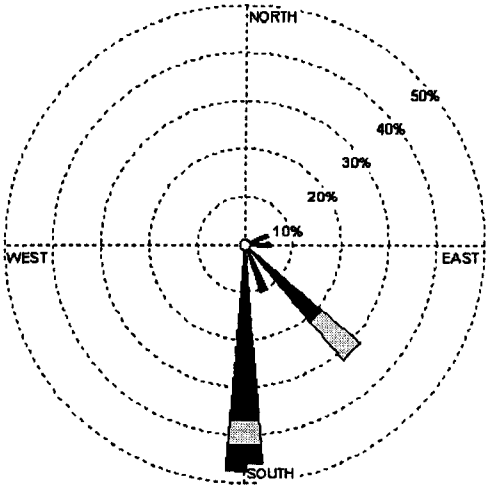

July 26-27, 2004 (3PM to 10AM)

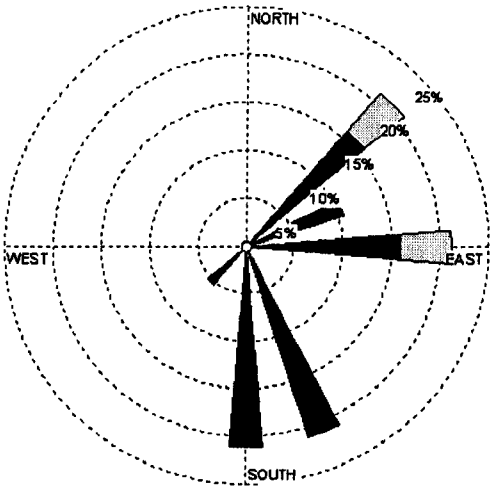

August 9-10, 2004 (1PM to 10AM)

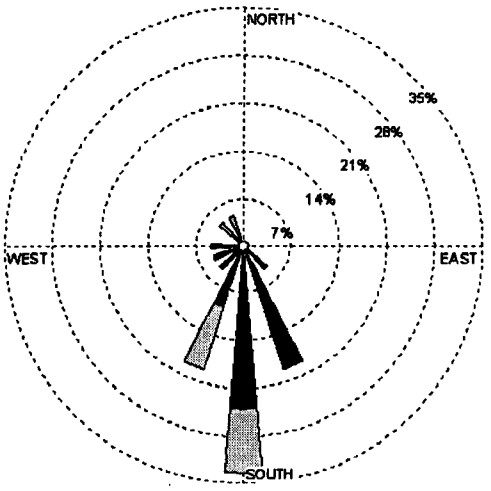

August 23-24, 2004 (2PM to 10AM)

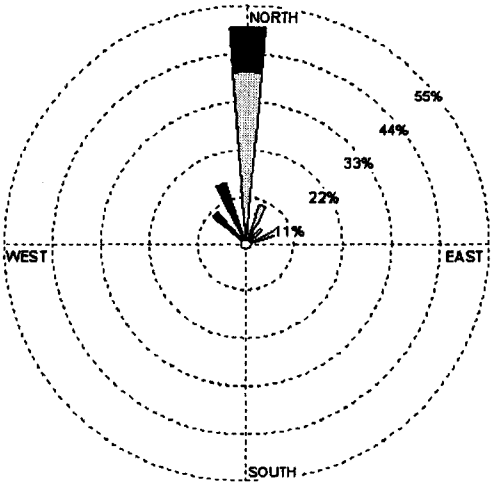

September 13-14, 2004 (3PM to 10AM)

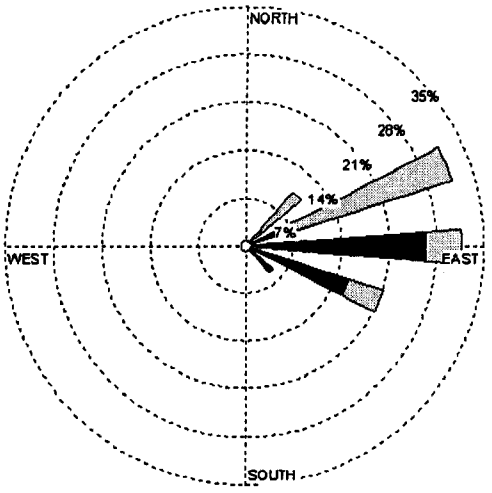

September 20-21, 2004 (1PM to 11AM)

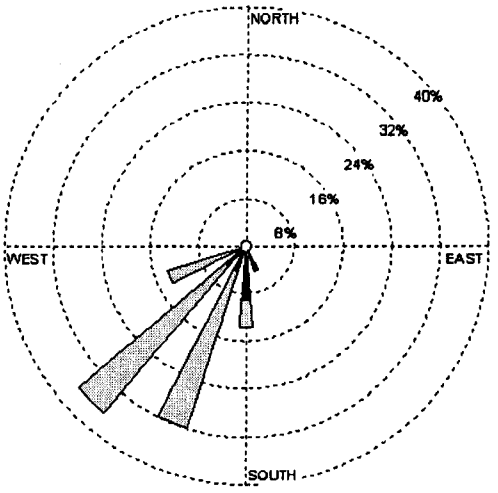

October 4-5, 2004 (1PM to 9AM)

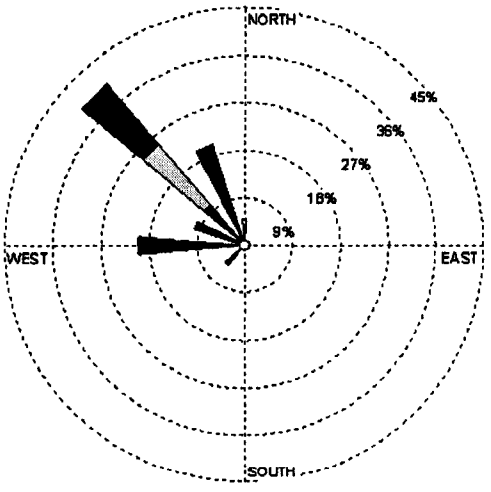

October 18-19, 2004 (2PM to 10AM)

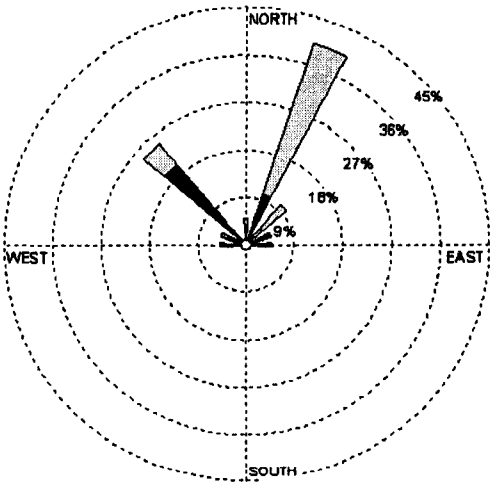

November 1-2, 2004 (1PM to 10AM)

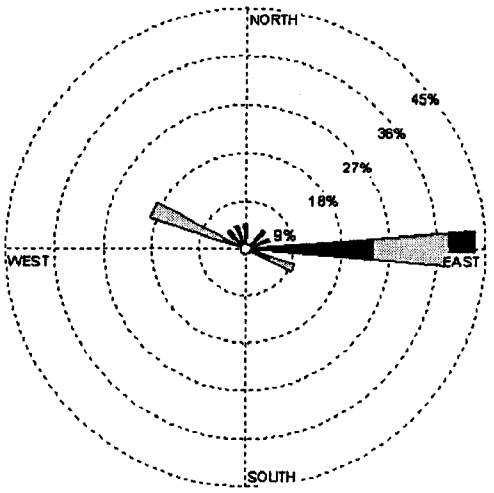

November 15-16, 2004 (1PM to 10AM)

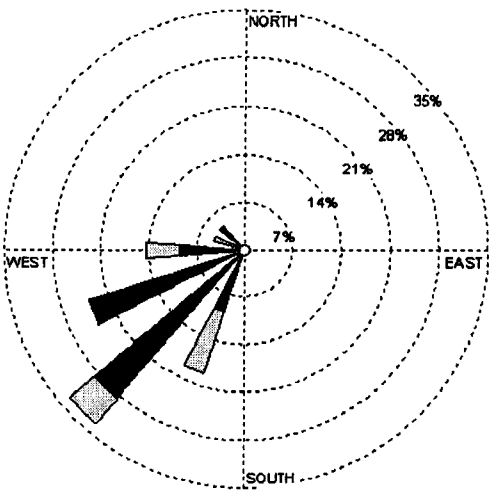

November 29-30, 2004 (1PM to 10AM)

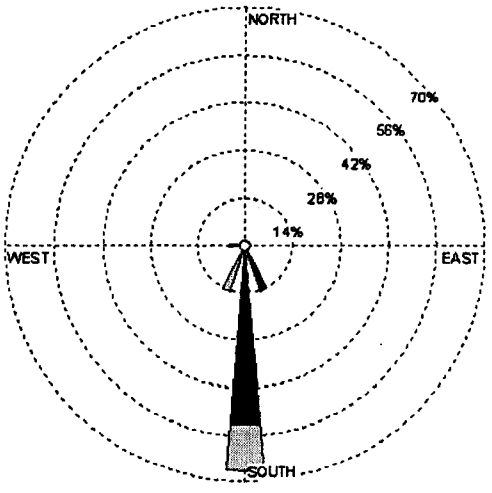

December 14-15, 2004 (2PM to 10AM)

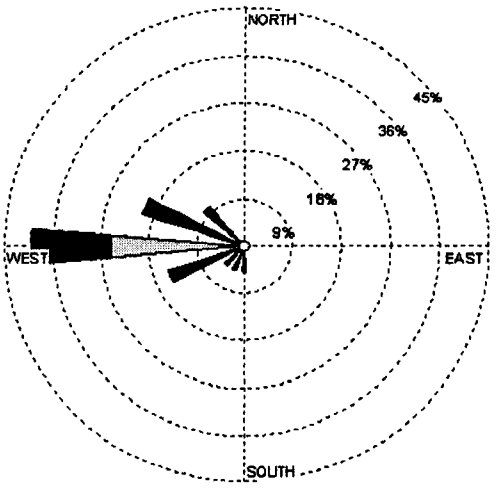

January 5-6, 2005 (2PM to 9AM)

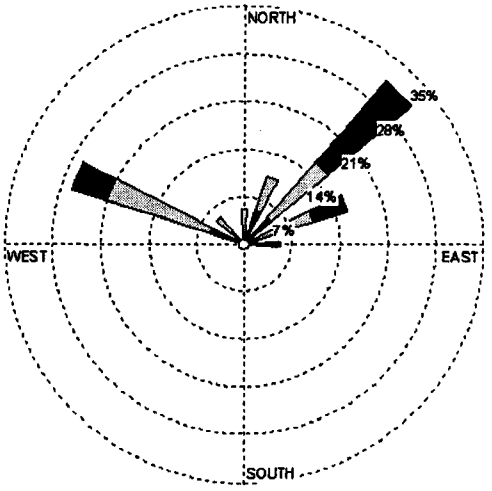

January 17-18, 2005 (2PM to 9AM)

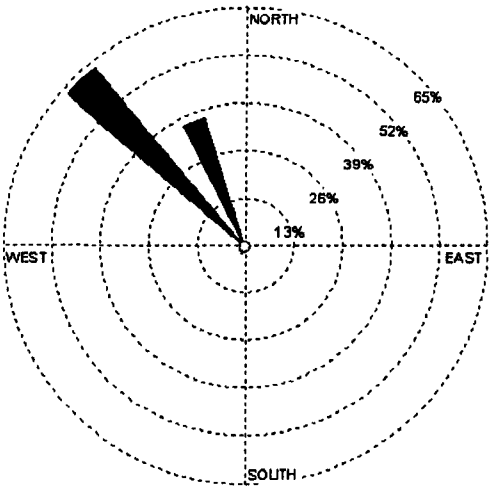

January 31 - February 1, 2005 (1PM to 9AM)

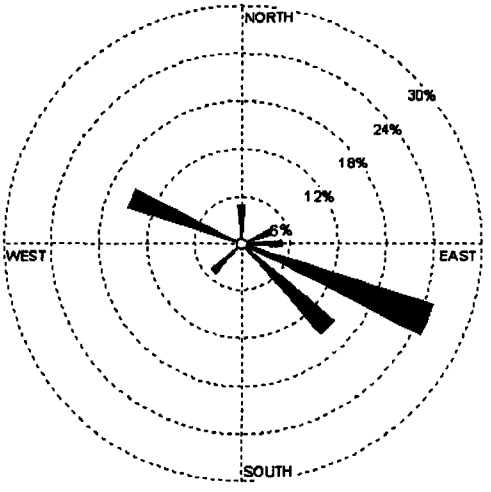

February 17-18, 2005 (12PM to 10AM)

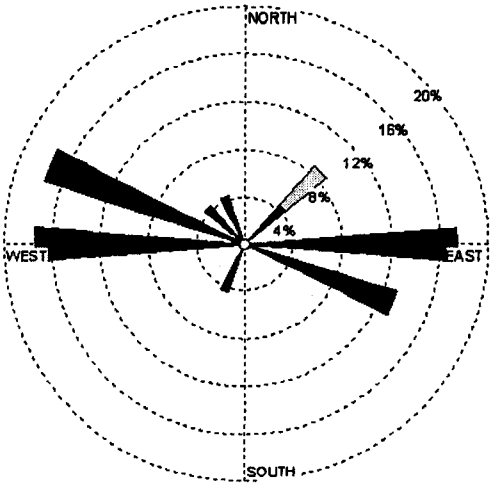

March 3-4, 2005 (2PM to 10AM)

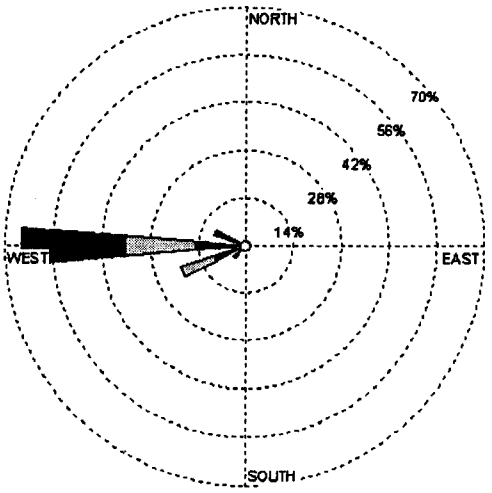

March 14-15, 2005 (2PM to 10AM)

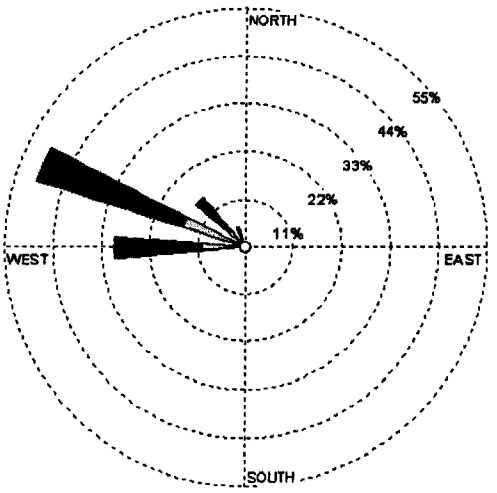

March 29-30, 2005 (10AM to 9AM)

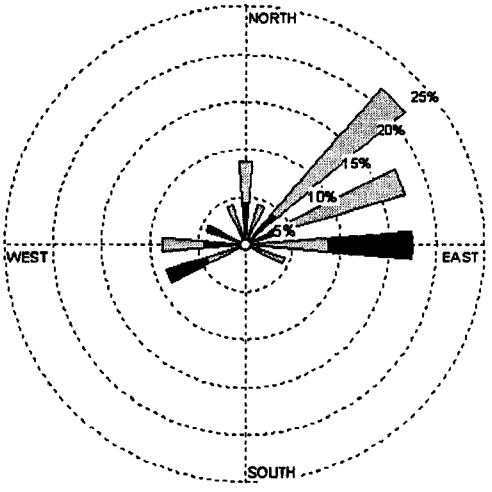

April 11-12, 2005 (2PM to 10AM)

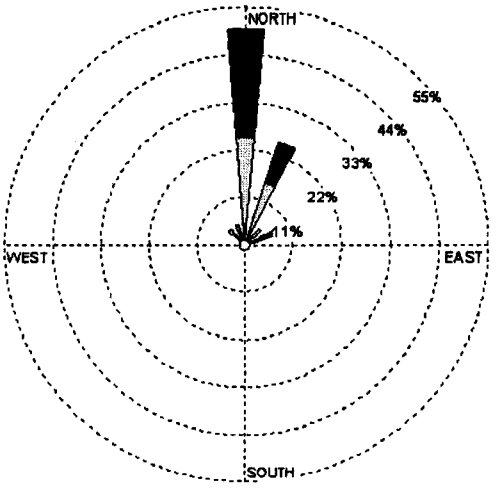

April 25-26, 2005 (2PM to 9AM)

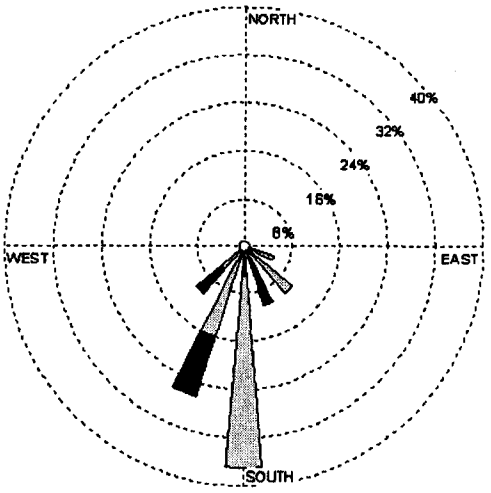

May 10-11, 2005 (12PM to 9AM)

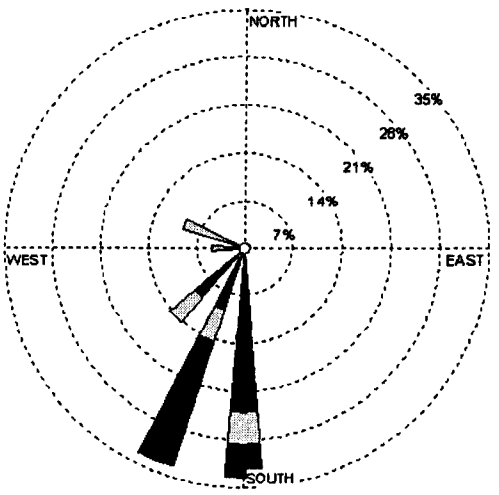

May 24-25, 2005 (2PM to 10AM)

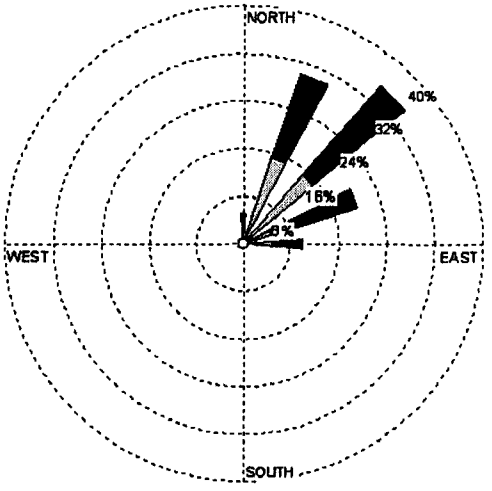

June 7-8, 2005 (2PM to 10AM)

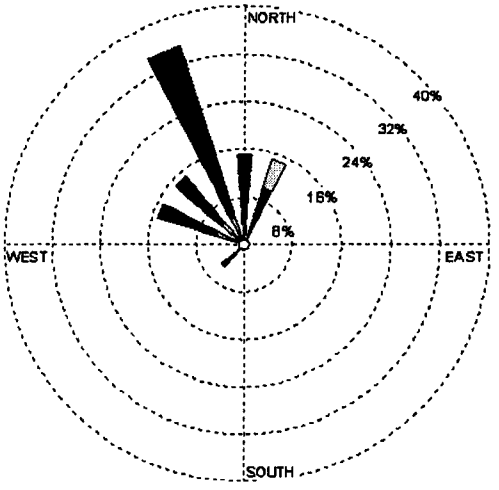

June 20-21, 2005 (2PM to 10AM)

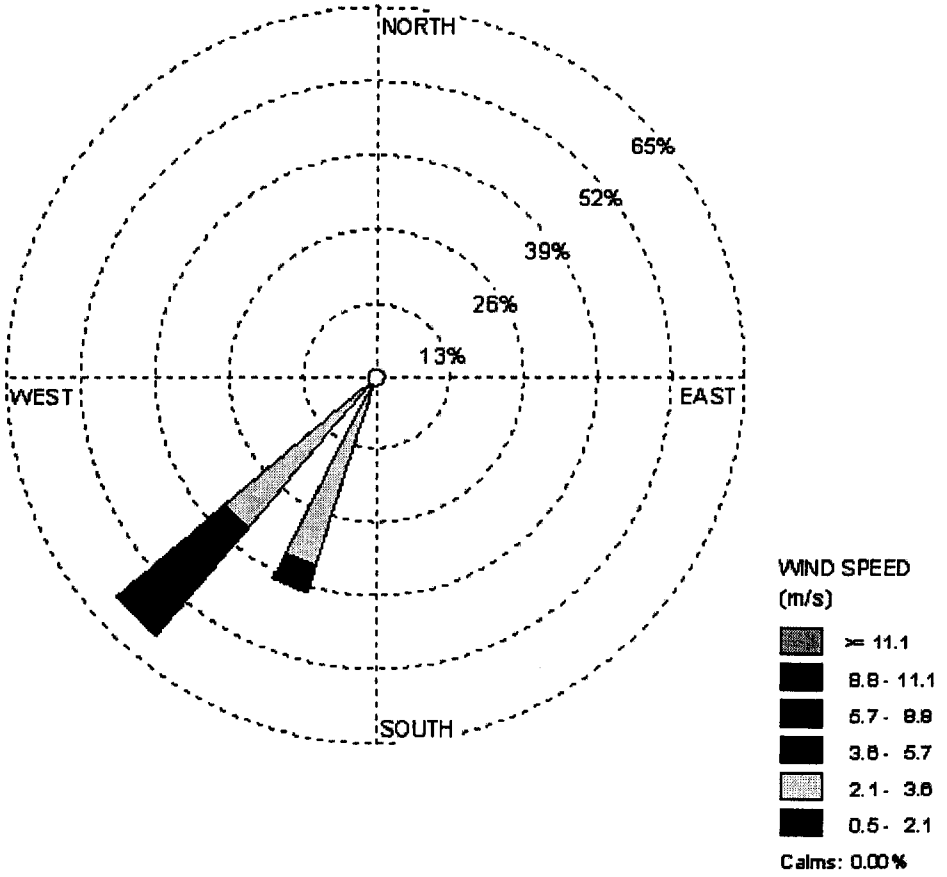

Air sampler calibration

The air sampler was calibrated using a standard calibration procedure for high-volume air samplers. The flow through the apparatus in m^3/min was calibrated against inches of H_2O magnehilic readings (Dwyer Model 2100). In this procedure pressure (inches of H_2O) is recorded using a manometer at different magnehilic pressure readings. Using the calibrated slope and intercept of the orifice, the standard flow rate (Qstd) is calculated according to each manometer reading using

$$Qstd\ (m^3/\min) = \frac{1}{m} \times \left(\sqrt{H_2O \times \frac{Atmos\ P\ (mmHg)}{760\ mmHg} \times \frac{298\ K}{T(K)}} - b \right)$$

where Qstd is the standard flow rate in m^3/min, m is the Qstd slope of the orifice, H_2O corresponds to the manometer reading during the calibration procedure, Atmos P is the atmospheric pressure in mm Hg, T is the ambient temperature in K, and b is the Qstd intercept of the orifice.

Also, the magnehilic readings during calibration are corrected according to current meteorological conditions using the following equation

$$Flow\ corrected\ (inches\ H_2O) = \sqrt{P_{H2O} \times \frac{Atmos\ P\ (mmHg)}{760\ mmHg} \times \frac{298\ K}{T\ (K)}}$$

where P_{H2O} is the magnehilic reading. The corrected flow is then plotted against the standard flow rate (Qstd) and a linear relationship is observed. The slope and intercept are determined. The determination coefficient (R^2) should be above 0.99.

The first calibration was realized from January 19th to 22nd, 2004, prior to the start of the study. A second calibration procedure was done July 20th to 26th 2004.

Air sampler calibration

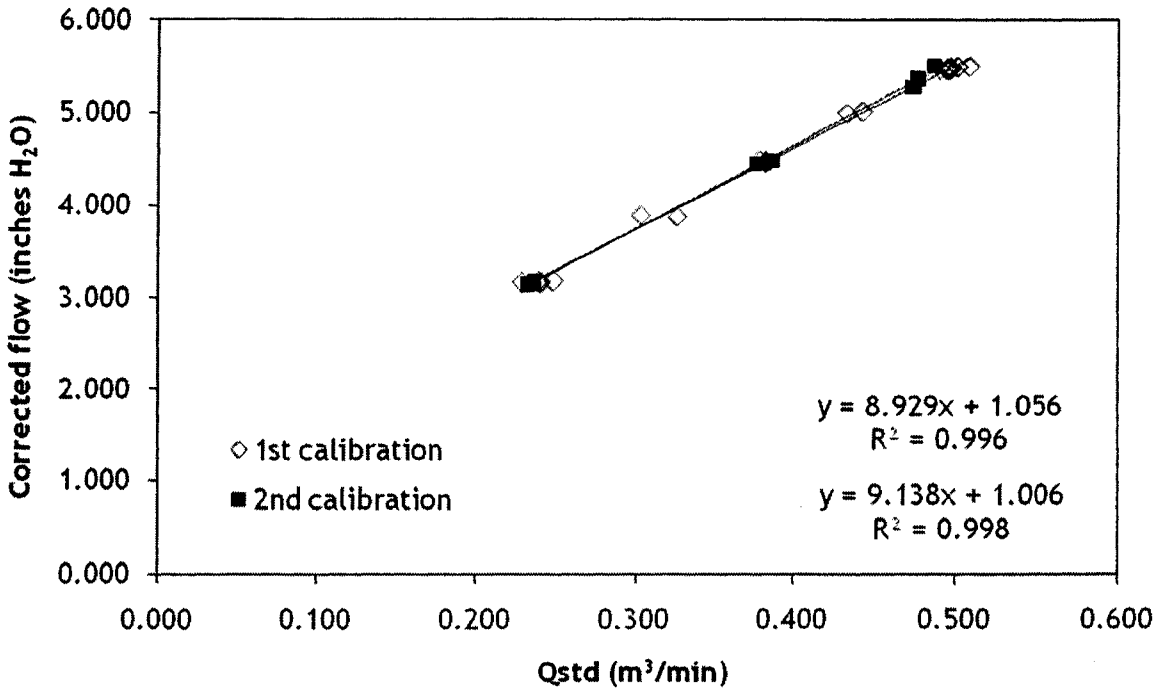

Magnehilic readings were recorded at the beginning and at the end of each sampling session. Using the calibration slope and intercept, an initial and final flow rates were calculated (with the following equation), averaged and used to obtain sample volume.

$$Flow\ rate\ (m^3/\min) = \frac{1}{m} \times \left(\sqrt{P_{H2O} \times \frac{Atmos\ P\ (mmHg)}{760\ mmHg} \times \frac{298\ K}{T(K)}} - b \right)$$

Backward trajectories

February 17, 2004 (8AM)

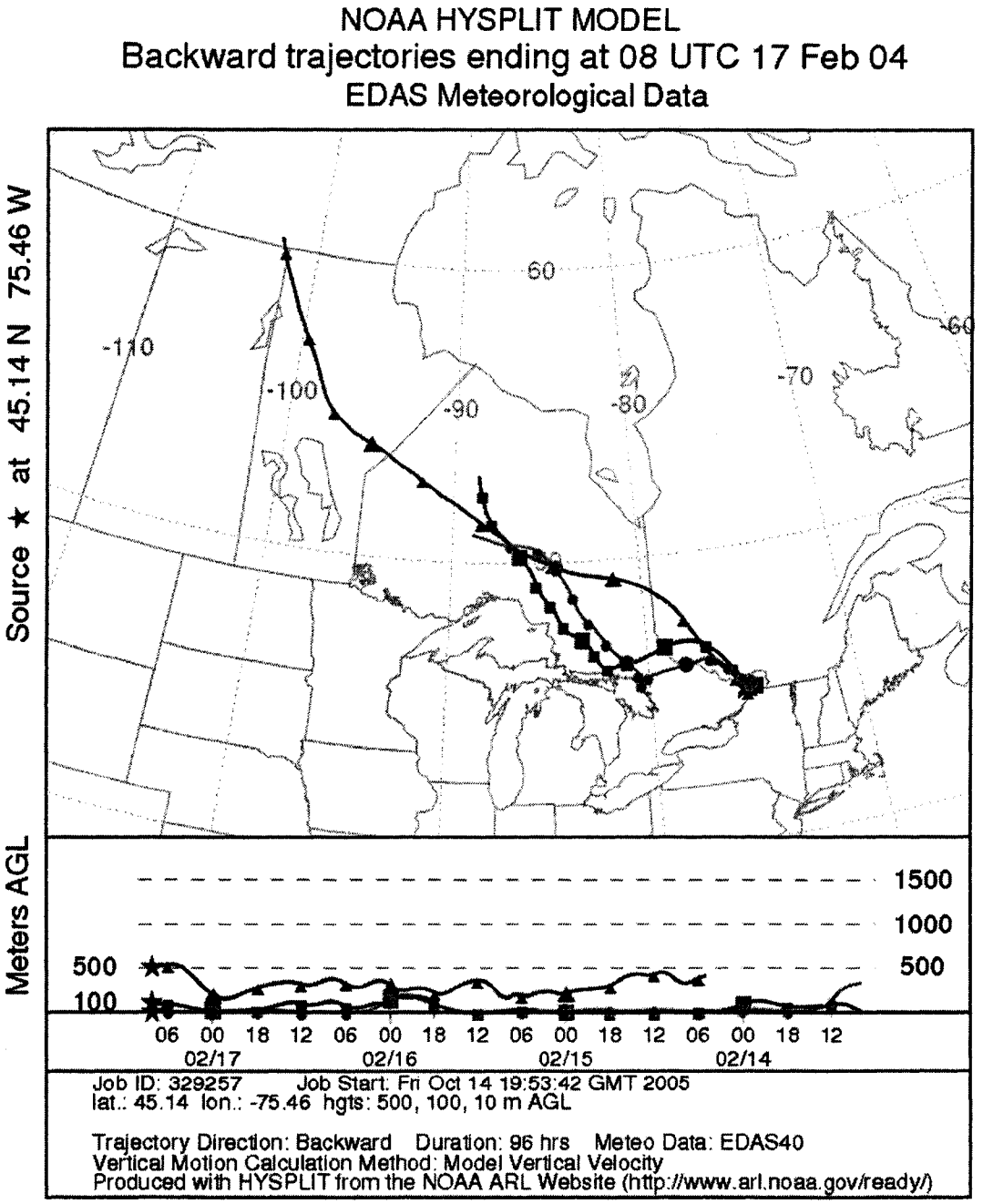

February 25, 2004 (9AM)

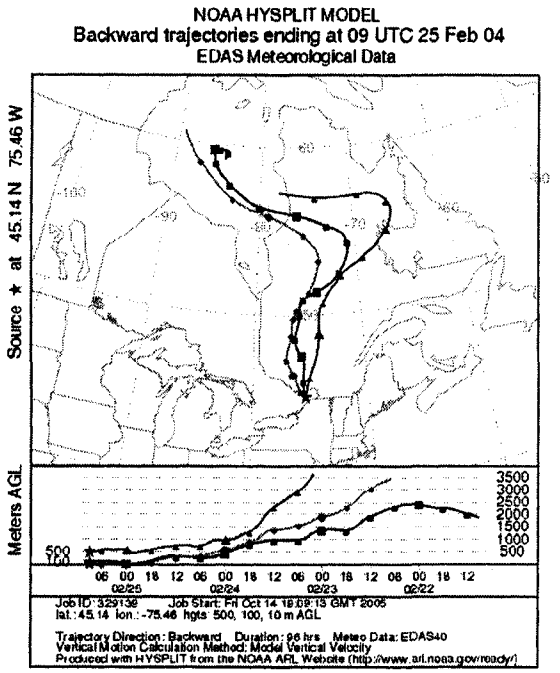

March 3, 2004 (9AM)

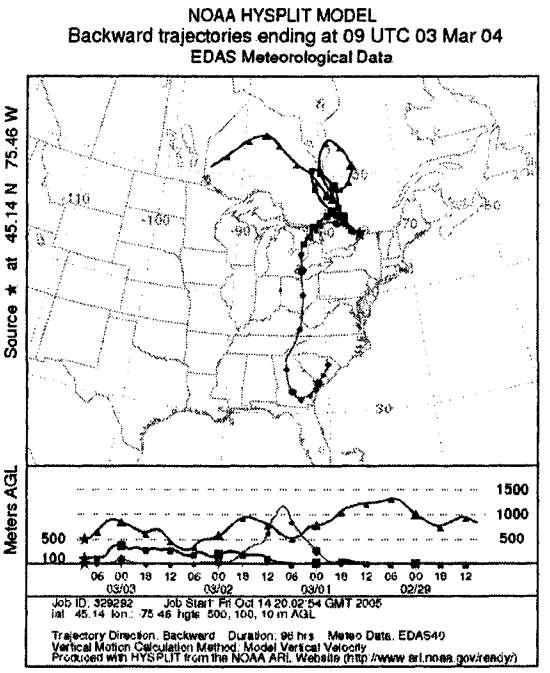

March 10, 2004 (4PM)

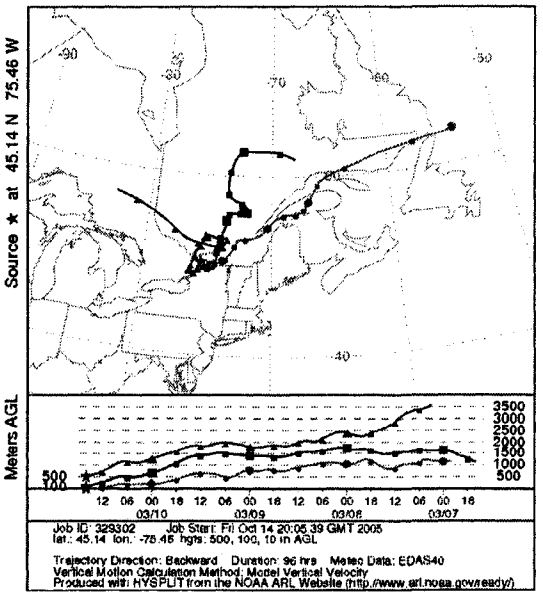

March 23, 2004 (4PM)

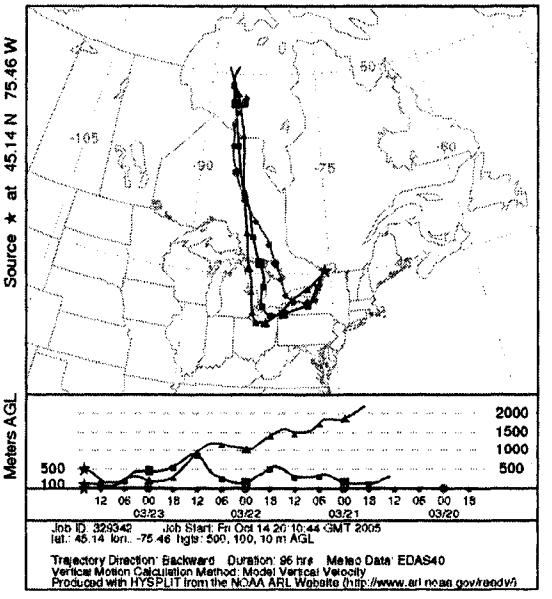

April 6, 2004 (4PM)

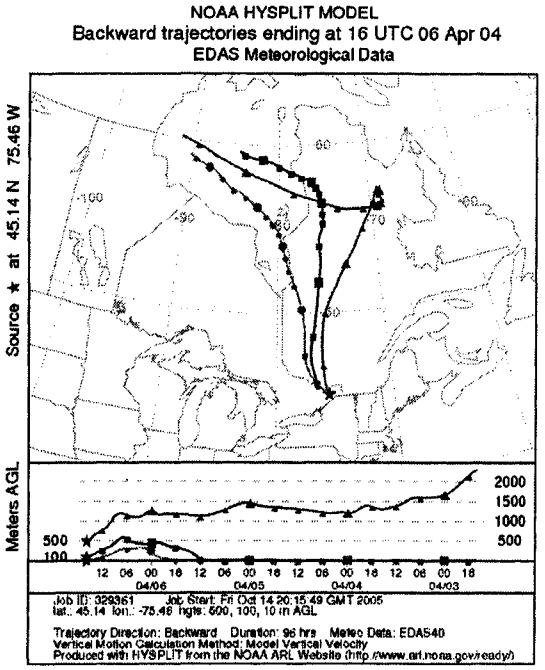

April 21, 2004 (8AM)

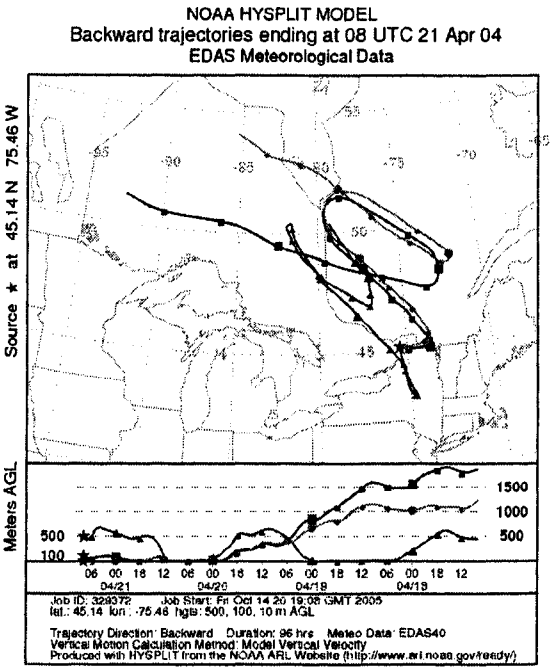

May 4, 2004 (10AM)

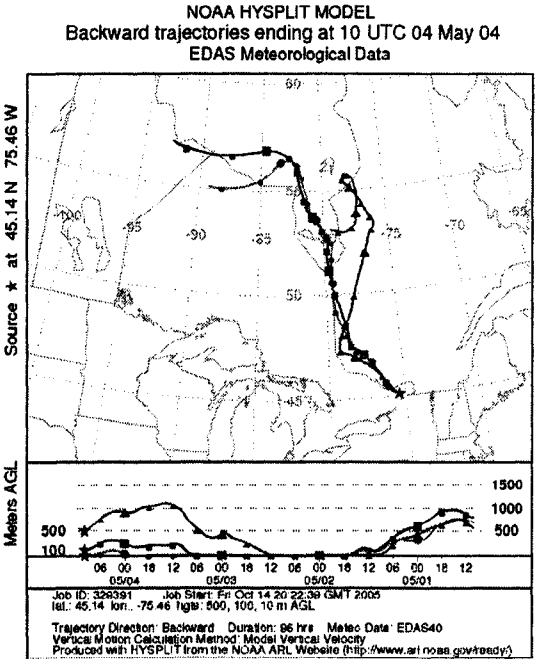

May 18, 2004 (11AM)

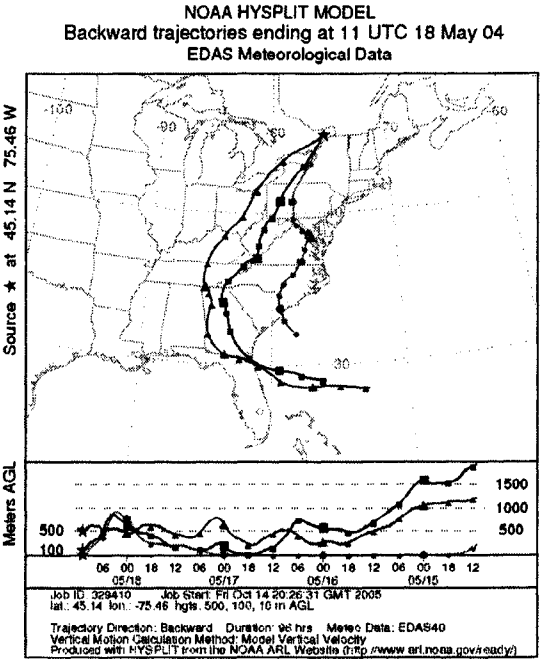

June 1, 2004 (10AM)

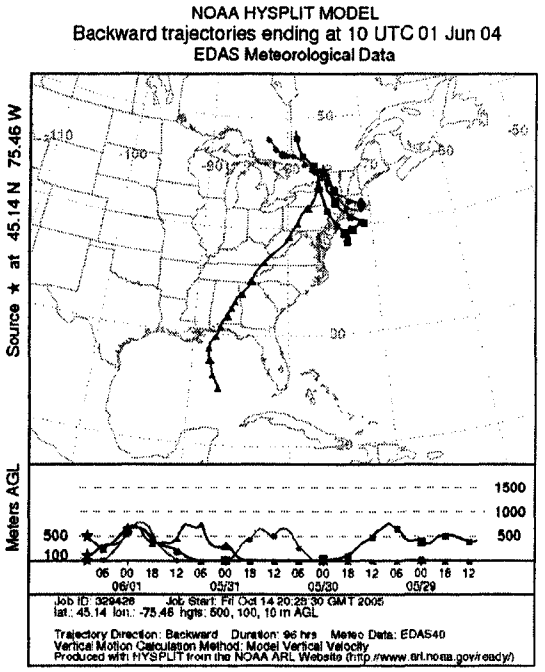

June 15, 2004 (11AM)

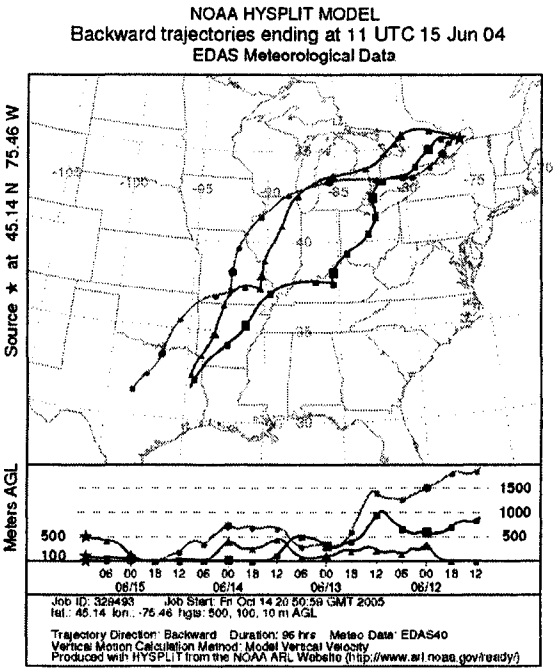

June 29, 2004 (11AM)

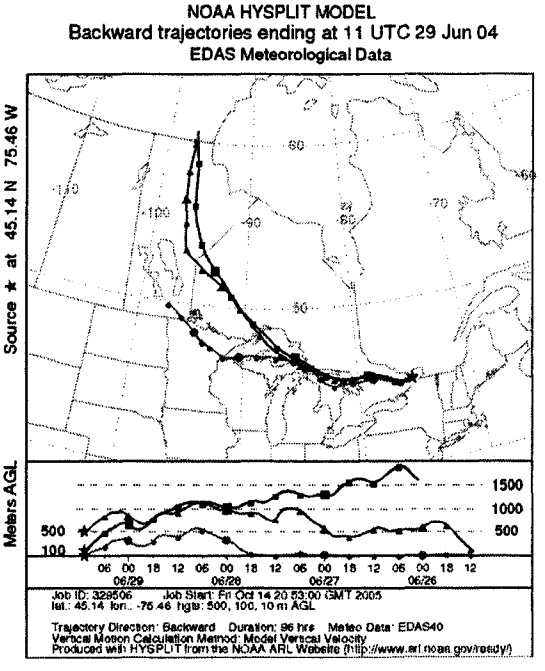

July 13, 2004 (9AM)

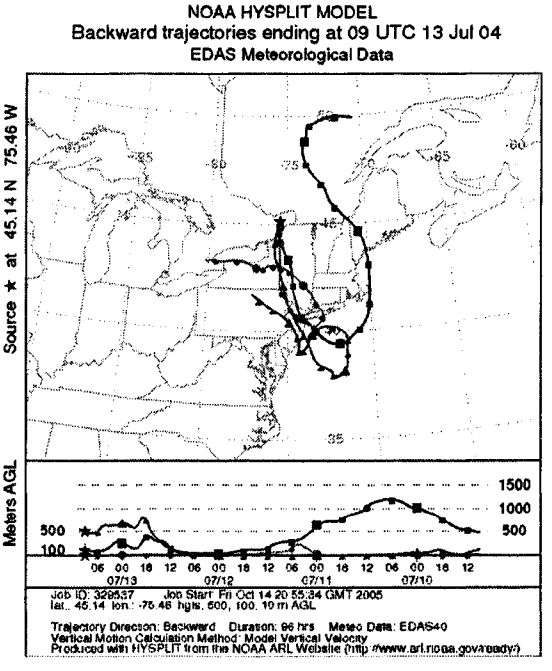

July 27, 2004 (10AM)

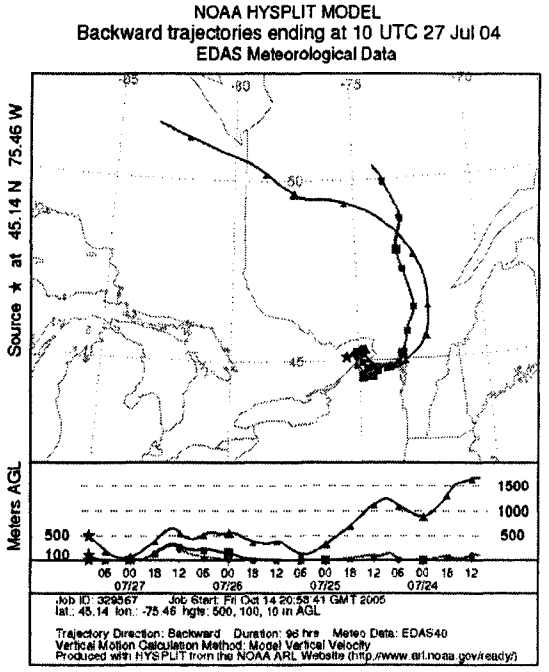

August 10, 2004 (10AM)

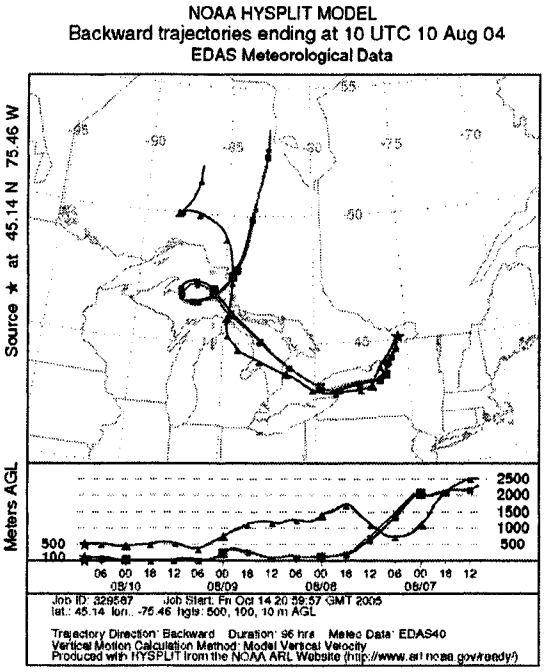

August 24, 2004 (10AM)

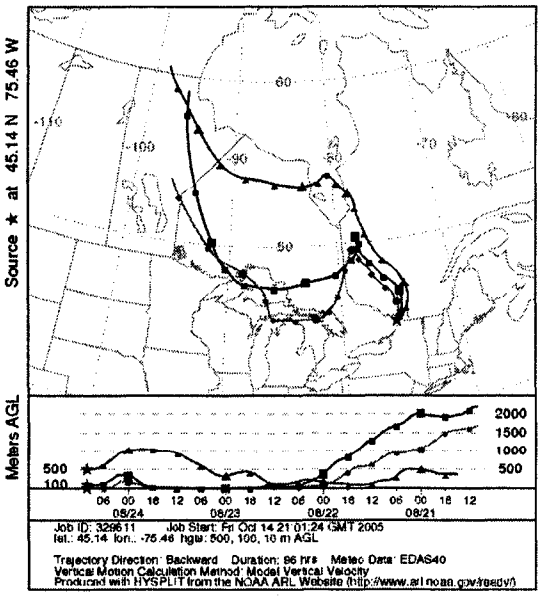

September 14, 2004 (10AM)

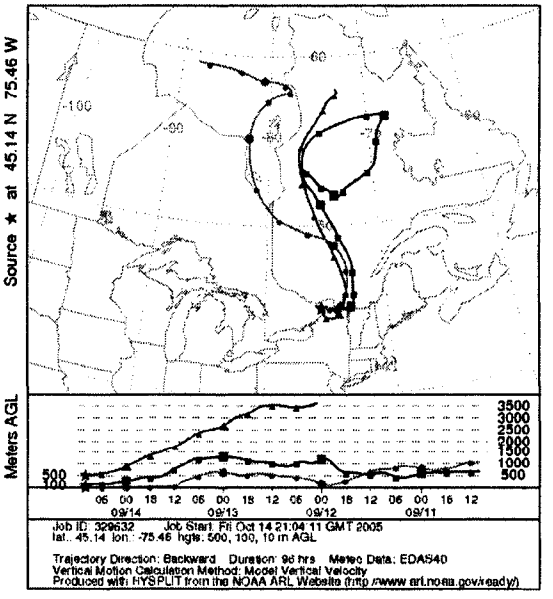

September 21, 2004 (11AM)

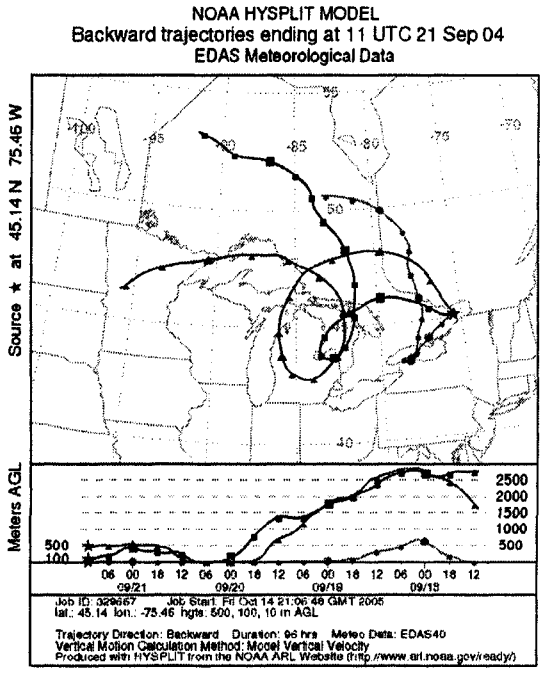

October 5, 2004 (9AM)

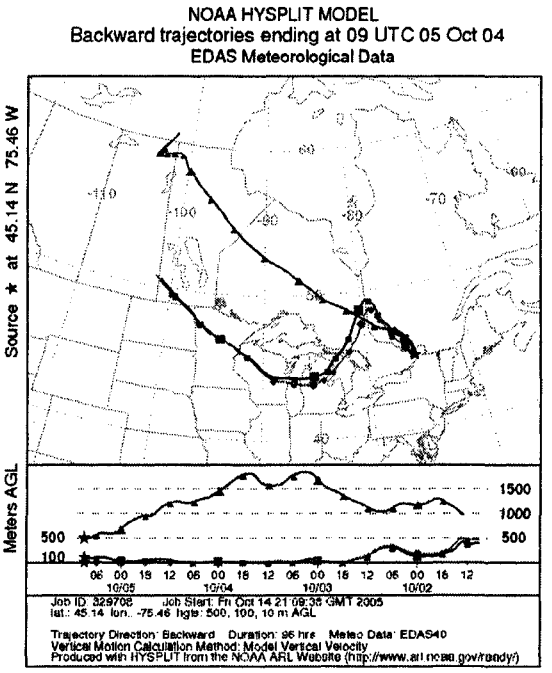

October 19, 2004 (10AM)

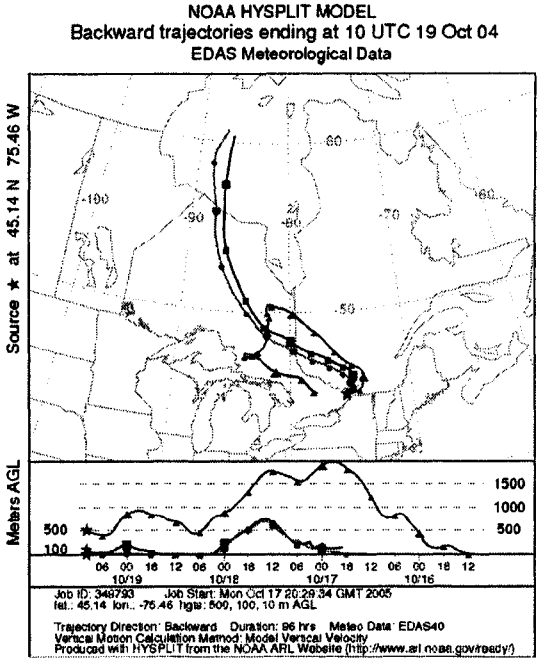

November 2, 2004 (10AM)

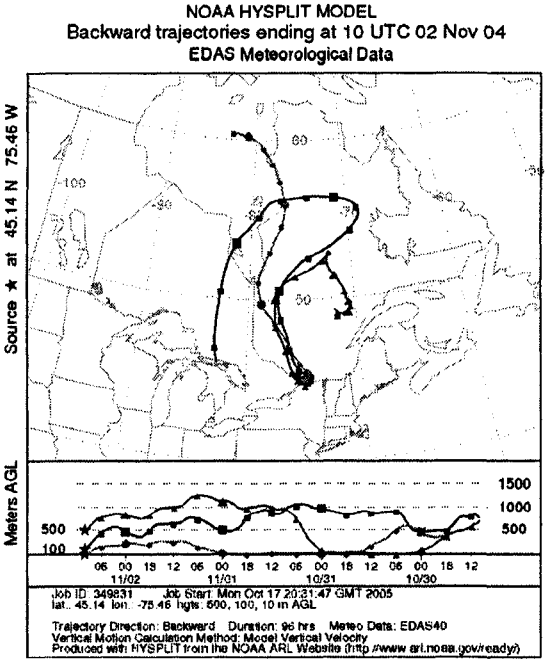

November 16, 2004 (10AM)

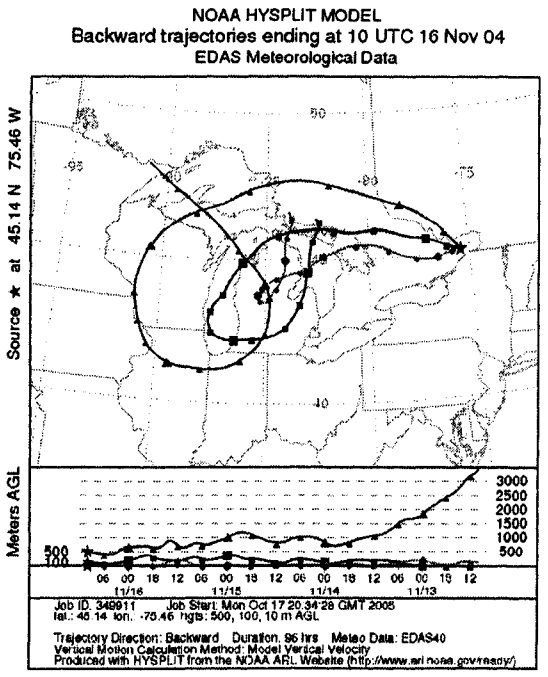

November 30, 2004 (10AM)

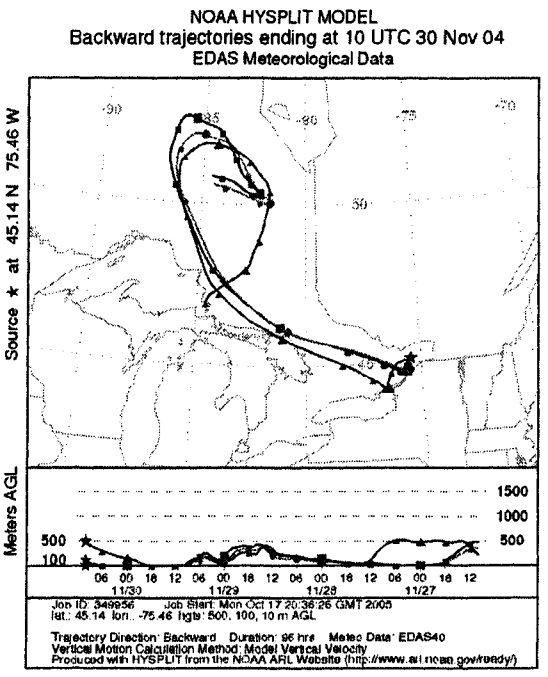

December 15, 2004 (10AM)

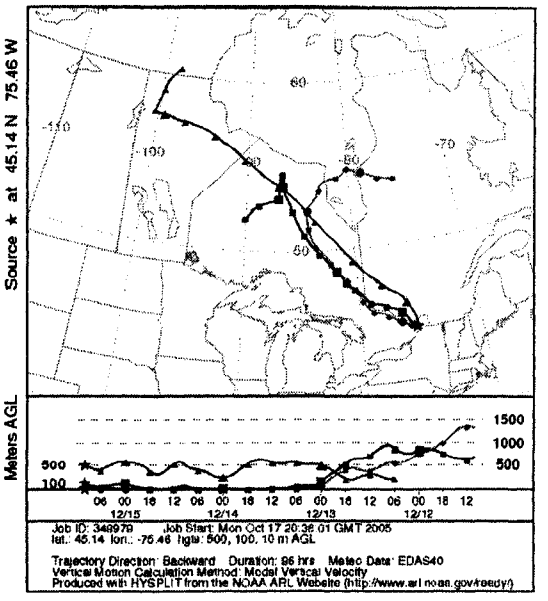

January 6, 2005 (9AM)

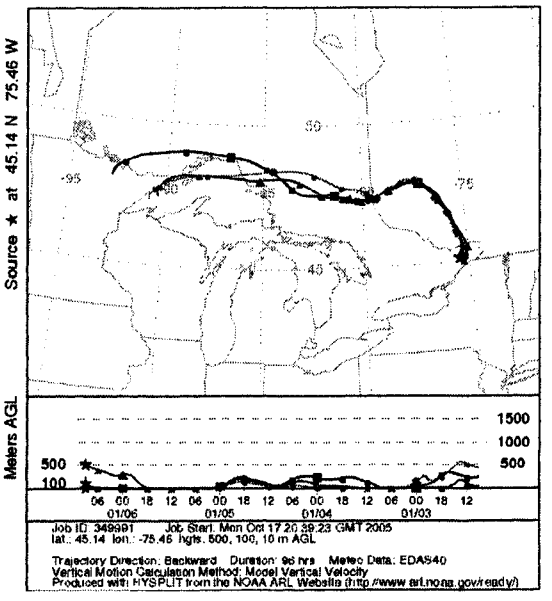

January 18, 2005 (9AM)

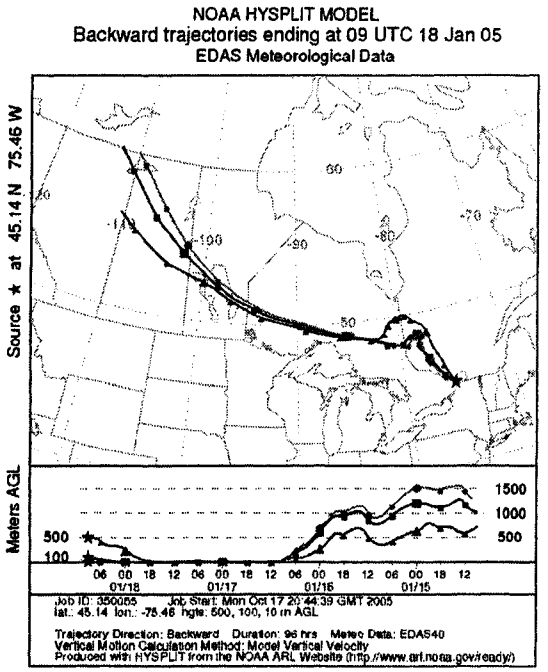

February 1, 2005 (9AM)

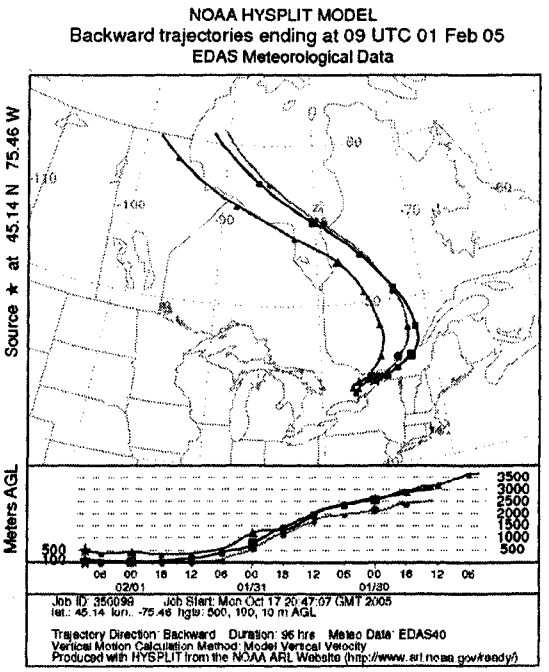

February 18, 2005 (10AM)

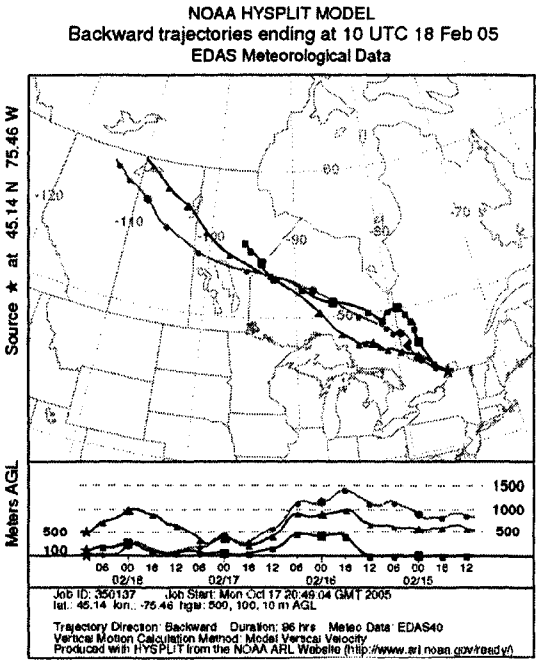

March 4, 2005 (10AM)

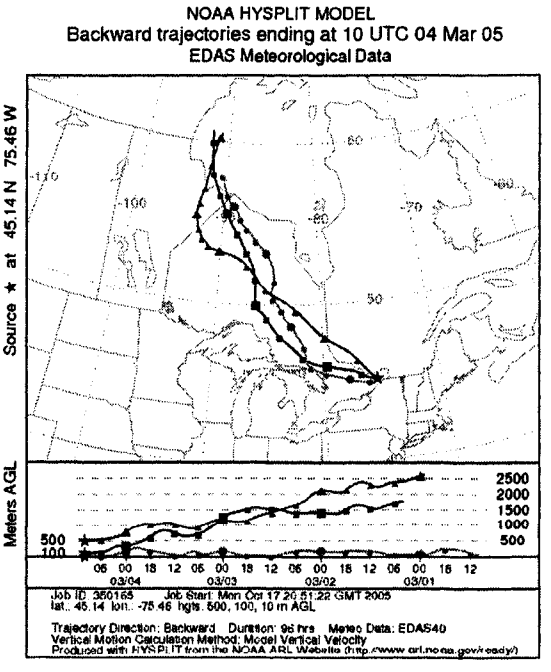

March 15, 2005 (10AM)

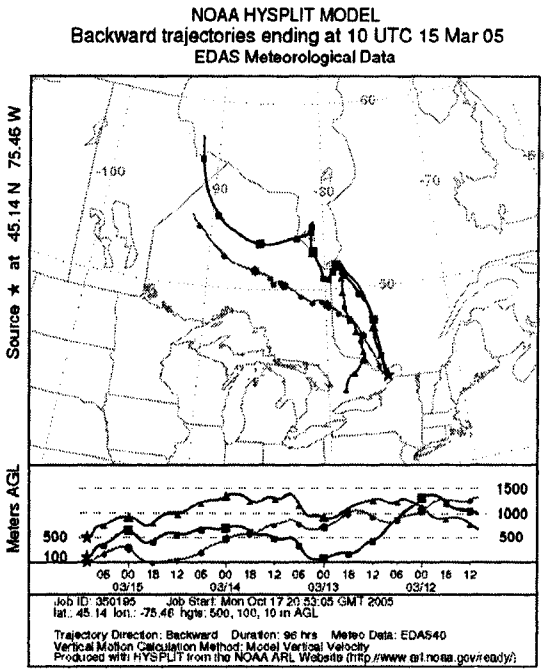

March 30, 2005 (9AM)

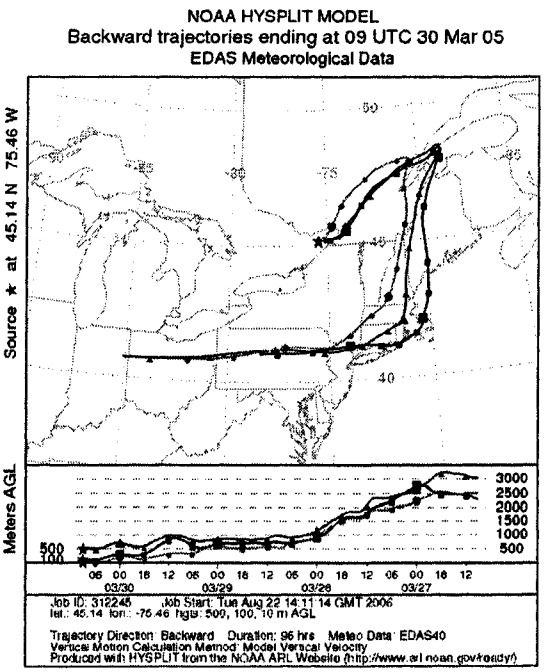

April 12, 2005 (10AM)

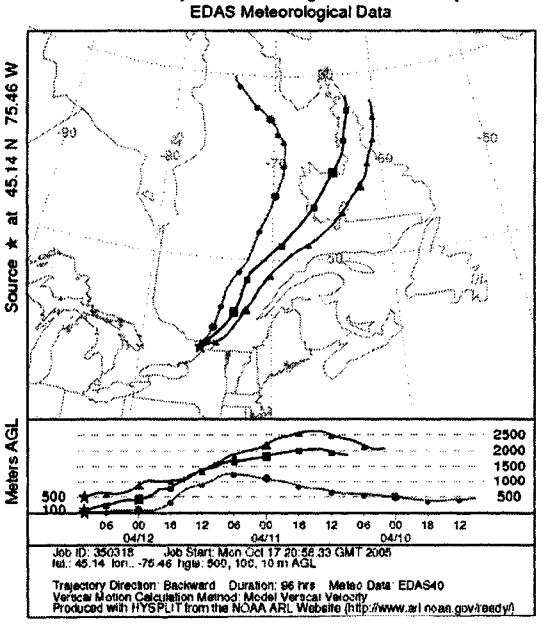

April 26, 2005 (9AM)

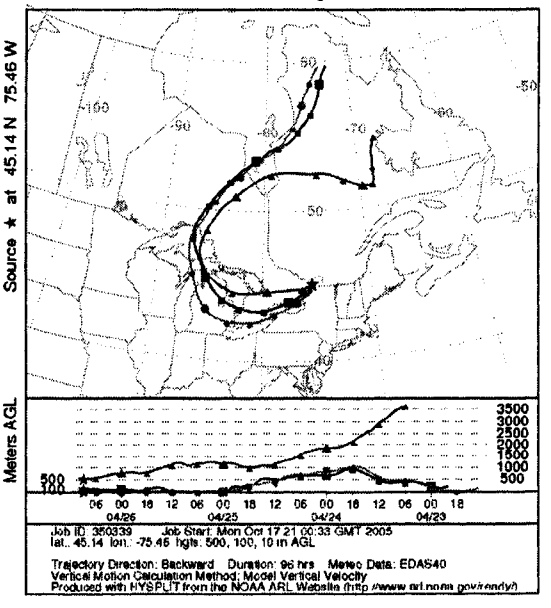

May 11, 2005 (9AM)

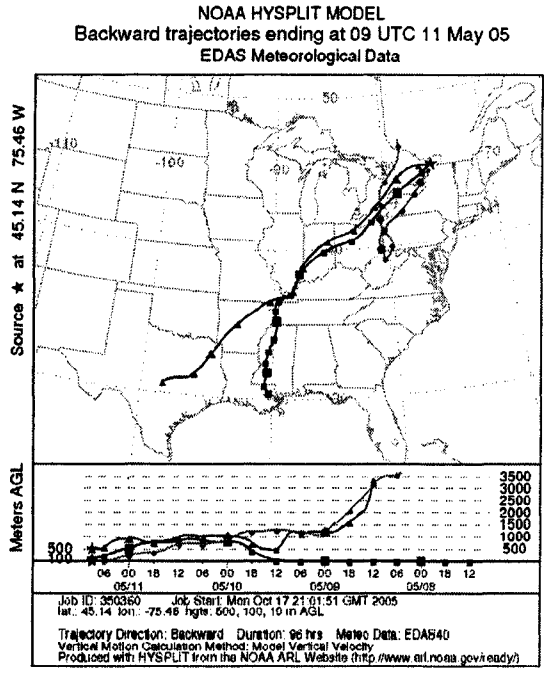

May 25, 2005 (10AM)

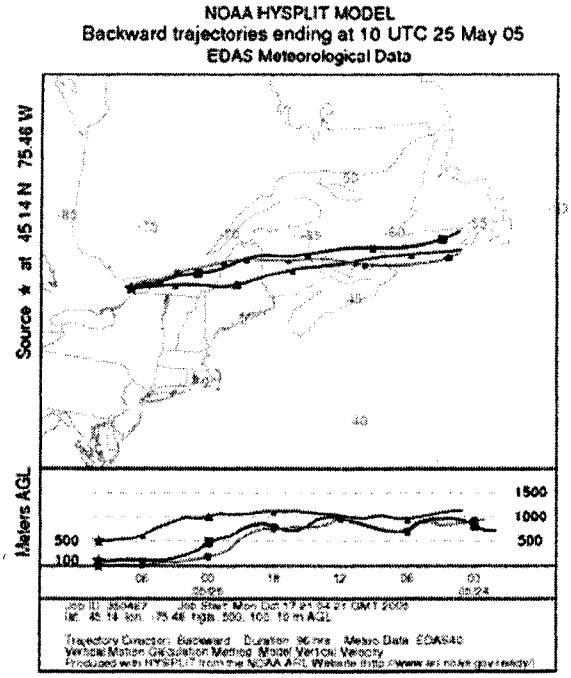

June 8, 2005 (10AM)

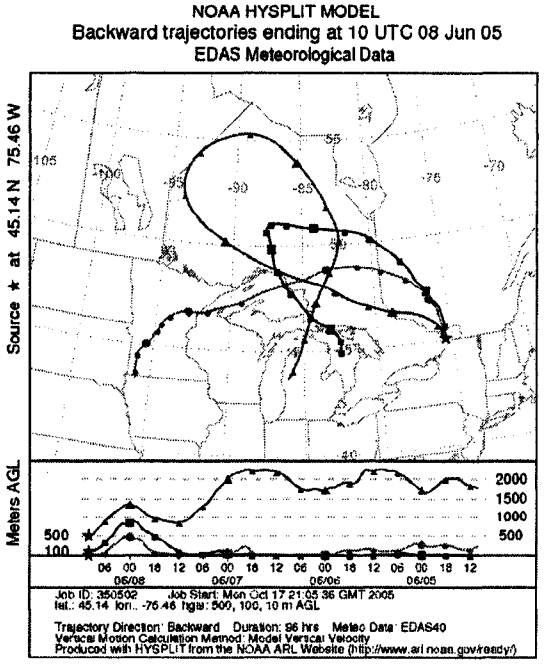

June 21, 2005 (10AM)

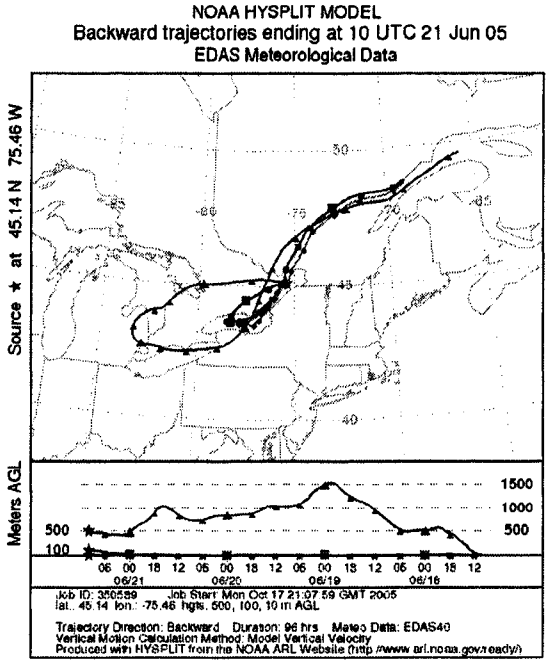

APPENDIX 2 - CHROMATOGRAMS AND RELATED DATA

Chromatographic data for tri to hepta PBDEs (optimized GC-MS method; 1 pg/μL standard)

Surrogate standards denoted with an asterisk

BDE	Retention time (min)	Peak width (min)	Resolution
17	3.464	0.024	
			5.3
28	3.599	0.027	
			27.9
71	4.296	0.023	
			3.8
47	4.387	0.025	
			5.2
66	4.518	0.025	
			7.7
77*	4.713	0.026	
			10.6
100	4.972	0.023	
			8.3
99	5.163	0.023	
			6.7
118*	5.323	0.025	
			6.8
85	5.482	0.022	
			6.6
154	5.623	0.021	
			11.2
153	5.880	0.025	
			14.1
138	6.246	0.027	
			17.0
183	6.729	0.030	
			20.0
190	7.507	0.048	

Note: BDE-209 quantified with a different GC-MS method.

$$R = \frac{(t_2 - t_1)}{0.5(w_2 + w_1)}$$

Chromatographic data for PAHs (optimized GC-MS method; 1 ng/μL standard)

PAH	Retention time (min)	Peak width (min)	Resolution
Acenaphthylene	1.139	0.021	
			25.5
Fluorene	1.840	0.034	
			43.4
Phenanthrene	3.490	0.042	
			2.2
Anthracene	3.591	0.051	
			52.5
Pyrene	6.502	0.060	
			30.3
Benzo(a)anthracene + Chrysene	9.411	0.132	
			16.8
Benzo(b)fluoranthene + Benzo(k)fluoranthene	11.754	0.147	
			4.8
Benzo(a)pyrene	12.368	0.110	
			24.4
Indeno(123-cd)pyrene	15.093	0.113	
			3.7
Benzo(ghi)perylene	15.667	0.200	

PBDEs - Examples of total ion chromatograms

Spruce needle sample (collected May 10, 2005)

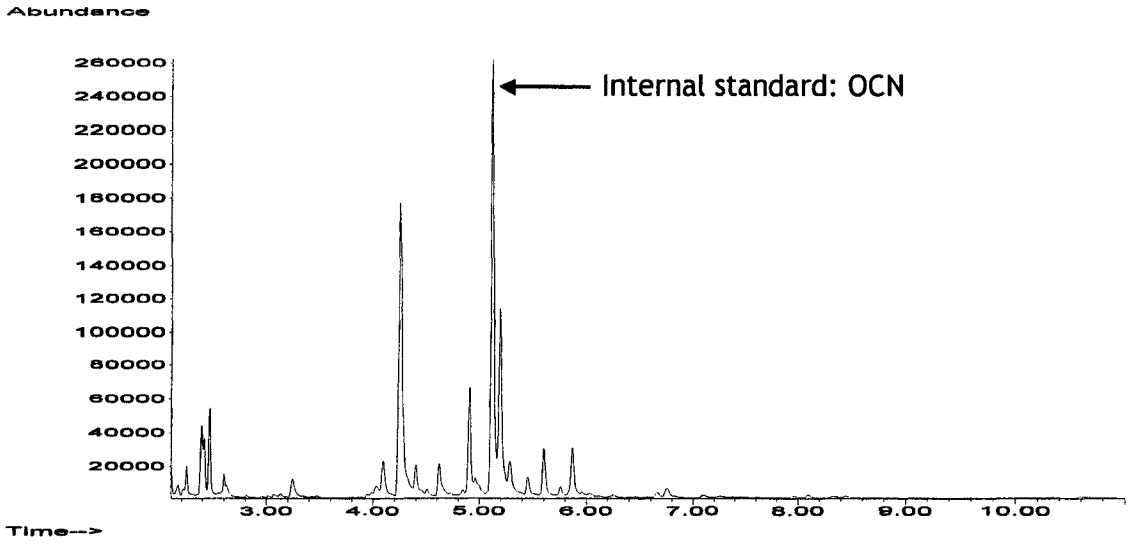

Filter sample (collected March 29, 2005)

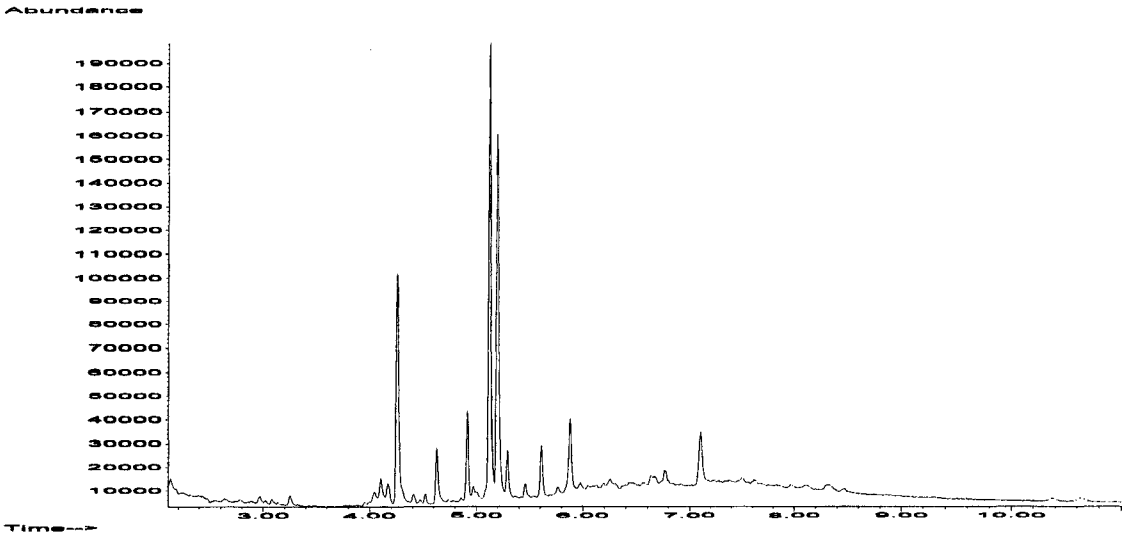

PUF sample (collected May 10, 2005)

Top

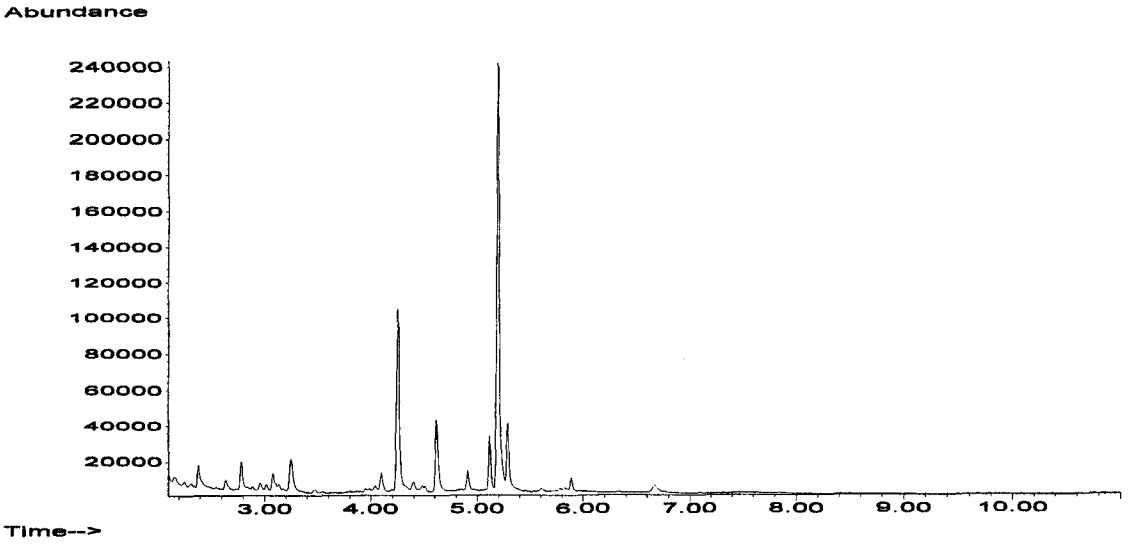

Bottom

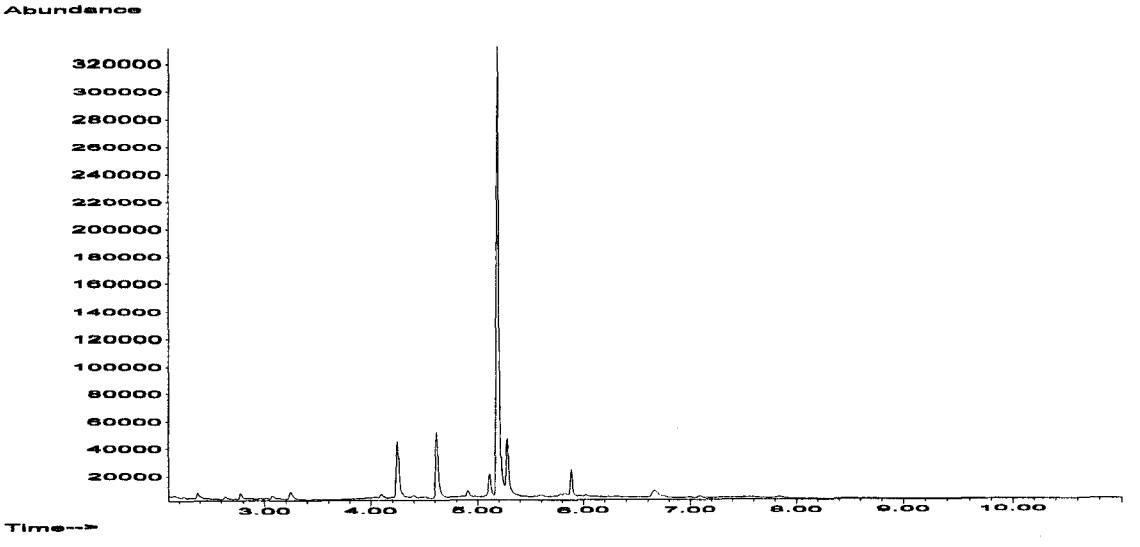

PAHs - Examples of total ion chromatograms PAHs

Spruce needle sample (collected March 15, 2005)

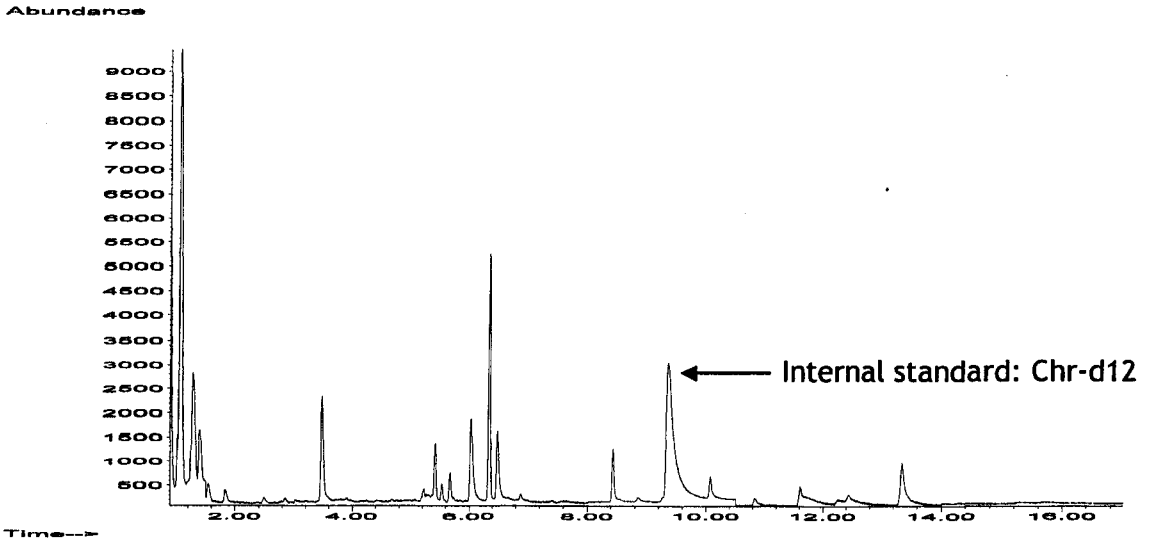

Filter sample (collected May 24, 2005)

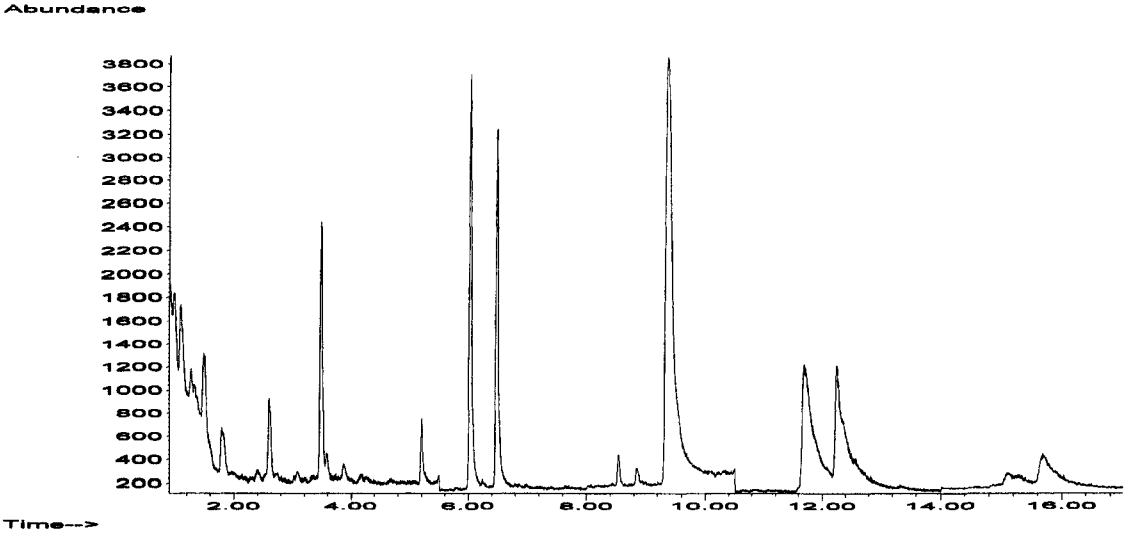

PUF sample (collected May 3, 2004)

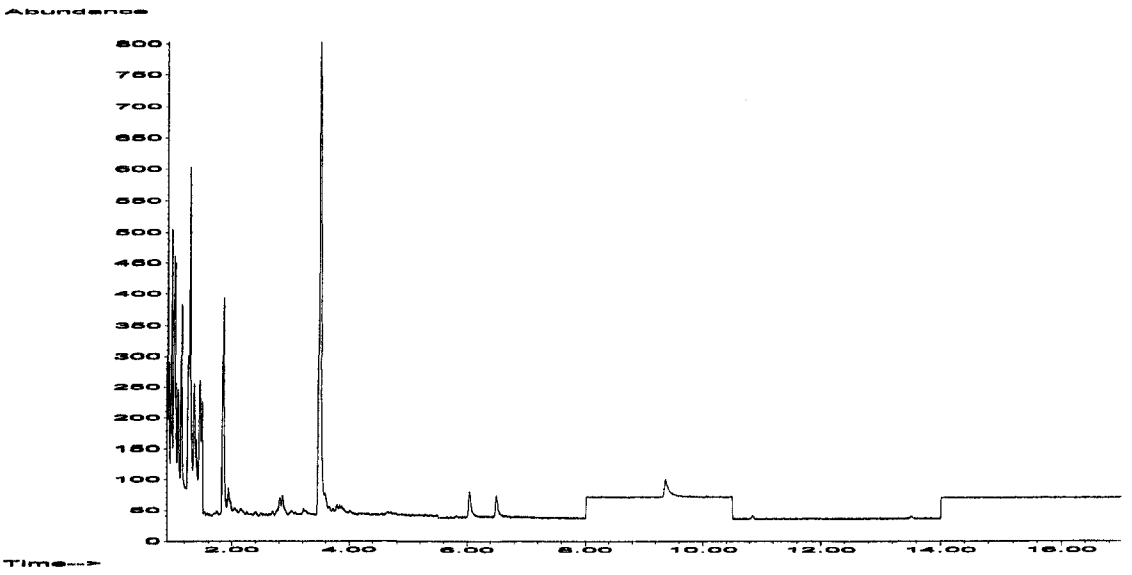

APPENDIX 3 - PBDE AND PAH SPRUCE NEEDLE AND ATMOSPHERIC CONCENTRATIONS

PBDE spruce needle concentrations (pg/g dry weight)

2003 growth year (February to June 2004)

BDE	16-Feb	24-Feb	2-Mar	9-Mar	22-Mar	5-Apr	20-Apr	3-May	17-May	31-May	14-Jun	28-Jun
17	BDL	BDL	BDL	6.95	BDL	3.43	BDL	BDL	BDL	BDL	BDL	BDL
28	17.47	11.54	13.62	16.03	8.31	6.75	1.34	2.36	BDL	3.77	2.86	5.82
71	BDL	BDL	BDL	BDL	BDL	BDL	BDL	BDL	BDL	BDL	BDL	BDL
47	298.93	197.36	197.14	185.76	133.07	98.36	BDL	17.29	BDL	46.19	35.22	72.87
66	23.32	24.08	21.25	21.31	13.23	9.85	BDL	2.36	BDL	4.71	4.07	9.42
100	79.54	76.66	71.05	61.23	63.34	40.31	5.13	11.42	2.53	34.80	21.32	47.97
99	313.44	218.91	217.37	165.40	170.71	116.37	10.94	30.32	BDL	116.03	76.64	157.10
85	12.77	6.83	4.78	3.15	3.54	3.07	BDL	BDL	BDL	1.38	1.69	3.81
154	30.77	28.14	23.88	18.35	39.41	16.38	4.47	6.29	3.56	20.03	13.98	28.31
153	37.52	26.29	22.34	15.18	23.83	15.07	3.49	5.45	2.28	23.55	16.15	33.27
138	10.58	9.94	2.10	1.57	7.18	2.93	0.63	BDL	1.83	2.12	3.04	4.50
183	21.15	14.18	9.10	6.10	12.32	9.00	2.35	4.67	2.65	9.51	7.93	17.66
190	BDL	13.79	BDL	BDL	BDL	BDL	BDL	BDL	BDL	BDL	5.72	BDL
209	BDL	625.94	786.20	330.11	683.24	376.57	177.38	276.70	277.84	2037.83	549.24	1987.06
Total	845.49	1253.66	1368.83	831.14	1158.18	698.09	205.73	356.86	290.69	2299.92	737.86	2367.79

2004 growth year (June to November 2004)

BDE	31-May	14-Jun	28-Jun	12-Jul	26-Jul	9-Aug	23-Aug	13-Sep	20-Sep	4-Oct	18-Oct	1-Nov
17	BDL	BDL	BDL	BDL	2.85	BDL	BDL	BDL	BDL	BDL	BDL	3.67
28	7.83	5.30	3.32	9.21	9.78	13.13	20.30	12.83	15.67	32.79	10.74	32.18
71	BDL	BDL	BDL	BDL	BDL	BDL	BDL	BDL	BDL	BDL	BDL	BDL
47	51.82	61.43	50.48	160.61	156.21	226.31	348.04	223.19	316.67	722.30	217.32	566.41
66	2.91	3.80	4.16	15.73	17.39	30.30	37.75	28.13	36.55	75.90	28.25	57.00
100	27.12	17.02	18.29	86.35	63.24	84.67	91.51	119.80	116.89	187.67	118.98	118.05
99	92.67	58.66	56.03	259.73	155.63	205.33	231.85	287.27	305.49	587.97	282.28	669.26
85	1.89	1.46	1.43	5.09	2.26	3.12	4.35	5.03	7.44	16.55	3.20	31.62
154	12.65	5.50	6.80	42.43	21.08	24.42	25.69	42.55	39.04	57.36	38.36	63.69
153	18.12	6.48	7.92	47.99	19.20	21.96	23.18	40.24	38.47	61.65	37.24	83.50
138	1.39	BDL	1.61	12.94	BDL	3.11	3.28	4.94	5.03	9.15	3.29	9.70
183	4.26	2.98	7.25	24.60	7.41	8.89	10.37	18.94	11.33	20.19	11.91	32.98
190	BDL	BDL	BDL	6.35	BDL	BDL	BDL	BDL	BDL	BDL	BDL	BDL
209	650.75	149.99	258.96	2255.56	1406.54	1392.65	1363.79	1553.07	916.05	2361.21	1096.30	3551.98
Total	871.41	312.62	416.25	2926.59	1861.59	2013.89	2160.11	2335.99	1808.63	4132.74	1847.87	5220.04

2004 growth year (November 2004 to April 2005)

BDE	15-Nov	29-Nov	14-Dec	5-Jan	17-Jan	31-Jan	17-Feb	3-Mar	14-Mar	29-Mar	11-Apr	25-Apr
17	3.84	4.23	BDL	3.43	3.89	3.16	BDL	BDL	4.73	3.64	4.12	3.84
28	24.49	19.15	25.04	23.83	48.53	22.49	32.92	40.28	23.92	24.23	29.73	24.49
71	BDL	BDL	BDL	BDL	BDL	BDL	BDL	BDL	BDL	BDL	BDL	BDL
47	458.94	491.08	352.86	431.51	450.05	401.35	495.18	668.58	456.34	359.12	438.57	458.94
66	44.84	49.89	36.90	44.30	47.01	37.03	53.93	77.43	45.42	34.96	48.32	44.84
100	101.61	110.95	79.72	96.27	92.11	90.94	104.71	136.29	97.13	82.29	103.99	101.61
99	540.62	545.43	373.15	461.44	438.41	394.00	470.12	606.15	557.64	410.57	477.57	540.62
85	25.68	24.67	18.72	21.46	18.30	18.27	19.63	25.66	24.08	18.02	20.21	25.68
154	55.26	49.57	36.25	43.62	42.94	36.43	44.55	62.98	56.98	40.98	49.38	55.26
153	64.37	66.81	45.66	52.32	49.41	39.32	45.33	69.39	74.85	55.89	57.10	64.37
138	8.00	8.25	BDL	BDL	BDL	BDL	BDL	BDL	BDL	8.13	9.47	8.00
183	25.58	27.60	18.25	18.24	11.48	14.39	16.29	66.69	35.19	25.95	37.35	25.58
190	BDL	BDL	BDL	BDL	BDL	BDL	BDL	BDL	BDL	BDL	BDL	BDL
209	2369.77	1473.07	616.59	873.82	459.07	785.72	1050.94	1391.91	2219.55	2002.55	1259.93	2369.77
Total	3723.00	2870.70	1603.14	2070.24	1661.20	1843.10	2333.60	3145.36	3595.83	3066.33	2535.74	3723.00

2004 growth year (May to June 2005)

BDE	10-May	24-May	7-Jun	20-Jun
17	6.86	5.14	3.53	6.89
28	34.48	33.60	21.43	46.77
71	BDL	BDL	BDL	BDL
47	534.31	610.10	444.73	907.25
66	56.05	56.77	41.06	91.63
100	127.06	138.30	144.63	293.88
99	654.56	739.99	803.71	1674.80
85	33.10	33.01	42.99	100.86
154	72.56	76.81	90.04	200.51
153	98.10	102.75	134.44	280.04
138	13.28	18.59	21.42	35.40
183	34.80	58.01	57.47	94.56
190	BDL	BDL	BDL	BDL
209	2843.37	3464.69	6219.87	6194.23
Total	4508.53	5337.76	8025.32	9926.82

PBDE particulate-bound concentrations (pg/m^3)

February to June 2004

BDE	16-Feb	24-Feb	2-Mar	9-Mar	22-Mar	5-Apr	20-Apr	3-May	17-May	31-May	14-Jun	28-Jun
17	BDL	0.43	0.01	0.01	BDL	0.02	0.01	0.01	BDL	BDL	BDL	BDL
28	0.06	0.37	0.02	0.02	0.01	0.04	0.03	0.02	0.01	0.12	BDL	0.01
71	BDL	BDL	BDL	BDL	BDL	BDL	BDL	BDL	BDL	BDL	BDL	BDL
47	1.74	11.56	0.73	0.78	0.36	1.47	1.15	1.09	0.12	0.28	0.17	0.10
66	0.07	0.64	0.06	0.05	0.02	0.09	0.06	0.06	0.01	0.15	0.01	0.01
100	0.31	2.78	0.19	0.28	0.08	0.46	0.36	0.34	0.04	1.57	0.06	0.02
99	1.27	13.59	0.86	1.20	0.40	2.26	1.77	1.68	0.20	8.43	0.29	0.11
85	0.05	0.53	0.03	0.05	0.02	0.09	0.07	0.07	0.02	0.38	0.03	0.01
154	0.11	0.89	0.08	0.13	0.03	0.22	0.17	0.16	0.03	1.02	0.04	0.01
153	0.22	0.97	0.15	0.31	0.06	0.36	0.28	0.24	0.04	1.89	0.07	0.02
138	BDL	0.16	0.02	0.03	BDL	0.05	0.05	0.04	BDL	0.23	BDL	BDL
183	0.12	0.18	0.05	0.38	0.07	0.14	0.24	0.20	0.03	0.51	0.11	0.05
190	BDL	BDL	BDL	BDL	BDL	BDL	BDL	BDL	BDL	BDL	BDL	BDL
209	4.72	BDL	BDL	2.92	1.39	10.37	7.91	6.20	0.91	67.05	1.25	0.71
Total	8.67	32.10	2.20	6.16	2.44	15.57	12.10	10.11	1.41	81.63	2.03	1.05

July to December 2004

BDE	12-Jul	26-Jul	9-Aug	23-Aug	13-Sep	20-Sep	4-Oct	18-Oct	1-Nov	15-Nov	29-Nov	14-Dec
17	BDL	0.03	BDL	0.04	BDL	BDL	BDL	0.02	BDL	BDL	BDL	BDL
28	0.02	0.05	0.02	0.06	0.03	0.02	0.01	0.07	0.03	0.06	0.04	BDL
71	BDL	BDL	BDL	BDL	BDL	BDL	BDL	BDL	BDL	BDL	BDL	BDL
47	0.50	3.09	0.38	2.75	0.90	0.74	0.55	0.79	0.94	0.97	0.67	0.25
66	0.04	0.14	0.02	0.13	0.06	0.04	0.03	0.04	0.06	0.07	0.06	BDL
100	0.14	1.23	0.10	0.85	0.32	0.19	0.20	0.25	0.38	0.31	0.23	0.08
99	0.55	6.92	0.40	4.70	1.51	0.98	0.93	1.04	1.73	1.82	1.24	0.32
85	0.05	0.28	0.03	0.19	0.07	0.05	0.05	0.04	0.06	0.11	0.13	BDL
154	0.07	0.70	0.05	0.47	0.17	0.09	0.11	0.12	0.18	0.29	0.28	0.03
153	0.10	1.08	0.06	0.81	0.27	0.13	0.17	0.17	0.29	0.42	0.34	0.03
138	BDL	0.16	BDL	0.12	0.04	BDL	0.04	0.04	0.05	BDL	BDL	BDL
183	0.08	0.54	0.13	0.70	0.14	0.10	0.11	0.16	0.13	0.33	0.40	BDL
190	BDL	BDL	BDL	BDL	BDL	BDL	BDL	BDL	BDL	BDL	BDL	BDL
209	5.11	130.86	5.01	90.50	11.29	13.57	8.61	13.90	12.20	9.84	4.76	BDL
Total	6.66	145.08	6.20	101.32	14.80	15.91	10.81	16.64	16.05	14.22	8.15	0.71

January to June 2005

BDE	5-Jan	17-Jan	31-Jan	17-Feb	3-Mar	14-Mar	29-Mar	11-Apr	25-Apr	10-May	24-May	7-Jun
17	BDL	BDL	BDL	BDL	BDL	BDL	0.07	0.08	BDL	1.59	0.13	1.28
28	BDL	0.02	BDL	BDL	0.05	0.06	0.17	0.22	0.03	0.08	0.28	0.12
71	BDL	BDL	BDL	BDL	BDL	BDL	BDL	BDL	BDL	BDL	BDL	BDL
47	0.45	0.37	0.41	0.25	0.27	0.50	2.18	3.80	0.26	0.77	3.58	0.62
66	0.15	BDL	0.04	0.02	BDL	0.13	0.32	0.27	BDL	0.22	0.37	0.14
100	0.18	0.08	0.09	0.06	0.09	0.21	0.91	1.16	0.07	0.48	1.67	0.35
99	0.70	0.32	0.50	0.34	0.49	0.87	5.05	7.18	0.44	2.47	10.67	1.90
85	0.21	BDL	0.03	BDL	0.03	0.24	0.55	0.35	0.00	0.40	0.84	0.28
154	0.31	0.02	0.06	0.03	0.04	0.36	1.06	0.88	0.04	0.68	1.57	0.31
153	0.28	0.02	0.10	0.04	0.07	0.61	1.91	1.66	0.06	1.03	2.53	0.51
138	BDL	BDL	BDL	BDL	BDL	BDL	0.91	0.17	BDL	BDL	0.47	BDL
183	BDL	BDL	BDL	BDL	BDL	0.61	1.32	0.55	BDL	1.04	1.12	0.34
190	BDL	BDL	BDL	BDL	BDL	BDL	BDL	BDL	BDL	BDL	BDL	BDL
209	1.43	BDL	4.62	BDL	1.99	1.80	3.04	4.71	BDL	4.22	32.51	3.80
Total	3.71	0.83	5.85	0.74	3.03	5.39	17.49	21.03	0.90	12.98	55.74	9.65

June 2005

BDE	20-Jun
17	0.33
28	0.04
71	BDL
47	0.53
66	0.05
100	0.25
99	1.61
85	0.12
154	0.25
153	0.45
138	BDL
183	0.28
190	BDL
209	1.81
Total	5.72

PBDE gaseous concentrations (pg/m^3)

February to June 2004

BDE	16-Feb	24-Feb	2-Mar	9-Mar	22-Mar	5-Apr	20-Apr	3-May	17-May	31-May	14-Jun	28-Jun
17	0.01		0.02	0.01	0.01	0.01	0.04	0.02	0.02	BDL	BDL	0.01
28	0.03		0.03	0.02	0.02	0.02	0.07	0.03	0.05	0.54	0.16	0.05
71	BDL		BDL	BDL	BDL	BDL	BDL	BDL	BDL	BDL	BDL	BDL
47	0.16		0.26	0.21	0.32	0.34	0.50	0.37	0.41	1.95	0.80	0.32
66	BDL		0.01	0.01	0.02	BDL	BDL	0.02	0.02	0.07	0.03	0.02
100	0.03		0.03	0.03	0.06	0.06	0.09	0.08	0.05	0.17	0.09	0.05
99	0.12		0.11	0.12	0.23	0.23	0.28	0.29	0.13	0.49	0.30	0.12
85	0.01		0.01	0.01	0.02	0.01	0.01	0.01	BDL	0.01	0.01	0.01
154	0.04		0.01	0.01	0.02	0.02	0.02	0.02	0.01	0.02	0.01	0.01
153	0.01		0.01	0.01	0.02	0.02	0.01	0.02	BDL	0.01	BDL	0.01
138	BDL		BDL	BDL	BDL	BDL	BDL	BDL	BDL	BDL	BDL	BDL
183	BDL		BDL	BDL	BDL	BDL	BDL	BDL	BDL	BDL	BDL	BDL
190	BDL		BDL	BDL	BDL	BDL	BDL	BDL	BDL	BDL	BDL	BDL
209	BDL		BDL	BDL	BDL	BDL	BDL	BDL	BDL	BDL	BDL	BDL
Total	0.41		0.49	0.43	0.72	0.71	1.02	0.86	0.69	3.26	1.40	0.60

July to December 2004

BDE	12-Jul	26-Jul	9-Aug	23-Aug	13-Sep	20-Sep	4-Oct	18-Oct	1-Nov	15-Nov	29-Nov	14-Dec
17	BDL	BDL	BDL	BDL	BDL	BDL	BDL	BDL	0.05	0.02	0.02	BDL
28	0.64	0.40	0.23	0.18	0.45	0.15	0.09	0.05	0.13	0.04	0.09	0.03
71	BDL	BDL	BDL	BDL	BDL	BDL	BDL	BDL	BDL	BDL	BDL	BDL
47	3.53	1.83	1.30	0.97	1.30	0.95	0.39	0.34	0.56	0.33	0.47	0.18
66	0.19	0.10	0.07	0.05	0.06	0.06	0.04	BDL	BDL	BDL	0.09	BDL
100	0.39	0.22	0.16	0.19	0.20	0.15	0.08	0.07	0.12	0.07	0.14	BDL
99	1.22	0.71	0.47	0.49	0.53	0.42	0.24	0.31	0.35	0.32	0.46	0.16
85	0.03	0.03	0.03	0.03	0.05	0.04	0.01	BDL	BDL	BDL	BDL	BDL
154	0.06	0.05	0.03	0.03	0.06	0.04	0.03	BDL	BDL	BDL	BDL	BDL
153	0.05	0.03	0.03	0.04	0.04	0.03	0.04	BDL	BDL	BDL	BDL	BDL
138	BDL	BDL	BDL	BDL	BDL	BDL	BDL	BDL	BDL	BDL	BDL	BDL
183	BDL	BDL	BDL	BDL	BDL	BDL	BDL	BDL	BDL	BDL	BDL	BDL
190	BDL	BDL	BDL	BDL	BDL	BDL	BDL	BDL	BDL	BDL	BDL	BDL
209	BDL	BDL	BDL	BDL	BDL	BDL	BDL	BDL	BDL	BDL	BDL	BDL
Total	6.11	3.37	2.32	1.98	2.69	1.84	0.92	0.77	1.21	0.78	1.27	0.37

January to June 2005

BDE	5-Jan	17-Jan	31-Jan	17-Feb	3-Mar	14-Mar	29-Mar	11-Apr	25-Apr	10-May	24-May	7-Jun
17	BDL	BDL	BDL	BDL	BDL	0.02	BDL	0.03	0.02	0.22	0.23	0.25
28	0.00	0.04	0.04	0.03	0.05	0.06	0.09	0.07	0.06	0.52	0.59	0.27
71	BDL	BDL	BDL	BDL	BDL	BDL	BDL	BDL	BDL	BDL	BDL	BDL
47	0.16	0.14	0.29	0.20	0.24	0.25	0.72	0.23	0.37	2.62	2.57	1.12
66	BDL	BDL	BDL	BDL	0.05	BDL	0.05	BDL	BDL	0.22	0.18	0.19
100	0.04	0.08	0.06	0.05	0.10	0.05	0.15	0.03	0.07	0.40	0.46	0.28
99	0.17	0.16	0.29	0.26	0.40	0.22	0.40	0.21	0.23	1.24	1.84	0.71
85	BDL	BDL	BDL	BDL	BDL	BDL	BDL	BDL	BDL	0.21	0.05	0.02
154	BDL	BDL	BDL	BDL	BDL	BDL	BDL	BDL	BDL	0.17	0.12	0.11
153	BDL	BDL	BDL	BDL	BDL	BDL	BDL	0.02	BDL	0.28	0.18	0.13
138	BDL	BDL	BDL	BDL	BDL	BDL	BDL	BDL	BDL	0.30	BDL	BDL
183	BDL	BDL	BDL	BDL	BDL	BDL	BDL	BDL	BDL	0.76	BDL	0.11
190	BDL	BDL	BDL	BDL	BDL	BDL	BDL	BDL	BDL	BDL	BDL	BDL
209	BDL	BDL	BDL	BDL	BDL	BDL	BDL	BDL	BDL	BDL	BDL	BDL
Total	0.37	0.42	0.68	0.54	0.84	0.60	1.41	0.59	0.75	6.94	6.22	3.19

June 2005

BDE	20-Jun
17	0.29
28	0.33
71	BDL
47	1.37
66	0.13
100	0.23
99	0.73
85	BDL
154	0.03
153	0.02
138	BDL
183	0.03
190	BDL
209	BDL
Total	3.16

PAH spruce needle concentrations (ng/g dry weight)

2003 growth year (February to June 2004)

PAH	16-Feb	24-Feb	2-Mar	9-Mar	22-Mar	5-Apr	20-Apr	3-May	17-May	31-May	14-Jun	28-Jun
AceN	0.10		0.19	0.13	0.26	0.13	0.04	BDL	BDL	0.09	0.10	0.26
Flu	0.38		0.32	0.28	0.30	0.21	0.09	0.06	0.07	0.10	0.07	0.27
Phe	2.40		2.60	2.10	1.64	1.09	0.25	0.25	0.24	0.35	0.34	1.22
Ant	0.17		0.23	0.21	0.20	0.15	0.05	0.08	0.06	0.41	0.11	0.27
Pyr	1.56		1.87	1.48	0.86	0.65	0.10	0.25	0.18	0.77	0.31	1.06
BaA+Chr	0.44		0.42	0.45	0.45	0.36	0.13	0.28	0.24	0.95	0.45	0.80
BbF+BkF	41.37		26.84	23.35	37.43	23.13	27.74	18.28	20.27	32.35	27.00	52.18
BaP	-		4.48	4.16	5.58	4.49	7.75	6.85	8.37	9.29	8.22	10.75
IndP	8.24		6.68	5.30	BDL	8.19	BDL	7.05	3.52	22.43	9.68	BDL
BghiP	0.53		0.35	0.59	BDL	0.81	BDL	0.75	0.21	2.05	0.80	BDL
Total	55.19		43.98	38.05	46.72	39.21	36.15	33.85	33.16	68.79	47.08	66.81

2004 growth year (June to November 2004)

PAH	31-May	14-Jun	28-Jun	12-Jul	26-Jul	9-Aug	23-Aug	13-Sep	20-Sep	4-Oct	18-Oct	1-Nov
AceN	BDL	0.20	0.07	0.13	0.17	0.13	0.11	0.09	0.13	0.29	0.23	0.21
Flu	0.06	0.27	0.10	0.17	0.11	0.09	0.14	0.08	0.10	0.27	0.09	0.12
Phe	0.44	1.31	0.47	0.59	0.53	0.37	0.70	0.35	0.49	1.49	0.40	0.65
Ant	0.13	0.28	0.07	0.13	0.10	0.08	0.18	0.09	0.12	0.24	0.12	0.12
Pyr	0.44	0.94	0.38	0.41	0.29	0.20	0.59	0.27	0.40	1.31	0.30	0.59
BaA+Chr	0.51	0.78	0.39	0.51	0.55	0.38	0.63	0.40	0.53	0.46	0.51	0.54
BbF+BkF	0.39	1.05	1.99	9.12	6.09	5.36	8.03	5.90	6.03	8.47	10.40	8.39
BaP	BDL	BDL	0.35	1.41	1.51	1.23	1.68	1.43	1.39	1.83	2.02	2.17
IndP	12.78	14.58	6.18	10.07	10.01	6.01	9.85	4.65	9.25	11.66	BDL	7.06
BghiP	1.41	2.02	0.66	0.76	1.16	0.78	1.25	0.68	1.00	1.36	BDL	0.83
Total	16.16	21.43	10.66	23.30	20.52	14.63	23.16	13.94	19.44	27.38	14.07	20.68

2004 growth year (November 2004 to April 2005)

PAH	15-Nov	29-Nov	14-Dec	5-Jan	17-Jan	31-Jan	17-Feb	3-Mar	14-Mar	29-Mar	11-Apr	25-Apr
AceN	0.28	0.31	0.27	0.44	0.33	0.63		0.34	0.36	1.20	0.46	0.52
Flu	0.77	0.92	0.78	1.12	0.82	2.40		0.83	2.25	3.96	1.39	1.06
Phe	4.39	4.67	5.06	8.82	6.20	19.20		5.80	12.40	26.72	7.61	4.63
Ant	0.54	0.55	0.49	0.88	0.52	1.37		0.56	1.51	3.08	0.89	0.56
Pyr	4.74	4.47	3.32	8.14	4.63	10.19		2.79	8.85	22.87	5.89	3.14
BaA+Chr	7.07	8.08	6.17	9.68	7.41	12.82		5.14	19.27	27.77	6.41	2.82
BbF+BkF	40.58	34.41	25.62	40.53	27.87	19.03		19.27	74.50	199.24	80.43	43.64
BaP	6.67	5.25	7.96	5.53	3.20	-		5.78	14.62	37.11	19.25	10.46
IndP	18.15	10.93	15.45	15.13	6.54	BDL		19.84	72.00	246.24	48.71	20.64
BghiP	4.30	4.09	3.95	4.48	2.25	6.41		2.11	11.69	39.85	7.27	2.27
Total	87.49	73.68	69.07	94.75	59.77	72.05		62.46	217.45	608.04	178.31	89.74

2004 growth year (May to June 2005)

PAH	10-May	24-May	7-Jun	20-Jun
AceN	0.59	0.43	0.48	0.70
Flu	0.86	1.08	0.87	1.82
Phe	4.25	4.57	6.11	10.06
Ant	0.68	0.56	0.68	1.22
Pyr	3.16	4.28	6.42	10.84
BaA+Chr	4.89	5.38	10.16	15.50
BbF+BkF	62.47	49.35	78.45	121.15
BaP	14.88	13.26	25.39	16.35
IndP	15.28	27.39	98.45	106.68
BghiP	4.45	3.58	13.17	16.56
Total	111.51	109.88	240.18	300.88

PAH particulate-bound concentrations (pg/m^3)

February to June 2004

PAH	16-Feb	24-Feb	2-Mar	9-Mar	22-Mar	5-Apr	20-Apr	3-May	17-May	31-May	14-Jun	28-Jun
AceN	16.05	10.63	BDL	1.06	BDL	1.16	1.06	BDL	BDL	BDL	BDL	BDL
Flu	15.48	9.27	BDL	1.04	BDL	1.06	BDL	BDL	BDL	1.16	BDL	BDL
Phe	259.51	201.50	3.95	14.33	6.14	13.42	7.67	6.28	3.21	11.00	2.16	2.08
Ant	17.98	30.15	BDL	1.77	BDL	1.14	1.05	BDL	BDL	1.55	BDL	BDL
Pyr	332.05	394.93	5.80	25.89	7.14	16.21	13.50	11.11	5.58	16.56	4.74	3.83
BaA+Chr	210.89	187.77	BDL	28.99	6.60	10.08	13.71	7.80	3.33	18.42	BDL	BDL
BbF+BkF	406.75	250.78	6.70	95.53	22.36	18.29	40.96	14.56	9.04	57.33	6.19	BDL
BaP	189.80	173.27	8.13	25.74	6.40	9.37	14.27	6.77	BDL	16.64	BDL	BDL
IndP	285.08	216.00	BDL	76.44	27.01	18.30	38.53	14.60	12.96	48.75	12.27	8.12
BghiP	136.57	103.61	BDL	36.27	10.74	9.70	18.24	7.88	5.51	23.12	5.90	BDL
Total	1870.16	1577.91	24.58	307.06	86.39	98.73	148.99	69.00	39.63	194.53	31.26	14.03

July to December 2004

PAH	12-Jul	26-Jul	9-Aug	23-Aug	13-Sep	20-Sep	4-Oct	18-Oct	1-Nov	15-Nov	29-Nov	14-Dec
AceN	BDL	BDL	BDL	BDL	BDL	BDL	1.13	1.87	1.68	1.28	2.14	2.91
Flu	BDL	1.61	BDL	1.02	BDL	BDL	1.28	1.42	2.11	1.38	2.10	2.93
Phe	3.04	12.14	3.82	10.04	6.15	5.89	8.68	10.92	17.85	13.92	20.51	45.28
Ant	BDL	3.54	1.01	2.05	1.33	2.85	1.56	2.29	3.98	12.31	12.98	6.46
Pyr	6.06	27.66	8.79	23.92	13.49	11.45	10.79	19.05	26.21	26.09	33.08	87.93
BaA+Chr	3.33	20.71	4.70	16.40	19.99	6.81	9.72	34.44	22.77	19.88	28.42	52.09
BbF+BkF	10.76	58.94	13.35	36.44	103.20	17.96	27.75	114.30	65.22	50.33	80.46	90.62
BaP	BDL	17.22	BDL	23.31	64.71	5.61	18.14	50.47	26.44	20.38	33.91	32.35
IndP	20.05	65.02	19.18	38.26	62.83	23.31	25.38	127.50	64.32	57.88	73.47	86.18
BghiP	7.68	32.10	9.70	23.23	35.12	13.20	14.58	62.86	30.25	26.33	35.27	44.18
Total	50.92	238.94	60.55	174.67	306.82	87.08	119.01	425.12	260.83	229.78	322.34	450.93

January to June 2005

PAH	5-Jan	17-Jan	31-Jan	17-Feb	3-Mar	14-Mar	29-Mar	11-Apr	25-Apr	10-May	24-May	7-Jun
AceN	4.91	4.19	9.49	1.68	2.45	1.16	3.21	5.47	BDL	BDL	1.31	BDL
Flu	3.78	4.14	7.01	BDL	2.05	1.04	2.79	5.05	BDL	BDL	1.80	BDL
Phe	64.12	42.95	136.59	13.10	27.92	12.53	37.63	61.50	6.07	8.50	15.70	4.40
Ant	5.95	4.84	13.51	2.03	2.75	1.55	5.24	9.44	1.03	1.89	3.53	1.54
Pyr	89.69	32.06	213.24	18.54	36.03	16.93	65.37	89.16	6.92	14.73	26.79	9.40
BaA+Chr	58.71	15.64	145.09	18.53	19.14	12.54	62.66	60.03	5.20	8.66	23.46	6.96
BbF+BkF	107.91	29.95	240.91	40.97	30.26	27.06	156.67	109.46	16.43	23.38	69.46	17.16
BaP	42.26	11.06	121.47	11.69	12.80	10.42	46.51	37.72	7.59	9.52	21.34	7.64
IndP	78.60	29.24	161.61	33.57	32.54	26.92	121.82	69.13	20.04	23.57	68.18	27.14
BghiP	41.58	13.64	73.91	17.53	15.93	11.87	69.74	51.27	7.91	10.69	36.96	12.66
Total	497.51	187.1	1122.83	157.64	181.87	122.02	571.64	498.23	71.19	100.94	268.53	86.90

June 2005

PAH	20-Jun
AceN	BDL
Flu	BDL
Phe	5.91
Ant	1.15
Pyr	8.67
BaA+Chr	5.33
BbF+BkF	12.92
BaP	BDL
IndP	12.20
BghiP	7.46
Total	53.64

PAH gaseous concentrations (pg/m^3)

February to June 2004

PAH	16-Feb	24-Feb	2-Mar	9-Mar	22-Mar	5-Apr	20-Apr	3-May	17-May	31-May	14-Jun	28-Jun
AceN	92.17			32.27	22.42	16.59	73.40	31.10	4.77	51.05	15.12	10.68
Flu	266.91			174.85	98.83	63.74	290.75	84.53	139.41	422.64	104.42	84.80
Phe	416.91			265.01	195.58	141.71	429.92	174.66	264.71	671.79	403.81	242.12
Ant	9.00			13.33	7.45	5.59	31.43	13.18	14.24	49.18	20.76	15.71
Pyr	14.50			35.29	30.61	11.07	45.95	21.96	29.84	68.52	52.41	27.62
BaA+Chr	BDL			5.17	BDL	BDL	4.79	BDL	4.30	5.26	5.72	3.72
BbF+BkF	BDL			6.99	6.86	BDL	BDL	BDL	BDL	BDL	BDL	BDL
BaP	BDL			BDL	BDL	BDL	BDL	BDL	BDL	BDL	BDL	BDL
IndP	BDL			BDL	13.70	BDL	14.25	BDL	BDL	13.67	15.09	19.43
BghiP	BDL			BDL	BDL	BDL	5.26	BDL	BDL	5.21	5.72	8.19
Total	799.49			532.91	375.45	238.70	895.75	325.43	457.27	1287.32	623.05	412.27

July to December 2004

PAH	12-Jul	26-Jul	9-Aug	23-Aug	13-Sep	20-Sep	4-Oct	18-Oct	1-Nov	15-Nov	29-Nov	14-Dec
AceN	10.24	40.66	27.20	191.07	87.77	24.27	55.44	342.08	106.04	128.36	97.09	348.52
Flu	227.80	347.58	156.95	335.14	553.83	191.62	213.64	265.56	423.25	312.78	308.06	698.73
Phe	739.01	649.72	352.46	702.45	658.81	319.44	320.23	408.17	666.76	536.36	598.52	1217.28
Ant	45.53	292.31	415.24	158.54	392.31	177.99	79.76	68.91	146.61	254.51	103.67	92.40
Pyr	74.74	79.48	54.17	101.12	102.73	48.06	50.13	48.81	82.73	60.40	94.03	105.46
BaA+Chr	8.76	4.67	4.58	5.41	19.85	4.46	6.06	BDL	BDL	BDL	4.67	2.89
BbF+BkF	10.04	BDL	BDL	BDL	12.36	7.76	BDL	BDL	5.13	BDL	BDL	BDL
BaP	BDL	BDL	BDL	BDL	BDL	BDL	BDL	BDL	BDL	BDL	BDL	BDL
IndP	26.27	BDL	BDL	BDL	BDL	17.83	BDL	12.98	22.85	14.40	12.53	18.68
BghiP	9.94	BDL	BDL	BDL	BDL	6.69	BDL	BDL	9.80	6.00	5.13	6.53
Total	1152.33	1414.42	1010.60	1493.73	1827.66	798.12	725.26	1146.51	1463.17	1312.81	1223.70	2490.49

January to June 2005

PAH	5-Jan	17-Jan	31-Jan	17-Feb	3-Mar	14-Mar	29-Mar	11-Apr	25-Apr	10-May	24-May	7-Jun
AceN	406.05	72.66	263.36	77.23	121.35	112.79	97.51	145.27	7.93	9.98	60.21	43.52
Flu	1039.88	218.82	382.92	236.42	361.67	415.13	767.33	449.43	70.86	184.37	656.60	218.64
Phe	1954.30	258.64	608.35	443.46	685.16	811.90	1047.21	948.33	140.60	433.26	1331.06	424.54
Ant	57.49	62.61	25.11	24.12	28.60	35.04	79.33	42.00	10.68	53.36	133.51	51.28
Pyr	194.07	22.13	38.24	54.62	64.73	61.07	104.39	84.48	19.82	34.57	116.38	52.82
BaA+Chr	5.97	BDL	BDL	BDL	4.09	BDL	6.17	BDL	4.61	4.08	5.32	5.93
BbF+BkF	BDL	BDL	BDL	BDL	BDL	BDL	BDL	BDL	BDL	BDL	BDL	12.57
BaP	BDL	BDL	BDL	BDL	BDL	BDL	BDL	BDL	BDL	BDL	BDL	BDL
IndP	13.93	BDL	27.05	BDL	BDL	BDL	BDL	BDL	18.95	BDL	14.35	30.63
BghiP	5.95	BDL	11.23	BDL	BDL	BDL	BDL	BDL	5.72	BDL	6.17	13.51
Total	3677.64	634.86	1356.26	835.85	1265.60	1435.93	2101.94	1669.51	279.17	719.62	2323.60	853.44

June 2005

PAH	20-Jun
AceN	7.72
Flu	107.41
Phe	238.37
Ant	22.89
Pyr	37.33
BaA+Chr	4.01
BbF+BkF	BDL
BaP	BDL
IndP	20.46
BghiP	6.68
Total	444.87